Investigations into the contributions of mitochondrial dynamics and function to platelet ageing and reactivity

Submitted in partial fulfilment of the requirements of the Degree of

Doctor of Philosophy

Queen Mary University of London

2016-2020

Harriet Elizabeth Allan

Blizard Institute
Barts and the London School of Medicine and Dentistry
Queen Mary University of London
London, United Kingdom

Statement of originality

I, Harriet Allan, confirm that the research included within this thesis is my own work or that where it has been carried out in collaboration with, or supported by others, that this is duly acknowledged below and my contribution indicated. Previously published material is also acknowledged below.

I attest that I have exercised reasonable care to ensure that the work is original, and does not to the best of my knowledge break any UK law, infringe any third party's copyright or other Intellectual Property Right, or contain any confidential material.

I accept that the College has the right to use plagiarism detection software to check the electronic version of the thesis.

I confirm that this thesis has not been previously submitted for the award of a degree by this or any other university.

The copyright of this thesis rests with the author and no quotation from it or information derived from it may be published without the prior written consent of the author.

Signature: Harriet Allan
Date: 08-01-2020

Acknowledgements

Firstly, I would like to thank Tim for giving me the opportunity to complete my PhD in the Warner lab. Thank you for your expert supervision, your support and loyalty and for giving me the freedom to explore my own ideas.

Thank you to the past and present members of the Warner Lab and Trauma Group. Mel, Melissa, Mari, Paul, Laura, Ivana, Trauma Paul, Scarlett and Plinio. Thank you for your support and encouragement; it has been a pleasure to work with you all, I have really enjoyed all our big days out and conferences together, it has been great to be part of such a fun team.

I would like to say a special thanks to Mel. You have been an incredible support to me both professionally and personally. Thank you for always making time for me, and for knowing when I just needed to be shown videos of fluffy animals.

Thank you to all my friends for providing me with a welcome break and distraction from work. I would like to say a particular thank you to Leigh and Melissa. You have both been incredibly supportive over the past few years, and I am so grateful for your friendship.

Lastly, I want to say a massive thank you to my family. Thank you for your unwavering encouragement and belief that I can do anything I set my mind to. I would not be where I am today without your support, and I will be forever grateful for everything you do for me.

Details of collaborations

The liquid chromatography tandem mass spectrometry analysis of the platelet proteome (Chapter 4) was carried out by Dr Simone Marcone at the Conway Institute mass spectrometry facilities at University College Dublin.

I would like to acknowledge the flow cytometry core facilities at the Blizard Institute and Charterhouse House Square, Barts and the London School of Medicine and Dentistry, Queen Mary University of London, for their support with the sorting of platelet samples (Chapter 4).

Details of publications

Papers

Vulliamy P, Gillespie S, Armstrong PC, **Allan HE**, Warner TD, Brohi K. Histone H4 induces platelet ballooning and microparticle release during trauma hemorrhage. Proc Natl Acad Sci USA. 2019 Aug 27;116(35):17444-17449

Unsworth AJ, Bye AP, Tannetta DS, Desborough MJR, Kriek N, Sage T, **Allan HE,** Crescente M, Yaqoob P, Warner TD, Jones CI & Gibbins JM Farnesoid X Receptor and Liver X Receptor Ligands Initiate Formation of Coated Platelets. Arterioscler Thromb Vasc Biol. 2017; 37: 1482–1493

Abstracts

Allan HE, Hayman MA, Marcone S, Chan MV, Menke L, Crescente M, Armstrong PC, Warner TD. Platelet ageing causes loss of mitochondrial and cytoskeletal proteins associated with a decline in haemostatic function and increases in apoptotic markers. Platelets. 2020; 31(1): 129-155

Allan HE, Hayman MA, Marcone S, Chan MV, Armstrong PC, Warner TD. Platelet ageing causes changes in key metabolic and structural proteins. ISTH Academy. Jul 7, 2019; 263636; PB0448 Topic: Platelet Proteomics & Genomics

Allan HE, Ferreira PMF, Crescente M, Warner TD. Characterisation of Platelet Microvesicles Containing Mitochondria and their Interaction with Neutrophils. ISTH Academy. Jul 7, 2019; 274040; OC 27.2 Topic: Platelet Function & Interactions

Allan HE, Ferreira PMF, Crescente M, Warner TD. Platelet Activation Causes Vesicle Release and Loss of Mitochondria. Cardiovascular Drugs and Therapy (2019) 33:261–274

Abstract

Platelets are essential for the physiological process of haemostasis, but also drive pathological thrombosis. Platelet lifespan is a tightly controlled process through which platelets exist for approximately 10 days within the circulation of healthy individuals. However, in a number of disease states this process is dysregulated leading to an accelerated platelet turnover. Indeed, there are a number of reports suggesting that newly formed platelets are hyper-reactive and their presence has been associated with a higher risk of thrombosis. Whilst there are these indications of hyper-reactivity in young platelets, there are few systematic studies. Here I have used proteomics coupled with functional studies and immunofluorescence to show that there is a progressive decline in mitochondrial and cytoskeletal proteins as platelets age and an increase in apoptotic pathways. Given the apparent importance of mitochondria in supporting the predetermined platelet lifespan, it raised the question as to whether mitochondria are important for other platelet functional processes. Therefore, I sought to elucidate the impact of platelet activation on mitochondrial function and dynamics. Physiological stimulation causes an increase in mitochondrial respiration, consistent with an increase in energy demand. Interestingly, $P2Y_{12}$ receptor inhibition causes a reduction in basal oxygen consumption, suggesting a dysregulation in mitochondrial function. Furthermore, this work highlights a role for mitochondria beyond energy production, with indications that stimulation causes platelets to package and release their mitochondria into microvesicles. Interestingly, these mitochondria-containing microvesicles have high P-selectin expression suggesting they may be more likely to interact with neutrophils than the rest of the microvesicle population. Indeed, incubation of neutrophils with mitochondria-positive microvesicles but not mitochondria-negative microvesicles causes alterations in the expression of surface markers; CD11b, CD66b and CXCR2, indicative of neutrophil activation potentially as a result of phagocytosis. This work highlights an important role of mitochondria in both platelet ageing and activation.

Table of Contents

Figures and Tables

Abbreviations

α2A	α2A-adrenergic receptors
AA	Arachidonic acid
ADP	Adenosine diphosphate
AMP	Adenosine monophosphate
AMR	Ashwell-Morell receptor
ASA	Aspirin
ATP	Adenosine triphosphate
AU	Arbitrary units
AUC	Area under curve
BCA	Bicinchoninic Acid
BSA	Bovine serum albumin
$CaCl_2$	Calcium chloride
cAMP	Cyclic adenosine monophosphate
CD11b	Integrin αM
CD40L	CD40 ligand
CD66b	Carcinoembryonic antigen-related cell adhesion molecule 8
cGMP	Cyclic guanosine monophosphate
COX-1	Cyclooxygenase-1
CS	Citrate synthase
CXCR2	C-X-C chemokine receptor type 2
DAG	1,2-diacyl-glycerol
DAMPs	Damage-associated molecular patterns
DDA	Data-dependent acquisition mode
DNM1L	Dynamin-1-like protein
DTS	Dense tubular system
$\Delta\Psi m$	Mitochondria membrane potential
ERp57	Endoplasmic Reticulum protein 57
FADH2	Flavin adenine dinucleotide
FASP	Filter aided sample preparation
FCCP	Carbonyl cyanide-p-trifluoromethoxyphenylhydrazone
FUNDC1	FUN14 domain-containing 1
GDP	Guanosine diphosphate
GPCRs	G protein coupled receptors
GPVI	Glycoprotein VI
GTP	Guanosine triphosphate
HBSS	Hank's Balanced Salt Solution
ICAM-1	Intracellular adhesion molecule 1
IMM	Inner mitochondrial membrane

IP_3	Inositol trisphosphate
IP_3R	Inositol trisphosphate receptor
IPA	Ingenuity pathway analysis
LC-MS/MS	Liquid chromatography tandem mass spectrometry analysis
LC3	Microtubule-associated protein light-chain
LFA-1	Lymphocyte function-associated antigen 1
LIR	LC3-interacting region
MCU	Mitochondrial calcium uniporter
Mfn1	Mitofusin 1
Mfn2	Mitofusin 2
miRNA	Micro ribonucleic acid
mitoPMV	Mitochondrial positive platelet microvesicles
mPTP	Mitochondrial permeability transition pore
mRNA	Messenger ribonucleic acid
MT-CO2	Cytochrome c oxidase subunit 2
MTH buffer	Modified Tyrode's HEPES buffer
NADH	Nicotinamide adenine dinucleotide
OCS	Open canalicular system
OMM	Outer mitochondrial membrane
PAR	Protease-activated receptor
PBS	Phosphate buffered saline
PDGF	Platelet-derived growth factor
PFA	Paraformaldehyde
PGE1	Prostaglandin E1
PGG2	Prostaglandin G_2
PGH2	Prostaglandin H_2
PGI2	Prostacyclin
PI3K	Phosphatidylinositide-3-kinase
PINK1	PTEN-induced kinase 1 (PINK1)
PIP2	Phosphoinositide-4,5-bisphosphate
PKA	Protein kinase A
PKC	Protein kinase C
PKG	Protein kinase G
PLC	Phospholipase C
PMV	Mitochondria negative platelet microvesicles
PRP	Platelet rich plasma
PSGL-1	P-selectin glycoprotein ligand-1
RNA	Ribonuleic Acid
SDS	Sodium dodecyl sulfate
SNAREs	SNAp Receptor
SOCE	Store operated calcium entry

STIM1	Stromal interaction molecule 1
TMRM	Tetramethylrhodamine, Methyl Ester
TOM	Translocase of the outer membrane
TP	Thromboxane prostanoid
tPA	Tissue-type plasminogen activator
TPO	Thrombopoietin
TRAP-6	Thrombin Receptor Activator for Peptide 6
TRPC6	Transient receptor potential channel 6
tSNAREs	Target SNAp Receptor
TXA_2	Thromboxane A_2
uPA	Urokinase-type plasminogen activator
VDAC	Voltage-dependent anion channel
VEGF	Vascular endothelial growth factor
vSNAREs	Vesicles SNAp Receptor
vWF	von Willebrand factor

1 Introduction

1.1 Haemostasis

The cardiovascular system is composed of the heart and a network of branching arteries, veins and capillaries. Fundamental for delivering nutrients throughout the body, this closed system is vital to maintain the functionality of every organ. Under physiological conditions, the maintenance of blood flow is achieved by haemostasis, a process which prevents excessive blood loss, preserves vascular integrity and provides a barrier for infection.

Haemostasis is a tightly regulated process intended to achieve a fine balance between excessive bleeding and thrombosis. Maintaining the haemostatic balance is a complex interplay between procoagulant and anticoagulant mechanisms and is achieved through four components; the vascular endothelium, platelets, the coagulation system and fibrinolysis.[1]

The role of the vascular endothelium is primarily providing a physical barrier between blood components and pro-thrombotic factors within the subendothelial layer. Furthermore, under basal physiological conditions, endothelial cells exhibit a number of anti-thrombotic properties including the production and secretion of a range of vasoactive mediators, affecting vascular tone, inhibiting platelet aggregation and coagulation and promoting fibrinolysis.[2] As a result of damage to the vasculature there is a reduction of nitric oxide and prostacyclin production by endothelial cells, which coupled with the exposure of the subendothelial extracellular matrix causes local, rapid platelet activation and aggregation. This initial phase of platelet activation is termed primary haemostasis.[3]

Subsequently, secondary haemostasis includes the activation of the coagulation system, which acts to stabilise the clot through the production of a fibrin network. This process is initiated by the exposure of phosphatidylserine and tissue factor, on the surface of activated platelets and endothelial cells.[4] The coagulation system is

separated into two pathways; the intrinsic pathway - a longer pathway - and the extrinsic pathway (Figure 1.1). Both pathways proceed in a step wise fashion through the activation of serine protease enzymes, which circulate as inactive zymogens, subsequently interacting with their substrates and cofactors.[5] The intrinsic and extrinsic pathways converge into the Common Pathway, with the activation of Factor X to Factor Xa, finally leading to the production of thrombin and fibrin. The composition of the fibres within the fibrin network determines the clot strength, and ultimately affects the rates of clot break down, and retraction, also known as fibrinolysis.[6]

As with the coagulation cascade, fibrinolysis is a tightly controlled process involving serine proteases, cofactors and inhibitors. This pathway proceeds with the cleavage of plasminogen into plasmin, by tissue-type plasminogen activator (tPA) or urokinase-type plasminogen activator (uPA) which are produced by endothelial cells and macrophages or monocytes respectively.[7] The active plasmin, subsequently acts to degrade the fibrin network within the clot network. These fibrin degradation products are then removed from the circulation and further degraded in the liver.[8]

Physiological haemostasis is a multifaceted process, with a number of steps that can become dysregulated causing pathological thrombosis or bleeding. In thrombotic scenarios, over-activation of platelets or the coagulation cascade can lead to occlusive thrombi, causing the onset of a stroke or myocardial infarction. On the other hand, impaired platelet aggregation or defective coagulation proteins may lead to uncontrollable bleeding.

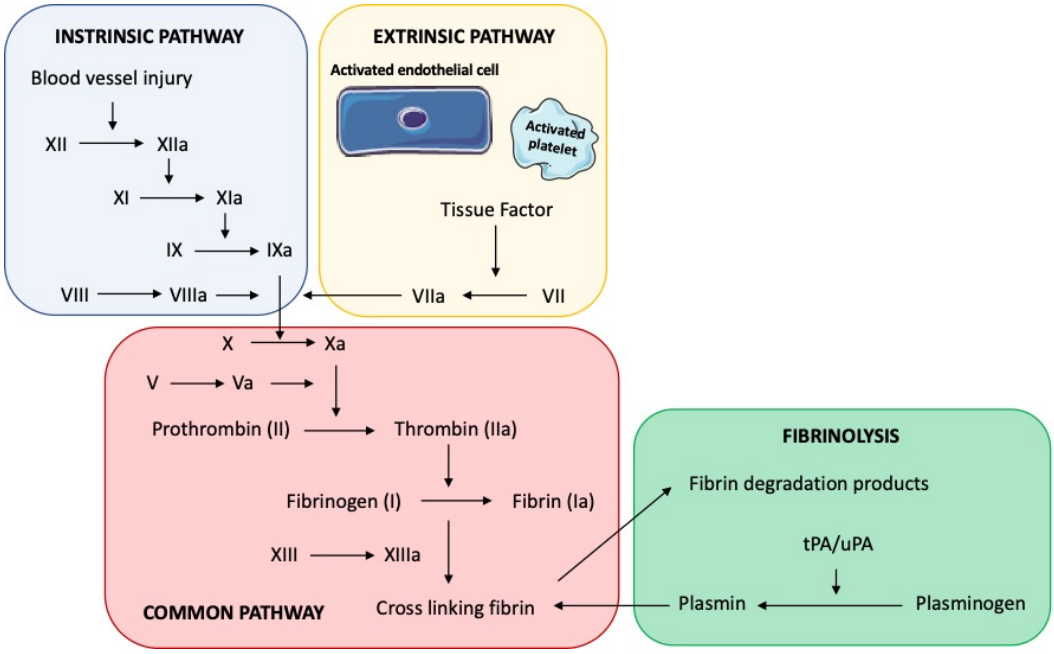

Figure 1.1 Schematic representation of the coagulation cascade

Schematic diagram of the coagulation cascade representing the intrinsic (blue) and extrinsic (yellow) pathways converging with the activation of factor X and the initiation of the common (red) pathway of coagulation in which there is thrombin generation and the conversion of fibrinogen to fibrin which is stabilised by cross-linking facilitated by factor XIII. The breakdown of the fibrin network proceeds through fibrinolysis (green) with the conversion of plasminogen to plasmin. Adapted from Loof et al, 2014.[9]

1.2 Platelet production

Platelets are small, anucleate cell fragments derived from megakaryocytes within the bone marrow. Platelet formation is a highly regulated, continuous process, in which 10^{11} platelets are produced and destroyed every day. Platelet biogenesis is a multi-step process during which megakaryocytes undergo maturation from haematopoietic stem cells.[10] During the early 1990s, the hormone thrombopoietin (TPO) was identified as a key regulator of megakaryocyte differentiation and maturation and consequently platelet production.[11] During the initial phases of biogenesis, haematopoietic stem cells exist in a hypoxic niche relying exclusively on anaerobic glycolysis for energy production. However, increases in TPO levels cause a metabolic switch in haematopoietic stem cells, with a rapid upregulation in mitochondrial activity which is accompanied by a preferential differentiation down the megakaryocyte lineage.[12]

Following the initial cell lineage commitment phase, megakaryocytes undergo endomitosis, a process of several cycles of DNA replication without cell division, leading to their transformation into large polyploid cells.[10] Endomitosis is important for priming megakaryocytes with sufficient protein and messenger ribonucleic acid (mRNA) to pass on to their platelet progeny, whilst not detracting from the maintenance of cellular functionality.[10] Indeed, the synthesis of large quantities of protein and lipids facilitates the development of an extensive invaginated membrane system continuous with the plasma membrane. This complex membrane supported by cytoskeletal fibres and spectrin networks develops throughout the megakaryocyte cytoplasm, acting as a reservoir of membrane structure for the production of proplatelets.[13] As megakaryocytes advance through ploidy cycles, the abundance of protein allows for the formation and packaging of granules for the subsequent trafficking into proplatelets.[14]

The initiation of proplatelet production begins with the disassembly of centrosomes, and the movement of microtubules to the cell cortex.[15] The formation of long pseudopodia originates from a single region of the megakaryocyte plasma

membrane, from which the proplatelet shaft elongates and narrows enabled by rapid microtubule polymerisation and sliding, forming linear bundles which loop back towards the proplatelet body at the free end.[16] Microtubule dynamics facilitate the trafficking of organelles and cellular components towards tandem arrays of platelet sized swellings along the length of the proplatelet shaft, elongating into the sinusoidal blood vessels.[17] The terminal phase of proplatelet production allows tandem swellings packaged with organelles, proteins and ribonucleic acids (RNA), connected by cytoplasmic bridges to bud off into the circulation as preplatelets. The process of cytoplasmic fragmentation and proplatelet formation continues, extending throughout the entire cell body, until the entire megakaryocyte is transformed into proplatelets, after which the nucleus is extruded and degraded. Unlike the proplatelets, preplatelets form a discoid shape with the characteristic platelet cortical microtubule band.[18] The processes involved in the maturation of preplatelets into platelets are poor defined, however there is evidence that they the undergo fission events producing singular circulating cell fragments.

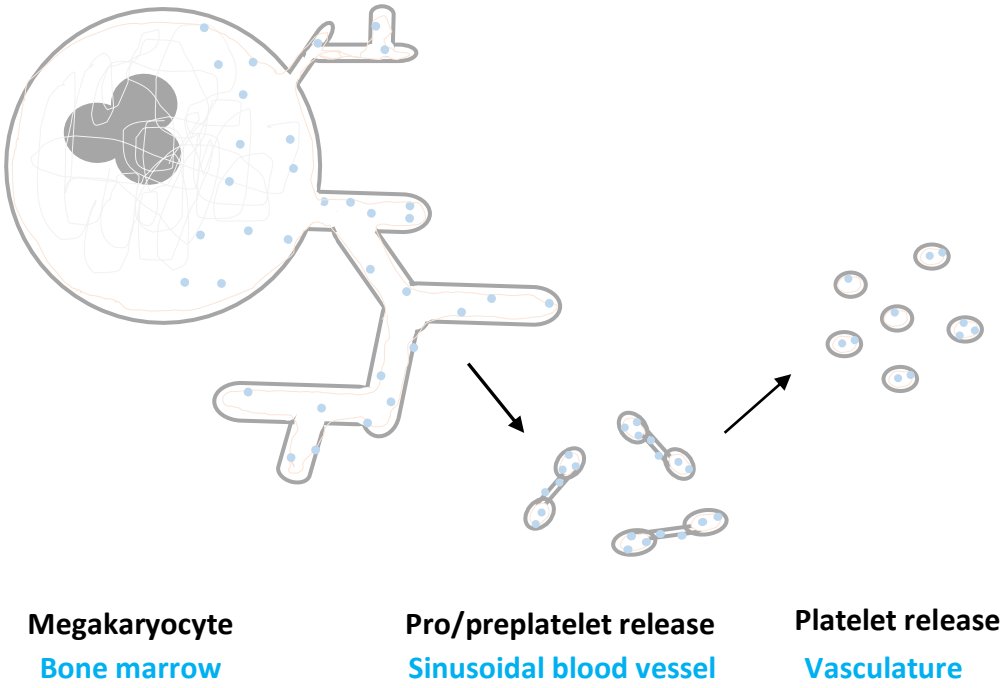

Figure 1.2 Pro-platelet model of platelet development

Megakaryocytes become polyploid cells, undergoing rapid cytoplasmic expansion, allowing the accumulation of cytoplasmic and granule proteins and the formation of a demarcation membrane system. Cytoplasmic reorganization leads to the formation of protrusions, termed pro-platelets, which elongate and branch facilitated by thick linear arrays of microtubules. Once cytoplasmic reorganisation is fully completed, pro-platelets with bulbous ends are released into the vasculature where they mature into platelets. Adapted from Patel et al, 2005[16].

1.3 Platelet turnover, lifespan and clearance

1.3.1 Platelet turnover

Following release into the circulation, platelets in a healthy person circulate for approximately 10 days.[19] Platelet turnover is a tightly regulated, continuous process maintained through a fine balance of platelet production and destruction.[20] It has been reported that in a number of pathological states, such as diabetes mellitus, chronic kidney disease and coronary artery disease, the rate of platelet turnover is altered, with the average lifespan reducing to approximately 5-7 days.[21] The triggers for the initiation of platelet clearance remain elusive. Early evidence suggested a 'multiple hits' model, in which the accumulation of external damage causes engagement of internal cell death pathways.[22,23] However, more recently there is data suggesting platelets have a predetermined lifespan, termed the 'molecular clock'.[24] Given that platelets are anucleate, without the capacity to produce large quantities of protein to repair themselves, it is probable that both models are contributors to the determination of platelet lifespan.

1.3.2 Platelet lifespan and clearance

Since the initial documentation of platelet lifespan in the 1950s, significant research has been conducted to understand the mechanisms governing the predetermined lifespan.[19] To date, a number of pathways of clearance have been proposed, however the mechanism of determining clearance under healthy, steady state conditions remains unclear.

One of the proposed mechanisms of clearance is through the intrinsic (or mitochondrial) apoptosis pathway mediated by Bak and Bcl proteins. It has been established that platelets have the ability to undergo apoptosis, however the conditions triggering this response and the physiological relevance remain to be determined.[25–27] Experiments, using both pharmacological inhibition as well as knockout murine models, have indicated that anti-apoptotic Bcl-X_L and pro-apoptotic

Bak are the major components governing the control of platelet lifespan via intrinsic apoptosis.[28] As platelets age, the progressive degradation of Bcl-X_L causes the balance of anti- and pro-apoptotic signals to shift, triggering Bak mediated apoptosis and subsequent clearance (Figure 1.3). The importance of the intrinsic pathway in platelet clearance has been highlighted in clinical trials of navitoclax, an anti-cancer drug targeting the Bcl proteins, in which its administration causes acute thrombocytopenia, due to the inhibition of Bcl-X_L.[29,30]

Another potential mechanism of clearance is through time-dependent surface modifications such as desialylation. The platelet surface is covered in glycoproteins, of which sialic acid acts as the terminal monosaccharide of both N- and O-linked glycans. The loss of sialic acid residues from these surface glycans acts to expose β-galactose, which is recognised by the Ashwell-Morell receptor (AMR); a lectin asialoglycoprotein receptor, and subsequently phagocytosed (Figure 1.3).[31] Reports have indicated that this surface modification is important in the clearance of several blood components including erythrocytes, and as such may be additionally applicable to platelet clearance. Indeed, both pharmacological inhibition of sialidase activity and knockout of the lectin asialoglycoprotein receptor cause a 30-35% increase in platelet lifespan, highlighting the importance of this pathway in platelet clearance.[32]

As there is convincing evidence that both the intrinsic apoptosis and desialyation pathways are important in the maintenance of platelet lifespan, it raises the question as to whether one pathway is basally active, maintaining the predetermined platelet 'internal clock', whilst the other is engaged under pathological conditions. Indeed, during platelet storage, the levels of sialic acid on the platelet surface decrease at a rate proportional to the storage length, facilitating an increase in phagocytosis by hepatic macrophages and subsequent increase in TPO levels.[33,34] Furthermore, evidence has indicated that sepsis associated thrombocytopenia is linked to increased levels of desialylation.[35] Given that platelet storage does not represent physiological conditions and research has highlighted increased desialylation in septic patients, I would speculate that intrinsic apoptosis is basally active,

maintaining physiological platelet turnover, whilst desialylation is engaged in pathological conditions.

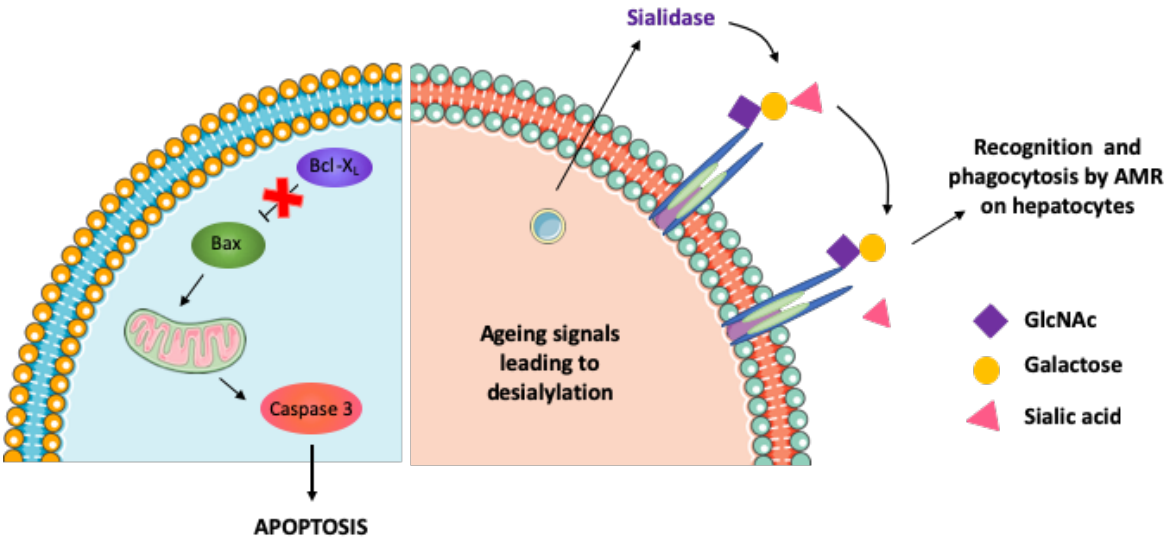

Figure 1.3 Proposed mechanisms of platelet clearance

Platelet clearance may be initiated through two pathways; intrinsic apoptosis and desialylation. Intrinsic apoptosis is controlled by the fine balance between Bcl-X_L and Bax, leading to the release of caspase 3 and subsequent phosphatidylserine exposure. Platelet ageing, causes the release of sialidase from lysosomes which acts to remove sialic acid from membrane glycoproteins, thereby exposing β-galactose which is subsequently recognised by the Ashwell-Morell receptor on hepatocytes. Adapted from McArthur et al, 2018 and Li et al, 2016.[24,36]

1.3.3 Alterations in platelet lifespan

As detailed above, the lifespan of a platelet within a healthy individual is approximately 10 days, however there are reports of alterations in platelet lifespan associated with various pathologies.

Accelerated platelet turnover has been demonstrated in patients with chronic kidney disease and diabetes mellitus, associated with an increased risk of thrombosis and coronary artery disease.[37,38] Indeed, newly formed platelets have been widely reported as being hyper-reactive based on higher thrombotic risk in patients with a higher proportion of young platelets. Whilst this association provides clues into the nature of changes in platelet reactivity in disease, it is hard to unpick the cause of the increased reactivity. For example, there are reports that patients with diabetes mellitus have an increased risk of thrombosis due to hyper-reactive platelets, which may be due to accelerated platelet turnover, or endothelial dysfunction, causing inappropriate platelet activation.[39]

In contrast to the changes observed in platelet turnover secondary to the main complications of diabetes mellitus and chronic kidney disease, altered platelet lifespan is central to immune thrombocytopenia. This autoimmune disease is characterised by an abnormally low platelet count as a result of increased destruction of platelets or impairment in platelet production.[40] It is caused by autoantibodies produced by autoreactive B cells, which target platelet and megakaryocyte glycoproteins, resulting in a shorter platelet lifespan.[40]

To monitor platelet turnover in these pathologies, the immature platelet fraction is measured using a diagnostic platform such as a Sysmex analyser and taken as an indicator of newly formed platelets, which are often referred to as reticulated platelets. Commonly used within the clinic, this automated machine uses a nucleic acid dye to stain platelet RNA acting as a surrogate marker for platelet age.[41]

1.4 Platelet structure and composition

Platelets are smooth, anucleate discoid cell fragments comprising a unique intracellular structure that that supports the rapid response required to maintain haemostasis.

1.4.1 Platelet membranes

The platelet plasma membrane is formed of a bilayer of asymmetric lipids maintained in balance by lipid transporters. Following physiological stimulation or the initiation of apoptosis this asymmetric distribution of anionic phospholipids is lost.[42] Whilst ATP-dependent flippase enzymes act to retain the asymmetric distribution of anionic phospholipids within the plasma membrane, the redistribution of phospholipids is facilitated by the actions of scramblases causing negatively charged lipids to become exposed on the outer leaflet of the plasma membrane.[43,44]

In addition to the plasma membrane, platelets have a vast, continuous and highly complex internal membrane formed from invaginations of the lipid bilayer called the open canalicular system (OCS).[45] This extensive membrane structure has a similar lipid and surface glycoprotein composition to the plasma membrane, providing a reservoir of membrane for the expansion of platelet surface area. Indeed, the OCS allows for the formation of filopodia and lamellipodia in response to vessel damage, facilitating an increase in platelet surface area of up to 420%.[46,47] Furthermore, the OCS is a complex structure of surface connected and interconnected channels, functioning to allow the rapid release of molecules during granule secretion, as well as the transport proteins and molecules from the plasma into the platelet cytosol where they are subsequently packaged into storage granules.[48]

1.4.2 Platelet cytoskeleton

To establish and maintain their discoid shape, platelets have a highly consistent and organised internal cytoskeleton, including a tyrosinated microtubule marginal band formed below the plasma membrane.[49] The circumferential marginal band, a unique

feature to platelets, is composed of a 7-12 filamentous microtubule rings encircling the periphery of the cytoplasm, which when in a quiescent state are heavily acetylated.[49]

Whilst circulating in their inactive form, approximately 50% of a platelet's actin is maintained in a filamentous form.[50] Upon, activation and adhesion rapid reorganisation occurs, causing the actin to form bundles and net-like arrangements facilitating the formation of pseudopodia and lamellipodia.[51] During adhesion, the assembly of these protrusions increases the platelet surface area which facilitates the prevention of blood loss at sites of injury.

1.4.3 Platelet organelles

Despite lacking a nucleus, platelets contain an array of organelles including the dense tubular system, granules, mitochondria, lysosomes and peroxisomes.

1.4.3.1 The dense tubular system

Forming a closed tubular network, the dense tubular system (DTS) is a remnant of the megakaryocyte endoplasmic reticulum playing an essential role in platelet activation.[52] The DTS is a structure discrete from the OCS, however in some circumstances these structures have been observed to be intertwined.[53]

As a major calcium store within platelets, the DTS sequesters and releases calcium in response to various stimuli.[52] In resting platelets, the DTS stem forms a long-elongated structure, acting to maintain a cytoplasmic calcium concentration of approximately 100nmol/L.[52] However, following the addition of a physiological stimulus such as thrombin, the DTS rapidly expels calcium through the inositol-1,4,5-trisphosphate receptor (IP3R) increases cytoplasmic calcium levels.[52] In addition to being an important calcium store, the DTS has been recognised as a site of prostaglandin endoperoxidase and thromboxane A_2 synthesis, as well as a store of protein disulphide isomerases.[54,55]

1.4.3.2 Platelet granules

Platelets contain a range of granules including α-granules, dense granules and lysosomes, which are packaged with a diverse repertoire of pro-inflammatory and pro-thrombotic molecules. The formation of platelet granules begins within the megakaryocyte, where granule proteins are synthesised within the endoplasmic reticulum before undergoing maturation in the Golgi apparatus. Following maturation, the granule cargo is packaged into small vesicular bodies and transported from the trans-Golgi network.[56] The subsequent trafficking of granules into the terminal ends of proplatelets is mediated by microtubule bundles and motor proteins. Following the release of platelets into the circulation, granules continue to mature, with proteins being taken up from the circulation through endocytosis and packaged and stored within platelet granules.[57]

Of the three types of granules, α-granules are the largest and most abundant; ranging from 200-500nm in size with approximately 50-80 per platelet.[57] These granules are heterogeneous with differing cargoes, including soluble factors such as platelet factor 4 as well as membrane associated molecules such as P-selectin.[58] The majority of the cargo within α-granules is trafficked through multivesicular bodies within the megakaryocyte, however a small proportion of factors are endocytosed from the circulation. Electron microscopy has revealed that α-granules have a unique structure, typically made up of four distinct morphological zones. This includes the membrane, a dense nucleoid comprising of proteoglycans and chemokines, a less dense area containing fibrinogen, and a peripheral zone containing von Willebrand factor.[56] Defects in α-granules are associated with a number of inherited bleeding disorders, including gray platelet syndrome and von Willebrand disease.[59]

Dense granules are less numerous than α-granules, with approximately 3-8 per platelet.[60] These acidic granules are rich in nucleotides and have a dark, dense appearance when viewed by electron microscopy. These storage granules, are packaged with pro-thrombotic small molecules including serotonin, adenosine diphosphate (ADP), adenosine triphosphate (ATP) and CD63.[61] Furthermore, they are

also important calcium stores within platelets accounting for approximately 60-70% of the total calcium.[61]

Further to the two secretory granules detailed above, platelets also contain approximately 1-3 lysosomes, comprising of molecules such as cathepsin, heparitinase and β-hexosaminidase. Generally, lysosomal contents are involved in degradation, however the function of lysosomes within platelets remains unclear.[57,62]

Early reports demonstrated that activated platelets lose protein, without disruption of the integrity of the membrane, indicating they may be undergoing granule exocytosis.[63] Originally termed the release reaction, recent work has indicated that this process is highly regulated with differential packaging and release of granular content in response to different stimuli.[63] Indeed, evidence suggests subsets of granules are released at different rates; small molecules packaged in dense granules are rapidly released, potentiating the activation signal, and facilitating the slower release of α-granule and lysosomal content.[64–66] The release of granular content is reliant on fusion machinery located on both the granule itself and the target membrane, either the open canalicular system or the plasma membrane.[67] During the release reaction, the granules proceed through two stages; docking of the granules and subsequent fusion.[61] These processes are mediated by fusion machinery encompassing SNAREs (SNAp REceptor), vesicles SNAREs (vSNAREs) present on the granule membrane and target SNAREs (tSNAREs) resident on the target membrane.[68]

1.4.3.3 Platelet peroxisomes

In addition to the granules detailed above, platelets have a small number of peroxisomes, but their function is unknown.[69] In other cell types they are involved in reactive oxygen species metabolism, fatty acid oxidation and lipid biosynthesis. As they are involved in oxidation reactions, they also produce harmful substances such

as hydrogen peroxide, and as such they are also a store for the enzyme catalase which is involved in the decomposition of these harmful substances.[70]

1.4.3.4 Platelet mitochondria

Despite lacking a nucleus, platelets contain a small number of fully functional mitochondria.[71] Given that platelets are significantly smaller than nucleated cells, the mitochondria resident within a platelet are much smaller and do not form mitochondrial networks, but rather are discrete organelles. While mitochondria in nucleated cells are involved in a myriad of processes their full contribution to platelet functionality remains to be fully characterised.[72] Further description of mitochondrial function in platelets is described in section 1.7.

1.4.3.5 Platelet Ribonucleic Acid

During biogenesis, platelets inherit a small amount of RNA from their parent megakaryocyte. As they are anucleate, this residual RNA is largely lost within the first few days following their release into the circulation.[73] Emerging evidence has identified that platelets contain translational machinery, and therefore have a limited capacity to synthesise new protein from inherited mRNA.[74]

In the last decade is has also become apparent that platelets contain an array of small non-coding RNAs, comprising approximately 500 microRNAs (miRNAs).[75] Maturation of pre-miRNA into miRNA is facilitated by miRNA processing machinery including Dicer, Argonaute-2, and RISC-loading complex subunit TARBP2.[76,77] These mature miRNAs exert their effects on protein-coding genes by interacting with mRNA, acting to regulate its translation.[78] Indeed, these miRNAs have also been shown to play a role in intracellular communication, as they have been detected in platelet derived microvesicles. Using microarray screening, the most abundant miRNAs within platelets and platelet-derived microvesicles have been identified as miR-223, miR-126, miR-196, miR-24 and miR-21.[78] There is evidence that the miRNA profile is linked to platelet activation and aggregation; with platelets having the capacity to control the expression of $P2Y_{12}$, therefore regulating their ability to aggregate.[79]

Interestingly, miRNA expression profiles have been linked with age, sex and disease states, and have been suggested as a potential biomarker for the progression of pathologies.[75,80]

1.5 Platelet activation, adhesion and aggregation

The main function of platelets is to maintain vascular integrity by preventing blood loss following vascular injury. In order to properly carry out their haemostatic function, platelets circulate within the bloodstream at the periphery of the blood vessel, in very close proximity to the endothelium. Platelet margination occurs as a result of the high concentration of circulating erythrocytes, which given their greater size push platelets towards the vessel wall.[81] Under normal physiological conditions, platelets gently roll along the lumen wall, being maintained in a quiescent state by the influence of nitric oxide and prostacyclin released from the endothelium. The presence of nitric oxide and prostacyclin causes an increase in cyclic adenosine monophosphate (cAMP) and cyclic guanosine monophosphate (cGMP) which inhibit platelet activation by the elevation of protein kinase A (PKA) and protein kinase G (PKG) levels.[82]

The close proximity of platelets to the endothelium allows for the rapid detection of vascular damage. Following the detection of exposed extracellular matrix components such as collagen along with shear forces, platelets arrest at the site of damage.[82] Initial tethering occurs in conjunction with von Willebrand factor (vWF) and the glycoprotein GPIb-V-IX complex, which allows for the subsequent activation of additional platelet receptors for collagen, glycoprotein VI (GPVI) and integrin $\alpha_2\beta_1$, thereby stabilising the interaction.[82–84] Initial platelet adhesion allows for sequential actions facilitating platelet activation and aggregation (Figure 1.4).[85]

The activation of the collagen receptors facilitates a series of intracellular signalling cascades, mediated by phospholipase C (PLC), protein kinase C (PKC) and phosphatidylinositide-3-kinase (PI3K).[86] The engagement of these pathways causes an elevation in intracellular calcium, facilitated by its release from the intracellular stores as well as entry through the plasma membrane. These processes are mediated by inositol-1,4,5-trisphosphate (IP_3) and 1,2-diacyl-glycerol (DAG) produced through the hydrolysis of phosphoinositide-4,5-bisphosphate (PIP_2) regulated by PLC.[82,87] Subsequently, IP_3 binds to IP_3 receptors on the intracellular stores, causing calcium

release into the cytoplasm. In parallel, DAG acts to facilitate calcium entry through the transient receptor potential channel 6 (TRPC6) within the plasma membrane. In addition, IP_3 can stimulate the uptake of extracellular calcium by stimulating store operated calcium entry (SOCE). Following calcium release from intracellular stores, the calcium sensor stromal interaction molecule 1 (STIM1) is redistributed within the membrane of the dense tubular system, where it interacts with the store operated calcium channel, Orai1, facilitating its opening and influx of calcium.[87]

The rapid increases in cytosolic calcium levels promotes the secretion of secondary mediators, and cytoskeletal rearrangement facilitating platelet shape changes.[82,88] The release of secondary mediators such as ADP and thromboxane A_2 potentiates the haemostatic response by binding to, and activating receptors on additional circulating platelets.[89]

Platelet activation causes a conformational change in the glycoprotein, GPIIb-IIIa receptor, which reveals the fibrinogen binding domain.[90] The high plasma concentration of fibrinogen readily binds to the GPIIb-IIIa receptor, thereby crosslinking adjacent activated platelets, and forming a platelet aggregate.[90] Stabilisation of the platelet aggregate proceeds through the initiation of the coagulation cascade.

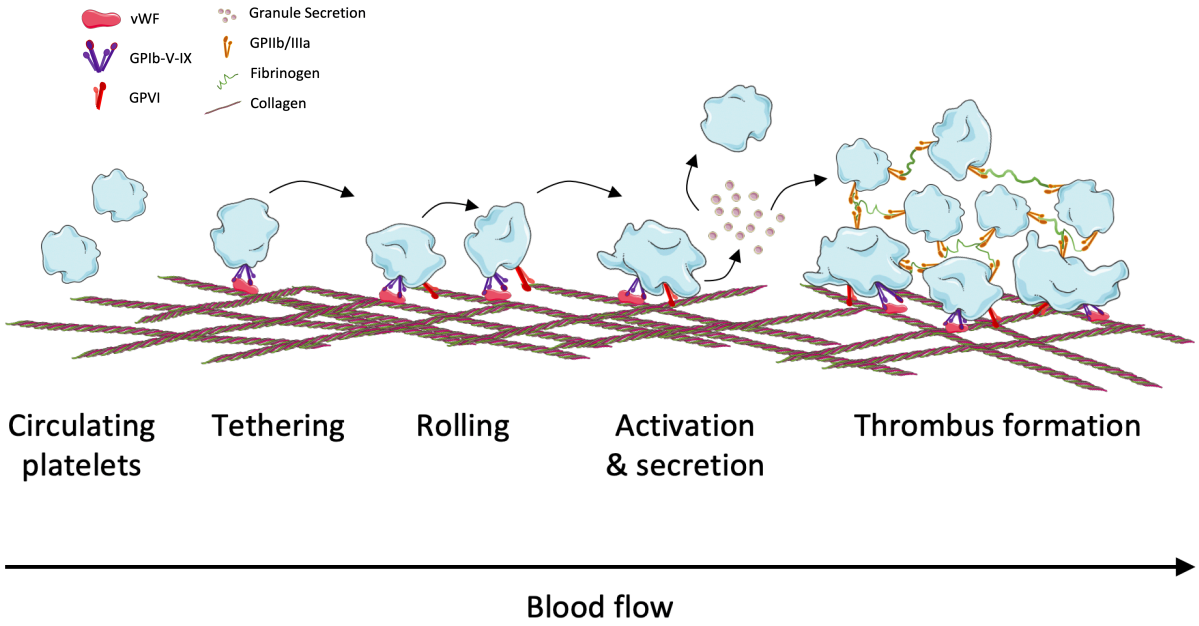

Figure 1.4 Schematic representation of platelet interactions with exposed extracellular matrix components in the vessel wall

Interactions between platelets and collagen within the exposed extracellular matrix. The initial interaction is mediated by vWF and the GPIb-V-IX complex, which given its weak nature promotes rolling of the platelet along the vessel wall. Subsequently, a more stable interaction between GPVI and collagen is established, facilitating platelet arrest and activation. During platelet activation, the secretion of secondary mediators signal for the recruitment of additional platelets to the growing thrombus which interact and form an aggregate by binding fibrinogen through the activated GPIIb-IIIa receptor. Adapted from Gibbins, 2004.[85]

1.6 Platelet activators and inhibitors

In order for platelets to undergo the adhesion, aggregation and activation pathways detailed above, platelets have a wide range of surface receptors which allow them to respond to a multitude of endogenously produced stimulatory and inhibitory mediators. The interaction between these surfaces receptors and their ligands initiates signalling cascades eliciting reactions with varying strengths and functions. These mediators, along with stable synthetic mimetics, are utilised in laboratory testing of platelet function (Figure 1.5).

The majority of the classical platelet activation pathways signal through G protein coupled receptors (GPCRs). These transmembrane receptors are formed of a single polypeptide chain folded forming a looped shape spanning the membrane seven times with an exposed extracellular tail.[91] Following ligand binding, GPCRs become activated undergoing a conformational change which alters their interaction with G proteins within the plasma membrane.[92] These G proteins are heterotrimeric, formed of alpha, beta and gamma subunits, and in their inactive state bind to guanosine diphosphate (GDP). Following activation, guanosine triphosphate (GTP) replaces GDP on the G protein, and causes the dissociation of the subunits, creating an alpha subunit and a beta-gamma dimer. There are four G protein families; Gs, Gi, Gq, $G_{12/13}$, which stimulate or inhibit different intracellular pathways, through second messenger signalling.[93,94]

1.6.1 Adenosine diphosphate

As touched on above, platelets contain secretory granules packed with pro-thrombotic molecules, such as ADP. Following the initial, primary wave of aggregation, platelets release ADP into the extracellular milieu, which activates additional platelets by binding to the $P2Y_{12}$ and $P2Y_1$ receptors.[95] Binding of these receptors activates both Gi and Gq signalling. The engagement of the Gi pathway facilitates the downstream activation of PI3K, Rap1b, Akt and potassium channels, as well as inhibition of adenylyl cyclase. The Gq pathway elicits its effects by activating PKC and calcium mobilisation.[96]

1.6.2 Arachidonic acid and thromboxane A_2

Following initial activation, increases in cytosolic calcium enable the activation of phospholipase A_2 enzymes, which subsequently cleave fatty acids facilitating the liberation of arachidonic acid from the plasma membrane. Arachidonic acid (AA) is then converted into thromboxane A_2 (TXA_2) through a series of two intermediate prostaglandins; cyclic endoperoxide prostaglandin G_2 and H_2 (PGG_2, PGH_2) produced by cyclooxygenase-1, which are then converted into thromboxane A_2 by thromboxane synthase.[97–99] The release of thromboxane A_2 acts as a positive feedback loop activating additional platelets by binding to the thromboxane prostanoid (TP) receptor which couples to Gq and G_{13} proteins.[86] The activation of these G proteins causes the stimulation of PLC, increasing IP_3 and DAG levels and therefore increases intracellular calcium levels and activation of PKC, facilitating platelet shape changes, potentiating platelet activation and aggregation.[100]

1.6.3 Collagen

As touched upon above, vascular damage causes exposure of the subendothelial extracellular matrix components including collagen. The interaction between collagen and platelets can be either indirect via von Willebrand factor and the glycoprotein Ib-V-XI complex, or direct via GPVI or integrin α2β1.[82] The activation of these collagen receptors, stimulates downstream signalling and platelet activation through PI3K and PLC.[82]

1.6.4 Epinephrine

Epinephrine is a weak platelet activator, acting to potentiate the effects of other platelet agonists following its binding to α2A-adrenergic receptors.[101] Activation of these receptors causes coupling to Gi and subsequent inhibition of adenylyl cyclase and a decrease in cAMP levels reducing the brake on other platelet activation pathways.[89]

1.6.5 Thrombin

Thrombin is a serine protease effector of the coagulation cascade produced locally at the site of vascular damage. Thrombin is the most potent platelet agonist causing strong activation through the proteolytic cleavage of the N-terminal tail of its GPCR, the protease-activated receptor (PAR), exposing the thrombin receptor activating-peptide, which subsequently acts a ligand to the transmembrane receptor.[89] In human platelets, thrombin is able to cleave PAR-1 and PAR-4, however these receptors have distinct activation differences. PAR-1 is a high-affinity thrombin receptor, responding to low concentrations of thrombin, eliciting a rapid and strong activation signal. On the other hand, PAR-4 is a low-affinity thrombin receptor, responding to high thrombin concentrations, with a slower and weaker activation signal.[102]

1.6.6 Fibrinogen and Fibrin

Recent work has highlighted a role for fibrinogen and fibrin in binding and activation of GPVI.[103,104] Unlike collagen activation of GPVI which requires receptor dimerization, there is conflicting reports on whether fibrin binding requires receptor clustering and dimerization.[105] Following activation of GPVI, intracellular signalling cascade facilitate spiking in cytoplasmic calcium, and promotes a conformational change in GPIIb-IIIa from a low to a high affinity fibrinogen state. Binding of fibrinogen to GPIIb-IIIa causes outside-in signalling through activation of PLC and calcium mobilisation, and causes cross-linking between adjacent platelets.[104]

1.6.7 Apyrase (ATP diphosphohydrolase)

Apyrase is an endogenous anti-haemostatic agent which hydrolyses ADP into adenosine monophosphate (AMP) thereby inhibiting the potentiation of aggregation following from binding of ADP to $P2Y_1$ and $P2Y_{12}$ receptors.[106]

1.6.8 Prostacyclin

Prostacyclin (PGI_2) is released from the endothelium and acts to maintain platelets in a quiescent state.[107] PGI_2 binds to the IP receptor, activating Gs which binds and activates adenylyl cyclase stimulating the conversion of AMP into cAMP. Subsequent activation of PKA causes inhibition of both calcium mobilisation and granule secretion.[82,107]

1.6.9 Prostaglandin E_1

Prostaglandin E_1 (PGE_1), synthesised from dihomo-gamma-linolenic acid, has anti-inflammatory and anti-platelet affects. This inhibitory mediator is longer lasting than PGI_2, but also binds to the IP receptor causing activation of adenylyl cyclase and subsequent elevation in cAMP levels, PKA activation and inhibition of calcium release.[108]

1.6.10 Pharmacological inhibitors

Cardiovascular disease is the leading cause of morbidity and mortality in the western world. As platelets are central to thrombotic disease, they are an attractive target for the prevention of thrombotic events. As platelets have a vast repertoire of surface receptors and activation mechanisms, there are numerous pharmacological agents targeted at different aspects of platelet activation.[109] The most widely prescribed is acetylsalicylic acid, more commonly known as aspirin. This anti-platelet therapeutic works by irreversibly inhibiting cyclooxygenase-1 (COX-1), the enzyme involved in the metabolism of arachidonic acid into thromboxane A_2.[110]

In addition to aspirin, $P2Y_{12}$ antagonists, such as prasugrel, ticagrelor and clopidogrel, have been shown to be efficacious in reducing the risk of thrombosis. This class of anti-platelet drug act by blocking the ADP receptors, therefore inhibiting the potentiation of platelet aggregation following release of ADP from granular stores.[111] In recent years, dual antiplatelet therapies using a combination of aspirin and $P2Y_{12}$ antagonists have become common place, and demonstrated to reduce thrombotic

events. Despite being effective at reducing thrombotic events there is an intrinsic risk of bleeding when using antiplatelet therapies, in particular within the gastrointestinal tract, and as such caution needs to be taken when prescribing.[112]

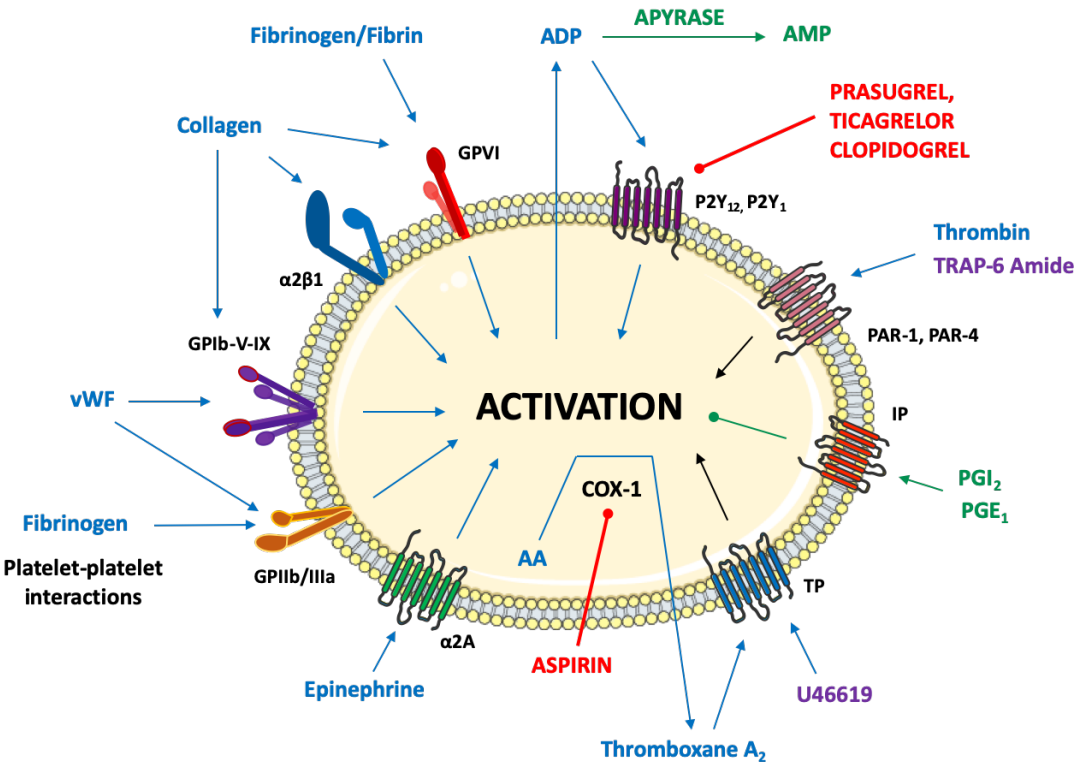

Figure 1.5 Schematic of platelet activation and inhibition pathways

Endogenous platelet activation (blue) and inhibition (green) pathways. Synthetic platelet activation (purple) and pharmacological inhibition (red) pathways. Initial tethering and adhesion processes are mediated by vWF and collagen binding to the GPIb-V-IX complex. Stable adhesion proceeds with collagen binding to GPVI and integrin α2β1. Activation by extracellular mediators such as thrombin, epinephrine and fibrinogen/fibrin, binding to PAR-1/PAR-4, α2A and GPVI receptors respectively facilitates the liberation of AA from the plasma membrane and subsequent conversion into TXA_2. Additionally, ADP is released from the dense granules. These secondary mediators bind to the TP and $P2Y_{12}/P2Y_1$ receptors, respectively, amplifying the activation response. Platelet aggregation is mediated by the activation and binding of fibrinogen to the GPIIb-IIIa receptor. In addition, activation can follow from exposure to TRAP-6, a synthetic agonist of the PAR-1 receptor, and U46619, a stable synthetic analogue of prostaglandin H_2 which binds to the TP receptor. PGI_2 and PGE_1 inhibit platelet activation by binding to the IP receptor and causing increases in intracellular cAMP. Apyrase inhibits platelet function by facilitating the conversion of ADP into AMP. Pharmacological inhibition by aspirin irreversibly blocks the action of COX-1 and therefore the conversion of AA into TXA_2. The $P2Y_{12}$ receptor antagonists, prasugrel, ticagrelor and clopidogrel, inhibit the $P2Y_{12}$ receptor and block ADP induced platelet activation.

1.7 Platelet mitochondrial function

1.7.1 Energy production

As touched upon previously, platelets have a small number of fully functional mitochondria. Most commonly described for their role in energy production, mitochondria produce ATP through oxidative phosphorylation (Figure 1.6).[113] In this process, ATP is generated by the transfer of electrons from nicotinamide adenine dinucleotide (NADH) and flavin adenine dinucleotide ($FADH_2$) to oxygen via a series of electron carrier proteins; complexes I-IV.[113]

Platelets are highly metabolically active cells, requiring a significant amount of energy to maintain themselves in a quiescent state, as well as for the rapid responses essential to maintain haemostasis.[114,115] Whilst every cell type has different energy requirements, with varying ratios of glycolysis to oxidative phosphorylation, it was originally proposed that under basal conditions, oxidative phosphorylation accounts for approximately 40% of energy production, whilst glycolysis is responsible for the remaining 60%.[116] In recent years, however, the rate of glycolysis has been demonstrated to been much lower, with only around 13% of glucose being converted into lactate. Interestingly, a recent report has highlighted an extramitochondrial source of oxidative phosphorylation has been identified in platelets which is active under resting conditions and increases following physiological stimulation.[117] This report highlights a high rate of NADH-fuelled oxygen consumption and ATP production, which is not affected by an inhibitor of the adenine nucleotide translocase, suggesting this process is happening at a site distinct from the mitochondria. [117] Indeed, the authors speculate the extramitochondrial oxidative phosphorylation machinery may be present within the dense tubular system as determined by colocalization of the endoplasmic reticulum marker calnexin and cytochrome c oxidase and ATP synthase.[117,118] Although this data provides an interesting theory of energy metabolism in platelets, this is a singular report of the existence of an extramitochondrial oxidative phosphorylation machinery, so would need further investigation to confirm this data.

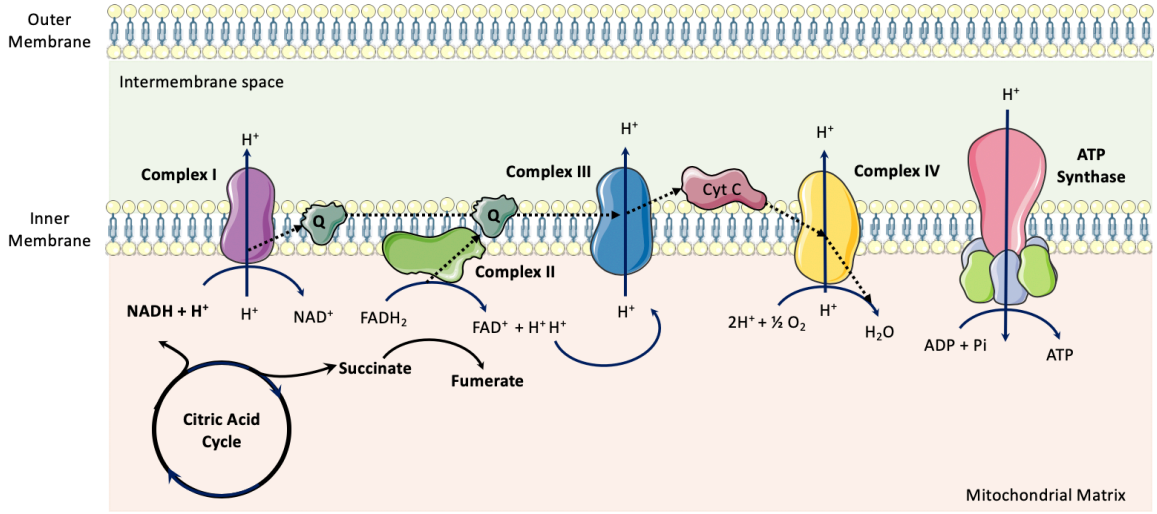

Figure 1.6 Schematic representation of oxidative phosphorylation

Oxidative phosphorylation is a process implemented to produce ATP following from the shuttling of electrons through a series of four electron transport proteins, generating a proton motive force which is harnessed for the formation of ATP. Electrons can enter the oxidative phosphorylation pathway at two points; the first point of entry is at Complex I (NADH-coenzyme Q oxidoreductase) where NADH generated from the citric acid cycle is oxidised by the coenzyme ubiquinone (Q). The reduction of ubiquinone causes a conformational change in the transporter, facilitating the movement of four protons (H^+) into the intermembrane space. The second point of entry is at Complex II (Succinate-Q oxidoreductase), where succinate from the citric acid cycle is oxidised to fumerate transferring electrons to ubiquinone. Subsequently, Complex III (cytochrome c oxidoreductase) oxidises ubiquinone to ubiquinol, enabling the movement of two protons into the intermembrane space, and the subsequent transfer of the electrons to cytochrome c. The final electron transport protein, Complex IV (cytochrome c oxidase) receives the electrons from cytochrome c, supplying them to oxygen (O_2), which is subsequently converted into water (H_2O) with four protons being transported into the intermembrane space. In the final step, ATP synthase uses the proton gradient to generate ATP from ADP.[119]

1.7.2 Reactive oxygen species production and metabolism

During oxidative phosphorylation, mitochondria generate a vast quantity of reactive oxygen species with effects on cellular health. As such, mitochondria possess a host of machinery that acts to minimise the detrimental effects, by metabolising the reactive oxygen species.[120] Indeed, reports have identified that patients with type II diabetes, a disease associated with high oxidative stress, have higher levels of the mitochondrial anti-oxidant enzymes superoxide dismutase-2 and thioredoxin-dependent peroxide reductase 3 compared to healthy controls.[121] Furthermore, the production of mitochondrial reactive oxygen species has been tightly linked with alterations in mitochondrial membrane potential, and is associated with increased platelet activation.[71]

1.7.3 Calcium buffering

Calcium is integral for platelet function, with higher cytoplasmic calcium levels associated with activation. As detailed previously, calcium flux can occur from the extracellular milieu or through release from intracellular calcium stores. In addition to the DTS and dense granules, mitochondria act as a calcium store and buffer by the passive flow of calcium from the cytoplasm across the ion impermeable inner membrane of the mitochondria as a result of the electrical and chemical gradient.[122] Interestingly, recent work has indicated that in a small subset of platelets, agonist stimulation causes an increase in mitochondrial calcium levels which facilitates the exposure of phosphatidylserine.[122]

1.7.4 Mitochondrial induced apoptosis

As described in section 1.3.2, platelet mitochondria are involved in the intrinsic apoptosis pathway facilitating the exposure of phosphatidylserine on the platelet surface. The intrinsic apoptosis pathway is mediated by a fine balance of pro- and anti-apoptotic factors. Degradation of the anti-apoptotic Bcl-X_L, allows activation of pro-apoptotic Bax thereby triggering mitochondrial damage and facilitating the release of cytochrome c.[123] Subsequent caspase-3 activation cleaves hundreds of

intracellular substrates resulting in impairment of important cellular process. Coupled with caspase activation is the exposure of phosphatidylserine on the platelet membrane. Phosphatidylserine can be exposed following platelet activation and apoptosis; however recent work has indicated that the pathways governing these outcomes vary with the former supporting the coagulation cascade, and the latter acting as an eat-me signal.[124] Phosphatidylserine exposure during apoptosis is not reliant on calcium flux, and may proceed through the caspase-3 cleavage of the scramblase Xkr8.[24,125]

1.7.5 Mitochondrial dynamics

Mitochondria are dynamic organelles which can undergo fission and fusion. These processes have been widely characterised in other cell types as a mechanism to maintain mitochondrial health, but it is unclear if platelets have the same capabilities. These processes are mediated by the dynamin family of proteins; fission is mediated by dynamin-1-like protein (DNM1L), whilst fusion is mediated by mitofusin 1 and 2 (Mfn1, Mfn2).[126] Proteomic analysis has revealed that platelets possess these proteins, but it remains unknown whether they are functional or are residual from the parent megakaryocyte.[127]

In addition to the fission-fusion pathways, damaged mitochondria can be marked for degradation by the autophagosome during a process termed mitophagy. Two mitophagy pathways have been described in platelets; firstly, the PTEN-induced kinase 1 (PINK1)/PARKIN pathway and secondly, the FUN14 domain-containing 1 (FUNDC1) pathway.[128,129]

When mitochondria are healthy, PINK1 is internalised from the outer mitochondrial membrane and degraded within the mitochondrial matrix. However, following loss of mitochondrial membrane potential, during mitochondrial damage, PINK1 remains on the outer leaflet of the mitochondrial membrane.[129] The presence of PINK1 on the outer membrane causes the recruitment of the translocase of the outer membrane (TOM) complex, and subsequent recruitment of PARKIN. Following translocation to

the mitochondrial membrane, PARKIN is phosphorylated and subsequently ubiquitylates membrane proteins, thereby recruiting cytoplasmic factors such as p62 and microtubule-associated protein light-chain (LC3) to the mitochondria, marking it for degradation by autophagy.[130]

The second mitophagy pathway identified in platelets is mediated by FUNDC1 and is initiated in response to hypoxia. This pathway proceeds with FUNDC1 becoming dephosphorylated, thereby increasing the interaction with LC3 via the LC3-interacting region (LIR).[128,131] Recent work by the same group has identified that Nix, a mitophagy receptor in erythrocytes, is also involved in platelet mitophagy, with knockout murine models showing an increased lifespan potentially as a result of higher Bcl-X_L levels.[132]

1.7.6 Alterations in mitochondrial function in disease

It is clear that mitochondria are important for platelet function as well as contributing to the control of lifespan, therefore mitochondrial dysfunction may cause impairments in platelet functional pathways. Given the ease of platelet isolation, platelet mitochondrial dysfunction has been described in a number of pathological states, including diabetes mellitus, sepsis, Alzheimer's, Huntington's and Parkinson's disease (Figure 1.7). Notably, these conditions exhibit mitochondrial dysfunction as a result of distinct functional changes.[133]

Reports have demonstrated that in Parkinson's, Alzheimer's and Huntington's disease there is a reduced expression or activity of electron transport proteins; Complex I-II, Complex III and IV and Complex I respectively.[134–137] Interestingly, the reduction in expression of complex I and II in Parkinson's does not cause alterations in mitochondrial membrane potential.[138] In addition to reductions in electron transport carrier proteins, platelets from Alzheimer's patients have a lower basal oxygen consumption rate, with suggestions that this may be as a result of reduced availability of substrate to the complexes, as it is restored following platelet permeabilisation.[135] Likewise, deficiencies in the activity of electron transport

proteins have also been described in patients with sepsis, most notably in complex I, III and IV.[139]

A number of studies have demonstrated mitochondrial dysfunction in patients with diabetes mellitus. Fengming and colleagues have attributed these findings to higher levels of reactive oxygen species and lower mitochondrial membrane potential.[140] Confirmation of these findings in a murine model of diabetes mellitus, indicated that diabetes causes abnormal mitochondria structures and significantly lower mitochondrial ATP content.[140] Additionally, the basal oxygen consumption rate is significantly lower in platelets from diabetic patients compared to healthy controls, showing a 40% reduction. Interestingly, these patients had significantly higher levels of mitochondrial antioxidant proteins, suggesting the reduction in mitochondrial function may be due to increased reactive oxygen species.[121]

Interestingly, a number of pharmacological agents have been shown to effect mitochondrial function in platelets. Metformin, commonly prescribed to treat diabetes mellitus, has been shown to have adverse effects on platelet mitochondrial health at high levels. Metformin overdose is rare, but can develop in patients with renal complications. In these conditions, metformin has been shown to reduce mitochondrial membrane potential and oxygen consumption.[141] Furthermore, statins used to reduce blood lipid levels have been shown to effect the function of Complex I of the electron transport chain.[142]

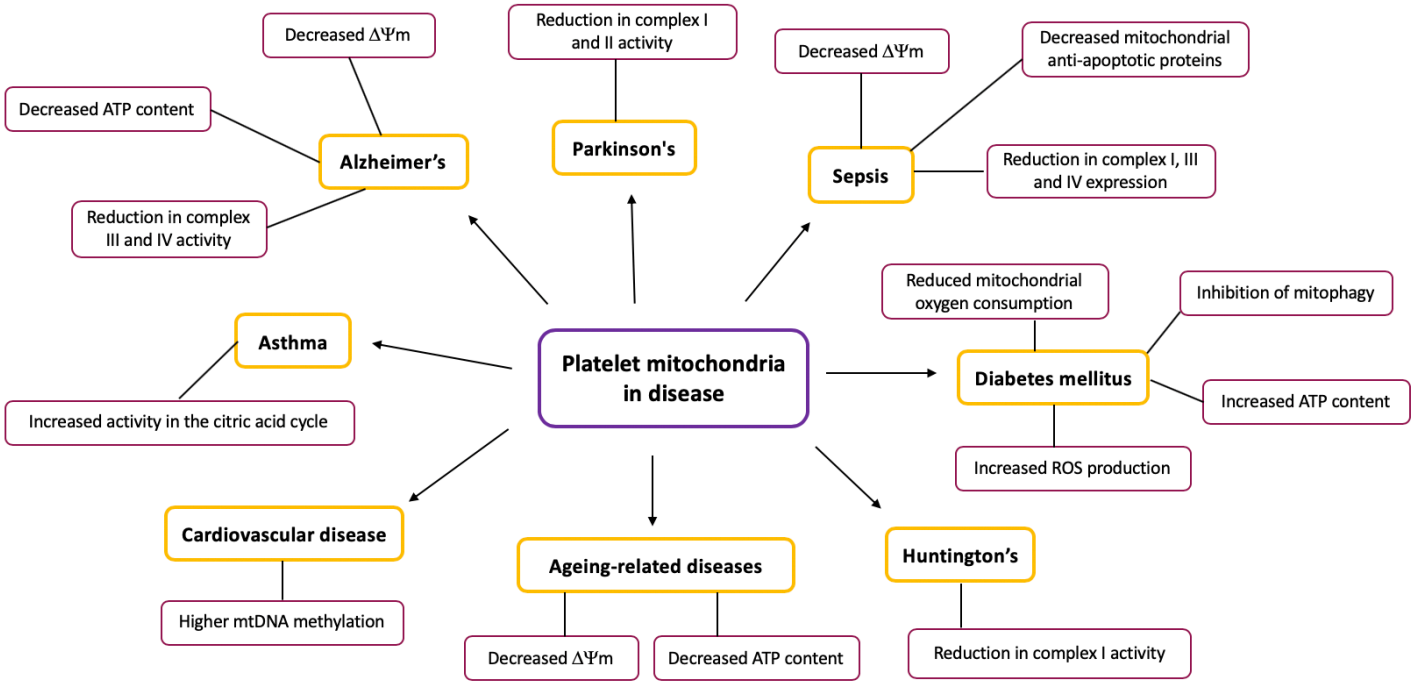

Figure 1.7 Alterations in platelet mitochondrial function in pathological states

Mitochondrial dysfunction has been reported in a number of disease states with alterations in varying aspects of mitochondrial function ranging from the expression and activity of complexes of the electron transport chain, to changes in ATP content and $\Delta\Psi m$.[121,133,135,137,138,143–148]

1.8 Platelet microvesicles

It has long been established that platelet activation causes the exocytosis of secondary mediators into the local site of injury to potentiate platelet recruitment and activation. However, in recent years it has become clear that during both physiological and pathological activation, platelets release small membrane-bound vesicles, termed microvesicles, into the circulation. Originally termed 'platelet dust' by Wolf in 1967, recent advances in technology have allowed for the identification and characterisation of these vesicles.[149] With the advancement in techniques, interest has flourished in the field of extracellular vesicle research, which can be found in numerous bodily fluids including blood, saliva urine, and synovial fluid and are produced by a range of different cell types.[150] The nomenclature within the vesicle field is varied, with the term extracellular vesicles encompassing a range of membrane bound vesicles varying in size and origin including exosomes (20nm-100nm), microvesicles (100nm-500nm) and apoptotic bodies (500nm-1000nm).[150]

1.8.1 Platelet-derived microvesicle production

Platelet-derived microvesicles can be formed and released into the circulation in response to a number of physiological stimuli including activation and apoptosis, in addition to physical stimuli such as shear stress.[151] The process of vesicle formation is crucially dependent on calcium, which is intimately linked to both the inhibition and activation of a number of enzymes.[151] Under resting physiological conditions, the platelet phospholipid membrane is maintained by flippases and floppases in a dynamic asymmetric configuration, in which phosphatidylserine and phosphatidylethanolamine are confined to the inner membrane, whereas phosphatidylcholine and sphingomyelin are restricted to the external membrane.[152] However, the presence of extracellular platelet activators causes outside-in signalling, leading to a rapid rise in intracellular calcium and cytoskeletal rearrangement. After the initial activation and engagement of membrane integrins and G-protein coupled receptors, platelets undergo a series of processes leading to the engagement of scramblase, a bi-directional lipid transporter which causes disruption of the phospholipid asymmetry.[152] The disturbance of the membrane

asymmetry causes disruption to the anchorage between the plasma membrane and the cytoskeleton, subsequently allowing for blebbing of the plasma membrane, allowing the formation and release of microvesicles.[151,153] In addition to budding from the plasma membrane, microvesicle formation can be initiated from the OCS, following release of granular and cytoplasmic contents.[154]

1.8.2 Platelet-derived microvesicle structure and composition

Microvesicles are a heterogeneous population of particles containing a myriad of cargoes inherited from their parent platelets; including surface receptors, soluble mediators, microRNAs and organelles encapsulated within a phospholipid bilayer (Figure 1.8).[155,156] As discussed previously, microvesicles can form in response to a number of stimuli and as a result can be formed into a number of different structures. These range from the most abundant structure consisting of a simple single membrane, to complex structures of multi-membrane vesicles.[153] In addition, multi-vesicular particles have been identified consisting of approximately 15 individual microvesicles. These structures can take two forms; the first is formed of multiple single membrane vesicles which are free to move within a restricted large membrane, the second lacks the restrictive membrane and the vesicles rather form tight contact sites with one another.[153] Despite the identification of these different structures, the roles of each subpopulation of microvesicle remain unclear. Proteomic analysis of platelet-derived vesicles indicates that they contain approximately 600 proteins, suggesting that they may play important roles in a wide range of process from haemostasis to inflammation.[157] Indeed, there is evidence to suggest platelet-derived vesicles may be selectively packaged with cargo consistent with the formation of distinct vesicle populations with varying functions.[158]

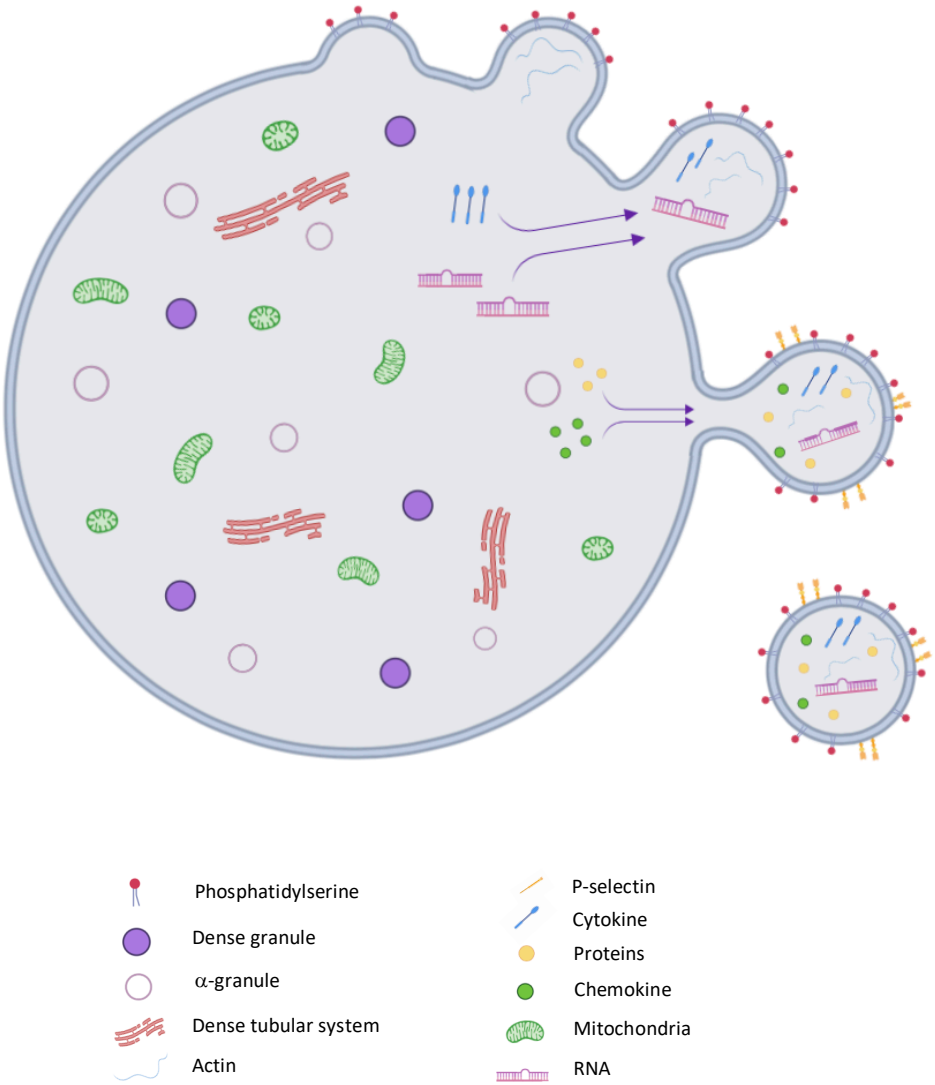

Figure 1.8 Formation and composition of platelet-derived microvesicles

Platelet-derived microvesicles are produced during platelet activation facilitated by the exposure of phosphatidylserine on the outer leaflet of the plasma membrane, cytoskeletal rearrangement and subsequent membrane blebbing. With the advances in the technologies, research has established that platelet-derived microvesicles contain varying content including cytokines, chemokines, organelles, and miRNA.[152,155]

1.8.3 Platelet-derived microvesicle function

Since their earliest characterisations it has become clear that platelet microvesicles play an important role in blood coagulation because of the exposure of phosphatidylserine on the vesicle surface. The asymmetric flipping of phosphatidylserine onto the outer membrane provides ideal conditions for the initiation and assembly of the coagulation cascade, causing thrombin generation through the contact pathway.[159] Indeed, reports suggest platelet vesicles have up to a 100-fold higher procoagulant activity than whole platelets.[160] Aside from their contribution to coagulation, emerging evidence suggests vesicles may play an important role in immune modulation and inflammation through interactions with leukocytes and the endothelium.[161,162] Despite the growing literature characterising microvesicles, their lifespan still remains unclear, with some groups reporting removal from the circulation within a few minutes, whilst others have been able to identify these particles circulating for up to four hours.[163]

1.8.4 Platelet-derived microvesicle in disease

Microvesicles from varied cellular origins are basally present in the plasma of healthy individuals, however the most abundant are platelet-derived microvesicles. Given the presence of microvesicles in healthy individuals, it would suggest they play a physiological role which remains to be identified.[151] However, it well established that circulating levels of platelet-derived microvesicles are increased in a number of pro-inflammatory and pro-thrombotic disease pathologies.

Notably, recent studies have indicated that patients with cardiovascular disease, diabetes mellitus and rheumatoid arthritis exhibit higher levels of platelet-derived microvesicles.[164–166] Indeed, these diseases are all associated with increased levels of platelet activation which is important for vesicle formation.[167] Furthermore, increased levels of platelet microvesicles have been reported in patients with active Crohn's disease. The associated microvesicle populations demonstrate significantly higher levels of angiogenic factors such as MMP9, MMP2 and PDGFα which are functionally active in promoting tubule formation in both endothelial cells and

interstitial cells.[168] Interestingly, platelet microvesicles appear to have a role in both chronic diseases, as detailed above, and acute injuries, such as traumatic injury. In this latter case, it has been reported that traumatic injury causes an increase in platelet-derived microvesicles and in platelet microvesicle-leukocyte interactions which correlate with injury severity score and prognosis.[169]

Given the plethora of research indicating elevated microvesicle number in disease pathologies, interest in recent years has focussed on using vesicles as biomarkers of disease.[170] The ease of isolation of vesicles from peripheral blood makes their use as a biomarker particularly appealing, as it is a far less invasive process than taking tissue biopsies. Although there are conflicting reports on microvesicle lifespan, following isolation and storage at -80˚C, microvesicles remain relatively stable and thus so may provide a potential novel disease biomarker.[170] Vesicles could be utilised as biomarkers in two ways; detection of specific origin vesicles or the detection of a specific surface markers on the vesicles. Analysing vesicles' cellular origin has been used in the investigation of experimental models such as myocardial infarction, which have identified an increase in cardiomyocyte extracellular vesicle number following reperfusion. Although an interesting observation, the use of cardiomyocyte extracellular vesicles as an acute biomarker of myocardial infarction is an unlikely avenue to pursue as it has been shown it takes 15 days for the levels to significantly rise.[171] On the other hand, the use of vesicle surface marker expression has proved useful in identifying glypican-1 as a potential marker of pancreatic cancer, as it has been shown to be specific to exosomes derived from cancer cells.[172]

Whilst microvesicles make an appealing non-invasive biomarker, there are a number of limitations using them in the diagnosis and prognosis of disease. Firstly, there are no standard procedures for the collection and analysis of microvesicles from blood samples, thus these would need to be established prior to the use of microvesicles as a biomarker.[173] Furthermore, it remains to be established how long elevated levels of microvesicles can be detected in the circulation. Thus, the time frame in which microvesicles may be a useful diagnostic or prognostic tool remains unknown. In

addition, research has not demonstrated the effect of co-morbidities of microvesicle number or composition, which may provide misleading results.

1.9 Platelet interactions

In addition to platelets interacting with one another, they also readily interact with endothelial cells and leukocytes, causing activation of pro-thrombotic and pro-thrombotic signalling pathways and subsequently altering the phenotype and modulating of the endothelium and leukocytes. While these interactions are detectable under physiological conditions, there are many reports of elevated levels under pathological conditions contributing to a potentiation of thrombotic and inflammatory responses.

1.9.1 Platelet-endothelial cell interactions

Given the close proximity to endothelial cells in which platelets circulate it is unsurprising that there is extensive cross talk between them. Platelets can communicate and interact with endothelial cells in a paracrine manner; through the release of bioactive mediators such as platelet-derived growth factor (PDGF) and vascular endothelial growth factor (VEGF), through transient interactions, and through receptor mediated adhesion.

Following platelet activation, CD40 ligand (CD40L) is translocated to the plasma membrane which subsequently promotes the interaction between platelets and endothelial cells by binding CD40.[174] Moreover, platelet rolling along the activated endothelium is supported by GPIb-V-IX complex and vWF released from the endothelial cells, with the aid of P-selectin and P-selectin glycoprotein ligand-1 (PSGL-1). The subsequent firm adhesion is mediated by the platelet integrin $\alpha_{IIb}\beta_3$ and the endothelial integrin $\alpha_V\beta_3$ and intracellular adhesion molecule 1 (ICAM-1).[175] In addition, platelet-endothelial interactions act as a bridge for the capture and activation of circulating leukocytes.[176] Sustained platelet-endothelial interactions are thought to contribute to low grade chronic inflammation, endothelial dysfunction and increased risk of cardiovascular diseases.[177,178]

1.9.2 Platelet-leukocyte interactions

As touched upon above, platelets interact with a range of white blood cells, including neutrophils, monocytes, T cells and macrophages.[179] Indeed, platelet-neutrophil and platelet-monocyte aggregates are detectable within peripheral blood samples from healthy individuals, with reports suggesting they account for approximately 20% of the leukocyte population (Figure 1.9).[180] These interactions are mediated by a number of platelet surface receptors and adhesion molecules including; P-selectin and PSGL-1, ICAM-1/2 and lymphocyte function-associated antigen 1 (LFA-1), and CD40 and CD40L for platelets and leukocytes respectively. [180,181]

The initial interaction between platelets and neutrophils is largely mediated by P-selectin and PSGL-1, which subsequently promotes a stable interaction between GPIb or fibrinogen bound to GPIIb-IIIa on platelets and the integrin αMβ2 on neutrophils.[181] The firm adhesion can also be mediated by ICAM-2 on platelets and LFA-1 on neutrophils.[181] Likewise, platelet-monocyte aggregates are mediated by the interaction between P-selectin and PSGL-1, and there is also evidence for a role of ICAM-1 binding to LFA-1 or to fibrinogen in facilitating this interaction.[182,183]

Activated platelets at the site of vascular injury play a crucial role in the recruitment of leukocytes to the growing thrombus, where they are captured by endothelial cells and subsequently undergo rolling and arrest on the activated endothelium.[184] Consequently, the leukocytes are able transmigrate into the surrounding inflamed tissue, with emerging evidence suggesting leukocytes bound to platelets have an increased capacity to undergo transmigration into inflamed tissue. [184,185]

Elevated levels of circulating platelet-leukocytes complexes have been reported in a number of disease states including coronary artery disease, liver inflammation, sepsis, diabetes mellitus and traumatic injury.[169,186–188] Identification of increases in these complexes may act as an indicator of increased platelet reactivity and inflammation within the vasculature.

A

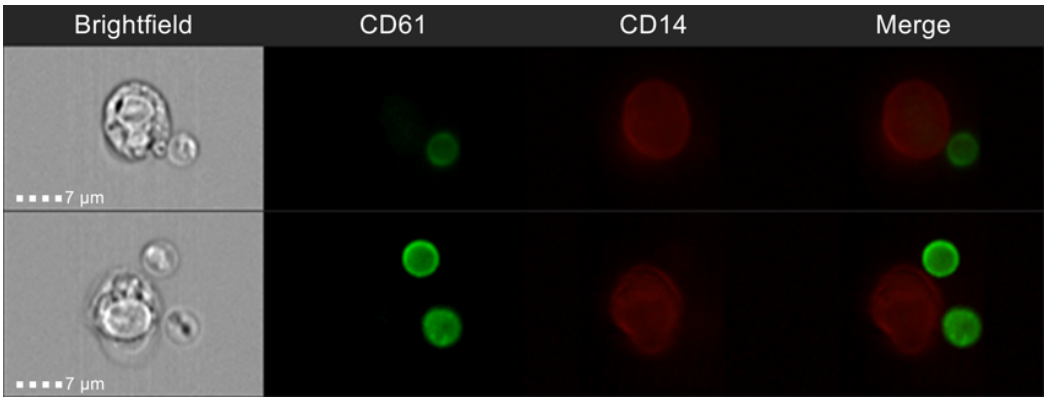

B

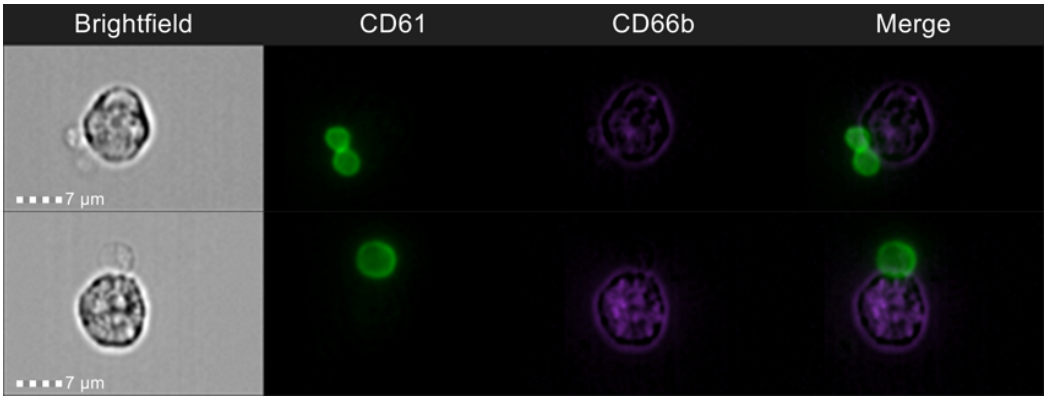

Figure 1.9 Representative Image Stream pictures of platelet-leukocyte aggregates

Interaction between platelets (CD61; green) and **A.** monocytes (CD14; red) and **B.** neutrophils (CD66b; purple) identified in lysed whole blood from a healthy individual.

1.10 Platelets in disease

As touched upon previously, under physiological conditions, circulating blood platelets are fundamental for maintaining haemostasis and vascular integrity, however under pathological conditions, platelets are key drivers of thrombosis. Additionally, in recent years it has been established that platelets are essential modulators of innate immunity and inflammatory responses, contributing to pathologies such as cancer, diabetes mellitus, autoimmune disorders, and allergic responses (Figure 1.10).[189]

1.10.1 Platelets and cardiovascular diseases

Cardiovascular disease is the leading cause of mortality and morbidity within the western world, with the most common vascular events being strokes and myocardial infarction as a result of coronary artery disease. Reports have clearly demonstrated that platelets play an essential role in the pathogenesis of ischemic stroke, exhibiting significantly higher activation markers such as PAC-1 binding, P-selectin expression and calcium secretion, than the platelets of healthy controls. Furthermore, proteomic analysis of platelets from patients with ischemic stroke show a marked alteration in protein expression, with a predicted contribution to inflammatory responses and haematological system.[190–192] Likewise, recent work has shown that platelets isolated from patients who have recently experienced an acute myocardial infarction have marked morphological differences such as extended pseudopodia, suggesting they have been activated.[193] In confirmation of this, platelets from patients with coronary artery disease express higher levels of P-selectin.[194] Furthermore, elevated levels of circulating platelet-leukocytes aggregates have been detected in patients with coronary artery disease and myocardial infarction.[194]

1.10.2 Platelets and cancer

Whilst the role of platelets in cardiovascular disease has long been recognised, research is now focussing on the contribution of platelets to other pathologies. Indeed, reports have indicated platelets may play a role in the pathogenesis of

several cancers, with an association between raised platelet counts and malignant tumours, with thrombosis being more common in a number of cancers.[195,196]

Reports have implicated platelets in several aspects of cancer progression. The elevation in thrombosis risk may be influenced by the exposure of extracellular matrix during intravasation of tumour cells into the circulation. In addition, the release of tumour by-products has been shown to cause platelet activation and aggregation, subsequently causing initiation of the coagulation cascade.[197] Further, tumour cell induced platelet activation has been identified to be involved in the promotion of angiogenesis by releasing bioactive mediators.[198] Moreover, research has detailed that platelets protect tumour cells within the circulation from damage by sheer stress and from detection by natural killer cells. Indeed, following tumour cell migration into the circulation, platelets become activated and encapsulate the tumour cells within aggregates masking them from detection and damage.[198] In addition, platelet aggregates interact with endothelial cells via surface receptors such as P-selectin, thereby promoting the arrest and extravasation of tumour cells out of the vasculature, facilitating their metastasis to secondary sites.[199,200]

Emerging evidence also suggests that within the tumour microenvironment, where there is a leaky vasculature, platelet-derived microvesicles can readily infiltrate and transfer miRNA into tumour cells.[201] Consistent with selective packing of microvesicle content detailed in section 1.8, evidence suggests miRNA transfer both supports and suppresses tumour progression dependent upon the miRNA present. For example, the transfer of miR-223 has been shown to increase the invasiveness of lung cancer cells, while miR-24 causes mitochondrial dysfunction and apoptosis and so suppresses tumour growth.[201]

1.10.3 Platelets and autoimmune diseases

Recent work has detailed a role for platelets in the pathogenesis of autoimmune diseases, including rheumatoid arthritis and systemic lupus erythematosus.[202,203] Elevated circulating platelet-leukocyte complexes have been identified in rheumatoid arthritis, associated with an increase in platelet activation markers P-

selectin and CD63.[204,205] Furthermore, research has detected increased levels of platelet-derived microvesicles, which as well as being detectable in the circulation are present within synovial fluid where they contribute to joint inflammation by the transfer of pro-inflammatory cytokines.[162,167]

1.11 Hypothesis and Aims

Until recently, the roles of mitochondria within platelets were largely overlooked, as their contribution was thought to be restricted to energy metabolism. However, given the ease of platelet isolation, the investigation of mitochondrial function in pathological conditions has flourished and with it our knowledge of platelet mitochondrial function in physiological conditions. Despite this advancement there are still a number of unanswered questions regarding mitochondrial biology in platelets.

This thesis will explore the hypothesis that mitochondria and mitochondrial function may become altered during the inherent process of platelet ageing and play an important role during platelet reactivity and cross-talk with other cells. To this end, this thesis is split into three chapters focussed upon exploration of the following questions:

1. How do different agonists and anti-platelet treatments affect classical platelet activation pathways and mitochondrial respiration?

2. Does the structure, composition and function of a platelet change as it ages within the circulation of healthy individuals?

3. How are mitochondrial dynamics affected by platelet activation, including microvesicle release and how does this affect other circulatory cells?

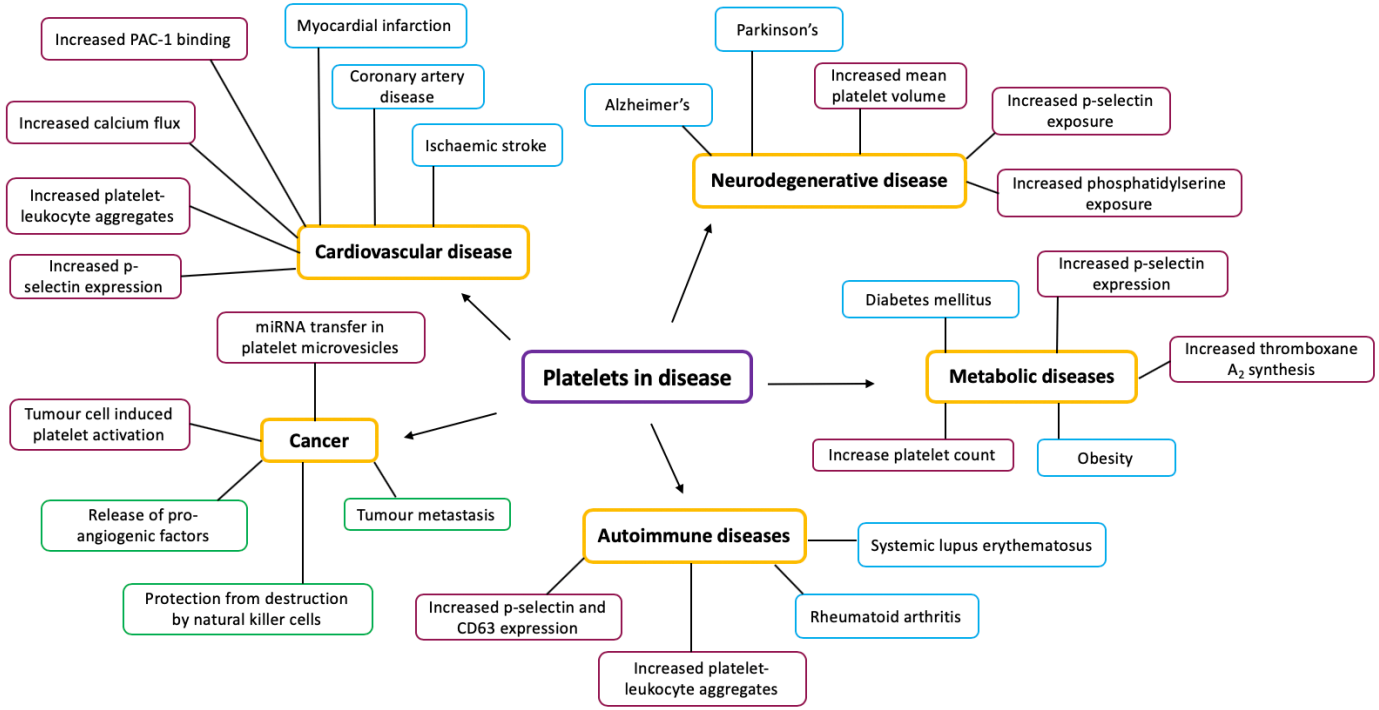

Figure 1.10 Overview of alterations in platelet function in different pathological states

Platelet function is altered in a number of pathological conditions and can drive disease progression. This diagram indicates diseases associated with changes in platelet function (blue boxes), reported alterations in platelet function (pink boxes) and functions that platelets facilitate and so aid disease progression (green boxes).[206,207]

2 Materials

2.1 Reagents

Product	Company
0.2µm filters	VWR, UK
24 well plate - Falcon™ Polystyrene Microplates	Thermo Fisher Scientific, UK
96-well flat-bottomed sterile plates	VWR, UK
96-well half-area microtitre plate	Thermo Fisher Scientific, UK
96-well round-bottomed sterile plates	VWR, UK
Acetylsalicylic acid	Sigma-Aldrich, UK
Annexin V APC	Biolegend, UK
Annexin V binding buffer	Biolegend, UK
Anti-human CD11b Brilliant Violet 421™	Biolegend, UK
Anti-human CD192 Brilliant Violet 421™	Biolegend, UK
Anti-human CD42b Brilliant Violet 421™	Biolegend, UK
Anti-Human CD45 PerCP-Cyanine5.5	Life Technologies, UK
Anti-Human CD61-APC	Life Technologies, UK
Anti-Human CD61-FITC	Life Technologies, UK
Anti-Human CD62-P APC	Biolegend, UK
Anti-human CD62L Brilliant Violet 421™	Biolegend, UK
Anti-human CD66b Pacific Blue™	Biolegend, UK
Anti-human CXCR2 Pacific Blue™	Biolegend, UK
Anti-mouse Alexa Fluor 488	Invitrogen, UK
Anti-mouse Alexa Fluor 555	Invitrogen, UK
Anti-mouse Alexa Fluor 647	Invitrogen, UK
Apyrase	Sigma-Aldrich, UK
AR-C 66096 tetrasodium salt	BioTechne, UK
Bovine serum albumin	Sigma-Aldrich, UK
Calbryte 630™	Stratech, UK
Calcium chloride	Sigma-Aldrich, UK
CD45 XP® Rabbit mAb	Abcam, UK
Cell Trace™ Violet Cell proliferation Kit	Life Technologies, UK
cOmplete™ Mini Protease Inhibitor Cocktail Tablet	Sigma-Aldrich, UK
Corning® Cell-Tak™ Cell and Tissue Adhesive	VWR, UK
D-Glucose	Sigma-Aldrich, UK
Dextran	VWR, UK
Dimethyl sulfoxide (DMSO)	VWR, UK
Donkey serum	Sigma-Aldrich, UK

Dulbecco's Phosphate Buffered Saline	Sigma-Aldrich, UK
Eptifibatide acetate	Sigma-Aldrich, UK
Ethanol	VWR, UK
Fluo-4 AM	Invitrogen, UK
Formalin	Sigma-Aldrich, UK
Hanks Buffered Salt Solution	Sigma-Aldrich, UK
Haemocytometer	VWR, UK
HEPES	Sigma-Aldrich, UK
Histopaque 1077	Sigma-Aldrich, UK
Horm Collagen	Takeda, Austria
Hydrochloric acid	Sigma-Aldrich, UK
Image-iT™ TMRM Reagent	Thermo Fisher Scientific, UK
Ionomycin	Life Technologies, UK
Isotonic glucose	Takeda, Austria
Magnesium chloride	Sigma-Aldrich, UK
Methanol	VWR, UK
MitoProbe™ DiIC1(5)	Invitrogen, UK
MitoTracker Orange CMTMRos	Life Technologies, UK
Mouse anti-TOM20	Santa Cruz, USA
Mouse anti-α-tubulin	Sigma-Aldrich, UK
Paraformaldehyde	VWR, UK
Phalloidin Alexa Fluor 488	Thermo Fisher Scientific, UK
Phalloidin Alexa Fluor 647	Thermo Fisher Scientific, UK
Phosphate buffered saline	Sigma-Aldrich, UK
Poly-l-lysine coverslips	VWR, UK
Potassium chloride	Sigma-Aldrich, UK
ProLong diamond antifade mount	Thermo Fisher Scientific, UK
Prostacyclin	BioTechne, UK
Prostaglandin E1	Sigma-Aldrich, UK
Rabbit anti-C4	Abcam, UK
Rabbit anti-ErP57	Abcam, UK
Rabbit anti-fibrinogen	Thermo Fisher Scientific, UK
Seahorse XF 1.0 M Glucose Solution	Agilent, USA
Seahorse XF 100 mM Pyruvate Solution	Agilent, USA
Seahorse XF 200 mM Glutamine Solution	Agilent, USA
Seahorse XF Base Medium	Agilent, USA
Seahorse XF Cell Mito Stress Test Kit	Agilent, USA
Seahorse XF24 FluxPak	Agilent, USA
Sodium bicarbonate	Sigma-Aldrich, UK
Sodium chloride	Sigma-Aldrich, UK

Sodium Dodecyl Sulfate	Sigma-Aldrich, UK
Sodium hydroxide	Sigma-Aldrich, UK
Sodium phosphate dibasic	Sigma-Aldrich, UK
Superfrost slides	VWR, UK
Thiazole Orange	Sigma-Aldrich, UK
TRAP-6 amide	Bachem, UK
Trisodium Citrate	Sigma-Aldrich, UK
Triton X-100	Sigma-Aldrich, UK
Trizma	Sigma-Aldrich, UK
Trypan Blue Solution, 0.4%	Thermo Fisher Scientific, UK
U46619	Enzo Life Sciences, UK
µ-Slide 8 Well Glass Bottom	IBIDI, UK

2.2 Equipment

Product	**Company**
BD FACS Aria III Fusion Cell Sorter	BD Bioscience, UK
BD LSRII	BD Bioscience, UK
Bio/Data PAP-8E aggregometer	Alpha Laboratories, UK
Bioshake plate IQ shaker	Quantifoil, Germany
Centrifuge 5247 R	Eppendorf, Germany
Heraeus Megafuge 16	Thermo Scientific, UK
Image stream^X MKII	Amnis, USA
LSM880 Confocal Microscope with airyscan	Zeiss, Germany
Nanodrop Spectrophotometer ND-1000	Thermo Scientific, UK
NanoSight NS300	NanoSight UK
pH meter PH1100L	VWR, UK
Seahorse XF24 Analyser	Agilent, USA
Tecan Sunrise plate reader	Tecan, Switzerland
Transsonic T310	CamLab, UK
Vortex Genie	VWR, UK

2.3 Software

Product	Company
FACSDiva acquisition software	BD Bioscience, UK
FlowJo Software v.8	TreeStar Inc, USA
GraphPad Prism version 8	GraphPad Inc, USA
IDEAS software	Amnis, USA
ImageJ software	NIH, USA
Ingenuity pathway analysis	Qiagen, USA
Nano Tracking Analysis (NTA2.1) software	NanoSight UK
Perseus	Max Plank Institute, Germany
STRING	STRING Consortium, Switzerland
Zen Software 2.3 SP1	Zeiss, Germany

3 Investigating platelet activation dynamics

3.1 Introduction

Platelet activation is a highly regulated process initiated by the binding of an agonist to its receptor on the platelet surface, proceeding in a largely sequential manner. This initial interaction stimulates intracellular signalling pathways, facilitating increases in intracellular calcium, cytoskeletal rearrangement, and proceeds through to the fusion of granules with the plasma membrane and the release of secondary mediators.[86] The successive nature of these events, allows for a rapid response needed to maintain haemostasis and prevent blood loss.[85]

Recent evidence has indicated that platelets are highly metabolically active cells even under basal conditions.[116] To control this balance and maintain platelets in a quiescent state, ion transporters are crucial to sequester cations into intracellular stores as well as causing the efflux into the extracellular milieu. These ion channels carry a high energy demand, requiring ATP to be fully functional, thus contributing to the high metabolic profile under basal conditions.[116] Furthermore, the processes of platelet activation and subsequent thrombus formation are highly energy dependent. Interestingly, platelets have been described as being metabolically flexible, being able to switch readily between glycolysis and oxidative phosphorylation.[115,208] Further, research has highlighted that these processes can act as compensatory mechanisms, as complete inhibition of platelet activation is achieved only when both pathways are inhibited.[209]

As well as its essential need for haemostasis, platelet activation and aggregation is also a key contributor to pathological thrombosis.[210–212] As such, therapeutics targeting platelet activation have been developed as treatment for the primary and secondary prevention of myocardial infarction and stroke.[213] As platelets have a myriad of activation pathways, a number of classes of anti-platelet drugs have been developed. Aspirin, the most commonly prescribed anti-platelet therapy, exerts its anti-platelet effects by acetylating serine530 on the cyclooxygenase-1, thereby

inhibiting its enzymatic activity and preventing the conversion of arachidonic acid into prostaglandin H_2 and subsequently thromboxane A_2.[110,214] Low dose aspirin reduces *ex vivo* platelet aggregation in response to arachidonic acid and low concentrations of collagen and its use is associated with a 25% reduction in recurrent thrombotic events. Some evidence suggests that in addition to inhibiting the formation of thromboxane A_2, aspirin reduces granule secretion, as measured by P-selectin and CD63 expression.[215,216]

A second class of anti-platelet drug, the thienopyridines, are often used in combination with aspirin, as a dual anti-platelet treatment.[217] These dugs exert their anti-platelet effect by inhibiting the $P2Y_{12}$ receptors which mediate ADP-induced platelet aggregation.[95,96,218] ADP, secreted from dense granules, is a weak platelet agonist involved in the secondary wave of aggregation, supporting the activation and subsequent binding of the fibrinogen receptor, GPIIb-IIIa. Thus, blockade of $P2Y_{12}$ receptors by therapeutics such as clopidogrel, ticagrelor and prasugrel, will affect the secondary wave of aggregation important for the potentiation of the aggregation response.[217]

Broadly speaking, platelet function can be assessed in two different ways; either an end point assay, measuring the expression of activation markers or aggregation after a defined period, or an assay measuring the dynamics of the response.[219] Whilst the first of these offers more flexibility in terms of the number of samples assessed simultaneously, it provides no information on the kinetics and dynamics of the response. Thus, in this chapter I will explore the dynamics of calcium flux and P-selectin exposure in platelets. Furthermore, I will investigate alterations in mitochondrial membrane potential ($\Delta\Psi m$) and mitochondrial respiratory capacity following stimulation. Finally, I will examine the effect of anti-platelet treatment on platelet activation pathways and mitochondrial function.

3.2 Methods

3.2.1 Blood collection

Blood was obtained from pre-screened healthy volunteers by venepuncture using a 19-gauge butterfly needle. Screening included the measurement of heart rate, blood pressure and body temperature. Exclusion criteria included smoking, >40 years of age and regular use of medication known to influence platelet function. All volunteers had abstained from taking any non-steroidal anti-inflammatory medication for at least 14 days prior to donation. Blood was drawn into 50ml syringes containing 3.2% trisodium citrate to achieve a final ratio of 1:9 anti-coagulant to blood. The procedure was approved by NHS St. Thomas' Hospital Research Ethics Committee (reference 07/Q0702/24).

3.2.2 Preparation of platelet rich plasma (PRP)

Citrated whole blood was transferred to 15ml Falcon tubes and centrifuged at 175 x g for 15 minutes at room temperature with a slow acceleration and deceleration to prevent white and red blood cell contamination. The straw-coloured plasma layer was transferred into a clean tube. The platelets were allowed to rest for approximately 30 minutes before beginning experiments.

3.2.3 Preparation of washed platelets

Isolated PRP was centrifuged at 1000 x g for 10 minutes in the presence of prostacyclin (PGI_2; 2µM) and apyrase (0.02 U/ml) to produce a platelet pellet. The pellet was resuspended in modified Tyrode's HEPES buffer supplemented with glucose (0.1% w/v) and apyrase (0.02U/ml), and subsequently centrifuged at 1000 x g for 10 minutes with the addition of PGI_2 (2µM). The supernatant was removed, and the pellet was resuspended in modified Tyrode's HEPES buffer to produce a pure platelet sample. The platelet count was adjusted to 3 x 10^8/ml, the suspension allowed to rest for 30 minutes and subsequently supplemented with calcium chloride ($CaCl_2$; 2mM).

3.2.4 Assessing calcium flux in washed platelets

Washed platelets were prepared and diluted to a concentration of 3 x 10^8/ml. Prior to the addition of $CaCl_2$, platelets were stained with Fluo-4 AM (2µM) for 45 minutes at 37˚C in the dark, followed by CD61-APC (1:100) for a further 15 minutes. The stained washed platelet sample was then diluted 1 in 10 with modified Tyrode's HEPES buffer and recalcified with 2mM $CaCl_2$. Calcium dynamics were measured over a 210 second period. Firstly, baseline Fluo-4 AM fluorescence was recorded for 30 seconds, followed by challenge with phosphate buffered saline (PBS), Thrombin Receptor Activator for Peptide 6 (TRAP-6; 25µM), or ionomycin (10µM) and subsequently recorded for a further 3 minutes. Samples were acquired on a BD LSRII flow cytometer using FACSDiva acquisition software and analysed using FlowJo v.8 software.

3.2.5 Assessing P-selectin expression in washed platelets

Washed platelets were prepared as described above, diluted to a concentration of 3 x 10^8/ml and supplemented with $CaCl_2$ (2mM). The rested washed platelet sample was stained with CD61-FITC (1:100) and CD62P-APC (1:100) for 20 minutes in the dark, and subsequently diluted 1 in 10 with modified Tyrode's HEPES buffer.

P-selectin expression dynamics were measured using a BD LSRII flow cytometer. Briefly, basal P-selectin expression was measured (CD62P-APC fluorescence) over 30 seconds to establish a baseline, followed by stimulation with PBS or TRAP-6 (25µM) for a further 180 seconds. Following acquisition, analysis was conducted was FlowJo v.8.

3.2.6 Assessing mitochondrial membrane potential

Washed platelets were prepared and diluted to a concentration of 3 x 10^8/ml supplemented with $CaCl_2$ (2mM). The washed platelet sample was stained with CD61-APC (1:100) and TMRM (Tetramethylrhodamine, Methyl Ester; 10nm) for 20 minutes in the dark, and subsequently diluted 1 in 10 with modified Tyrode's HEPES buffer.

Alterations in mitochondrial membrane potential ($\Delta\Psi m$) were measured using a BD LSRII flow cytometer; baseline TMRM fluorescence was established over 30 seconds, followed by addition of PBS or TRAP-6 (25µM) and recording for a further 180 seconds. Data analysis was conducted using FlowJo v.8.

3.2.7 Seahorse: Oxygen Consumption Rate

To understand platelet metabolism, the Agilent Seahorse XF24 was used to measure oxygen consumption rate under basal conditions and following stimulation. The XF24 calibration plate was loaded with 500µl of XF Calibrant Fluid and placed along with the Seahorse cartridge in the XF 37°C incubator with 0% CO_2 overnight.

XF24 cell cultures plates were coated with Cell Tak as per the manufacturer's guidelines. Briefly, 50µl of 2.4µg/ml Cell Tak was added to each well and incubated at room temperature for 20 minutes. The plates were then washed with sterile dH_2O and allowed to air dry.

Washed platelets were prepared as previously described and diluted to a concentration of 6 x 10^8/ml in Seahorse Base Medium supplemented with glutamine (2mM), glucose (25mM) and pyruvate (1mM) and allowed to rest for 30 minutes. Subsequently, 100µl of the 6 x 10^8/ml platelet sample was added to each well of the Cell Tak coated plate; achieving a final platelet concentration of 6 x 10^7 per well, leaving four empty wells as blanks. The plate was then spun for 20 seconds at 200 x g, the plate was rotated 180° and spun for a further 20 seconds to encourage the platelets to adhere. To the blank wells, 100µl of base medium was added. The plate was then transferred to the 37°C incubator with 0% CO_2 for 15 minutes. Afterward, 400µl of warmed Seahorse Base Medium (containing 2mM glutamine, 25mM glucose and 1mM pyruvate) supplemented with $CaCl_2$ (2mM) was added and the plate returned to the incubator for a further 30 minutes.

The Agilent XF MitoStress kit was used to assess mitochondrial function. Reagents were prepared according to the manufacturer's guidelines achieving a final concentration of 1µM Oligomycin, 0.7µM FCCP (Carbonyl cyanide-*4*-(trifluoromethoxy) phenylhydrazone), 0.5µM Rotenone and Antimycin A, and subsequently loaded into the appropriate wells in the XF cartridge (Figure 3.1).

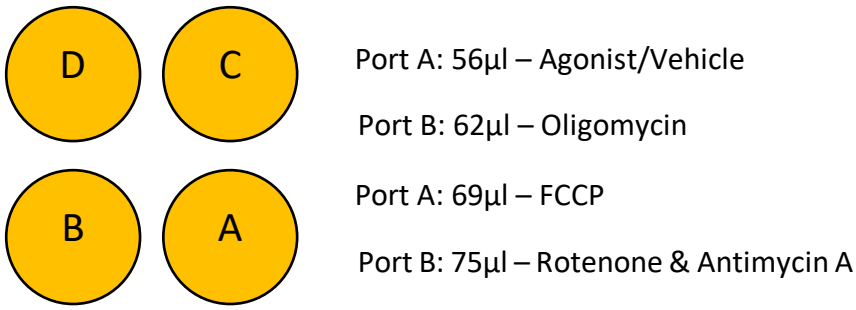

Figure 3.1 Injection port layout for the XF24 Seahorse cartridge

Orientation of the injection ports for the XF24 Seahorse cartridge which are sequentially injected. Port A was loaded with 56µl of vehicle or agonist (TRAP-6 20µM). Port B was loaded with 62µl of oligomycin (10µM) to achieve a final concentration of 1µM. Port C was loaded with 69µl of FCCP (7µM) to achieve a final concentration of 0.7µM and Port D was loaded with 75µl of rotenone and antimycin A (5µM) to achieve a final concentration of 0.5µM.

The calibrant plate and cartridge were placed in the XF24 Seahorse Analyser and the protocol shown in Figure 3.2 was initiated. After the initial calibration phase of the protocol, the calibrant plate was ejected and the plate containing the platelets was inserted.

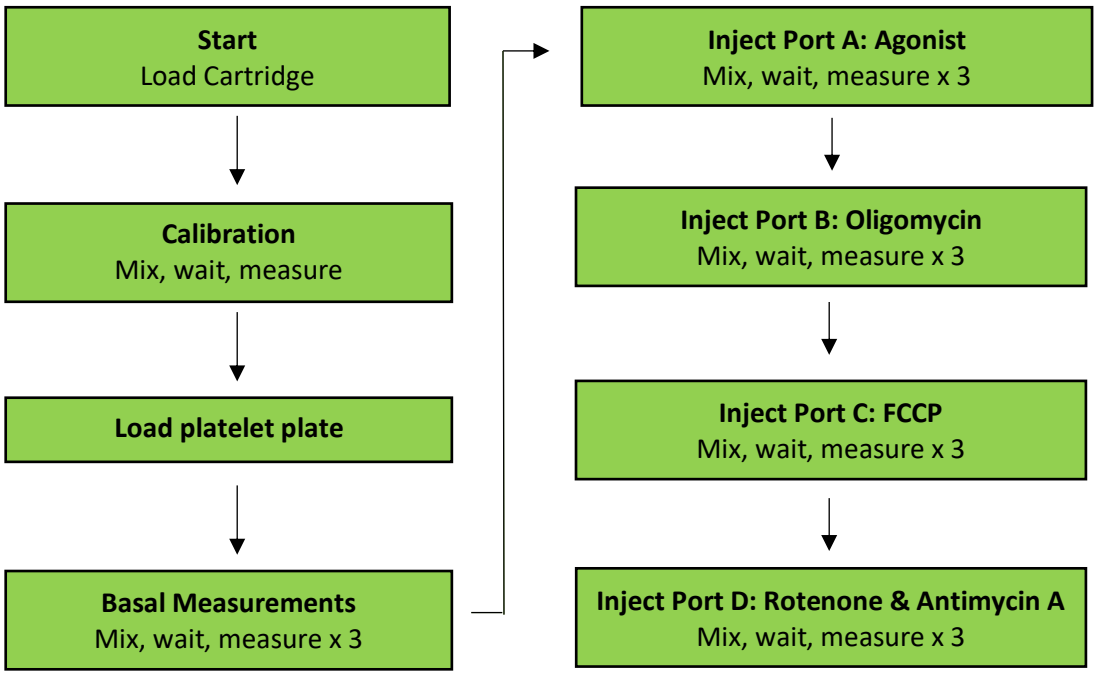

Figure 3.2 Agilent Seahorse running protocol

MitoStress Seahorse injection port protocol. The sequential injection of the four ports (A-D) allows the measurement of oxygen consumption rate following exposure to agonist or vehicle (Port A), and subsequently following the inhibition of individual complexes of the electron transport chain; Port B – injection of oligomycin inhibits ATP synthase; Port C – injection of FCCP inhibits complex IV; Port D – injection of rotenone and antimycin A inhibit complex I and III.

The Seahorse analyser measures the oxygen consumption rate over 95 minutes, producing a characteristic trace indicated in Figure 3.3. The injection of oligomycin, inhibits ATP synthase, causing a reduction in oxygen consumption. The subsequent injection of FCCP inhibits Complex IV, causes the uncoupling of the electron transport chain and subsequent increase in oxygen consumption. Finally, the dual injection of rotenone and antimycin A inhibits Complex I and III, thereby completely shuts down the electron transport chain and causes a reduction in oxygen consumption.

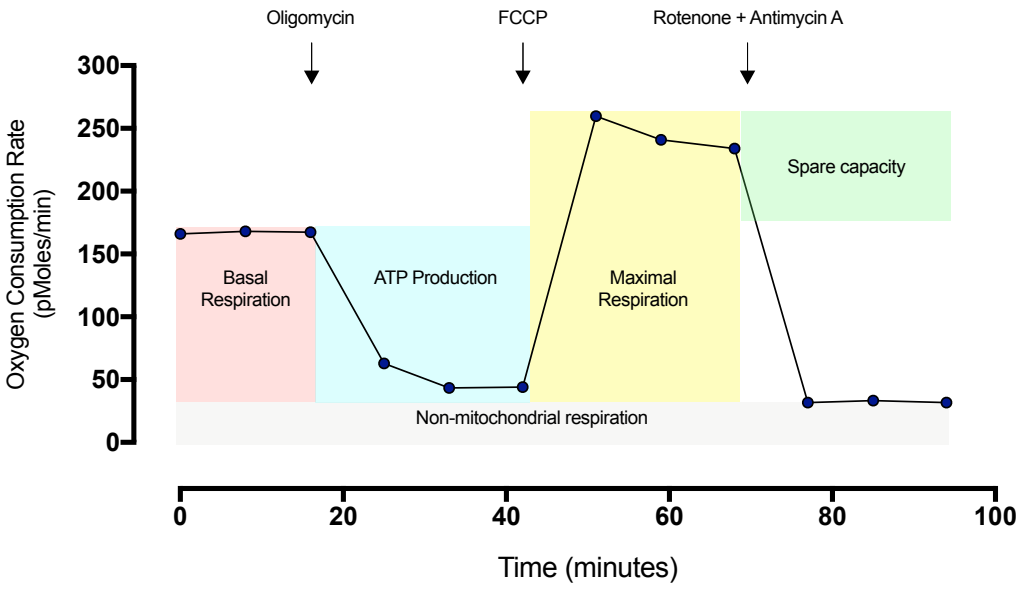

Figure 3.3 Representative trace diagram for XF Seahorse MitoStress test

The MitoStress test is measured based on the oxygen consumption rate following the injection of inhibitors of the electron transport chain to assess a number of parameters including basal respiration, ATP production, maximal respiration and spare reserve capacity. The arrows indicate the injection of oligomycin which inhibits ATP synthase, therefore preventing ATP generation; FCCP inhibits Complex IV of the electron transport chain causing mitochondrial uncoupling, allowing the measurement of maximal respiration; rotenone and antimycin A inhibit Complex I and III respectively, and cause the complete inhibition of the oxidative phosphorylation machinery.

3.2.8 Anti-platelet treatment of washed platelets

The effects of anti-platelet drugs on platelet activation, calcium flux and P-selectin expression, as well as mitochondrial function including mitochondrial membrane potential and respiratory capacity were assessed.

Briefly, washed platelets were prepared at 3 x 10^8/ml as previously described in 3.2.3. Following resting of the samples for 30 minutes, the platelets were treated with aspirin (30µM), AR-C66096 (1µM) or vehicle for 30 minutes at 37°C. Samples were then processed following the protocols detailed in sections 3.2.4-3.2.7

3.2.9 Statistical analysis

Graphs and statistical analysis were generated using GraphPad Prism v.8. Data were expressed as mean±SEM and all statistics were generated using a paired students t-test or a one-way ANOVA, with Dunnett's multiple comparisons test. Significance was defined as $p<0.05$.

3.3 Results

3.3.1 Platelet activation causes a rapid increase intracellular calcium

Calcium flux is integral to platelet activation and is a convergent point in all platelet activation pathways. Given that activation signals vary in strength and activate different intracellular signalling cascades, it is predictable that the calcium flux will vary amongst different pathways. Following exposure to PBS, Fluo-4 fluorescence remained relatively stable indicating no fluctuations in intracellular calcium over the 3-minute recording period (Figure 3.4A-C, G). The addition of the thromboxane A_2 mimetic, U46619, caused an increase in intracellular calcium which was sustained above baseline for the recording period (Figure 3.4A, B, D and H). Stimulation with the stronger agonist, TRAP-6, induced a more rapid increase in intracellular calcium, reaching its peak fluorescence at 20 seconds post stimulation, compared to 40 seconds post U46619 stimulation. Furthermore, the intracellular calcium signal was maintained at a higher level when stimulated with TRAP-6 compared to U46619 (Figure 3.4A, B, E and I). As expected, the addition of the calcium ionophore, ionomycin, caused a rapid and substantial rise in intracellular calcium levels, reaching a peak 20 seconds after addition (Figure 3.4A, B, F and J). Further, the percentage of platelets positive for Fluo-4 fluorescence at the end of the 3-minute recording, was significantly higher following stimulation with ionomycin (PBS, 1.1±0.1; U46619, 6.1±1.3; TRAP-6, 18.1±3.7; ionomycin, 71.7±1.8; $p<0.01$ for ionomycin vs. PBS, U46619 and TRAP-6; Figure 3.4G-J).

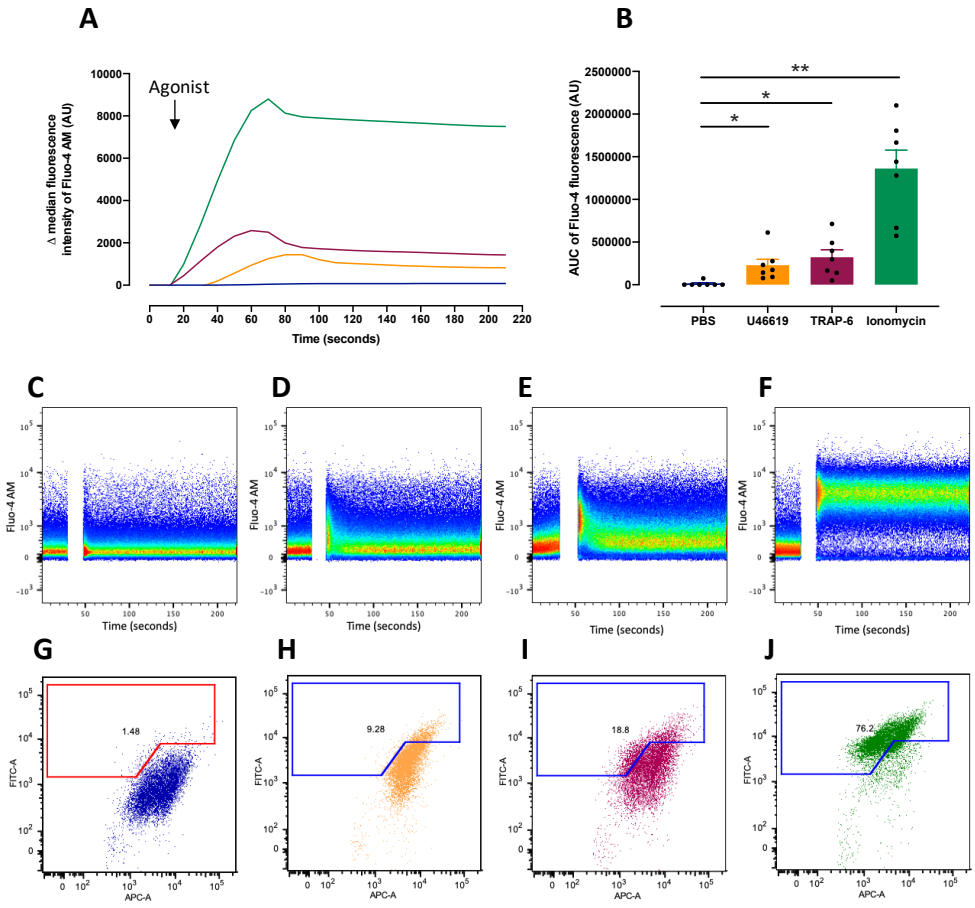

Figure 3.4: Measurement of calcium flux during platelet activation

A. Representative calcium (Fluo-4) dynamic traces following incubation of platelets with PBS (blue), U46619 (orange), TRAP-6 (magenta) and ionomycin (green). **B.** Quantification of area under the curve of Fluo-4 fluorescence following incubation with PBS, U46619, TRAP-6 and ionomycin. Representative density plot of Fluo-4 fluorescence over time following incubation with **C.** PBS **D.** U46619 **E.** TRAP-6 and **F.** Ionomycin. Representative dot plots showing the percentage of Fluo-4 positive platelets following incubation with **G.** PBS **H.** U46619 **I.** TRAP-6 and **J.** ionomycin after 210 seconds. Data presented as mean±SEM, significance was determined by one-way ANOVA with Dunnett's multiple comparisons (n=6, *p<0.05, **p<0.01).

3.3.2 Platelet activation causes P-selectin expression to change at a slower rate than calcium flux

Granule secretion is a key step in platelet activation, facilitating the release of soluble mediators which potentiate the activation response by causing a secondary wave of aggregation. As granule secretion occurs secondary to calcium flux, it can be predicted that the release and exposure of P-selectin from α-granules would occur at a slower rate than calcium flux. Stimulation of washed platelets with PBS caused no alteration in CD62P fluorescence, indicative that there was no change in the expression of P-selectin on the outer leaflet of the platelet membrane (Figure 3.5A-B). Stimulation with U46619, caused a weak and gradual increase in P-selectin expression over the 3-minute recording period (Figure 3.5A-B). Consistent with the calcium flux, TRAP-6 stimulation elicited a stronger and more rapid increase in P-selectin expression. Indeed, quantification of area under the curve of the P-selectin expression dynamics indicated that TRAP-6 activation provokes a response that was more than twice as strong as that triggered by U46619.

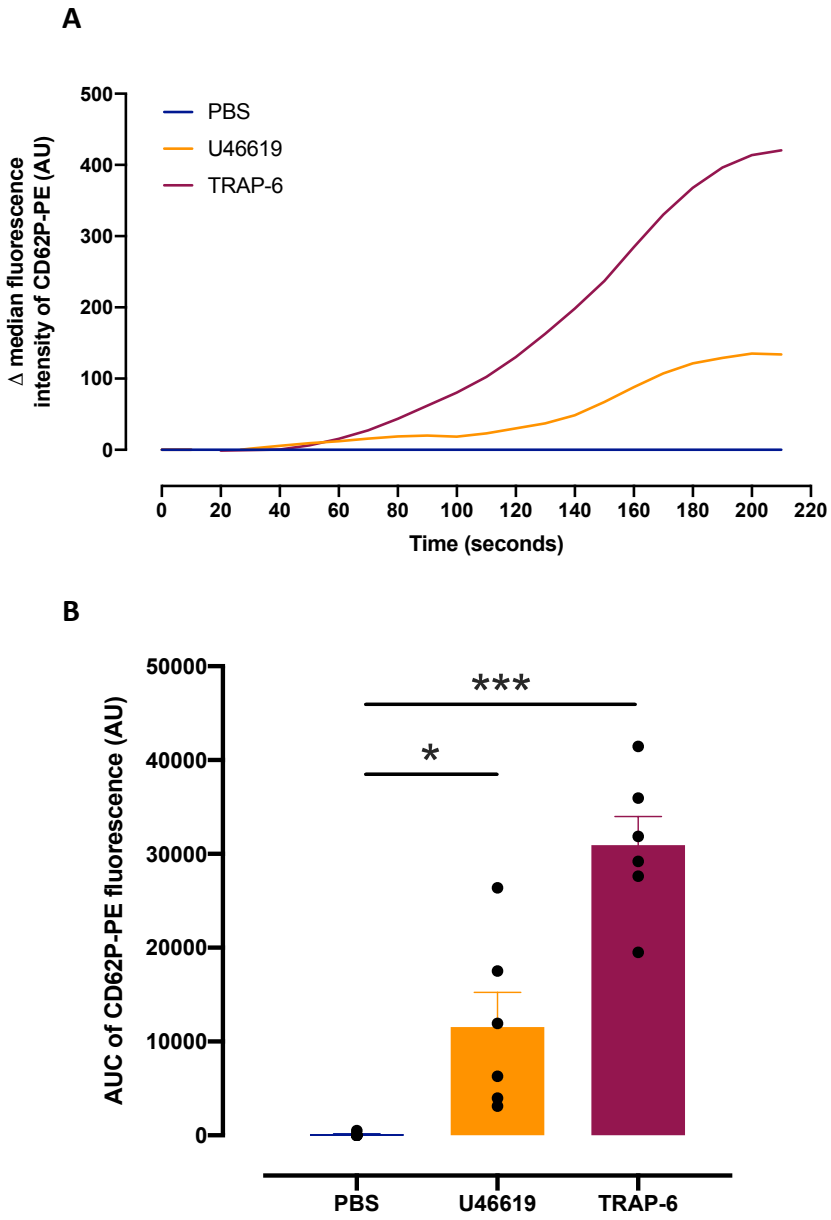

Figure 3.5: Measurement of P-selectin expression during platelet activation

A. Representative P-selectin (CD6P-PE) dynamic traces following incubation of platelets with PBS (blue), U46619 (orange) and TRAP-6 (magenta). **B.** Quantification of area under the curve of CD62P-PE fluorescence following incubation with PBS, U46619 and TRAP-6. Data presented as mean±SEM, significance was determined by one-way ANOVA with Dunnett's multiple comparisons (n=6, *<0.05, **p<0.01).

3.3.3 Platelet activation causes alterations in mitochondrial membrane potential

The effect of platelet activation on P-selectin expression and calcium flux is well documented, however the influence of platelet activators on mitochondrial membrane potential remains unknown. The transmembrane potential of the mitochondria is crucial for maintaining cellular health, regulated by the proton motive force generated during the transfer of electrons along the electron transport chain. Given its dynamic nature, mitochondrial membrane potential can become hyperpolarised or depolarised. Sustained hyper- or depolarisation can lead to deleterious effects and cause mitochondrial damage. Here I have shown that activation with U46619, caused an initial increase in TMRM fluorescence, suggesting the mitochondrial membrane has become hyperpolarised (Figure 3.6A; orange line) Interestingly, after approximately 60 seconds the TMRM fluorescence begins to reduce, returning towards baseline. After 170 seconds the membrane potential passes baseline reading, indicating that the mitochondrial membrane potential is becoming more positive. Consistent with the calcium flux and P-selectin expression, TRAP-6 caused mitochondrial membrane hyperpolarisation to a greater extent than U46619 and with a consistently greater area under the curve (Figure 3.6).

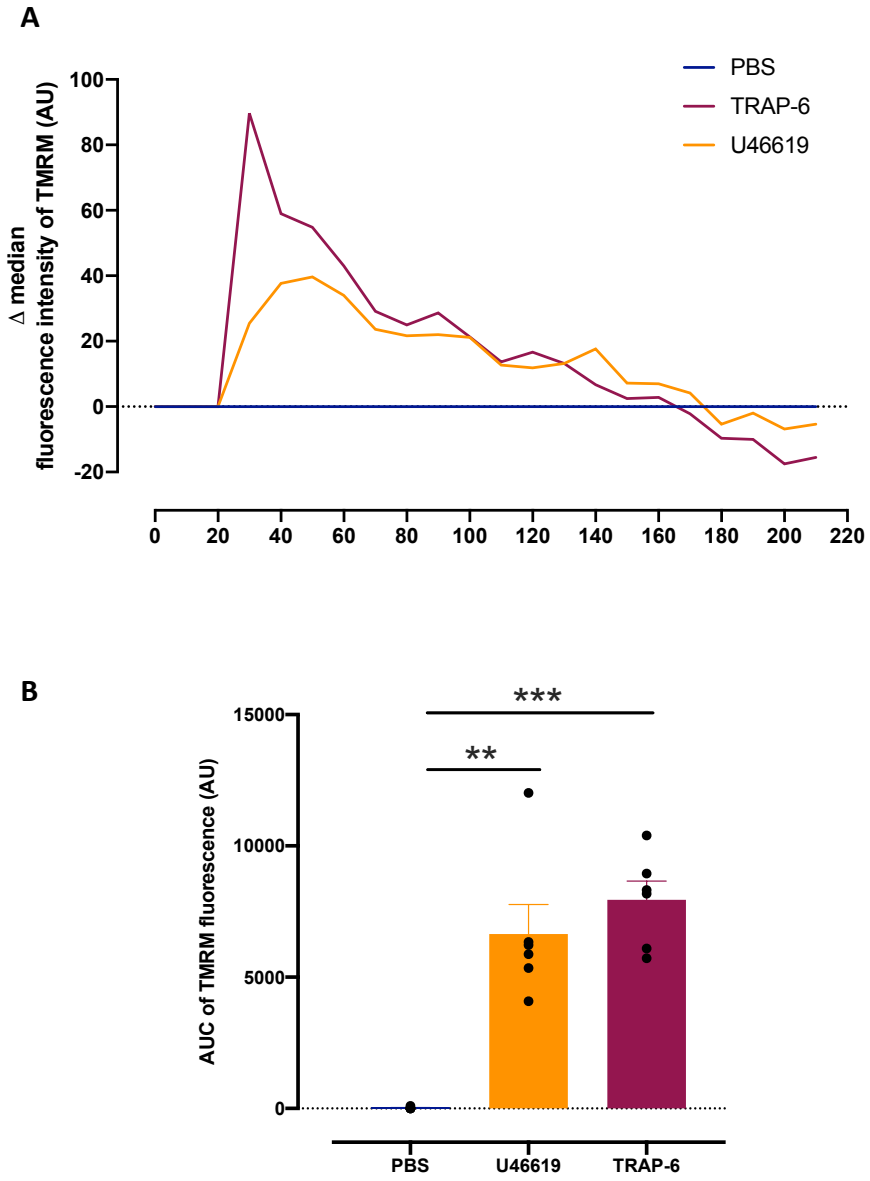

Figure 3.6: Assessment of mitochondrial membrane potential following stimulation

A. Representative change from baseline (blue) of mitochondrial membrane potential (TMRM) dynamic traces in response to U46619 (orange) and TRAP-6 (magenta). **B.** Quantification of area under the curve of TMRM fluorescence following incubation with PBS, U46619 and TRAP-6. Data presented as mean±SEM, significance was determined by one-way ANOVA with Dunnett's multiple comparisons (n=6, **p<0.01, ***<0.001).

3.3.4 Platelet activation causes an increase in mitochondrial respiration

Following on from the identification of alterations in mitochondrial membrane potential following activation raised the question as to whether this is influencing the respiratory capacity. Oxygen consumption rate, as a measure of mitochondrial activity, was assessed in washed platelets following the addition of TRAP-6 or vehicle. Using the Agilent Seahorse Analyser, I determined that under basal conditions, washed platelets (6×10^7) consume 105±5pmoles of oxygen per minute. The addition of TRAP-6 (20µM) caused a significant increase in oxygen consumption rate to 137±18pmoles/minute, which was maintained over the 15-minute recording period (Figure 3.7A-B).

After the addition of the platelet agonist or vehicle, a series of mitochondrial inhibitors were injected to assess if platelet activation influences other parameters of the respiratory chain. Injection of the ATP synthase inhibitor, oligomycin (1µM), allows for the calculation of the oxygen consumption rate coupled to ATP production. Following stimulation with TRAP-6, the oxygen consumption coupled to ATP production was significantly higher than that in the presence of vehicle (95±9pmoles/min vs. 61±8pmoles/min, $p<0.05$; Figure 3.7C). The injection of the subsequent two mitochondrial inhibitors, caused marginal but not significant changes in respiratory parameters. Indeed, maximal respiration, as assessed by FCCP (0.7µM) treatment, showed a slight increase in platelets incubated with TRAP-6 compared to vehicle (135±27pmoles/min vs. 110±18pmoles/min; Figure 3.7D). Consistent with an increased oxygen consumption rate following the addition of TRAP-6, the spare respiratory capacity was reduced compared to vehicle (-2±11pmoles/min vs. 14±10pmoles/min; Figure 3.7E). Finally, there was no significant change in the non-mitochondria respiration following exposure to TRAP-6 compared to vehicle (12±6pMoles/min vs. 8±5pMoles/min; Figure 3.7F).

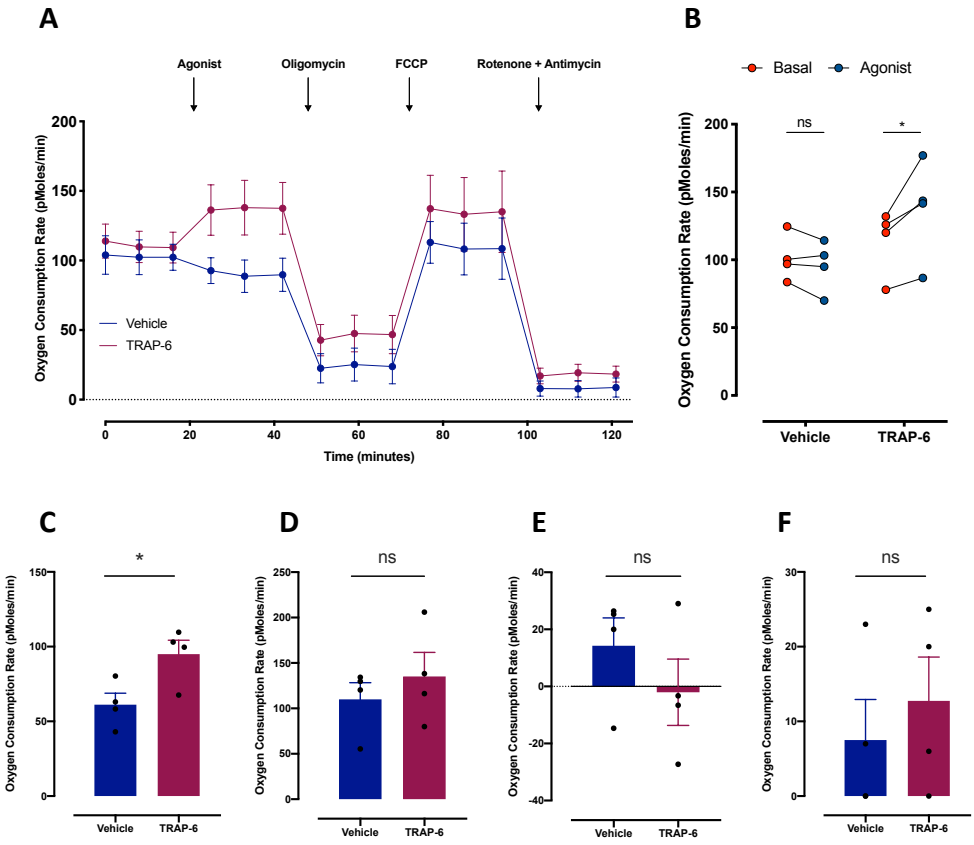

Figure 3.7: Seahorse oxygen consumption rate following physiological stimulation

A. Agilent Seahorse oxygen consumption rate trace following the addition of vehicle (blue) or TRAP-6 (magenta) and the subsequent injection of the mitochondrial inhibitors oligomycin, FCCP and rotenone and antimycin A **B.** Quantification of oxygen consumption rate under basal conditions (red) and following the addition of vehicle or TRAP-6 (blue) **C.** Quantification of oxygen consumption rate linked to ATP production, assessed by inhibition of ATP synthase with oligomycin **D.** Quantification of the maximal oxygen consumption rate assessed following uncoupling of the electron transport chain, by inhibiting complex IV following the addition of FCCP **E.** Quantification of the spare respiratory capacity calculated from the maximal respiration and agonist induced oxygen consumption **F.** Quantification of the non-mitochondrial respiration measured following the addition of rotenone and antimycin A which inhibit complex I and III, completely shutting down the electron transport chain. Data presented as mean±SEM, significance was determined by paired t-test (n=4, *p<0.05).

3.3.5 Aspirin treatment does not affect calcium flux in platelets

It is well established that aspirin causes a reduction in platelet aggregation, however the effect of this anti-platelet drug on calcium flux is less clear. As indicated in Figure 3.8, pre-treatment of platelets for 30 minutes with aspirin did not affect calcium flux following exposure to U46619 (AUC vehicle vs. aspirin, 270325±85551AU vs. 259523±133025AU; Figure 3.8B), TRAP-6 (AUC vehicle vs. aspirin, 529080±156104AU vs. 430378±16753AU; Figure 3.8D) or ionomycin (AUC vehicle vs. aspirin, 1273262±212867AU vs. 1088789±125238AU). Despite no change in the area under the curve of Fluo-4 fluorescence (Figure 3.8B, D and F), the kinetics of the U46619 response appeared altered following incubation with aspirin. As indicated in the representative trace in Figure 3.8A, platelets pre-treated with aspirin took longer to exhibit an increase in intracellular calcium which was subsequently sustained over the 3-minute recording period. On the other hand, TRAP-6 and ionomycin stimulation elicited a similar calcium dynamic trace (Figure 3.C, E).

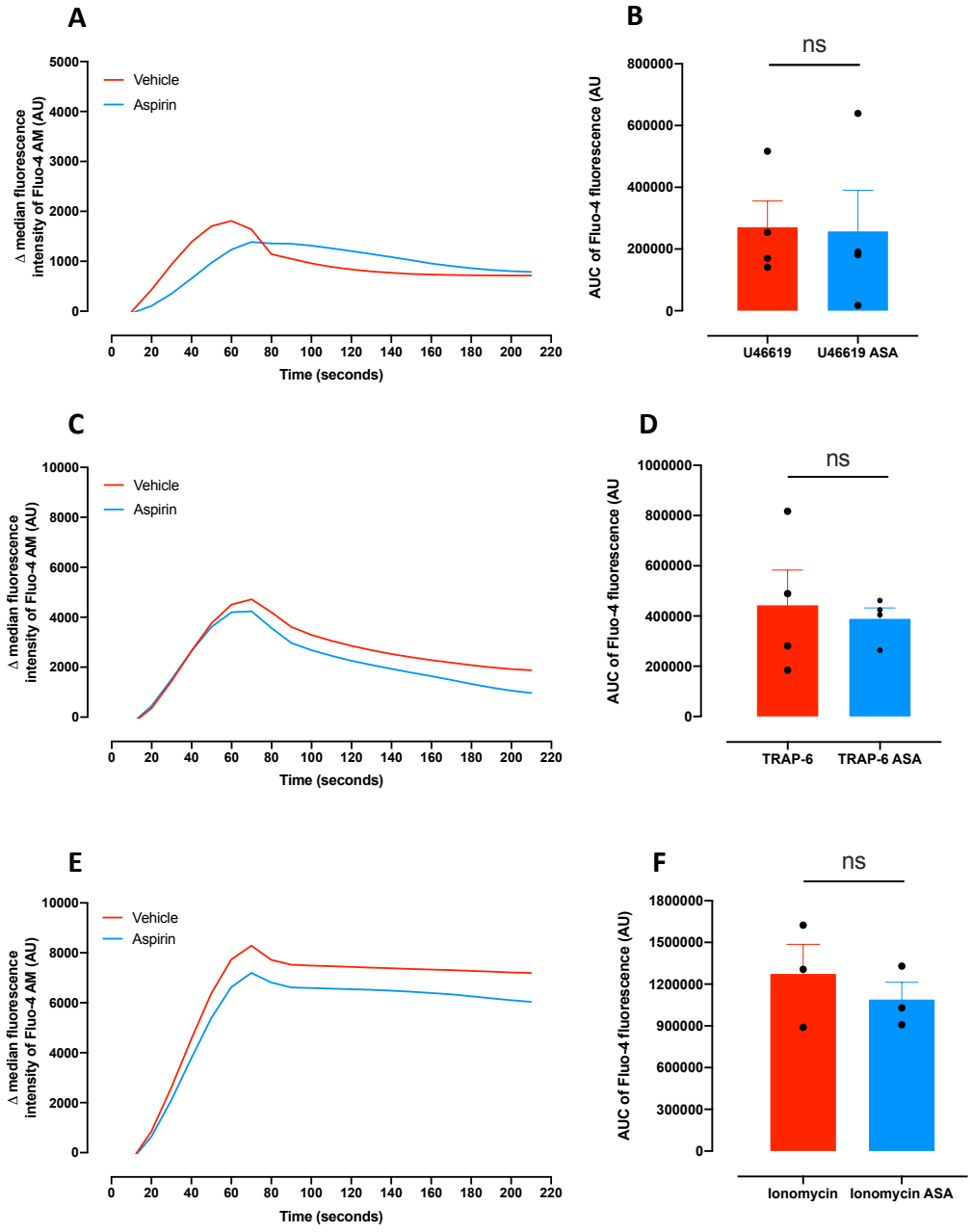

Figure 3.8: The effect of aspirin treatment on calcium flux following platelet activation

Representative calcium (Fluo-4) dynamic traces in response to **A.** U46619 **C.** TRAP-6 and **E.** ionomycin in the presence of vehicle (red) or aspirin (blue). Quantification of area under the curve of Fluo-4 fluorescence following incubation with: **B.** U46619, or aspirin (ASA) plus U46619; **D.** TRAP-6, or aspirin (ASA) plus TRAP-6; and **F.** ionomycin or aspirin (ASA) plus ionomycin. Data presented as mean±SEM, significance was determined by paired t-test (n=4)

3.3.6 Aspirin treatment reduces P-selectin exposure following stimulation of platelets with U46619

As detailed above, platelet activation is a sequential process with P-selectin exposure occurring secondary to rises in intracellular calcium. Here I have identified that treatment of platelets with aspirin caused a reduction in P-selectin expression following exposure to U46619 over a 3-minute recording period (AUC vehicle vs. aspirin, 6694±307AU vs. 4374±810AU; Figure 3.9A-B). Interestingly, this reduction in expression was not observed following incubation with the stronger agonist, TRAP-6 (AUC vehicle vs. aspirin, 20078±3250AU vs. 18233±3487AU; Figure 3.9C-D).

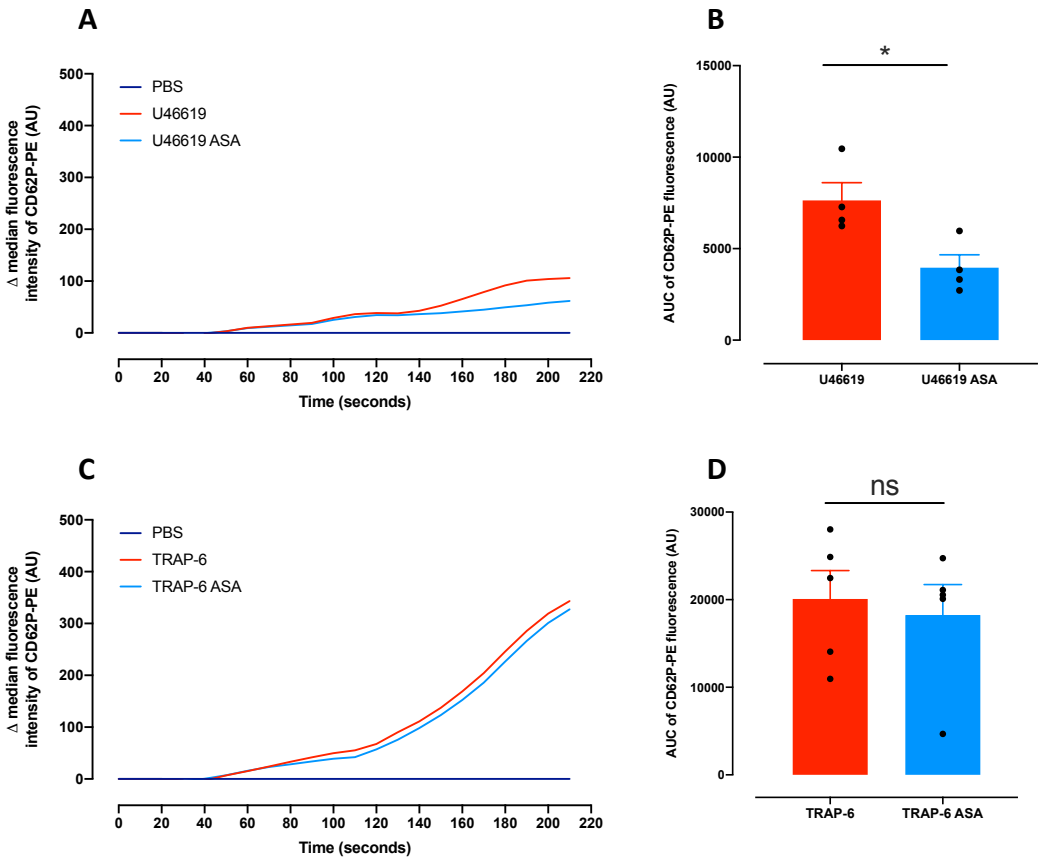

Figure 3.9: The effect of aspirin treatment on P-selectin expression following platelet activation

Representative P-selectin (CD62P) expression traces following incubation with **A.** U46619 and **C.** TRAP-6 in the presence of vehicle (red) or aspirin (blue). Quantification of area under the curve of CD62P fluorescence following incubation with: **B.** U46619, or aspirin (ASA) plus U46619; and **D.** TRAP-6, or TRAP-6 plus aspirin (ASA). Data presented as mean±SEM, significance was determined by paired t-test (n=4, *<0.05).

3.3.7 Aspirin treatment does not alter fluctuations in mitochondrial membrane potential observed following platelet activation

As I identified that platelet activation caused mitochondrial membrane hyperpolarisation, I wanted to assess the effect of aspirin treatment on mitochondrial membrane potential. Platelet stimulation with U46619 caused mitochondrial membrane hyperpolarisation to a similar extent in vehicle treated and aspirin treated platelets (AUC vehicle vs. aspirin, 3005±596AU vs. 2603±842AU; Figure 3.10A-B). Consistent with P-selectin expression and calcium flux, there was no change in mitochondrial membrane potential following TRAP-6 stimulation between vehicle-treated and aspirin-treated platelets (AUC vehicle vs. aspirin, 4053±1074AU vs. 4887±646AU; Figure 3.10C-D). Interestingly, despite no change in area under the curve, the mitochondrial membrane hyperpolarisation exhibited a more sustained response in the presence of aspirin (Figure 3.10A, C).

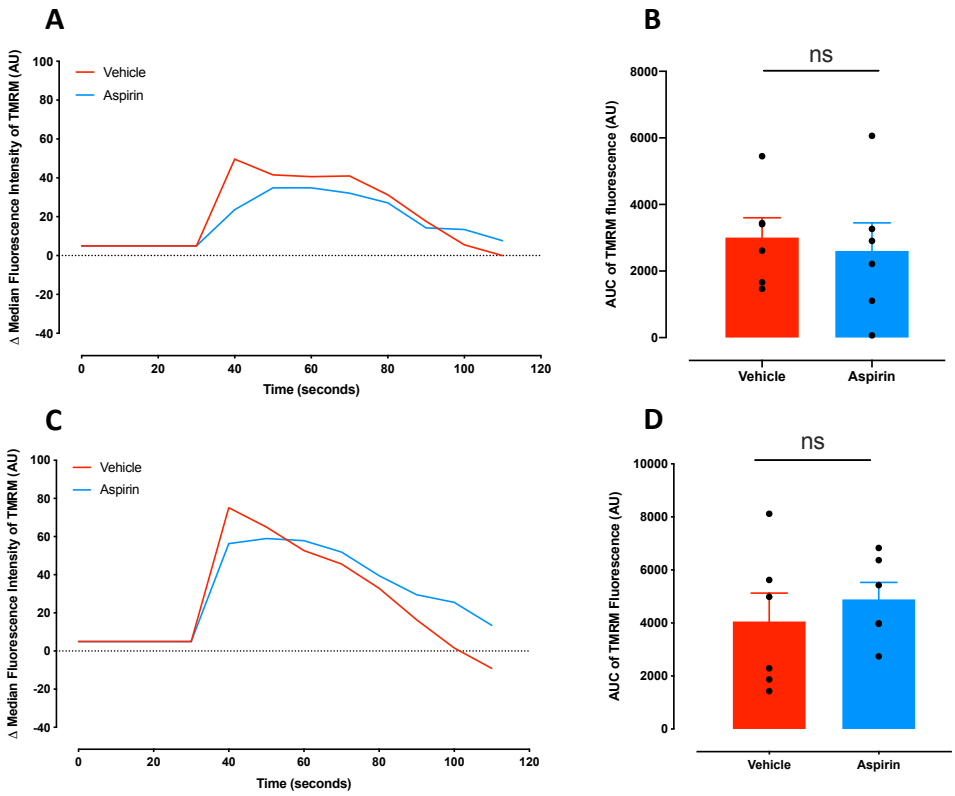

Figure 3.10: The effect of aspirin treatment on mitochondrial membrane potential following platelet activation

Representative TMRM fluorescence traces as an indicator of mitochondrial membrane potential in response to **A.** U46619 and **C.** TRAP-6 in the presence of vehicle (red) or aspirin (blue). Quantification of area under the curve of TMRM fluorescence following stimulation with: **B.** U46619, or aspirin plus U46619; and **D.** TRAP-6, or aspirin plus TRAP-6. Data presented as mean±SEM, significance was determined by paired t-test (n=6).

3.3.8 Aspirin treatment does not affect mitochondrial respiration

Consistent with no alterations in mitochondrial membrane potential, aspirin did not cause alterations in oxygen consumption rate as an indicator of mitochondrial activity (Figure 3.11A). Indeed, 30-minute pre-treatment of platelets with aspirin caused no changes in basal mitochondrial respiration (vehicle vs. aspirin, 127±46pmoles/min vs. 131±41pmoles/min; Figure 3.11B) or ATP-linked oxygen consumption (vehicle vs. aspirin, 72±15pmoles/min vs. 86±23pmoles/min; Figure 3.11C). Further, the maximal respiratory capacity was unchanged following aspirin treatment (vehicle vs. aspirin, 196±93pmoles/min vs. 218±104pmoles/min; Figure 3.11D) and thus the spare respiratory capacity remained unaltered (vehicle vs. aspirin, 69±49pmoles/min vs. 87±62pmoles/min; Figure 3.11E). Finally, aspirin treatment did not affect non-mitochondrial respiration (vehicle vs. aspirin, 66±48pmoles/min vs. 51±33pmoles/min; Figure 3.11F).

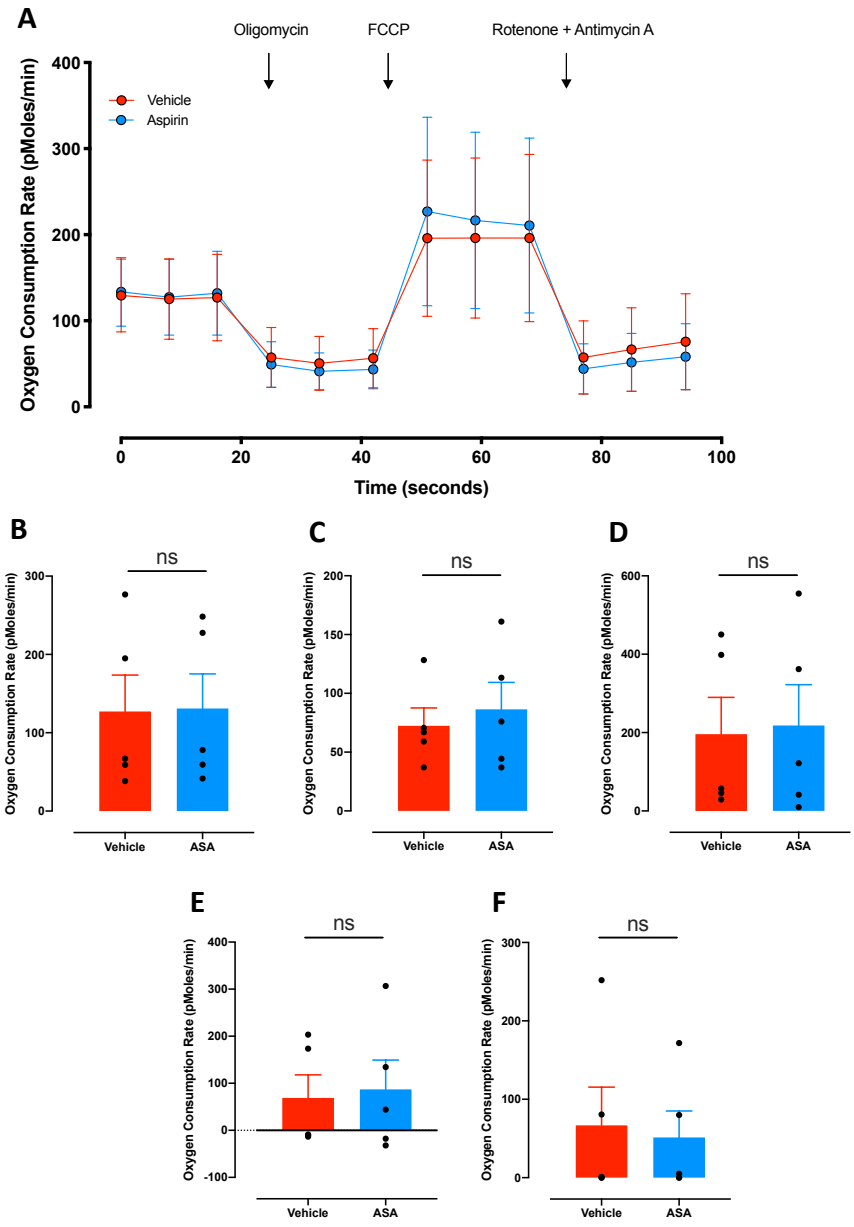

Figure 3.11: The effect of aspirin treatment on oxygen consumption rate

A. Agilent Seahorse oxygen consumption rate trace following incubation of platelets with vehicle (red) or aspirin (blue) and the subsequent injection of the mitochondrial inhibitors oligomycin, FCCP and rotenone plus antimycin **A.** Quantification of oxygen consumption rate: **B.** under basal conditions; **C.** linked to ATP production, assessed by inhibition of ATP synthase with oligomycin; **D.** maximal oxygen consumption rate; **E.** spare respiratory capacity; and **F.** non-mitochondrial respiration. Data presented as mean±SEM, significance was determined by paired t-test (n=5).

3.3.9 Inhibition of the $P2Y_{12}$ receptor causes a reduction in agonist-induced rises in intracellular calcium and P-selectin exposure in response to U46619

Aspirin is the gold-standard of antiplatelet therapies, however $P2Y_{12}$ receptor antagonists, such as prasugrel and clopidogrel, are now commonly prescribed for the secondary prevention of myocardial infarction. Given that the mode of action of this class of antiplatelet drugs differs from aspirin, I sought to identify if they have differential effects on platelet activation and mitochondrial function.

Interestingly, treatment with the $P2Y_{12}$ receptor antagonist, AR-C66096, caused a reduction in calcium flux following incubation of platelets both U46619 or TRAP-6 compared to vehicle (AUC U46619 vehicle vs. AR-C66906, 236277±7812AU vs. 160856±23164AU; AUC TRAP-6 vehicle vs. AR-C66906, 412503±23928AU vs. 242832±10444AU; Figure 3.12A-D). However, the maximal calcium flux capacity of platelets treated with AR-C66096 remained unchanged compared to vehicle (AUC ionomycin vehicle vs. AR-C66096, 1111457±84318AU vs. 1172395±86723AU).

Consistent with a reduced calcium flux, $P2Y_{12}$ inhibition caused a reduction in P-selectin expression following incubation with U46619 (AUC U46619 vehicle vs. AR-C66906, 5402±1411AU vs.1927±753AU; Figure 3.13A-B). On the other hand, $P2Y_{12}$ inhibition did not affect P-selectin expression following exposure to TRAP-6 (AUC TRAP-6 vehicle vs. AR-C66906, 34348±9878AU vs.36968±18284AU; Figure 3.13C-D).

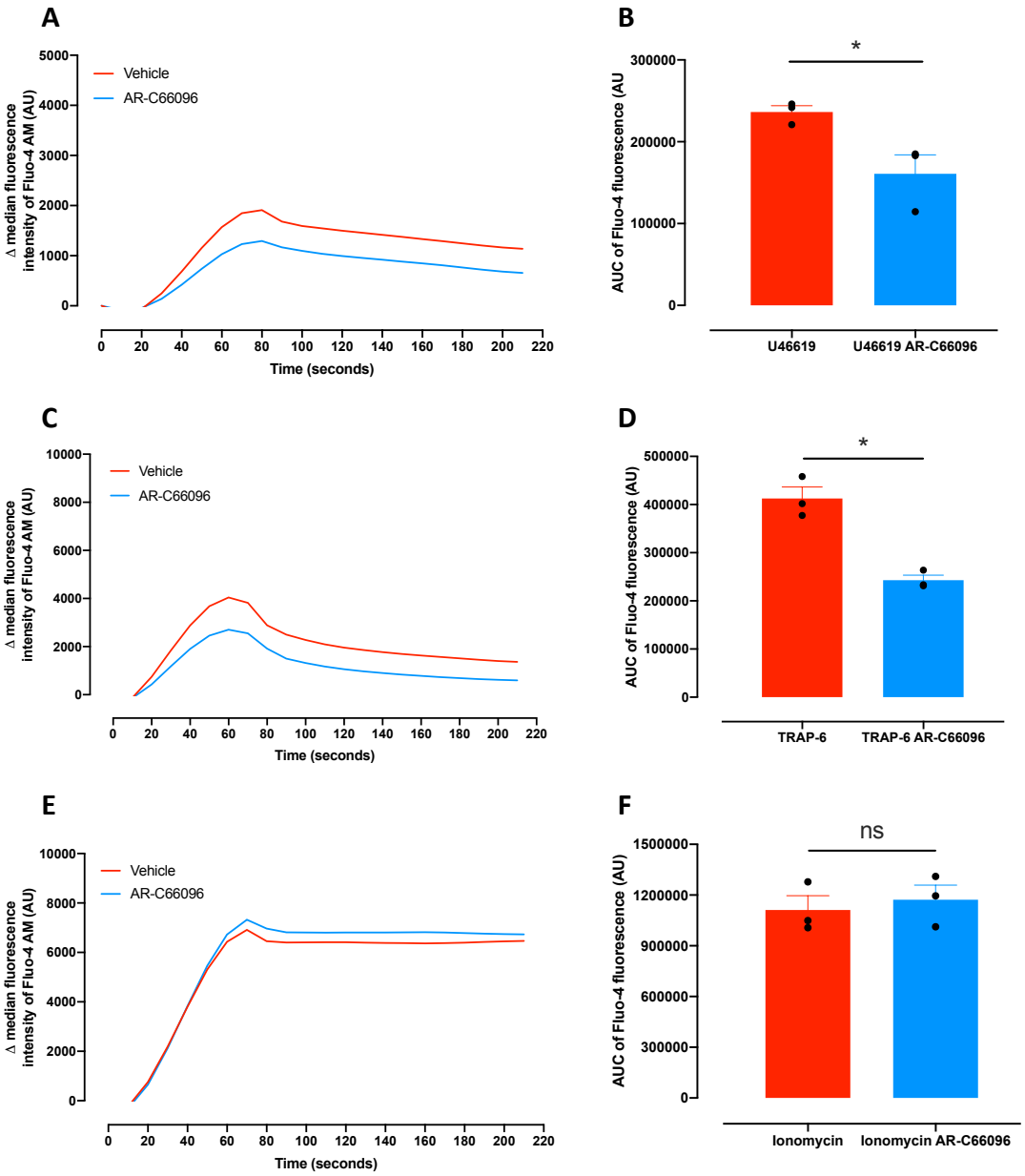

Figure 3.12: The effect of $P2Y_{12}$ inhibition on calcium flux during platelet activation

Representative calcium (Fluo-4) dynamic traces in response to **A.** U46619 **C.** TRAP-6 and **E.** ionomycin in the presence of vehicle (red) or AR-C66096 (blue). Quantification of area under the curve of Fluo-4 fluorescence following incubation with: **B.** U46619, or AR-C66096 plus U46619; **D.** TRAP-6, or AR-C66096 plus TRAP-6; and **F.** ionomycin or AR-C66096 plus ionomycin. Data presented as mean±SEM, significance was determined by paired t-test (n=3, *p<0.05).

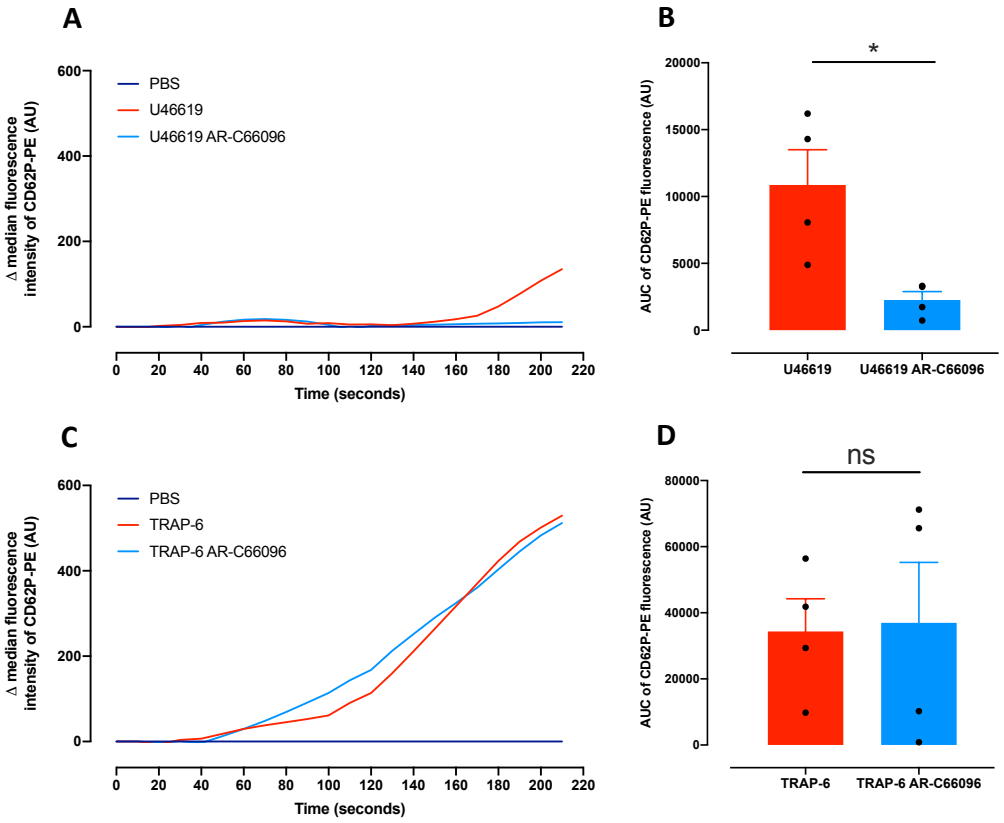

Figure 3.13: The effect of $P2Y_{12}$ inhibition on P-selectin expression

Representative P-selectin (CD62P) expression traces following exposure to **A.** U46619 and **C.** TRAP-6 in the presence of vehicle (red) or AR-C66096 (blue). Quantification of area under the curve of CD62P fluorescence following incubation with: **B.** U46619, or AR-C66096 plus U46619; **D.** TRAP-6, or AR-C66096 plus TRAP-6. Data presented as mean±SEM, significance was determined by paired t-test (n=4, *p<0.05).

3.3.10 Inhibition of the $P2Y_{12}$ receptor alters the dynamic of mitochondrial membrane hyperpolarisation following U46619 activation

As detailed above, platelet activation after incubation with both U46619 and TRAP-6, caused mitochondrial membrane hyperpolarisation. Here I have shown that $P2Y_{12}$ inhibition caused alterations in the $\Delta\Psi m$ dynamics. Interestingly, the initial rapid increase in TMRM fluorescence following U46619 stimulation, indicative of $\Delta\Psi m$ hyperpolarisation, was not observed following pre-treatment of platelets with AR-C66096. Indeed, 10 seconds after the addition of U46619, there was a significant difference in TMRM fluorescence between vehicle and AR-C66096 treated platelets (251±91AU vs. -70±45AU, respectively; $p<0.001$; Figure 3.14A). Despite this initial $\Delta\Psi m$ depolarisation, a subsequent sustained membrane hyperpolarisation equated to no significant change in the area under the curve (AUC U46619 vehicle vs. AR-C66096, 7955±4610AU vs. 3596±2732AU; Figure 3.12B). On the other hand, exposure of platelets to TRAP-6 in the presence of $P2Y_{12}$ inhibition caused $\Delta\Psi m$ hyperpolarisation to a similar extent as that seen in vehicle treated platelets (AUC TRAP-6 vehicle vs. AR-C66096, 13014±8161AU vs.12651±6345AU; Figure 3.14C-D).

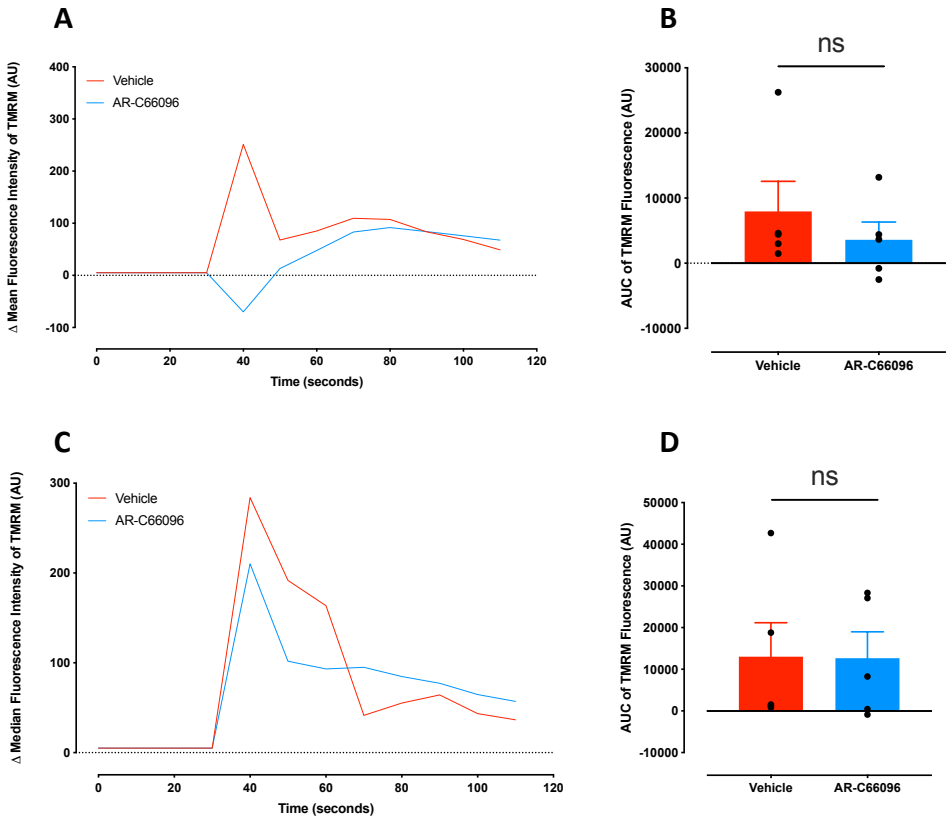

Figure 3.14: The effect of $P2Y_{12}$ inhibition on mitochondrial membrane potential

Representative TMRM fluorescence traces as an indicator of mitochondrial membrane potential in response to **A.** U46619 and **C.** TRAP-6 in the presence of vehicle (red) or AR-C66096 (blue). Quantification of area under the curve of TMRM fluorescence following stimulation with: **B.** U46619, or AR-C66096 plus U46619; and **D.** TRAP-6, or AR-C66096 plus TRAP-6. Data presented as mean±SEM, significance was determined by paired t-test (n=5).

3.3.11 Inhibition of the $P2Y_{12}$ receptor with AR-C66096 causes a reduction in mitochondrial respiration

Unlike treatment of platelets with aspirin, treatment with AR-C66096 caused a significant reduction in basal oxygen consumption rate (129±34pmoles/min vs. 72±10pmoles/min in vehicle and AR-C66096 respectively; Figure 3.15B) and subsequent reduction in ATP-linked oxygen consumption from 87±24pmoles/min in vehicle treated platelets to 36±15pmoles/min in AR-C66096 treated platelets (Figure 3.15C). Despite a marked reduction in maximal respiratory capacity following AR-C66096 treatment (Figure 3.15A), this did not reach significance; 193±70pmoles/min vs. 114±38pmoles/min for vehicle and AR-C66096, respectively (Figure 3.15D). Further, there was no significant change in the spare respiratory capacity following AR-C66096 treatment; 85±20pmoles/min vs. 57±41pmoles/min; Figure 3.15E). Likewise, there was no significant change in the non-mitochondrial respiration; 43±40pmoles/min vs. 32±20pmoles/min in vehicle and AR-C66096 treated platelets (Figure 3.15F).

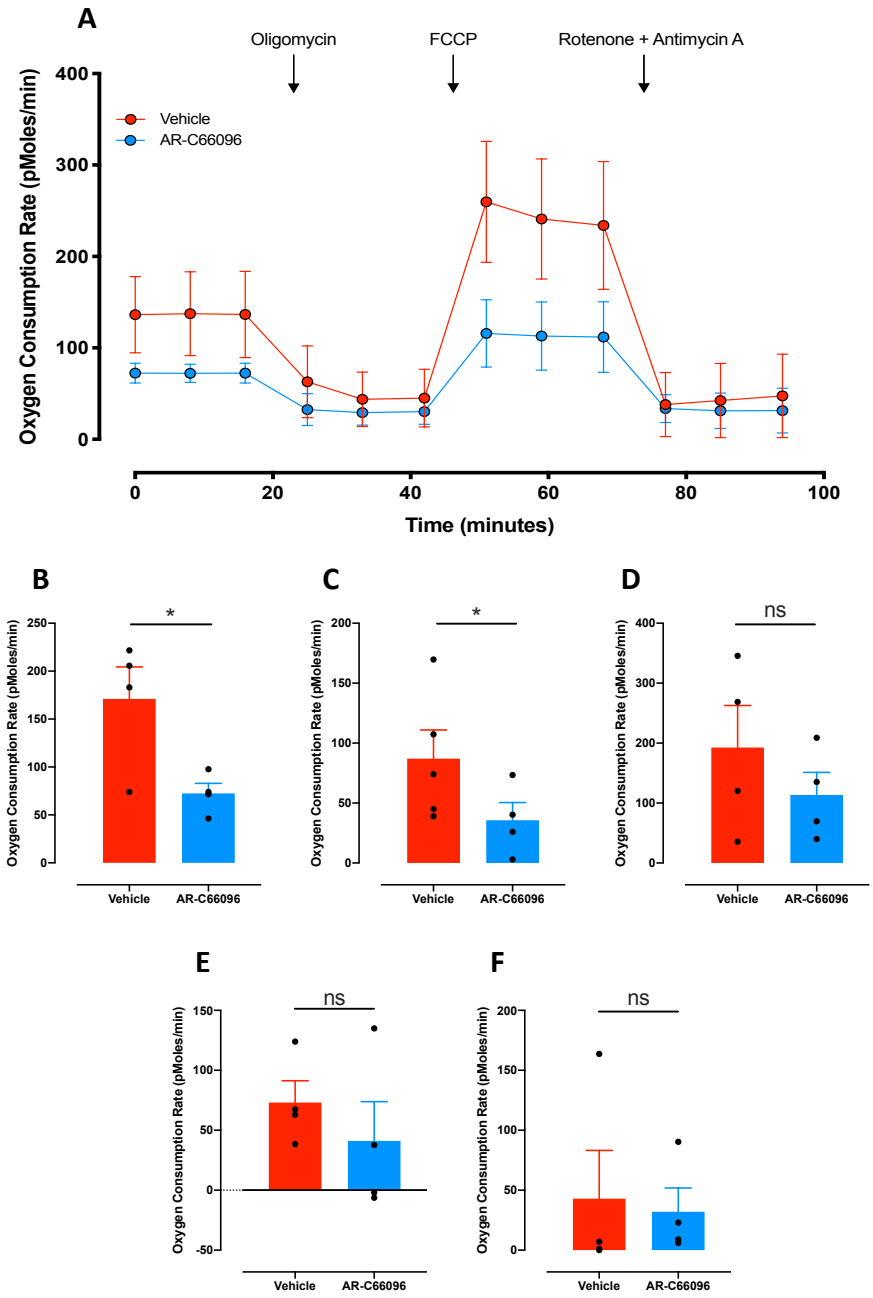

Figure 3.15: The effect of $P2Y_{12}$ inhibition on oxygen consumption rate

A. Agilent Seahorse oxygen consumption rate trace following treatment with vehicle (red) or AR-C66096 (blue) and the subsequent injection of the mitochondrial inhibitors oligomycin, FCCP and rotenone and antimycin **A**. Quantification of oxygen consumption rate: **B.** under basal conditions; **C.** linked to ATP production, assessed by inhibition of ATP synthase with oligomycin; **D.** maximal oxygen consumption rate; **E.** spare respiratory capacity; and **F.** non-mitochondrial respiration. Data presented as mean±SEM, significance was determined by paired t-test (n=4, * $p<0.05$).

3.4 Discussion

Platelet activation initiated by an external agonist binding to surface receptors facilitates intracellular signalling cascades, involving PLC and IP_3 which stimulate release of calcium from intracellular stores. Subsequently, this stimulates influx of calcium through the plasma membrane which is controlled by a number of mechanisms, including store-operated calcium entry mediated by STIM1 and Orai1.[87] Furthermore, the receptor-operated calcium channel, $P2X_1$ and TRPC6 facilitate the entry of calcium through the plasma membrane.[87] Here I have shown that platelet activation with both U46619 and TRAP-6, causes a significant increase in intracellular calcium. Unsurprisingly, activation with the stronger agonist, TRAP-6, causes a more rapid and sustained increase in intracellular calcium. Interestingly, the maximal calcium flux capacity of these platelets, examined using the calcium ionophore ionomycin, is approximately four times higher than the response elicited by TRAP-6. This observation could lead me to speculate that platelets may not require their maximal calcium signalling capacity to stimulate platelet activation. However, ionomycin elicits its function by creating pores within the membrane, thus allowing a substantial influx of calcium from the extracellular environment, which could subsequently overwhelm the intracellular calcium signalling. To better understand a platelets endogenous maximal calcium signalling capacity, the assay could be repeated without recalcification of the sample. This would allow for an indication of the release of calcium from within the intracellular stores, and would be less affected by the influx of calcium from the extracellular milieu.

Measuring calcium flux using flow cytometry has a number of limitations. Firstly, when using flow cytometry, the samples need to be diluted enough to ensure that the platelets do not aggregate, as this may cause obstruction in the cytometer. The dilution of platelets allows for a read out of the initial platelet activation pathways, but may be limited in terms of the secondary wave, following the release of secondary mediators. Thus, in this assay, I am looking at the calcium response following platelet activation, but not aggregation. Indeed, this assay may not be sensitive enough to fully understand the effect of anti-platelet therapies on calcium

signalling. Both aspirin and $P2Y_{12}$ antagonist target the secondary wave of aggregation, involving the release of secondary mediators, which given the diluted nature of the samples may not have elicited their full affects.

Whilst this data provides indications as to the nature of the effect of different agonists and anti-platelet drugs on calcium signalling, the technical limitations of the equipment means I have to be careful in drawing solid conclusions. Platelets inherently want to stick together, therefore measuring calcium flux in system where I am trying to prevent the samples aggregating does not mimic a physiological environment. Indeed, when looking at a growing thrombus, research has indicated that platelets exhibit a sustained high intracellular calcium which subsequently undergoes oscillations. Further, it has been proposed that platelets with high intracellular calcium communicate the calcium activation status to adjacent platelets.[220] Although far more time consuming and technically challenging, using a more physiological system, looking at calcium dynamics using adherent platelets and fluorescence microscopy may provide a better measure of calcium response during platelet aggregation, activation and thrombus formation, and subsequent effect of anti-platelet therapeutics.

The initial rise in intracellular calcium facilitates cytoskeletal rearrangement, promoting the movement and fusion of granules with the plasma membrane. Following the binding of vSNAREs on the granule and tSNAREs on the membrane, the granular content is released into the extracellular milieu and exerts its actions through both autocrine and paracrine manners.[60] Here I have shown that the exposure of P-selectin on the outer leaflet of the plasma membrane occurs at a slower rate than the rise in intracellular calcium, confirming the sequential nature of platelet activation. Further, stronger platelet stimulation with TRAP-6 causes a quicker and more robust increase in P-selectin expression than following stimulation with U46619. Interestingly, although TRAP-6 and U46619 activate different surface receptors, PAR-4 and TP respectively, the intracellular signalling pathways are overlapping, which raises the question as to why the responses are different.[82] The differences may be accounted for due to their role in the haemostatic response;

thrombin and therefore TRAP-6 is a strong platelet agonist, which stimulates the primary wave of aggregation, whilst thromboxane A_2 and therefore U46619, is an important secondary mediator which amplifies the activation response. Furthermore, these differences in the strength of the signal may be accounted in part by different receptor copy numbers which may limit the rate of response.

In recent years there has been growing interest in understanding mitochondrial function in platelets. Given the ease of isolation, platelets may provide a potential system to understand mitochondrial function and health at a more global level.[71] Thus, understanding platelet mitochondrial parameters; such as $\Delta\Psi m$ and oxygen consumption rate, in healthy individuals under both basal and activated conditions may allow us to establish if this information can be more widely applicable to mitochondrial health and function within other cells, and may allow the characterisation of differences in disease pathologies. In other cell types, it is well established that maintaining healthy mitochondria with an intact $\Delta\Psi m$, is necessary for the maintenance of cellular functionality, however it still remains elusive as to the importance of mitochondria function in platelets. Here I have shown that following activation, platelet mitochondria undergo a short, transient period of hyperpolarisation, as marked by an increase in the fluorescence of the mitochondrial membrane dye, TMRM. This increase in fluorescence is indicative of a more negative membrane potential as a result of increased proton motive force generated by an increase in oxidative phosphorylation.[221]

Interestingly, the kinetics of mitochondrial membrane potential follow a similar pattern to calcium dynamics, suggesting these two processes may be intimately linked. Whilst it has long been established that mitochondria are a reservoir of calcium, acting a buffer for cytosolic calcium. The data presented here may suggest that a rise in intracellular calcium is important for the transient $\Delta\Psi m$ hyperpolarisation. Indeed, research has shown that calcium imported into mitochondria may participate in the oxidation of mitochondrial substrates, therefore increasing the oxidative phosphorylation capacity.[222] Whilst it has been established calcium is essential for mitochondrial function in other cell types, the relationship in

platelets remains unknown. To examine the role of mitochondrial calcium during platelet activation, inhibition of the mitochondrial calcium uniporter (MCU) may provide interesting insights into the association between calcium flux and $\Delta\Psi m$ in platelets. Furthermore, the use of the mitochondrial specific calcium probe Rhod-2 would provide additional understanding of these processes. In this work, I have demonstrated that platelet activation causes a transient $\Delta\Psi m$ hyperpolarisation, whilst recent research has indicated that sustained $\Delta\Psi m$ hyperpolarisation enhances procoagulant platelet formation. Further, genetic deletion of MCU has highlighted an positive association between $\Delta\Psi m$ hyperpolarisation, calcium entry through MCU, and subsequent formation of the mitochondrial permeability transition pore (mPTP).[122,223]

The changes I identified in $\Delta\Psi m$ following platelet activation led me to speculate that platelet activation would cause an increase in mitochondrial respiration through oxidative phosphorylation. Under resting conditions, platelets derive approximately 60% of their ATP from glycolysis with the remaining 40% derived from oxidative phosphorylation within the mitochondria.[116] Using a Seahorse analyser, I found that platelet activation with TRAP-6 causes a significant increase in oxygen consumption rate, indicative of an increase in oxidative phosphorylation. Despite this increase from baseline oxygen consumption rate, platelet activation does not cause subsequent alteration to any additional respiration parameters. Interestingly, research has indicated that platelets have a relatively high basal oxygen consumption rate in comparison to some leukocytes, such as monocytes.[116] Given that platelets are far smaller than leukocytes, it may be surprising that their basal oxygen consumption is higher. The reasons behind the high basal oxygen consumption remain unknown, however as detailed previously, it may be due to platelets having to maintain their quiescent state and prevent inappropriate activation. In addition, platelets may need to maintain strong ion gradients such that they are able to respond rapidly to breaks within the vasculature or to soluble mediators thereby preventing excessive blood loss.

The Seahorse analyser is a useful tool to look at oxygen consumption, however there are a number of limitations with using this method for the measurement of mitochondrial function in platelets. Firstly, platelet activation is a rapid process in which platelets lose their discoid shape undergoing cytoskeletal rearrangement and thereby facilitating granule secretion. These processes are largely complete within 5-10 minutes following activation, however the Seahorse analyser protocol is limited by the time and frequency of the measurements. Following the injection of TRAP-6, the oxygen consumption rate was not measured for 3 minutes, therefore any initial alterations would have been missed. Despite this time delay in measuring the oxygen consumption, I was still able to demonstrate an increase in oxygen consumption, suggesting that the increased respiration is maintained past the initial platelet activation period. These findings support previous work showing an increase in oxygen consumption following activation of platelets by thrombin.[209,224] An alternative approach to measure mitochondrial respiration in platelets, would be using high resolution respirometry. This technique is more sensitive to small changes in oxygen consumption and would allow for the determination of earlier alterations in mitochondrial function following the addition of a platelet activator.[224] Whilst more labour intensive, high resolution respirometry is a more flexible and sensitive assay. Unlike Seahorse analyser, it allows for the manual injection of numerous compounds, through ports within the chamber stopper, and consistently measures the oxygen consumption within the sealed chamber. This technique would provide more detailed analysis of the rapid, dynamic nature of the platelet activation response. The measurement of oxygen consumption as an indicator of mitochondrial respiration is widely used, however it can be a misleading measurement as it does not consider the oxygen consumption contribution of oxidative enzymes, such as cyclooxygenase-1.[225] Thus, the increase in oxygen consumption following platelet activation may in part be attributable to the activation of cyclooxygenase-1 and lipoxygenases, facilitating the conversion of arachidonic acid into thromboxane A_2 and hydroxyeicosatetraenoic acids (HETEs).[226,227]

Anti-platelet therapeutics are commonly prescribed for the secondary prevention of cardiovascular events. There is a plethora of literature demonstrating alterations in

platelet aggregation, and the effectiveness of aspirin and $P2Y_{12}$ inhibitors in reducing platelet activity, however the dynamics of these responses have not been investigated. In this work, I have shown that $P2Y_{12}$ inhibition, but not aspirin treatment causes a reduction in calcium flux following stimulation with U46619 and TRAP-6, without affecting the overall calcium signalling capacity following incubation with ionomycin, supporting recent work indicating reduced calcium signalling following ticagrelor or AR-C69931.[228] As discussed previously, given the dilute nature of the sample, the inhibition of the secondary wave of aggregation may be masked, therefore not showing the true effect of these anti-platelet treatments.

Interestingly, recent work has indicated that aspirin affects the release of pro-inflammatory mediators independent of cyclooxygenase, by influences on calcium signalling pathways.[229] This work has highlighted that low and high concentrations of aspirin have differential effects on calcium entry into mast cells. Indeed, low concentrations stimulate a stronger influx of calcium, whilst high concentrations inhibit the uptake of calcium.[229] The anti-platelet effects of aspirin occur at low doses, and as such one might expect to see an increase in calcium signalling following activation. These reports have highlighted a modification in calcium signalling in T cells and mast cells, so may not be directly applicable to platelets, however repeating the calcium flux assay using a spectrofluorometer may provide a more accurate and sensitive assessment of calcium signalling. Further, using a spectrofluorometer would provide a more physiologically relevant environment as the samples do not need to be diluted, therefore allowing the platelets to aggregate and trigger the secondary wave of aggregation.

Further investigation of platelet activation pathways revealed that blockade of the $P2Y_{12}$ receptor and inhibition of cyclooxygenase-1 reduces P-selectin exposure following stimulation with U46619, but not TRAP-6. This data supports recent work that has shown that both the $P2Y_{12}$ and $P2Y_1$ receptors are involved in the secretion and exposure of P-selectin on the platelet surface.[217]

Interestingly, in the presence of aspirin, mitochondrial function was unaltered, following a similar dynamic $\Delta\Psi m$ hyperpolarisation following platelet activation, and a consistent oxygen consumption rate under basal conditions. This data indicates that pharmacological inhibition of cyclooxygenase-1 does not cause alterations in platelet metabolism. Conversely, pharmacological inhibition of the $P2Y_{12}$ receptor causes alterations in mitochondrial function. Notably, in response to U46619, the initial $\Delta\Psi m$ hyperpolarisation is replaced with a $\Delta\Psi m$ depolarisation, which was not observed in response to TRAP-6. Furthermore, analysis of mitochondrial respiration revealed that under basal conditions, AR-C66096 treated platelets had a significantly lower oxygen consumption rate than vehicle treated platelets, suggesting that pharmacological blockade of the $P2Y_{12}$ receptor is affecting mitochondrial function and health. This reduction in mitochondrial respiration could be a toxic side effects of AR-C66096 or as a result of disruption of the ADP associated pathways within the platelet. To determine if these findings are as a result of toxic effects, additional experiments using alternative $P2Y_{12}$ inhibitors could be performed. Interestingly, work has indicated the presence of $P2Y_{12}$ receptors on mitochondria within astrocytes.[230] While it is unknown whether platelets also express $P2Y_{12}$ receptors within their mitochondrial membranes, if they do it may provide an alternative explanation for the disruption in mitochondrial function following incubation with a $P2Y_{12}$ receptor antagonist.

Whilst in this work I have investigated the role of mitochondrial energy production within a small number of platelet activation pathways, further work exploring the contribution of glycolysis to these processes would provide interesting insights into platelet metabolism and compensatory mechanisms between these two pathways. Indeed, it would be exciting to explore whether either of these two pathways is engaged preferentially in response to certain agonists. In general terms, I have discussed the process of platelet activation occurring in a sequential manner, which in terms of soluble agonist induced activation appears to be true. However, it remains unclear whether platelet activation following from other stimuli, high shear stress being a particular example, proceeds in the same sequential nature.[65] My data

illustrates that measuring the dynamics of platelet activation pathways allows a deeper understanding of the response can be achieved and through this an opportunity to unpick differences in responses. As an example, using an end point fluorescence assay to measure TMRM fluorescence rather than a dynamic assay would not have allowed measurement of any of the changes seen in the initial stages of platelet activation and so a much poorer understanding of $\Delta\Psi$m.

This data presented in this chapter confirms the sequential nature of platelet activation, highlighting an importance of changes in mitochondrial membrane potential and increases in mitochondrial respiration. Anti-platelet treatment with AR-C66096, but not aspirin, affects calcium flux and P-selectin expression following activation. Furthermore, AR-C66096 affects mitochondrial function, under basal conditions causing a significant reduction in the oxygen consumption rate. This interesting observation warrants further investigation to unpick the impact of this reduction in oxygen consumption and its significance on platelet function.

The work presented in this chapter investigates response of platelets when considered as a whole population, however it is well established that platelets form a heterogenous population of ages, sizes and function. In the next chapter, I will explore differences in platelet function and composition in two subpopulations of different ages.

4 Characterisation of differently aged platelets

4.1 Introduction

Blood platelets form a heterogenous population of different ages which exist within the circulation of a healthy individual for approximately 10 days. During platelet biogenesis from the progenitor megakaryocyte, platelets are packaged with mRNA, lipids, proteins and organelles which are needed for their functionality within the circulation.[231] Given that platelets are anucleate, they lack the capacity to generate new mRNA, and as such, following release from the parent megakaryocyte, the mRNA rapidly degrades within the first few days.[73] This results in a small subpopulation of platelets, the newly formed, having the highest levels of mRNA.

Along with RNA, platelets also inherit ribosomes and translational machinery from the progenitor megakaryocyte. Historically, it was thought that the platelet proteome is stable, with the vast majority of proteins obtained during platelet biogenesis or taken up from the plasma via endocytic pathways. However, emerging evidence has revealed that platelets have a limited capability to translate mRNA into protein, although it remains to be established under what circumstances this occurs.[232] In addition to these recent observations that platelets are able to translate RNA, there are reports that they can also transfer RNA to other cells within the circulatory system and so influence their function.[233–235]

Understanding the functional changes across platelet lifespan is of particular research interest as newly formed platelets have been described as being hyper-reactive and associated with an increased risk of thrombotic disease.[236] Interestingly, in a number of diseases such as chronic kidney disease and diabetes mellitus, there are reports of increased platelet turnover resulting in a higher proportion of young platelets in the circulation, with a related increase occurrence of acute coronary events.[237] Furthermore, increased platelet turnover and the associated increase in the proportion of newly formed platelets have been linked to suboptimal responses to anti-platelet therapies.[238] Despite many reports of these newly formed platelets

being hyper-reactive, there are few systematic studies that have sought to understand functional changes between young and old platelets in healthy individuals.

In this chapter, I use proteomics, immunofluorescence and functional assays to investigate the differences between young and old platelets isolated from peripheral blood of healthy individuals.

4.2 Methods

4.2.1 Blood collection and preparation of PRP

Blood was collected from healthy volunteers and PRP was prepared as previously described in sections 3.2.1 and 3.2.2.

4.2.2 Flow cytometric sorting of young, intermediate and old platelets

Using flow cytometry cell sorting, platelets of different ages were separated for functional studies. Briefly, PRP was incubated with 200ng/ml thiazole orange for 30 minutes at room temperature in the dark. The sample was diluted 1 in 8 with filtered modified Tyrode's HEPES buffer (pH 7.4) and supplemented with prostaglandin E_1 (PGE_1; 2µM). Platelets were sorted on a BD FACS Aria III Fusion Cell Sorter (70µm nozzle, 70 Ps) into three subpopulations based on gating on thiazole orange fluorescence intensity (Figure 4.1). The sorting protocol identified platelets on forward scatter area (FSC-A) and side scatter area (SSC-A), removed doublets based on side scatter width (SSC-W) and subsequently gated on thiazole orange fluorescence intensity; young platelets were defined as top 10%, thiazole orange bright; intermediate platelets were defined as middle 50%; and old platelets were defined as bottom 30%, thiazole orange dim. Following cell sorting on thiazole orange intensity, platelet subpopulations were pelleted at 1000 *x g* for 10 minutes in the presence of prostacyclin (PGI_2; 2µM) and resuspended in modified Tyrode's HEPES buffer and allowed to rest for 30 minutes.

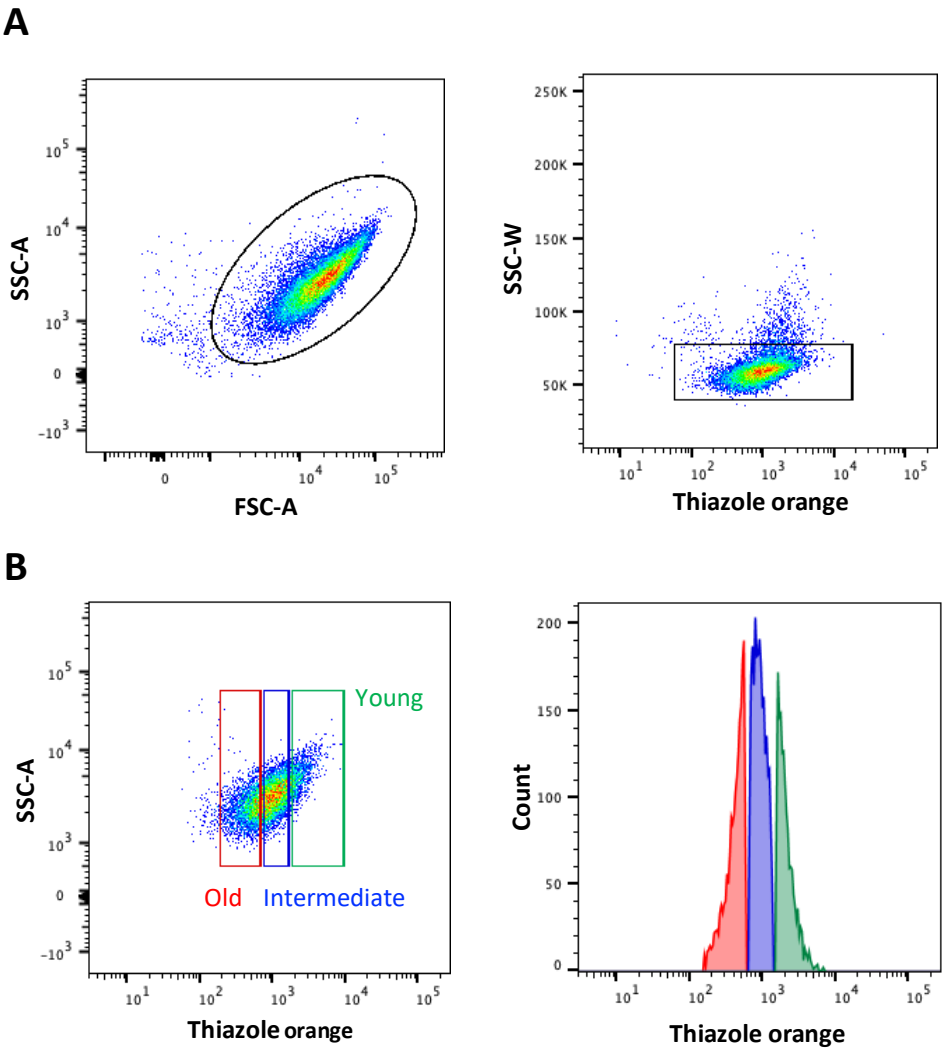

Figure 4.1 Thiazole orange isolation of young, intermediate and old platelets

Flow cytometric cell sorting protocol based on **A.** SSC-A/FSC-A and SSC-W/Thiazole Orange fluorescence intensity **B.** Representative dot plot of SSC-A/Thiazole Orange demonstrating the gating strategy to isolate young platelets (top 10%), intermediate platelets (middle 50%) and old platelets (bottom 30%) based on thiazole orange fluorescence intensity.

4.2.3 Proteomic analysis of sorted platelet subpopulations

Following sorting of 65 million platelets per subpopulation, platelet pellets were lysed on ice in 250µl buffer containing 100mM TRIS (pH 7.4), 2% sodium dodecyl sulfate (SDS) with 1 cOmplete™ Mini Protease Inhibitor Cocktail Tablet. The samples were sonicated twice at 20W for 5 seconds, and centrifuged at 18,000 *x g* for 7 minutes at 4˚C. The supernatant was removed, placed in a fresh microcentrifuge tube and stored at -80˚C until required. Protein content of platelet subpopulations was measured using a Nanodrop Spectrophotometer ND-1000.

The extracted protein samples were sent to Simone Marcone at University College Dublin, Ireland for liquid chromatography tandem mass spectrometry analysis (LC-MS/MS). Samples were prepared as previously described[239]. From each sample, 50µg of protein was used for trypsin digestion and filter aided sample preparation (FASP). For LC-MS/MS analysis, 2µg of purified protein was injected using an Ultimate3000 nano-LC system coupled to a hybrid quadrupole-orbitrap mass spectrometer (Q Exactive). All data was acquired operating in automatic data-dependent acquisition mode (DDA, shotgun).

Downstream analysis of the platelet proteomic data was performed by Perseus software (version 1.6.0.7); only proteins present in at least 50% of samples in at least one group of differently aged platelets were considered identified. The proteomic data is presented as a Z-score, expressing the relationship between each individual value and the mean of all values for that protein. Proteins found to be differentially expressed between groups (p value <0.05) were subjected to pathway mapping analysis using ingenuity pathway analysis (IPA) and STRING database (Version 10.5). The molecular activation prediction algorithm in IPA was used to predict upstream and downstream effects of activation and inhibition of associated network functions. STRING was used to generate protein-protein interaction networks.

4.2.4 Immunofluorescence of young and old platelets

Sorted young and old platelets (2 million per population) were fixed with paraformaldehyde (PFA; 4%) for 10 minutes and centrifuged onto poly-l-lysine coverslips at 600 *x g* for 5 minutes. Non-adherent platelets were removed from the coverslips by washing with filtered PBS. Samples were blocked and permeabilised with filtered permeabilising buffer (0.2 % Triton, 2% donkey serum and 1% bovine serum albumin; BSA, in PBS) for 30 minutes at room temperature. After removal of the blocking buffer, the coverslips were incubated with primary antibodies as indicated in Table 4.1 for 1 hour in the dark at room temperature. The primary antibody was removed with three wash steps using filtered PBS. Subsequently, the samples were incubated for 45 minutes with the secondary antibody in the dark at room temperature (Table 4.1). The secondary antibody was removed with three filtered PBS washes. The coverslips were mounted using ProLong Diamond antifade mount and allowed to set overnight in the dark at room temperature. Samples were then stored at 4°C and imaged on the Zeiss LSM880 confocal microscope with airyscan; 63x objective, 1.4 DICII; imaging at least 5 different fields of view per sample collecting a minimum of 30 platelets per sample. Image processing and analysis was conducted using Zen Software (2.3 SP1) and ImageJ.

Table 4.1 Antibodies used for immunofluorescence of sorted platelets

Target	Primary antibody	Dilution	Secondary antibody	Dilution
Actin	Phalloidin Alexa Fluor 647	1:200	-	-
Tubulin	Mouse anti-αTubulin	1:500	anti-mouse Alexa Fluor 647	1:500
Mitochondria	Mouse anti-TOM20	1:500	anti-mouse Alexa Fluor 555	1:500
Dense tubular system	Rabbit anti-ErP57	1:200	anti-rabbit Alexa Fluor 647	1:500
Fibrinogen	Rabbit anti-fibrinogen	1:200	anti-rabbit Alexa Fluor 647	1:500
Complement 4	Rabbit anti-C4	1:200	anti-rabbit Alexa Fluor 647	1:500

4.2.5 Measuring mitochondrial membrane potential in young and old platelets

Sorted young and old platelets (3 million per population in 250µl) were supplemented with 2mM $CaCl_2$ and stained with MitoProbe™ DiIC1(5) (50nM) and CD42b BV421 (1:250) for 15 minutes at room temperature in the dark. Samples were acquired using the BD LSRII, collecting 10,000 CD42b events and assessing MitoProbe fluorescence. Samples were analysed using FlowJo v.8.

4.2.6 Measuring phosphatidylserine exposure in young and old platelets

Sorted young and old platelets (3 million per population in 250µl) were supplemented with $CaCl_2$ (2mM), diluted in 150µl Annexin V binding buffer and stained with annexin V APC (1:150) and CD42b BV421 (1:250) for 15 minutes at room temperature in the dark. Samples were acquired using the BD LSRII, collecting 10,000 CD42b events and assessing annexin V fluorescence. Samples were analysed using FlowJo v.8.

4.2.7 Assessing platelet spreading on collagen in young and old platelets

Glass coverslips were coated in collagen (100µg/ml) overnight at 4˚C and subsequently washed with filtered PBS. The coverslips were blocked with BSA (1%) for 1 hour at room temperature and then washed with filtered PBS.

Following sorting, young and old platelets (3 million per population) were supplemented with $CaCl_2$ (2mM) and allowed to adhere to collagen coated coverslips for 1 hour at 37˚C. Non-adherent platelets were removed by three washes with filtered PBS. Samples were fixed with PFA (0.2%) for 10 minutes, washed with filtered PBS and subsequently permeabilised with Triton (0.2%). Following permeabilization, samples were once again washed with filtered PBS and stained with Phalloidin 647 (1:200) for 1 hour at room temperature in the dark. Platelet samples were washed with filtered PBS and mounted onto Super Frost coverslips using Prolong Diamond antifade mount. Samples were then stored at 4˚C and imaged on the Zeiss LSM880 confocal microscope with airyscan; 63x objective, 1.4 DICII,

imaging at least 5 different fields of view per sample collecting a minimum of 30 platelets per sample. Image processing and analysis was conducted using Zen Software (2.3 SP1) and ImageJ.

4.2.8 Assessing calcium dynamics young and old platelets

Sorted young and old platelets (10 million per population in 1000µl) were stained with Calbryte 630™ (2µM) for 30 minutes at 37°C, and CD42b BV421 (1:200) for 15 minutes at room temperature and supplemented with $CaCl_2$ (2mM). Baseline Calbryte 630™ fluorescence was recorded for 30 seconds, followed by challenge with Thrombin Receptor Activator for Peptide 6 (TRAP-6; 10µM and 25µM), or ionomycin (10µM) and subsequent recording of fluorescence for 2 minutes. Samples were acquired on a BD LSRII flow cytometer using FACSDiva acquisition software, and analysed using FlowJo software.

4.2.9 Statistical analysis

Graphs and statistical analysis were generated using GraphPad Prism v.8. Data was expressed as mean±SEM and all statistics were generated using a paired students t-test or a one-way ANOVA, with a Tukey's post-test. Significance was defined as $p<0.05$.

4.3 Results

4.3.1 Protein content declines with platelet age

Measurement of the total protein concentration in differently aged platelets demonstrated a significant reduction in protein content as platelets age. Young platelets (thiazole orange high) contained 8.7±2.6pg of protein per platelet, reducing to 6.6±0.72pg per platelet in the intermediate subpopulation and 4.7±1.2pg per platelet in old platelets (Figure 4.2A).

Mass spectrometry analysis revealed that the reduction in protein content was associated with a marked decrease in the number of different detectable proteins; 484±23, 297±34 and 281±43 proteins in in young, intermediate and old platelet subpopulations, respectively (Figure 4.2B).

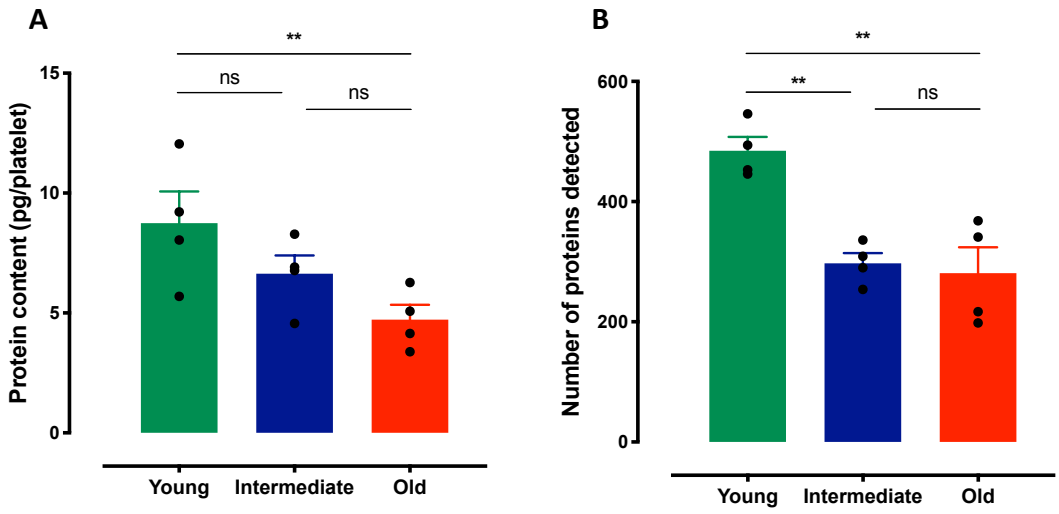

Figure 4.2 Assessment of protein content and number in platelet subpopulations

A. Quantification of protein content per platelet in young, intermediate and old subpopulations. **B.** Quantification of the number of detected proteins by mass spectrometry in young, intermediate and old subpopulations. Data presented as mean±SEM, significance was determined by one-way ANOVA with Tukey's multiple comparisons test (n=4, **p<0.01).

4.3.2 Platelet ageing causes alterations in protein expression

Shotgun mass spectrometry identified a total of 583 different proteins (Figure 4.3; Appendix 1) within the three platelet subpopulations. When comparing all three subpopulations, there was a significant difference in the expression of 94 different proteins (Figure 4.3B; Appendix 2).

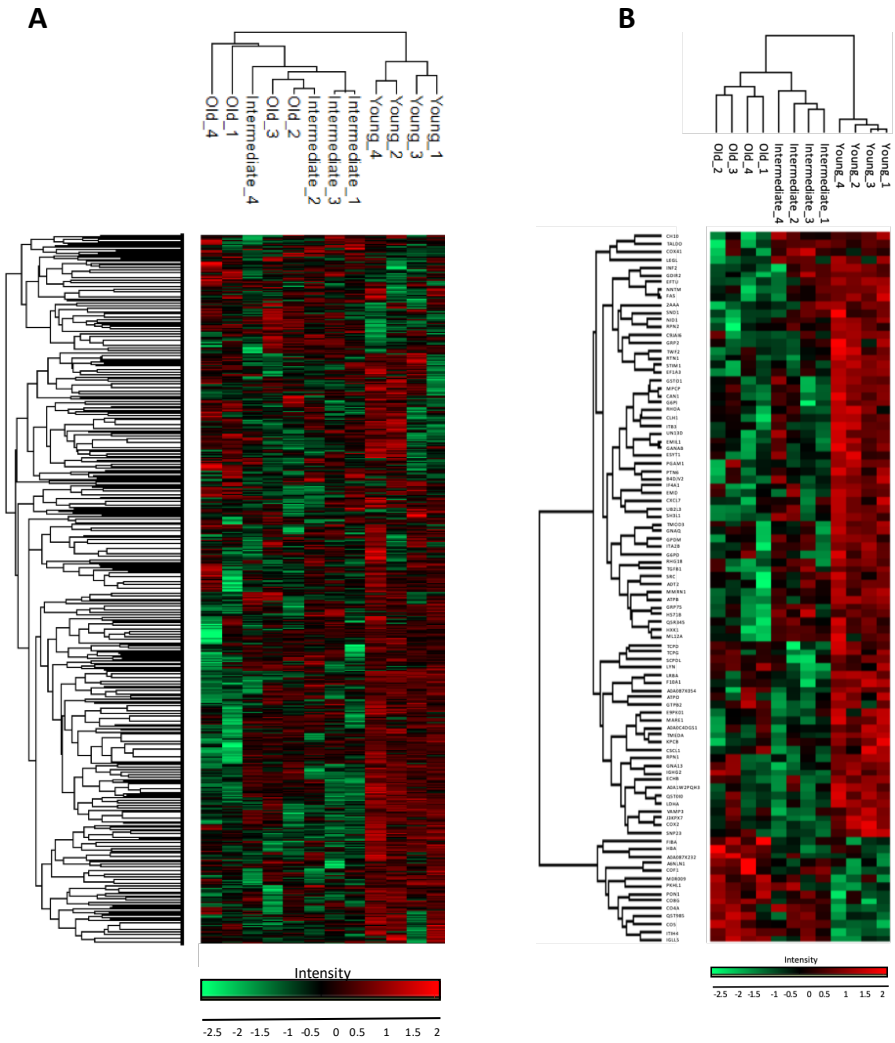

Figure 4.3 Hierarchal clustering of the sorted platelet proteome

A. Hierarchal clustering heat map of 583 proteins identified in the proteomic analysis of platelet subpopulations **B.** Hierarchal clustering heat map of the 94 proteins significantly altered between the three platelet subpopulations. Data presented as z-score (red indicates a relative increase, green indicates a relative decrease in expression).

Focussed analysis looking at differences in protein expression specifically between young and old platelets indicated a significant modulation in 78 different proteins (Figure 4.4; Appendix 3). Hierarchal clustering of these proteins indicated 64 proteins had a relatively higher expression in young platelets, whilst old platelets had a relatively higher expression of 14 proteins.

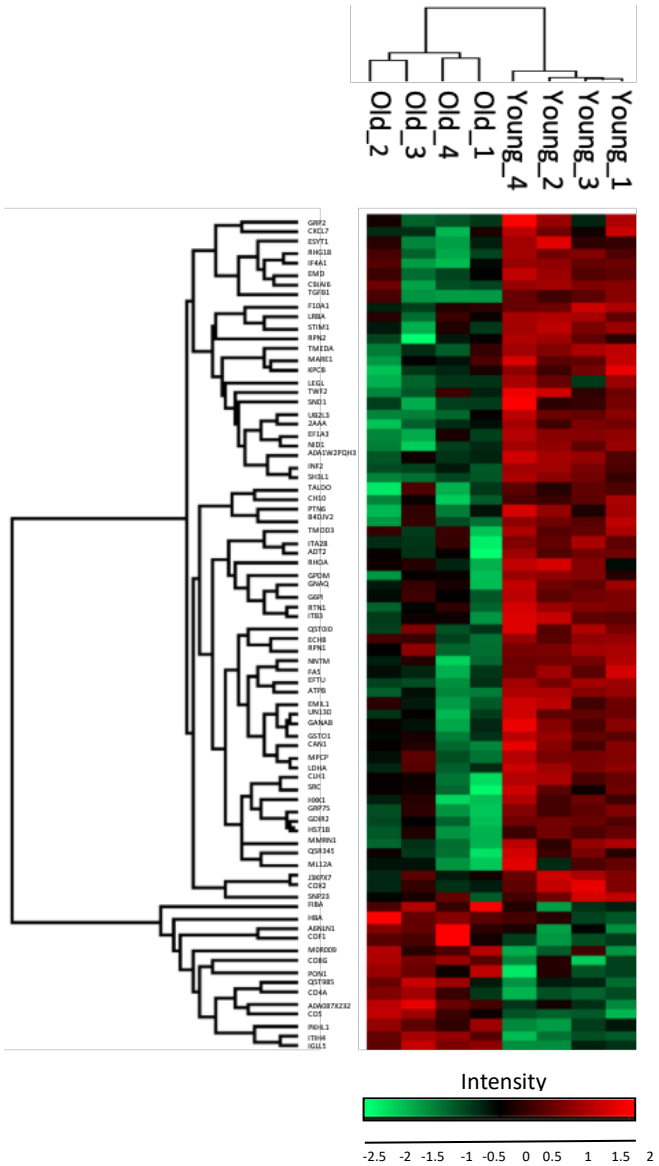

Figure 4.4 Protein alterations between young and old platelets

Hierarchal clustering heat map of 78 proteins significantly altered between young and old platelets. Data presented as z-score (red indicates a relative increase, green indicates a relative decrease in expression).

4.3.3 Alterations in protein expression affect key biological functions

Downstream analysis of the protein alterations using STRING analysis indicated that the proteins expressed relatively more highly in young platelets have a strong interaction network. Of particular interest, STRING analysis highlighted a large number of mitochondrial proteins and cytoskeletal-proteins with significantly higher expression levels in young platelets (Figure 4.5A). The analysis also indicated that there was an interaction between a number of mitochondrial (shown in red) and cytoskeletal proteins (blue). Further investigation examining the biological functions that may be affected as a result of higher expression of these proteins indicated that 15 of these proteins are involved in haemostasis (shown in green) and form interactions with cytoskeletal-associated proteins. Interestingly, only a small number of these proteins do not have an interaction partner within the group, suggesting the reduction in the protein levels may be due to specific degradation of proteins involved in certain pathways or potential release of these proteins in microvesicles.

The number of proteins that were identified as having a higher expression in old platelets was far lower than that identified in young platelets. Interestingly, however, these proteins tended to be circulating proteins suggesting they may have accumulated over the platelet's lifespan. STRING analysis demonstrated that these proteins are involved in the immune system response (red) and the stress response (blue), which may suggest that old platelets have a different function compared to young platelets (Figure 4.5B).

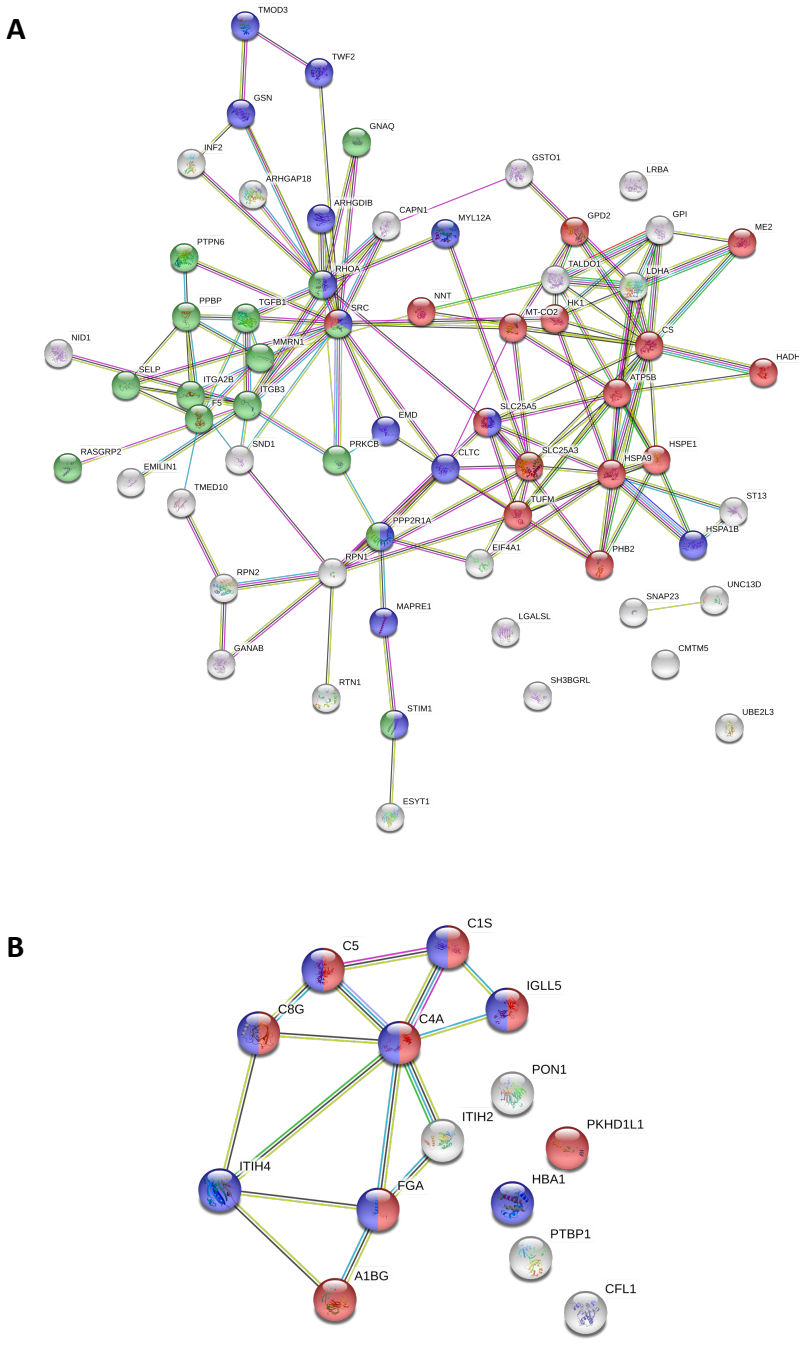

Figure 4.5 STRING analysis of protein interactions and associated functions affected by protein alterations

A. STRING analysis showing proteins more highly expressed in young platelets indicating mitochondrial (red) and cytoskeletal-associated proteins (blue) and proteins involved in haemostasis (green). **B.** STRING analysis showing proteins more highly expressed in old platelets involved in the immune system response (red) and the stress response (blue).

Downstream analysis of the altered proteome profile using ingenuity pathway analysis identified a total of 29 biological functions and pathways that may be affected by the altered protein expression (Figure 4.6). Of these, 22 functions were predicted to be higher in the young platelets; including haemostasis, binding and adhesion of blood platelets and organisation of the cytoskeleton. On the other hand, old platelets had a predicted increase in necrosis, apoptosis and senescence pathways, as well as an increase in the generation of reactive oxygen species.

Figure 4.6 Biological functions affected by protein alterations

Ingenuity pathway analysis of biological functions and pathways predicted to be affected by the identified protein alterations between young and old platelets. Data presented as z-score; orange indicates a predicted increase, blue indicates a predicted decrease in biological function.

Targeted analysis looking at the proteins involved in the predicted increase in haemostasis in young platelets identified 11 proteins that were differentially expressed and which may be contributing towards this enhanced function (Figure 4.7). All but two of these proteins were more highly expressed in the young platelets, however the plasma protein fibrinogen was detected at higher levels in the old platelets. In further support of young platelets having a predicted higher haemostatic function, IPA also indicated young platelets have a predicted increase in calcium flux, a process fundamental for platelet activation pathways (Figure 4.8).

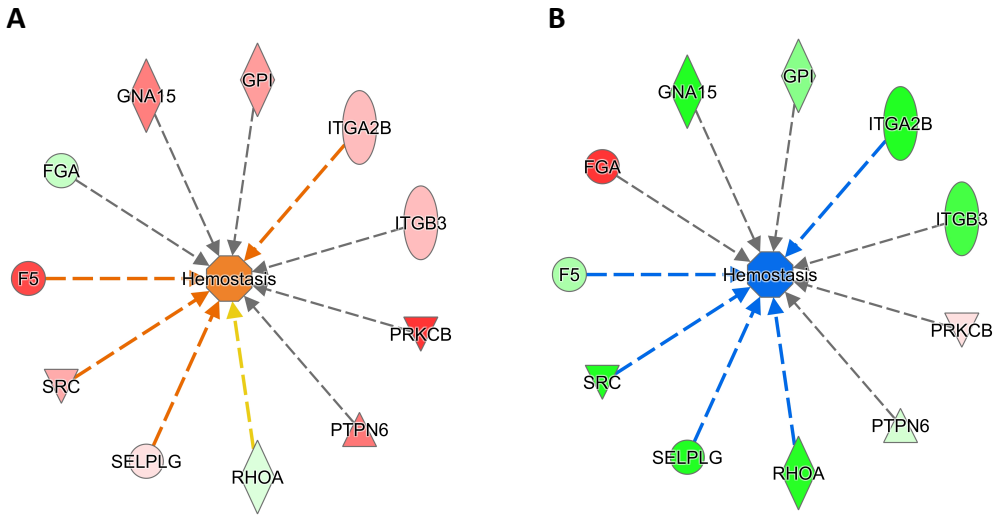

Figure 4.7 Proteins contributing to the predicted difference in haemostasis

IPA functional protein network indicating the expression and contribution of differentially expressed proteins to haemostatic function in **A.** young platelets and **B.** old platelets. IPA predicted regulatory relationships between upregulated (red) and downregulated (green) proteins contributing to an expected increase in haemostasis in young platelets indicated (indicated by orange lines), and a negative regulation in old platelets (indicated by blue lines).

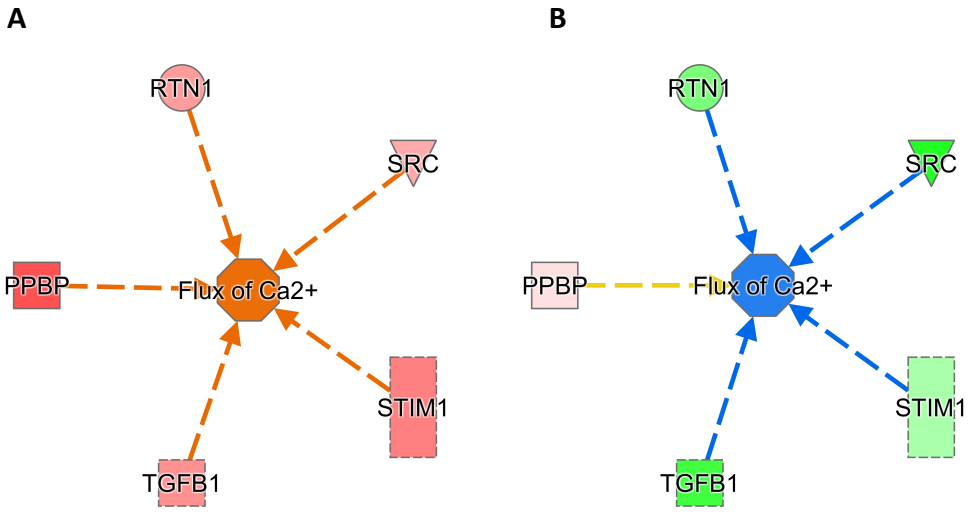

Figure 4.8 Proteins contributing to the predicted difference in calcium flux

IPA functional protein network indicating the expression and contribution of differentially expressed proteins on calcium flux in **A.** young platelets and **B.** old platelets. IPA predicted regulatory relationships between upregulated (red) and downregulated (green) proteins contributing to an expected increase in haemostasis in young platelets indicated (indicated by orange lines), and a negative regulation in old platelets (indicated by blue lines).

Interrogation of the proteins involved in cytoskeletal organisation demonstrated a further 11 proteins influencing these processes (Figure 4.9A-B). Interestingly only a small number of these proteins are directly linked to the cytoskeleton; twinfilin-2, gesolin and cofilin-1. Indeed, a number of surface receptors were significantly altered between young and old platelets, highlighting an intimate link between membrane structures and the cytoskeleton.

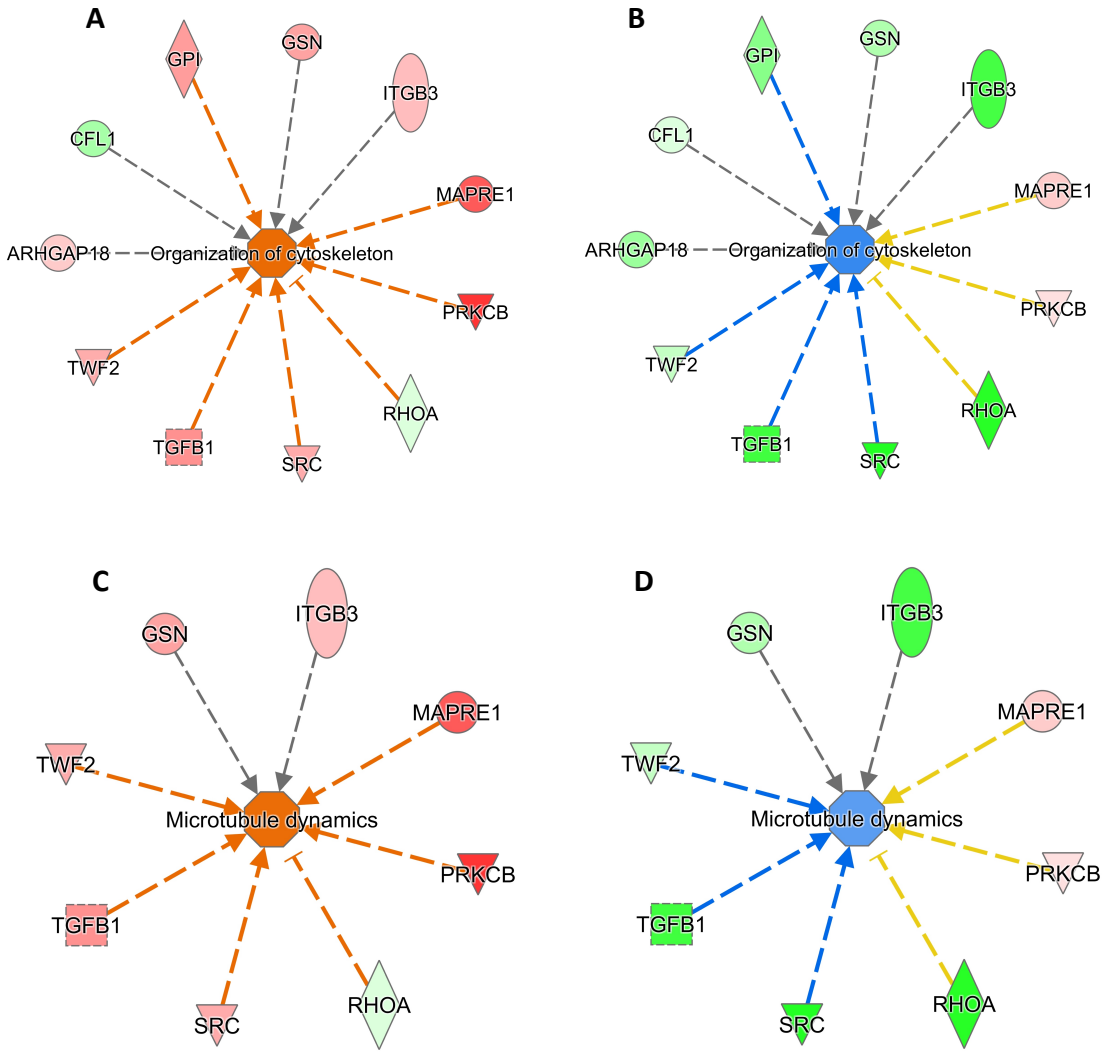

Figure 4.9 Proteins contributing to the predicted difference in cytoskeletal organisation

IPA functional protein network indicating the expression and contribution of differentially expressed proteins to the organisation of the cytoskeleton in **A.** young and **B.** old platelets and microtubule dynamics in **C.** young and **D.** old platelets. IPA predicted regulatory relationships between upregulated (red) and downregulated (green) proteins contributing to an expected increase in haemostasis in young platelets indicated (indicated by orange lines), and a negative regulation in old platelets (indicated by blue lines).

Given that old platelets had a predicted downregulation in conventional platelet function pathways, it is interesting to note that they had a predicted increase in pathways associated with cell death; both necrosis and apoptosis (Figure 4.10). The functional protein networks indicated the contribution of over 19 proteins to the upregulation of these pathways in old platelets compared to young platelets. A reduction in the expression of 21 proteins including RhoA, CS, HK1, ITGB3, PTPN6, GSN in old platelets would facilitate the activation of pathways causing the induction of necrosis. Similarly, downregulation of the expression of 16 proteins in old platelets led to a prediction of increased apoptotic pathways in old platelets compared to young platelets.

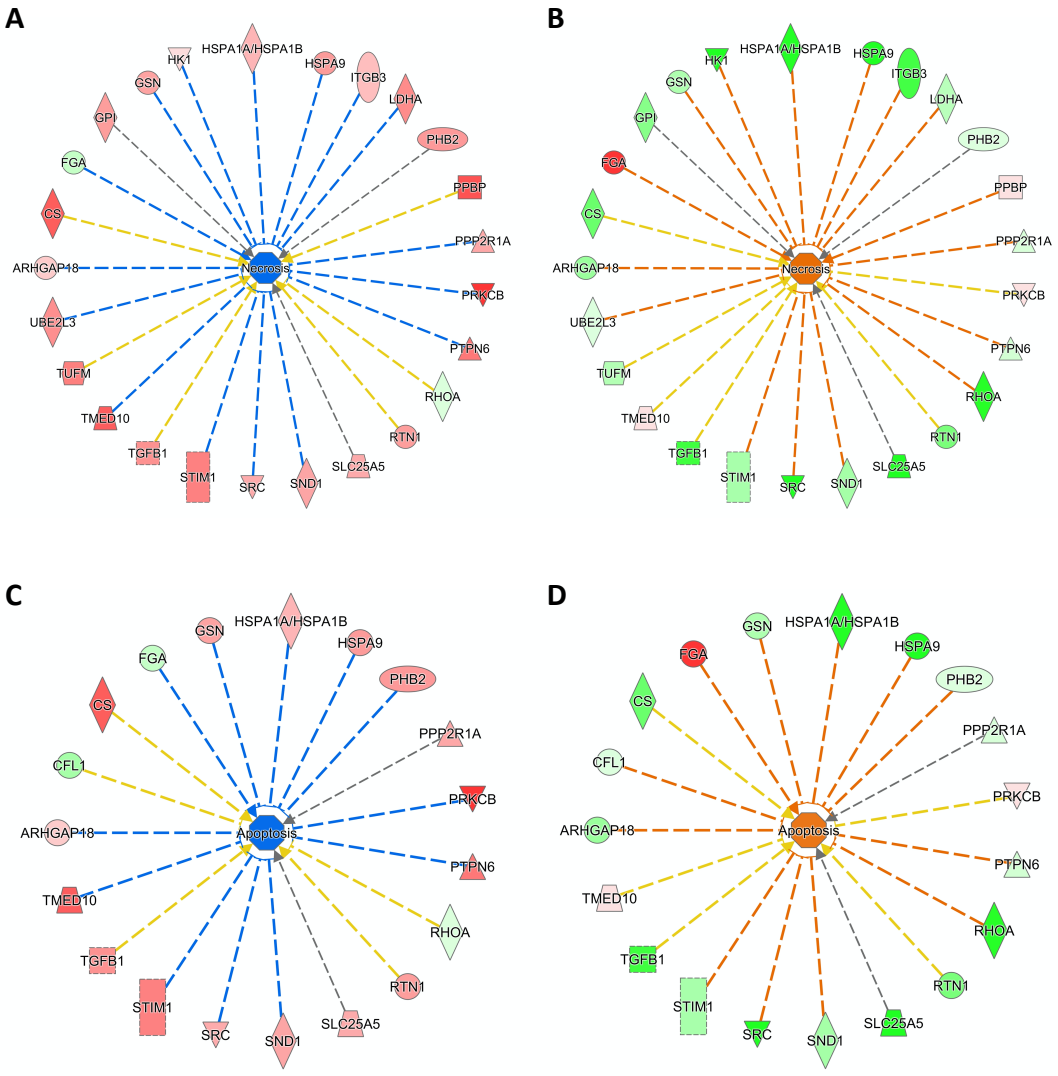

Figure 4.10 Proteins contributing to the predicted difference in necrosis and apoptosis

IPA functional protein network indicating the expression and contribution of differentially expressed proteins to necrosis in **A.** young platelets and **B.** old platelets and apoptosis in **C.** young and **D.** old platelets. IPA predicted regulatory relationships between upregulated (red) and downregulated (green) proteins contributing to an expected increase in haemostasis in young platelets indicated (indicated by orange lines), and a negative regulation in old platelets (indicated by blue lines).

4.3.4 Platelet ageing causes a reduction in mitochondrial parameters

Proteomics and STRING analysis revealed a reduction in key mitochondrial proteins in old platelets including citrate synthase, ATP synthase subunit beta and cytochrome c oxidase subunit 2. Interestingly, further examination of mitochondrial characteristics identified reduction in a number of features in old platelets compared to young platelets (Figure 4.11).

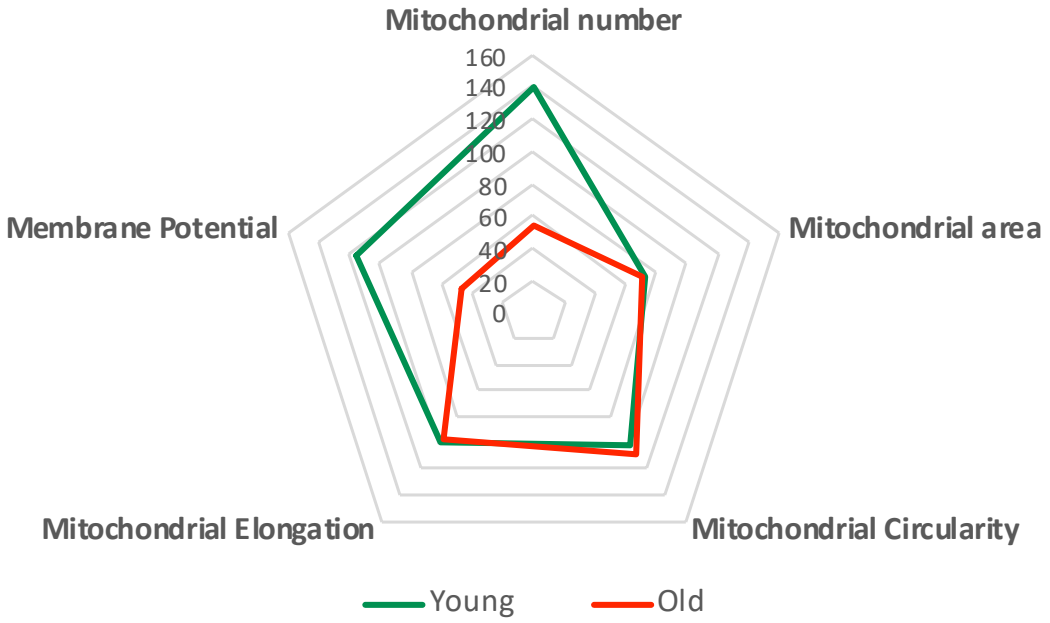

Figure 4.11 Analysis of mitochondrial parameters

Representation of the percentage differences in mitochondrial parameters in young (red) and old (green) relative to an unsorted population.

Most notably, using confocal microscopy, it was established that the decreased expression of mitochondrial proteins was accompanied by a reduction in the number of mitochondria per platelet. In unstimulated conditions, young platelets have 10±1 mitochondria per platelet compared to 5±1 mitochondria per platelet in old platelets (Figure 4.12A-C).

As mitochondria are dynamic organelles, having the capacity to undergo fission and fusion, I sought to establish if the reduction in mitochondria number in old platelets was as result of mitochondrial-fusion events, giving rise to fewer but larger mitochondria. Quantification of mitochondrial cross-sectional area, as a surrogate for mitochondria volume, indicated that there was no significant difference in the mitochondrial area 176±13nm^2 vs. 151±28nm^2 in young vs. old platelets (Figure 4.12D). Given that the mitochondria do not change size, this data indicates that loss of mitochondria during platelet ageing was not a result of mitochondrial fusion events. Indeed, further analysis of mitochondrial shape revealed there was no significant difference in overall shape, as indicated by mitochondrial elongation and circularity (Figure 4.12E-F).

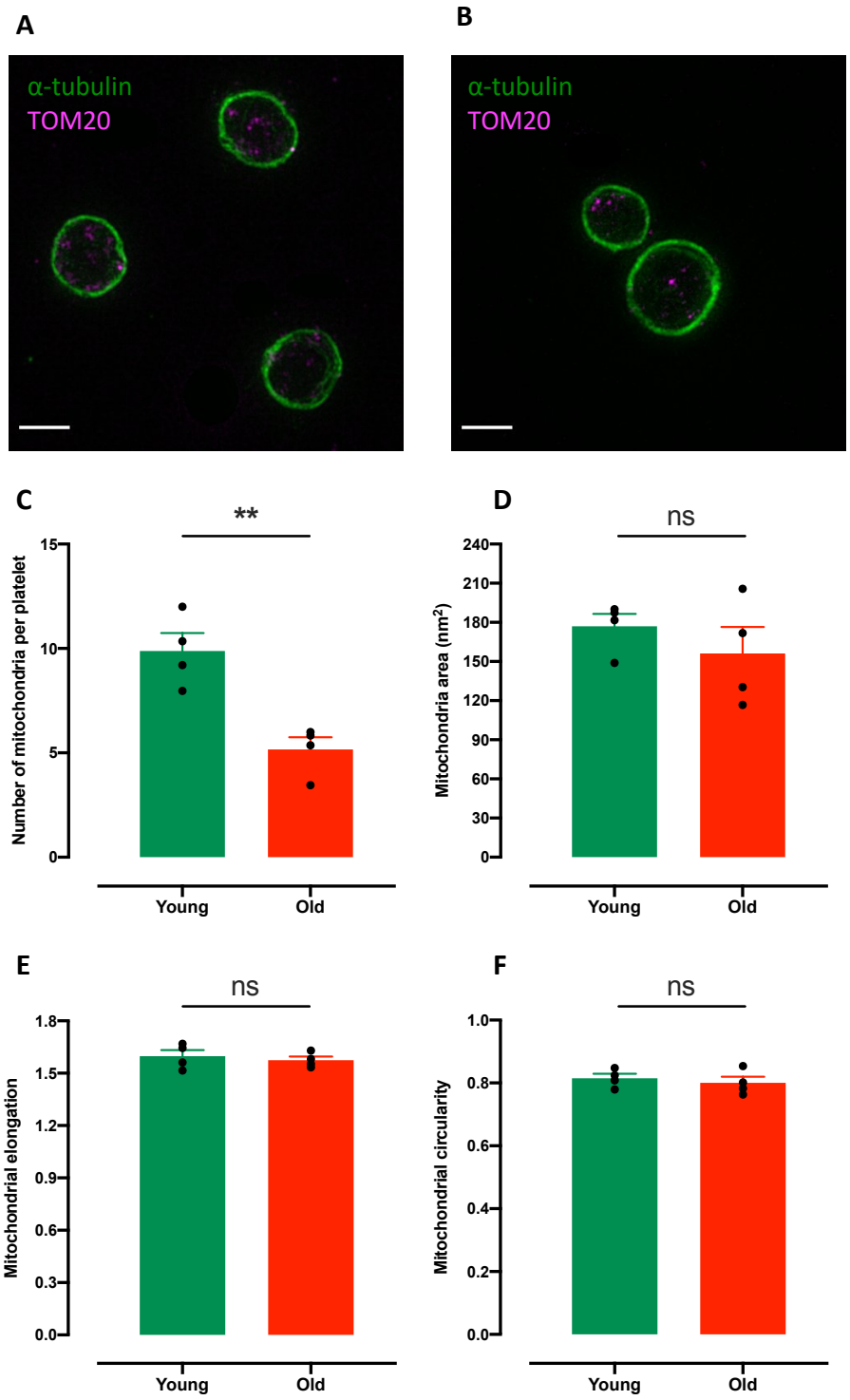

Figure 4.12 Immunofluorescence of mitochondria in young and old platelets

Immunofluorescence showing α-tubulin (green) and TOM20 (magenta; mitochondria) in **A.** young platelets and **B.** old platelets. Scale bar represents 2µm. Quantification of **C.** average number of mitochondria per platelet **D.** mitochondrial area **E.** mitochondrial elongation and **F.** mitochondrial circularity in young and old platelets. Data presented as mean±SEM, significance was determined by paired t-test (n=4, **p<0.01).

The reduction in mitochondrial number in old platelets supports the ingenuity pathway analysis prediction of a reduction in transmembrane potential of mitochondria. Flow cytometric analysis of MitoProbe^{TM} $DiIC_1(5)$ indicated that old platelets may have a significantly lower mitochondrial membrane potential compared to young platelets 86.4±9.7 arbitrary units (AU) vs. 191.7±28AU (Figure 4.13A). Interestingly, the lower mitochondrial membrane potential in old platelets was accompanied by an increase in phosphatidylserine exposure on the outer leaflet of the membrane, as indicated by a 3.1±1.3-fold change in annexin V binding relative to young platelets (Figure 4.13B).

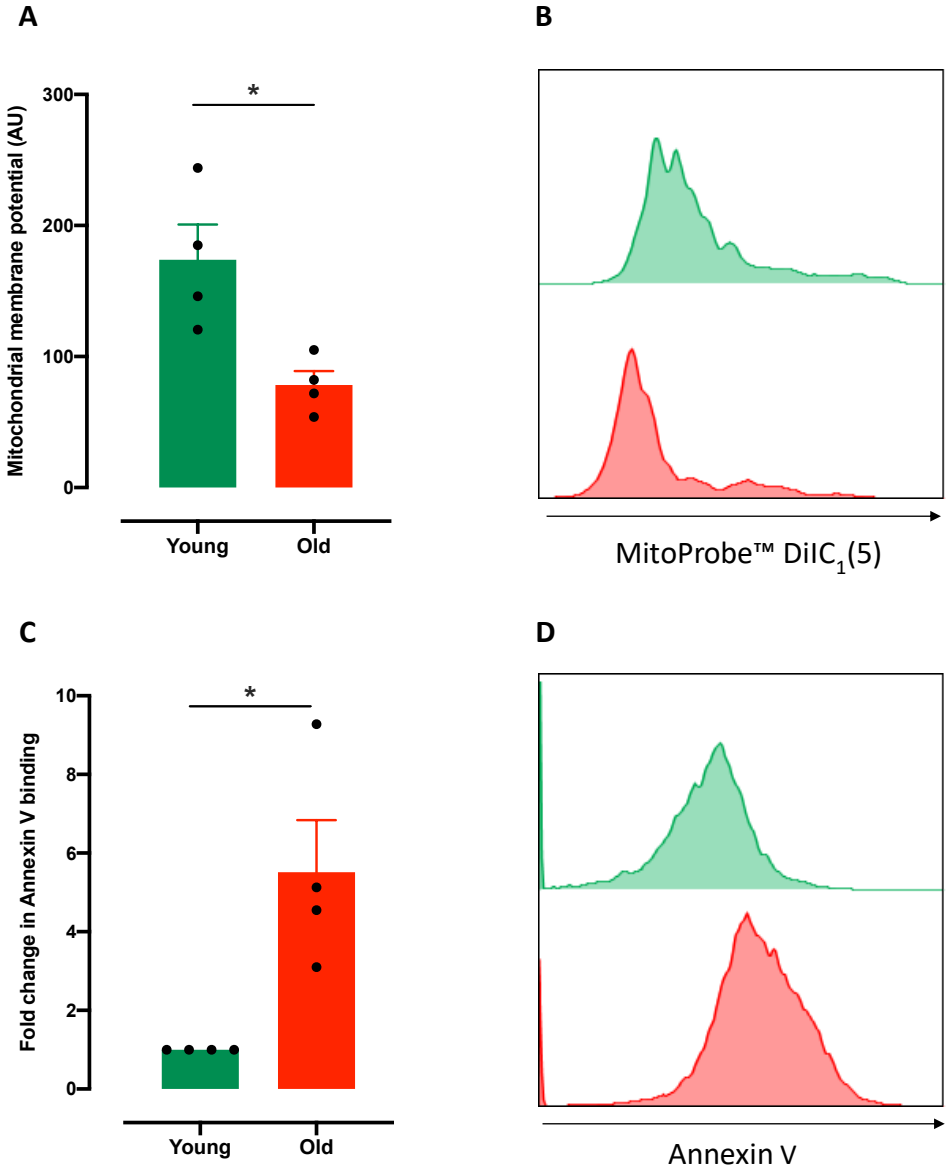

Figure 4.13 Flow cytometric analysis of young and old platelets

A. Flow cytometric analysis of mitochondrial membrane potential (MitoProbe™ $DiIC_1(5)$ fluorescence) in young and old platelets **B.** Representative histogram of MitoProbe™ $DiIC_1(5)$ fluorescence in young (green) and old (red) platelets. **C.** Analysis of phosphatidylserine exposure (annexin V binding) in young and old platelets. **D.** Representative histogram of annexin V fluorescence in young (green) and old (red) platelets. Data presented as mean±SEM, significance was determined by paired t-test (n=4, *p<0.05).

4.3.5 Platelet ageing causes a decrease in cytoskeletal-associated proteins and reduction in adhesive capacity

In addition to a reduction in mitochondrial proteins, proteomic analysis also identified a reduction in a number of cytoskeletal-associated proteins including gesolin, emerin, and twinfilin-2. Therefore, using immunofluorescence and confocal microscopy, I sought to understand if this reduction in cytoskeletal-binding proteins was associated with an altered cytoskeletal structure. Staining of resting platelets for α-tubulin demonstrated that old platelets have a significantly lower integrated fluorescence intensity of α-tubulin compared to young platelets seen as a reduction from 2435±354AU to 1034±79AU (Figure 4.14A-C). Notably, despite a reduction in α-tubulin there was no significant difference in platelet cross-sectional area, 8.0±0.5μm^2 vs. 7.6±0.6μm^2 in young vs. old platelets (Figure 4.14D).

Consistent with the loss of α-tubulin during platelet ageing, further investigation into the cytoskeletal structure identified a significant reduction in the integrated fluorescence intensity of F-actin from 2166±110AU in young platelets to 1364±139AU in old platelets (Figure 4.15).

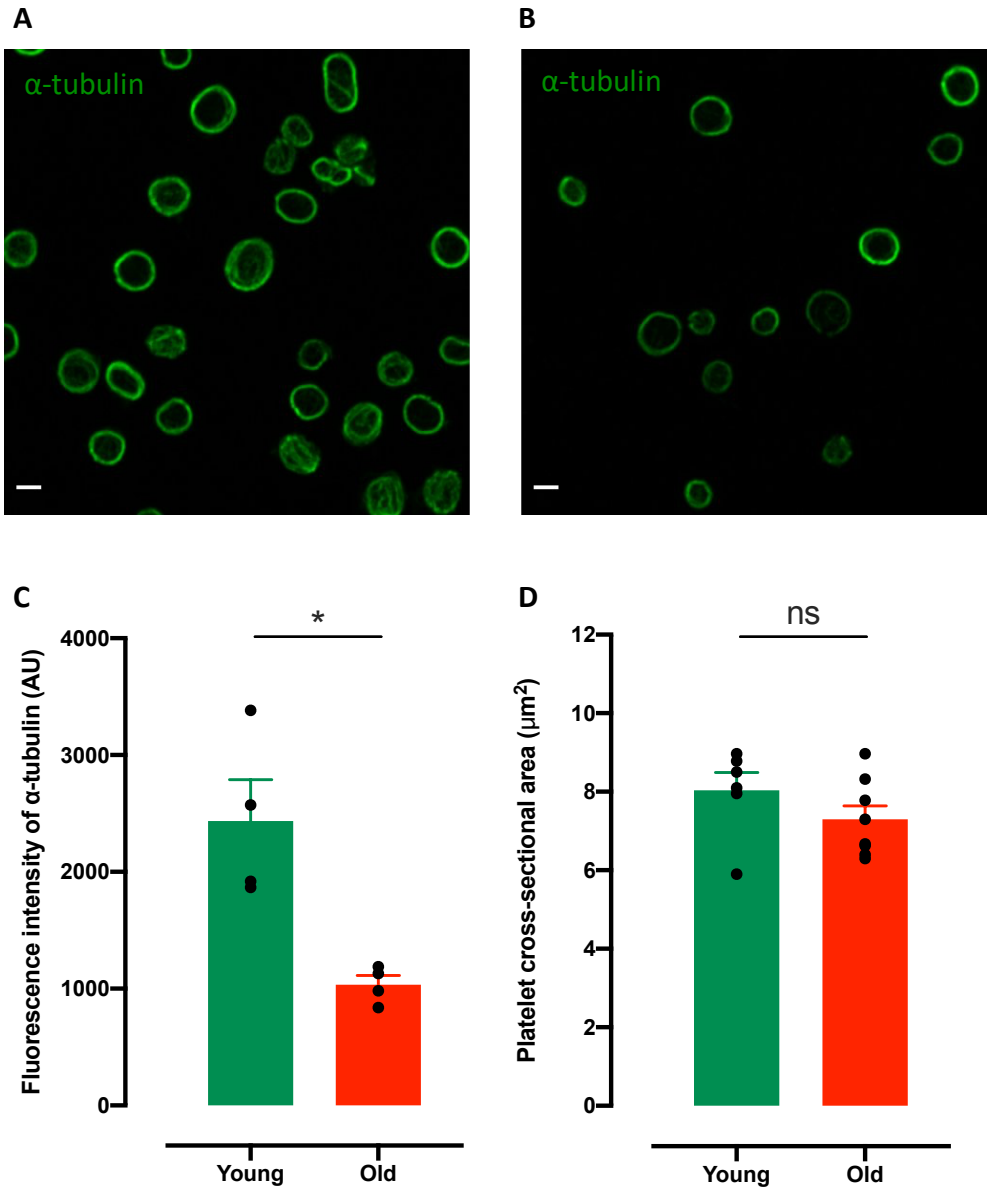

Figure 4.14 Immunofluorescence of α-tubulin in platelet subpopulations

Representative confocal images of **A.** young and **B.** old platelets stained for α-tubulin. Scale bar represents 2μm. **C.** Quantification of integrated fluorescence intensity of α-tubulin **D.** Quantification of platelet cross-sectional area. Data presented as mean±SEM, significance was determined by paired t-test (n=4-6, *p<0.05).

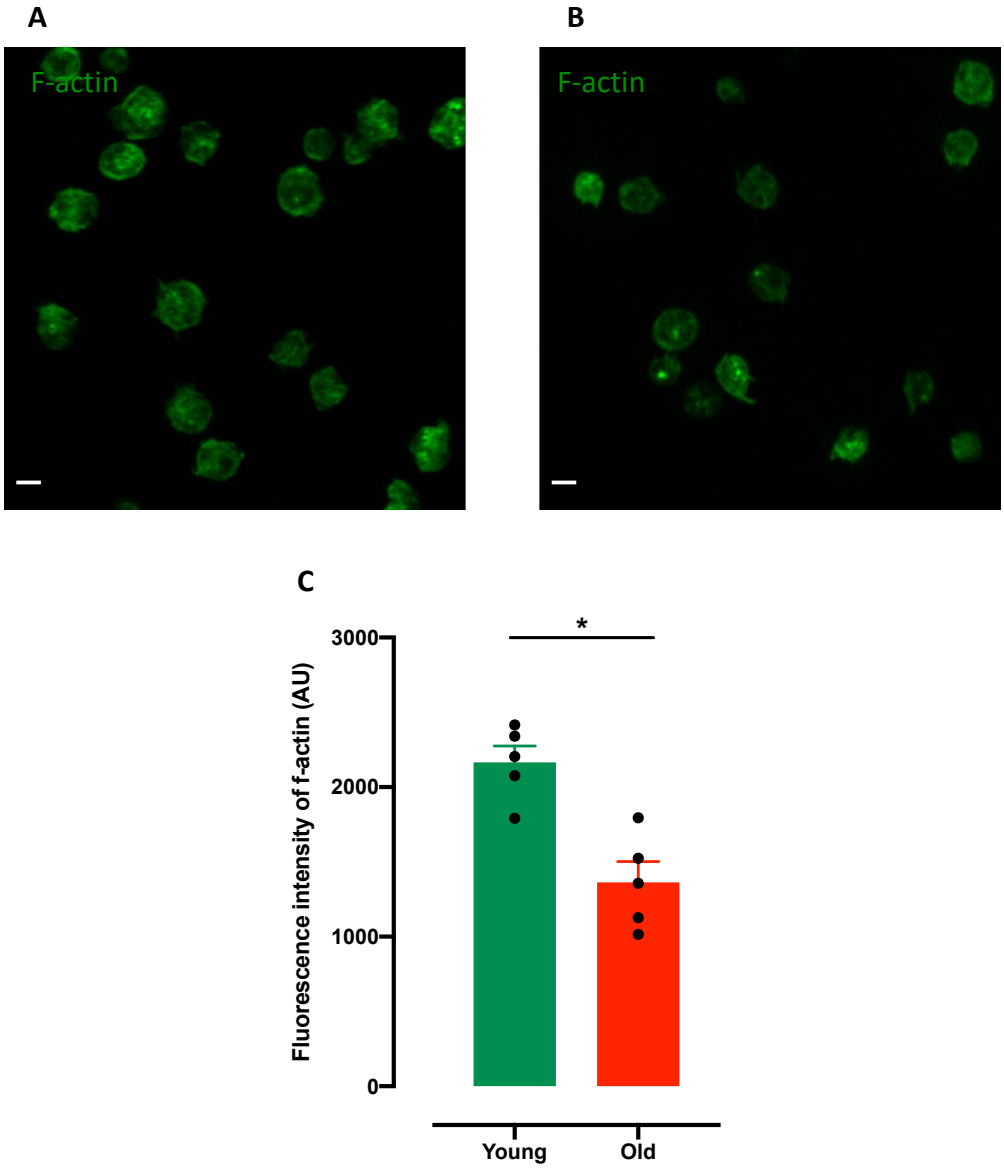

Figure 4.15 Immunofluorescence of F-actin in platelet subpopulations

Representative confocal images of **A.** young and **B.** old platelets stained for F-actin. Scale bar represents 2µm. **C.** Quantification of integrated fluorescence intensity of F-actin. Data presented as mean±SEM, significance was determined by paired t-test (n=4, *p<0.05).

As there was a notable decrease in the abundance of both α-tubulin and F-actin, it raised the question as to whether this alteration in the cytoskeletal structure impacted on the ability of platelets to adhere and spread. Using a static adhesion assay, it was established that old platelets have a marked defect in the adhesion and spreading response (Figure 4.16A-B). Following incubation on collagen, young platelets had adhered and spread, reaching a spread area of 14.8±3.2μm^2 (Figure 4.16A, C). Conversely, old platelets adhered, but did not spread, covering a significantly smaller area 6.2±0.5μm^2 (Figure 4.16B-C). Platelet adhesion and spreading proceeds through four stages (i) adherent but not spread, (ii) filopodia, (iii) lamellipodia and (iv) fully spread. Interestingly old platelets seem to arrest at the filopodia stage, whereas young platelet advance through to forming lamellipodia (Figure 4.16D).

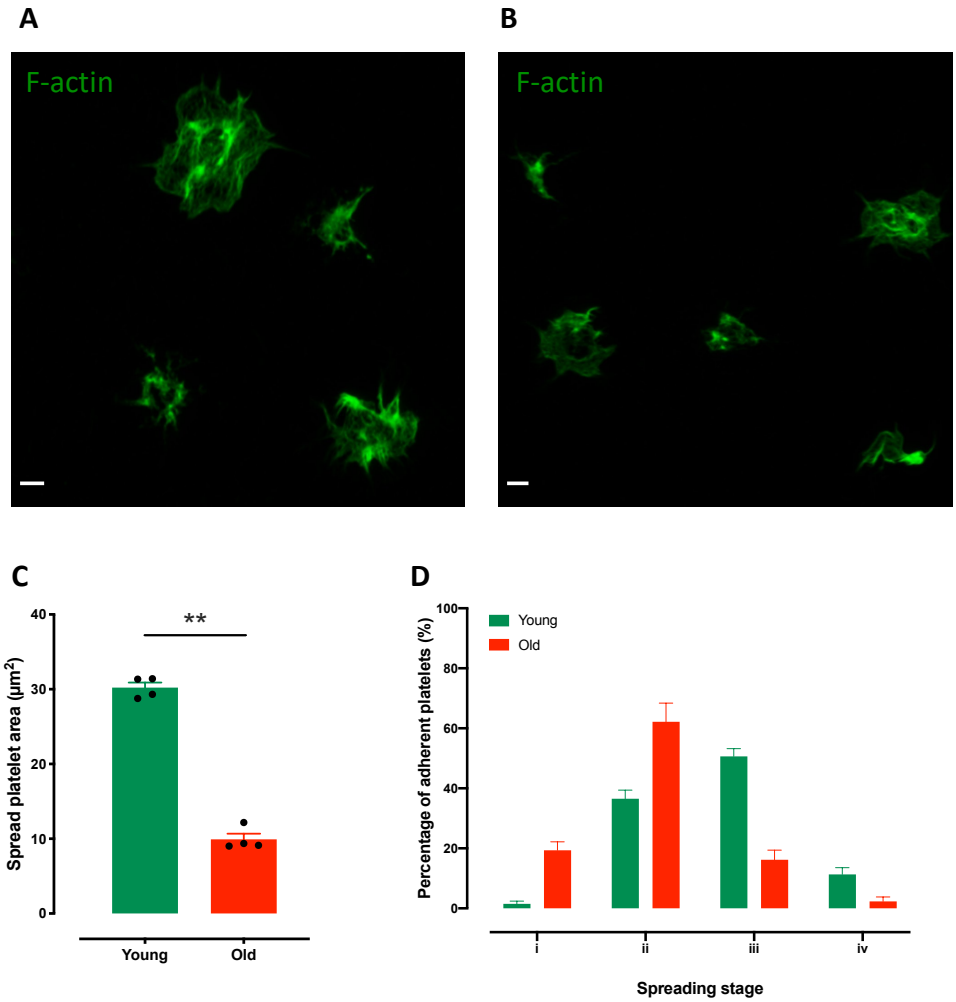

Figure 4.16 Immunofluorescence of adherent platelets spread on collagen

Representative confocal images of **A.** young and **B.** old platelets spread on collagen and stained for F-actin. Scale bar represents 2µm. **C.** Quantification of spread platelet area **D.** Quantification of stage of platelet spreading; adhered but not spread (i), filopodia (ii), lamellipodia (iii) and fully spread (iv). Data presented as mean±SEM, significance was determined by paired t-test (n=4, **p<0.01).

4.3.6 Intracellular protein components alter as platelets age

Amongst the proteins identified to have a significantly higher expression in young platelets were an array of organelle-associated proteins (Table 4.2). In addition to the reduction in mitochondria in old platelets, there is also a reduction in proteins associated with granules and the dense tubular system.

Table 4.2 Organelle-associated proteins with altered expression levels

Gene Name	Protein Name	Young Z-score	Old Z-score	p value
ATP5F1B	ATP synthase subunit beta, mitochondrial	1.168	-0.991	0.0001
CS	Citrate synthase	0.957	-0.812	0.0063
ESYT1	Extended synaptotagmin-1	0.854	-0.799	0.0247
GPD2	Glycerol-3-phosphate dehydrogenase, mitochondrial	0.813	-0.894	0.0147
HADHB	Trifunctional enzyme subunit beta, mitochondrial	0.957	-0.304	0.0224
HK1	Hexokinase-1	0.697	-1.049	0.0234
HSP70-10	10 kDa heat shock protein, mitochondrial	0.656	-1.105	0.0074
HSPA9	Stress-70 protein, mitochondrial	0.719	-1.007	0.0107
ME2	Malic enzyme	1.102	-0.534	0.0014
MT-CO2	Cytochrome c oxidase subunit 2	1.208	-0.325	0.0039
NNT	NAD (P) transhydrogenase, mitochondrial	0.927	-0.856	0.0096
RTN1	Reticulon-1	1.159	-0.534	0.0032
SLC25A3	Phosphate carrier protein, mitochondrial	0.996	-0.448	0.0127
SLC25A5	ADP/ATP translocase 2	0.805	-0.858	0.0305
SNAP23	Synaptosomal-associated protein 23	1.069	-0.134	0.0388
STIM1	Stromal interaction molecule 1	1.164	-0.671	0.0038
TUFM	Elongation factor Tu, mitochondrial	1.114	-0.908	0.0001

Immunofluorescence and confocal microscopy were used to confirm the proteomic analysis detailing a reduction in proteins associated with the dense tubular system. Analysis of unstimulated young and old platelets indicated a significant reduction in the fluorescence of ERp57 (Endoplasmic Reticulum protein 57), a protein localised within the dense tubular system, in old platelets compared to young platelets (93.5±10.7AU vs. 929.3±62.0AU; Figure 4.17).

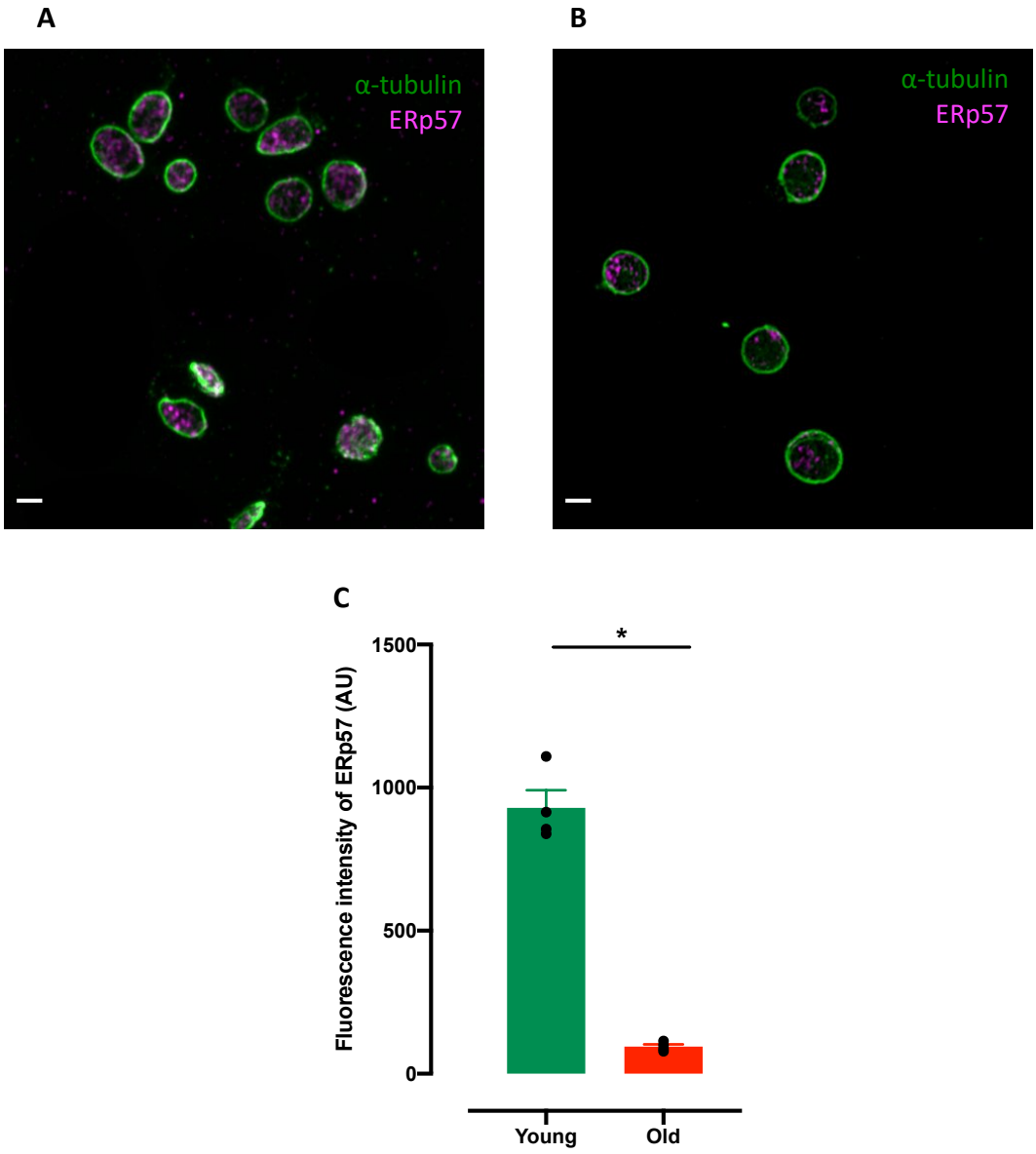

Figure 4.17 Immunofluorescence of ERp57 in platelet subpopulations

Representative confocal images of **A.** young and **B.** old platelets stained for ERp57 (magenta) and α-tubulin (green). Scale bar represents 2µm. **C.** Quantification of integrated fluorescence intensity of ERp57. Data presented as mean±SEM, significance was determined by paired t-test (n=4, *p<0.05).

Despite proteomic analysis revealing a relative decline in protein content, interestingly there was a small subset of proteins with a higher expression level in old platelets (Table 4.3). This subset was largely composed of circulating proteins including complement proteins, fibrinogen and haemoglobin, which may have been bound and internalised as the platelet aged within the circulation.

Table 4.3 Proteins with higher expression levels in old platelets

Gene Name	Protein Name	Young Z-score	Old Z-score	p value
A1BG	Alpha-1B-glycoprotein	-0.943	0.837	0.0193
C1S	Complement C1s subcomponent	-0.659	1.091	0.0063
C4A	Complement C4-A	-1.125	0.436	0.0153
C8G	Complement component C8 gamma chain	-0.983	0.956	0.0065
CFL1	Cofilin-1	-0.943	0.784	0.0149
CO5	Complement C5	-1.169	0.718	0.0042
FGA	Fibrinogen alpha chain	-0.639	1.059	0.0218
HBA	Hemoglobin subunit alpha	-0.284	1.080	0.0309
IGLL5	Immunoglobulin lambda-like polypeptide 5	-0.980	1.008	0.0008
ITIH2	Inter-alpha-trypsin inhibitor heavy chain H2	-0.881	0.755	0.0160
ITIH4	Inter-alpha-trypsin inhibitor heavy chain H4	-1.222	0.895	0.0002
PKHD1L1	Fibrocystin-L	-0.999	0.766	0.0023
PON1	Serum paraoxonase/arylesterase 1	-0.926	0.801	0.0248
PTBP1	Polypyrimidine tract binding protein 1,	-0.799	0.955	0.0207

To further explore the observed increases in protein expression, immunofluorescence analysis of complement proteins and fibrinogen was performed. In support of the proteomics, confocal microscopy confirmed that old platelets have significantly higher levels of fibrinogen compared to young platelets, 1438±178.8AU vs. 751.8±93.3AU (Figure 4.18). In further agreement with the proteomics, immunofluorescence indicated a significant increase in complement C4 levels from 1044±150.4AU in young platelets to 1866±180.7AU in old platelets (Figure 4.19). Interestingly, both fibrinogen and complement C4 were predominantly localised within the platelet cytoplasm, suggesting they are being bound and endocytosed.

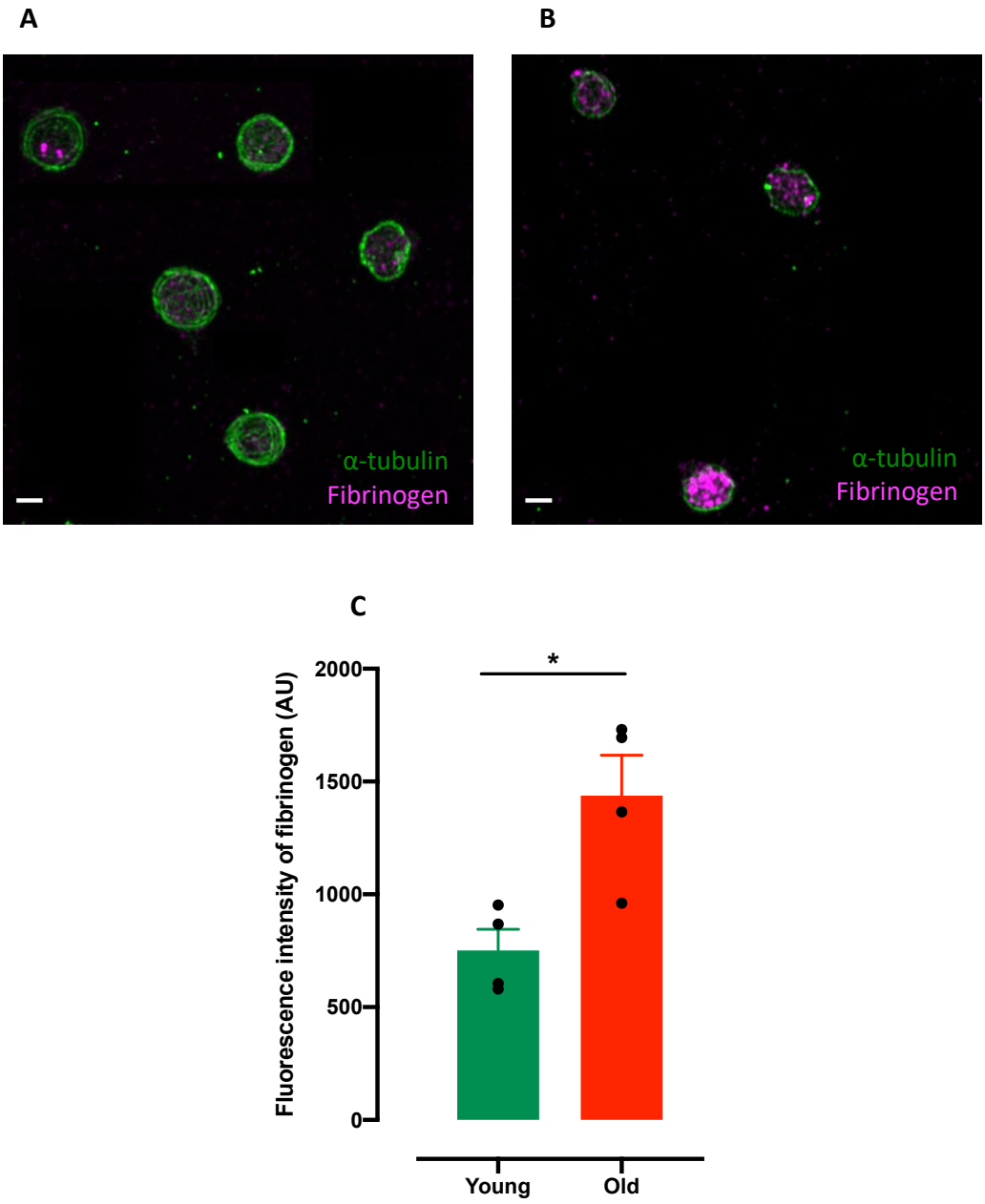

Figure 4.18 Immunofluorescence of fibrinogen in platelet subpopulations

Representative confocal images of **A.** young and **B.** old platelets stained for fibrinogen (magenta) and α-tubulin (green). Scale bar represents 2µm. **C.** Quantification of integrated fluorescence intensity of fibrinogen. Data presented as mean±SEM, significance was determined by paired t-test (n=4, *p<0.05).

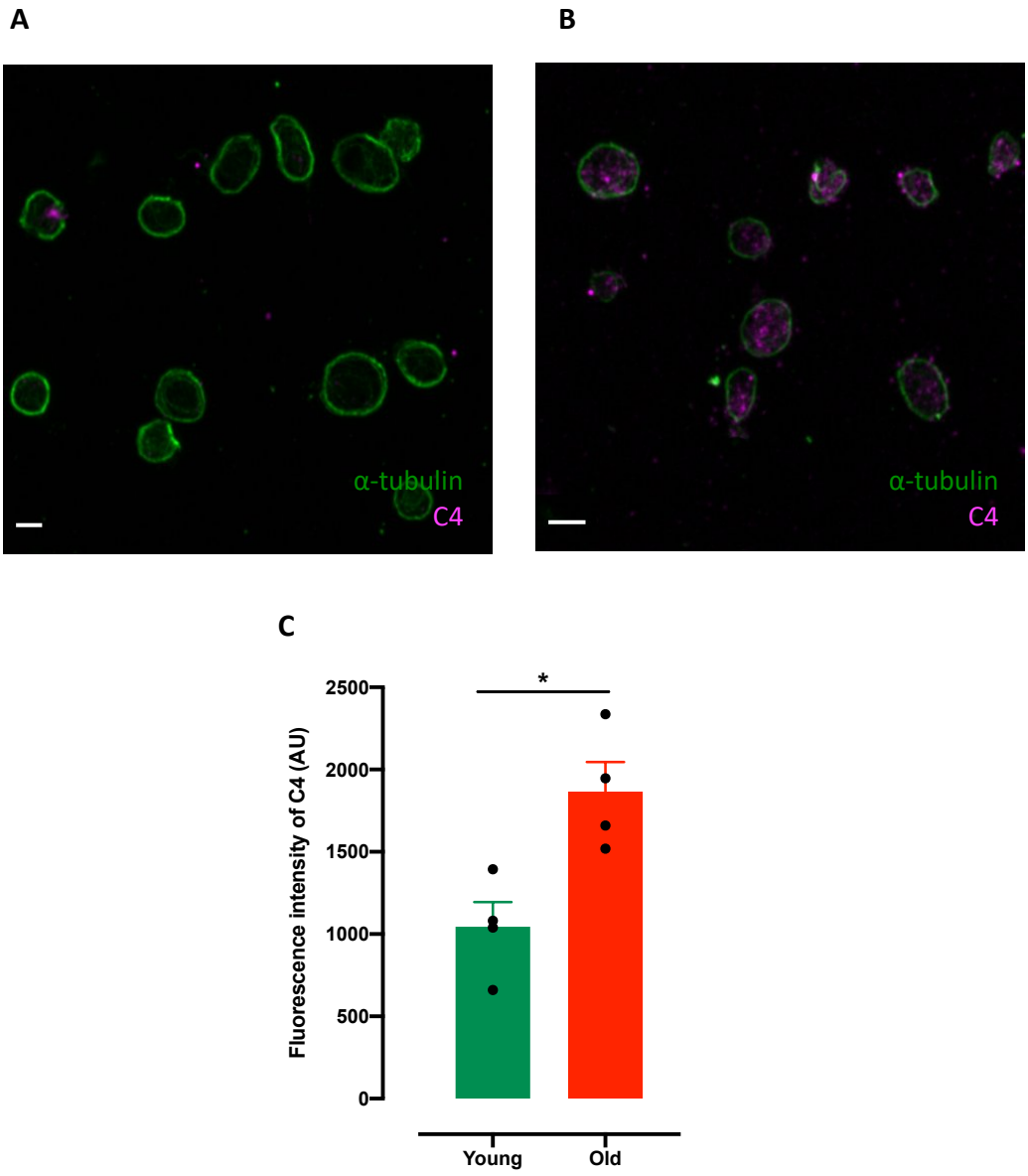

Figure 4.19 Immunofluorescence of complement C4 in platelet subpopulations

Representative confocal images of **A.** young and **B.** old platelets stained for complement C4 (magenta) and α-tubulin (green). Scale bar represents 2µm. **C.** Quantification of integrated fluorescence intensity of fibrinogen. Data presented as mean±SEM, significance was determined by paired t-test (n=4, *p<0.05).

4.3.7 Young platelets have an increased calcium signalling capacity

Proteomic analysis identified differential expression of a number of proteins involved in calcium handling and mobilisation, most notably STIM1, and subsequent ingenuity pathway analysis predicted that young platelets have an enhanced calcium flux as well as increased calcium quantity, compared to old platelets (Figure 4.8). As calcium signalling is fundamental for platelet activation pathways, it may be a contributing factor towards the predicted reduction in haemostatic function in old platelets. Therefore, to confirm the predicted differences, I sought to explore differences in calcium dynamics in young and old platelets.

Following stimulation with TRAP-6, young platelets had a more rapid and sustained calcium signal compared to old platelets. This stronger calcium signal was observed both at 10µM (AUC 7712±1684 vs. 2532±1221 in young vs. old platelets; Figure 4.20A-B) and 25 µM (AUC 8548±3024 vs. 3726±2053 in young vs. old platelets; Figure 4.20C-D). Indeed, stimulation with ionomycin revealed that young platelets have a higher maximal calcium signalling capacity compared to old platelets (AUC 69830±12864 vs. 27973±10195 in young vs. old platelets; Figure 4.20E-F).

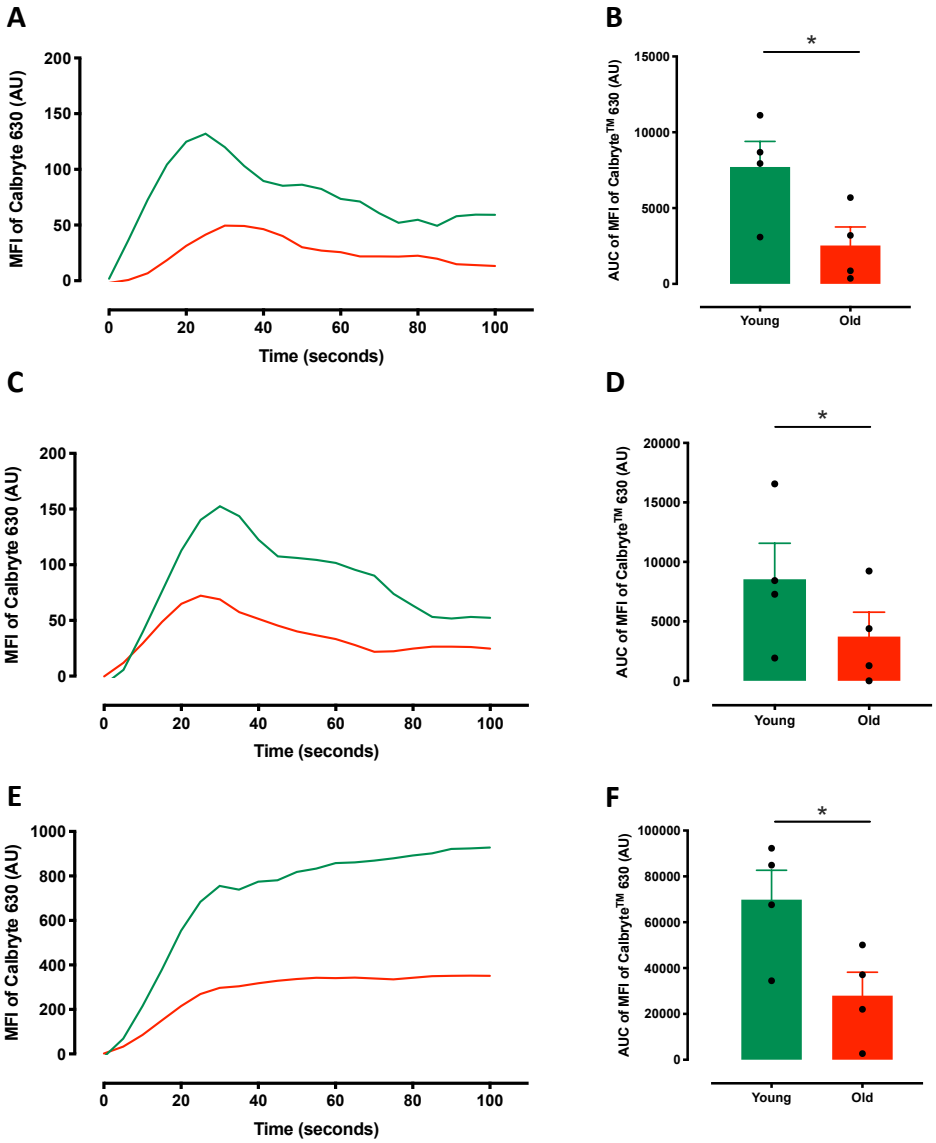

Figure 4.20 Calcium signalling in young and old platelets

Representative calcium dynamic trace (Calbryte 630 fluorescence) showing young (green) and old (red) platelets following incubation with **A.** 10µM TRAP-6 **C.** 25µM TRAP-6 **E.** 10µM ionomycin. Quantification of the area under the curve of Calbryte 630 fluorescence following incubation with **B.** 10µM TRAP-6 **D.** 25µM TRAP-6 **F.** 10µM ionomycin. Data presented as mean±SEM, significance was determined by paired t-test (n=4, *p<0.05).

4.4 Discussion

Understanding differences in platelet function across their lifespan is of particular interest due to emerging evidence suggesting alternative functions beyond haemostasis. In addition, young platelets are often described as being hyper-reactive, with a number of diseases in which there is heightened platelet turnover being associated with elevated thrombotic risk. Despite a number of studies indicating that young platelets are hyper-reactive, this work has been conducted using samples from individuals with underlying disease, such as diabetes or coronary artery syndrome, which may well influence other aspects of platelet function and the haemostatic response.[37]

The use of nucleic acid dyes to differentiate newly formed platelets is not a new technique and has been harnessed for routine assessment of platelet turnover.[41,240–242] However, our group is the first to use this approach to isolate differently aged platelet sub-populations with preserved function based on their RNA content. Interestingly, recent research has shown that thiazole orange staining correlates with the immature platelet fraction assessed by Sysmex XE-2100, however it has highlighted a stronger correlation with the nucleic acid dye, SYTO 13, and shows a long-lasting staining in comparison to thiazole orange.[243] Thus it may be beneficial to explore alternative nucleic acid staining protocols to ensure robust, long-lasting staining.

There have been conflicting reports on the utility of using nucleic acid dyes and platelet size to differentiate between newly formed and old platelets.[241] However, in my work I have definitively shown that separation of platelets based on thiazole orange fluorescent intensity results in two populations of platelets with comparable cross-sectional areas.

Proteomic analysis of sorted platelet subpopulations allowed me to gain a global understanding of changes in protein levels during platelet ageing and subsequently the pathways that could be affected. Given that platelets lack a nucleus and have a

very limited translation capacity, it is unsurprising that protein content progressively declines during platelet ageing, along with the number of detectable proteins. Using the absorbance 280nm (A280) protein setting on the NanoDrop may not have been the most accurate method to calculate the protein content of the sorted platelets as these values may have been influenced by the absorbance of RNA.[244] Whilst there is inbuilt intelligence technology to detect nucleic acid contaminants and correct the protein concentration based of this, these values should be used with caution. Using the bicinchoninic acid (BCA) assay would have been preferable to establish a more robust protein concentration however in these circumstances I was restricted by the volume of sample I was able to use before the proteomic analysis.[244]

Analysis of protein expression patterns in the whole platelet proteome indicated that intermediate and old platelets cluster together with a similar expression profile, suggesting that the progressive degradation of protein begins very soon after release into the circulation. In addition to protein degradation pathways, the reduction in proteins may be as result of microvesicle release, a process that has been well documented in platelets.[152] Classically, the shedding of microvesicles occurs in response to stimuli such as activation, sheer stress or apoptosis, however it may be possible that microvesicles are passively released as platelets age within circulation.[151] Interestingly, the proteins that exhibited the greatest decline were proteins involved in dynamic processes, most notably those associated with mitochondria and the cytoskeleton. Here I propose, that the reduction in these subsets of proteins may be influencing two main pathways; platelet activation and apoptosis.

The striking reduction in mitochondrial proteins revealed by proteomic analysis raised the question as to whether the number of mitochondria changes as platelets age. In agreement with the proteomic data, confocal microscopy demonstrated a reduction in the overall number of individual mitochondria. This observed reduction supports recent work indicating that old murine platelets have fewer mitochondria than newly formed platelets.[245]

The mechanism behind the reduction in mitochondria remains unclear, however I speculate that it could be as a result of the engagement of two pathways; firstly, mitochondrial fusion and secondly, mitophagy. Mitochondria are dynamic organelles with the ability to undergo both fission and fusion. During mitochondrial fusion, the dynamin-related GTPases Mfn1 and Mfn2 facilitate the coordinated fusion of the outer and inner membranes, forming a larger mitochondrion or network of mitochondria.[246] As there was no observed increase in the cross-sectional area of mitochondria it can be concluded that the reduced number of mitochondria was not as a result of fusion events. The use of confocal microscopy to determine mitochondria number and size needs to be used with caution. As platelet mitochondria are small, I was working close to the resolution limit of the airyscan confocal microscope, meaning that it may not have provided accurate measurements of the mitochondria size. Quantification of mitochondria number using the airyscan microscope is more robust than mitochondria size, however it may be an underestimation of number. Whilst Z-stack images allow the for the visualisation of mitochondria in multiple fields of view, there is a possibility that some of the mitochondria may be masked behind each other. The ideal method to determine mitochondria number and size would be to use electron microscopy as the resolution limit is far greater. This technique would prove challenging, as the quantities of platelets that can be sorted is too low to create a visible pellet, and thus the samples would not be suitable to be prepared of electron microscopy.

As mitochondrial fusion appears to be unaltered during platelet ageing, I therefore propose that the reduction of mitochondria is as a result of mitophagy. As platelets age within the circulation, they will encounter cellular stresses leading to the accumulation of mitochondrial damage. Mitochondrial stress will lead to a loss of mitochondrial membrane potential initiating the PINK1/PARKIN mediated mitophagy pathway.[247] In this process, loss of mitochondrial membrane potential causes PINK1 to remain on the outer mitochondrial membrane therefore recruiting PARKIN from the cytosol to the outer mitochondrial membrane. The presence of PARKIN facilitates the ubiquitination of membrane substrates, subsequently recruiting cytoplasmic factors, such as p62 and LC3.[248] The engagement of these proteins, may target the

damaged mitochondria for autophagosomal degradation leading to a reduced number of mitochondria in old platelets. Whilst I have shown that old platelets have a mitochondrial membrane potential, which may be a trigger for the engagement of mitophagy, this data may be misleading as the lower fluorescence intensity may be indicative of the reduction in the number of mitochondria rather than membrane potential. To fully understand whether there is a reduction in membrane potential in old platelets, flow cytometry using two mitochondrial dyes; a mitochondrial mass dye and a mitochondrial membrane potential dye, would allow for the calculation of a ratio between mass and membrane potential. Unfortunately, the mitochondrial mass dye has substantial spectral overlap with thiazole orange and thus this was not possible.

My data indicates that platelet ageing is associated with a loss in mitochondria which may affect two functional pathways; platelet activation and apoptosis. Platelets are highly metabolically active, relying on both glycolysis and oxidative phosphorylation, the latter of which accounts for approximately 40% of the total ATP synthesis.[116] Following activation, the energy demand for platelets rapidly increases resulting in an upregulation in ATP synthesis via oxidative phosphorylation at the mitochondria.[209] The dramatic reduction in mitochondrial number observed in old platelets will result in a markedly reduced capacity for ATP synthesis via oxidative phosphorylation that may well reduce old platelets' ability to undergo full activation and adhesion, resulting in an impairment in haemostasis. In addition to the data presented here, our laboratory has shown that old platelets have a reduced capacity to synthesise eicosanoids and express P-selectin on their surface, supporting the notion that as platelets age their haemostatic function declines.

The decline in cytoskeletal proteins may also be a contributing factor towards the reduction haemostatic function. It is well documented that the cytoskeleton is intimately linked to platelet activation, adhesion and secretion, therefore a loss of cytoskeletal proteins will affect platelet haemostatic functions.[249] Here, I have shown that old platelets have an impaired ability to spread on collagen, arresting at the filopodia stage, failing to form lamellipodia and fully spread. Proteomic analysis

revealed a decline in several actin-binding proteins including twinfilin-2, emerin and gelsolin. These proteins are involved in actin dynamics facilitating the conversion between globular and fibrillar actin via polymerisation at the actins barbed ends.[250] Platelet adhesion and spreading begins by platelets losing their characteristic discoid shape, becoming smaller and rounder. The cytoskeletal rearrangement then proceeds by the polymerisation of actin leading to the formation of long protrusions called filopodia.[50] The marked defect in spreading of old platelets is highly suggestive of the loss of cytoskeletal-associated proteins having a detrimental effect on these processes.

Mitochondria loss may also influence the engagement of apoptotic pathways. As detailed above, a key step of mitophagy, is the loss of mitochondrial membrane potential, this phase is also a trigger for the exposure of phosphatidylserine on the outer leaflet of the platelet membrane.[251] Further supporting the higher levels of phosphatidylserine exposure, emerging evidence suggests that the cytoskeleton plays an important role in maintaining the asymmetric distribution of anionic phospholipids within the platelet plasma membrane.[252,253] Degradation of actin and tubulin as identified in old platelets, may cause an instability, leading to an imbalance in the asymmetry of the lipid membrane and so facilitating the exposure of phosphatidylserine on the platelet outer membrane.[254]

The exposure of phosphatidylserine has two functions; firstly, acting as procoagulant platform, and secondly, and perhaps more relevantly, acting as an apoptotic signal.[255] In my work, phosphatidylserine exposure was found to be significantly higher in unstimulated old platelets. Under these circumstances, it is unlikely that the increased phosphatidylserine exposure would be a procoagulant trigger, as these platelets were unstimulated and did not demonstrate elevation in additional markers of activation, such as P-selectin, nor did they show an increase in size associated with ballooning procoagulant activity.[256] Therefore, I suggest that old platelets may be committing to an apoptotic fate, with the phosphatidylserine exposure acting as an ‘eat-me’ signal, marking them for destruction and clearance from the circulation.

Interestingly, knockout murine models two of proteins identified as having significantly lower expression levels in old platelets, twinfilin-2 and SNAP23, have shown an accelerated platelet turnover suggesting these proteins may be instrumental in determining platelet lifespan.[257,258] However, these studies reported that hyper-reactive platelets may be a contributing factor to an enhanced clearance, and therefore turnover. Conversely, I speculate that the decline in twinfilin-2 in my work, may be contributing to a reduction in structural integrity and therefore a decline in function.

My data provides novel insights into the mechanisms that may be influencing platelet lifespan. Understanding the increased exposure of phosphatidylserine, which may be controlled by both mitochondrial and cytoskeletal loss, may provide interesting insights into the increased platelet turnover in pathological states. Emerging evidence has revealed that oxidative stress plays an important role in the progression and pathogenesis of diabetes mellitus, a disease associated with accelerated platelet turnover. Further research has indicated that oxidative stress is linked to alterations in mitochondrial function in diabetic patients.[259] This interesting research in the context of the data presented in the chapter may indicate that oxidative stress experienced during the pathogenesis of diabetes mellitus leads to the accumulation of mitochondrial damage within the platelet. The resulting depolarisation of the mitochondrial membrane facilitates the exposure of phosphatidylserine on the outer leaflet of the plasma membrane, acting as a signal for the destruction of the platelets and so accelerating platelet turnover. In confirmation of this theory, a recent study has demonstrated that mitochondrial dysfunction in platelets isolated from diabetic patients is associated with higher phosphatidylserine exposure and increased mitophagy.[148]

It is widely debated whether newly formed platelets are larger, with a number of studies showing an association between mean platelet volume and thrombotic risk.[236,260] However, in my work I demonstrate clearly no association between platelet age and size, despite the significant reduction in structural proteins. These findings may support research from the 1980s, in which it was proposed that buoyant

density, but not size, is an accurate indicator of platelet age.[261] With the loss of large quantities of structural proteins as well as mitochondria and dense tubular proteins, it seems probable that the old platelets will be less dense than young platelets despite maintaining a similar size. Interestingly, the report from the 1980s, the indicated that platelets with a greater buoyant density were more metabolically active, which may be indicative of a greater mitochondrial number.[261] Despite the discrepancies in platelet size, a recent proteomic study looking at differences between large and small platelets revealed a reduction in a number of mitochondrial and cytoskeletal proteins in small platelets.[262]

Here I have shown that the decline in protein content associated with ageing is linked to a reduction in calcium signalling capacity, suggesting a reduction in haemostatic function. Indeed, this work supports research conducted by my colleague indicating that old platelets have a marked reduction in both α- and dense granule secretion, measured by P-selectin expression and ATP luminescence (unpublished data). Interestingly the ingenuity pathway analysis predicted a reduction in calcium flux and quantity of calcium, which I confirmed using flow cytometry. However, these samples were analysed in the presence of extracellular calcium and as such it is surprising that there were large changes in the calcium signal induced following stimulation with ionomycin. This could be for two reasons: firstly, the intracellular stores of calcium could be significantly lower in old platelets, such that they can't potentiate the signal from outside; secondly, given the observed differences in the cytoskeletal structure, this might be affecting the membrane and the subsequent uptake of the calcium dye.

Platelet ageing is associated with a general decline in protein content, but interestingly I identified a small subset of proteins that increase in abundance as platelets age within the circulation. Within this subset, the majority are circulating proteins which could be bound and accumulate within the platelet as they circulate within the vasculature. It is now widely accepted that platelets have the ability to sequester molecules from within the circulation, with a number of studies indicating a role for platelets in the transport of angiogenic and metastatic factors. [263,264] Here, I have shown that old platelets have increased levels of proteins involved in immune

responses such as complement proteins and immunoglobulin polypeptides. Interestingly, these proteins localise predominantly within the cytoplasm suggesting they are being bound by the platelet and actively endocytosed. With the growing body of evidence detailing the role of platelets in inflammation and immunity, the accumulation of this subset of proteins raises the question as to whether platelet ageing may be associated with a switch in phenotype from a rapid haemostatic role to an inflammatory regulatory role.[265,266]

The data presented in the chapter may provide insights into the mechanisms governing platelet lifespan and the associated changes in function. Here I propose, that platelet ageing is characterised by a progressive decline in mitochondrial and cytoskeletal proteins, affecting the buoyant density, but not the overall size of the platelet. In addition, newly formed, young platelets are rapid haemostatic responders with an enhanced adhesive ability coupled to strong calcium signalling capacity. Whilst beyond the scope of this work, the increased levels of circulating proteins associated with old platelets, raises interesting questions as to whether old platelets may have a role distinct from young platelets.

Given the importance and central role of mitochondria highlighted here, the following chapter will explore the effect of platelet activation on platelet mitochondria and the subsequent effects these may have upon other cells.

5 Investigating mitochondrial dynamics during platelet activation and the significance of the production of platelet-derived microvesicles

5.1 Introduction

Mitochondria have a myriad of functions from energy production, calcium buffering, and reactive oxygen species metabolism to involvement in apoptosis pathways.[267] Extensive characterisation of mitochondria in other cell types such as neurons has revealed controlled transport of mitochondria and their appropriate distribution is essential for cell survival.[268] Indeed, mitochondrial distribution is controlled through complex coordination of microtubules and actin microfilaments, mediating long-range and short-range movement respectively.[269–271] Given that platelets are significantly smaller than neurons and they do not exhibit the same cell polarisation, the need for mitochondrial trafficking is unclear.

In addition to appropriate mitochondrial distribution, maintenance of mitochondrial health is crucial to support cellular integrity. Highly regulated processes seek to resolve mitochondrial impairments, through fission and fusion, and subsequently remove damaged mitochondria, through mitophagy. As platelets have a short lifespan of approximately 10 days, the necessity of these pathways to control mitochondrial health can be questioned. Interestingly, two mitophagy pathways have been described in platelets, PINK1/PARKIN and the FUNDC1 pathway, the latter of which is engaged under hypoxic conditions.[128,131] Despite the identification of these two pathways, recent work has demonstrated that PINK1, a fundamental part of PINK1/PARKIN mitophagy is dispensable for platelet function.[129] However, the induction of mitophagy in platelets from diabetic patients has been shown to be beneficial, protecting the platelets from severe oxidative stress.[148]

Beyond the pathways involved in maintaining mitochondrial health, the majority of interest in platelet mitochondria has focussed on their role in supplying energy

required for adhesion, aggregation and secretion. However, the role of mitochondria in platelets is ever expanding. Recent evidence suggests an important role in mitochondria in apoptosis and the control of platelet lifespan, with the progressive decline of Bcl-X_L, facilitating BAX activation and subsequent permeabilization of the outer mitochondrial membrane (OMM).[123] Consequently, loss of mitochondrial membrane potential allows the release of cytochrome C, thereby enabling the exposure of phosphatidylserine on the platelet outer membrane.[24]

Moreover, strong agonist stimulation, has been shown to cause mitochondrial membrane depolarisation, and subsequent opening of the mPTP in the inner mitochondrial membrane (IMM).[272] This process is reliant on the mitochondrial matrix protein, cyclophilin D, interacting with the adenine nucleotide translocator, in the IMM and the voltage-dependent anion channel in the OMM.[273] Interestingly, recent work has shown that the formation of the mPTP is involved in some of the initial stages of platelet activation, including phosphatidylserine exposure and fibrinogen retention.[273,274] However, the opening of the mPTP occurs only in a small subset of platelets, enabling them to become highly activated, and often procoagulant. While potentially very important, the molecular processes governing the mPTP formation and its functional significance remain elusive.[275]

Interestingly, recent research has indicated that platelets have the capacity to release their mitochondria.[156] The functional relevance of this process remains to be demonstrated, but early data indicates that they may be acting as an inflammatory stimulus to other target cells. Indeed, mitochondria release has been identified from a number of cell types, with mitochondria released from activated monocytes exerting an inflammatory response on endothelial cells.[276] Despite many observations classifying mitochondria as damage-associated molecular patterns (DAMPs), and therefore inducing inflammatory responses, other research has detailed transfer of mitochondria between cells, which has been shown to be beneficial as it can rescue deficiencies in respiration, and replenishment of mitochondrial DNA.[277] This research demonstrates that mitochondria can be released as free organelles or encapsulated within a single membraned

microvesicles. It is well established, that platelets readily produce microvesicles during activation as well as apoptotic pathways, with higher levels being reported in a number of pathological states.[152] This poses the question as to whether microvesicle and mitochondria release may cooperate in affecting other cells within the vasculature, either through alterations in surface marker expression or by uptake and changes intracellularly.

To date, research into platelet organelles has focussed primarily on granules, presumably as these are a unique feature to platelets, and are fundamental for the haemostatic response. As such, until recently, research into platelet mitochondria has been largely overlooked, as their role was thought to be limited to energy production. However, current work has highlighted that mitochondria may play an important role beyond energy production both in modulating platelet phenotype, as well as influencing the behaviour of other cells within the circulation. Despite the recent advances in platelet mitochondrial research, the contribution of mitochondria to platelet function still remains to be fully explored. Thus, in this chapter I will investigate the role of mitochondria dynamics during platelet activation, and the subsequent effect of the presence of extracellular mitochondria on leukocyte function.

5.2 Methods

5.2.1 Blood collection, preparation of PRP and washed platelets

Blood was collected from healthy volunteers and PRP was prepared as previously described in sections 3.2.1-3.2.3

5.2.2 Immunofluorescence confocal microscopy of activated platelet samples

Washed platelets (3 x 10^8/ml) were stained with MitoTracker Orange CMTMRos (20nm) for 15 minutes at room temperature in the dark and subsequently incubated with eptifibatide (4µM) for 5 minutes. Platelets were incubated with PBS or TRAP-6 (25µM) for 5 minutes at 1200rpm, 37˚C and subsequently fixed with pre-warmed PFA (4%) for 10 minutes. Samples were prepared for immunofluorescence as described in 4.2.4. Briefly, samples were centrifuged onto poly-l-lysine coverslips at 600 *x g* for 5 minutes. Non-adherent platelets were removed from the coverslips by washing with filtered PBS. Samples were blocked and permeabilised with filtered permeabilising buffer (0.2 % Triton, 2% donkey serum and 1% BSA in PBS) for 30 minutes at room temperature. After removal of the blocking buffer, the coverslips were incubated with mouse anti-α-tubulin (1:200) for 1 hour at room temperature in the dark. The primary antibody was removed with three wash steps using filtered PBS. Subsequently, the samples were incubated with anti-mouse Alexa Fluor 488 (1:500) for 45 minutes in the dark at room temperature. The secondary antibody was removed with three filtered PBS washes. The coverslips were mounted using ProLong Diamond antifade mount and allowed to set overnight in the dark at room temperature. Samples were then stored at 4˚C and imaged on Zeiss LSM880 with airyscan; 63x objective, 1.4 Oil DICII; imaging at least 5 different fields of view per sample collecting a minimum of 30 platelets per sample. Image processing and analysis was conducted using Zen Software (2.3 SP1) and ImageJ.

5.2.3 Assessing mitochondrial fission following platelet activation

Washed platelets (3 x 10^8/ml) were stained with MitoTracker Orange CMTMRos (20nm) for 15 minutes at room temperature in the dark and subsequently incubated with eptifibatide (4µM) for 5 minutes. Platelets were activated with PBS or TRAP-6 (25µM) for 5 minutes or 30 minutes at 1200rpm, 37˚C and subsequently fixed with pre-warmed PFA (4%) for 10 minutes. Samples were prepared for immunofluorescence as outlined in 5.2.2.

5.2.4 Microvesicle production in response to collagen activation

Ibidi chambers were incubated with collagen (100µg/ml) for 1 hour, subsequently blocked with fatty acid free BSA (1%) for 1 hour and then washed with modified Tyrode's HEPES buffer. Washed platelets were stained by incubation (37˚C in the dark) with Fluo-4 AM (2µM) for 30 minutes and MitoTracker Orange CMTMRos (10nm) for 15 minutes. Stained platelets were allowed to settle and activate on the collagen coated chambers and images were recorded for 15 minutes, capturing 2 frames per second.

5.2.5 Preparation of platelet-derived microvesicles

Washed platelets were statically incubated with PBS or TRAP-6 (25µM) at 37˚C for 2 hours in non-stick Eppendorf microcentrifuge tubes. Subsequently, platelets were centrifuged at 1000 *x g* for 10 minutes and the supernatant was removed and transferred into a fresh non-stick Eppendorf microcentrifuge tube. The supernatant was then centrifuged at 18,000 *x g* for 45 minutes to pellet the platelet-derived microvesicles. The supernatant was removed and discarded, and the microvesicle pellet was resuspended in 100µl of filtered PBS. Samples were stored at -80˚C until required.

5.2.6 NanoSight Tracking analysis

NanoSight tracking analysis (NS300 NTA) was used to determine the size and concentration of platelet-derived microvesicles. Briefly, nanoparticle tracking is based on Brownian motion, and measures the diffusion constant as determined by the scattering of a laser beam by the particles which is detected by an ultramicroscope. Based on the laser scattering, the software tracks the particles' movement and provides a measure of their size and concentration. Microvesicles samples were diluted 1 in 10 in 1ml filtered PBS and analysed using a flow rate of 50AU. To determine microvesicle size and concentration, 5 videos of 60 seconds were acquired and analysed per sample.

5.2.7 Flow cytometric characterisation of platelet-derived microvesicles

Platelet microvesicles were prepared as described in 5.2.5. However, prior to stimulation, washed platelets were stained with MitoTracker Orange CMTMRos (10nm) for 15 minutes. Following stimulation, the remaining platelet pellet was retained, stained with CD61-APC (1:200) and analysed on a BD LSRII to determine the fluorescence of MitoTracker Orange CMTMRos. The purified platelet-derived microvesicles were stored at -80˚C until required. Samples were thawed at 4˚C prior to staining and incubated with antibody cocktails detailed in Table 5.1 for 30 minutes in the dark and analysed on either a BS LSR II or an Image Stream^{x} MKII.

To determine differences in the number of microvesicles produced following incubation with PBS or TRAP-6, samples were analysed for 60 seconds based on side scatter for basal number or PE triggered for mitochondria positive vesicles.

Table 5.1 Antibodies used for flow cytometric analysis of platelet microvesicles

	Antibody	Concentration
Sample 1	Cell Trace Violet CD41 APC	1:50 1:200
Sample 2	CD41 Pacific blue CD62P APC	1:200 1:150
Sample 3	CD41 Pacific blue Annexin V APC	1:200 1:150

5.2.8 Assessment of mitochondrial function, measure by oxygen consumption in a XF24 Seahorse in platelet-derived microvesicles

To understand if the mitochondria in platelet-derived microvesicles are active, the Agilent Seahorse XF24 was used to measure oxygen consumption rate under basal conditions. The Seahorse XF24 plate and cartridge were prepared as described in section 3.2.7. Briefly, the XF24 calibration plate was loaded with 500µl of XF Calibrant Fluid and placed along with the Seahorse cartridge in the XF 37°C incubator with 0% CO_2 overnight. XF24 cell cultures plates were coated with Cell Tak as per the manufacturer's guidelines. Briefly, 50µl of 2.4µg/ml Cell Tak was added to each well, and incubated at room temperature for 20 minutes. The plates were then washed with sterile dH_2O and allowed to air dry.

Platelet-derived microvesicles were prepared as described in 5.2.5, however with the modification that the microvesicles isolated from the platelet preparation were resuspended in 100µl of warmed Seahorse base medium (containing 2mM glutamine, 25mM glucose and 1mM pyruvate) and transferred to the Cell Tak coated XF24 seahorse plate (Figure 5.1) The plate was spun at 200 *x g* for 1 minute. To the blank wells, 100µl of base medium was added. The plate was then transferred to the 37°C incubator for 15 minutes. Afterward, 400µl of warmed Seahorse Base Medium (containing 2mM glutamine, 25mM glucose and 1mM pyruvate) supplemented with

2mM $CaCl_2$ was added and the plates returned to the incubator for a further 30 minutes. The calibrant plate and cartridge were then placed in the XF24 Seahorse Analyser for initial calibration. Subsequently, the calibrant plate was ejected and the plate containing the platelet-derived microvesicles was inserted and the oxygen consumption rate was measured over a period of 20 minutes.

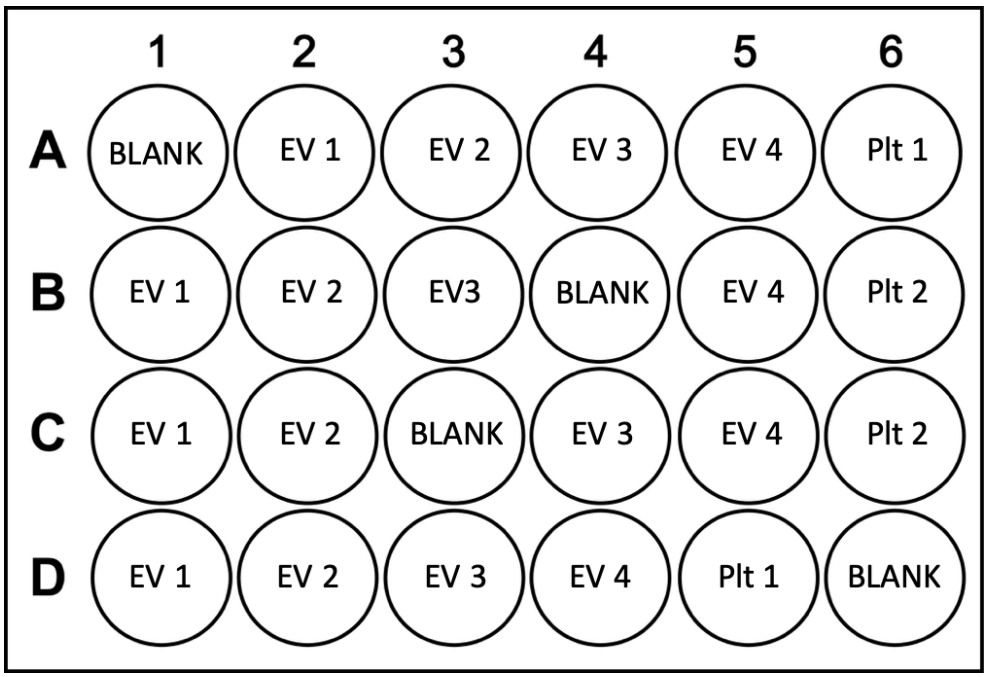

Figure 5.1 Agilent XF24 Seahorse plate layout for platelet microvesicles

Plate layout for the measurement of oxygen consumption rate in platelet microvesicles (indicated EV) and platelets (indicated as Plt) to act as controls. Wells A1, B4, C3 and D6 were left blank and only contained Seahorse Base Medium.

5.2.9 Neutrophil isolation

Citrated whole blood was transferred into a 50ml Falcon tube and centrifuged at 130 *x g* for 20 minutes with a slow acceleration and deceleration. Subsequently, the majority of the PRP was removed and 10ml of filtered PBS (without calcium or magnesium) was gently layered on top of the remaining red and white blood cells. On top of the PBS, 8ml of filtered 6% dextran was layered. The sample was slowly inverted to mix together the sample layers and subsequently left for 15 minutes at room temperature to sediment the red blood cells. After transfer to a fresh 50ml Falcon, 10ml of room temperature Histopaque 1077 was added and the leukocyte layer removed from the dextran separated sample. The Histopaque-leukocyte sample was centrifuged at 400 *x g* for 30 minutes. The remaining platelets, PBMC layer and Histopaque were removed and discarded. To lyse the red blood cells in the remaining layer, 9ml of ice cold dH_2O was added to the sample and left for 30 seconds. The sample was then diluted with 1ml of 10 x Hank's Balanced Salt Solution (HBSS) and made up to 50ml with filtered PBS (without calcium and magnesium). The sample was centrifuged at 300 x g for 10 minutes to wash the neutrophils. Lastly, the neutrophil pellet was resuspended in 1ml of filtered PBS (without calcium and magnesium), and the cell count determined using trypan blue staining.

5.2.10 Visualising platelet and neutrophil interactions with platelet microvesicles containing mitochondria

Washed platelets (3 x 10^7/ml) or isolated neutrophils (5 x 10^6/ml) were incubated with platelet-derived microvesicles stained with MitoTracker Orange CMTMRos for 30 minutes or 60 minutes. Samples were prepared for immunofluorescence and confocal microscopy as described in 5.2.2. Platelet-platelet microvesicle samples were stained with mouse anti-α-tubulin (1:200), and anti-mouse Alexa Fluor 488 (1:500). Neutrophil-platelet microvesicle samples were stained with anti-mouse LAMP1 (1:200), followed by anti-mouse Alexa Fluor 488 (1:500) and DAPI (10nm).

5.2.11 Cell sorting of platelet-derived microvesicles

To separate microvesicles containing mitochondria from the rest of the population, microvesicles were prepared as described in 5.2.5, stained with MitoTracker Orange CMTMRos (10nm). Prior to storing at -80˚C, samples were sorted using a BD FACS Aria III Fusion Cell Sorter (70µm nozzle, 70 Ps), based on the fluorescence intensity of MitoTracker Orange CMTMRos. The gating strategy is shown in Figure 5.2, with the top 20% of MitoTracker fluorescence sorted as mitochondria positive (mitoPMV) and the bottom 80% as mitochondria negative (PMV) Following sorting, microvesicles were pelleted at 18,000 *x g* for 45 minutes, resuspended in filtered PBS and stored at -80˚C until required.

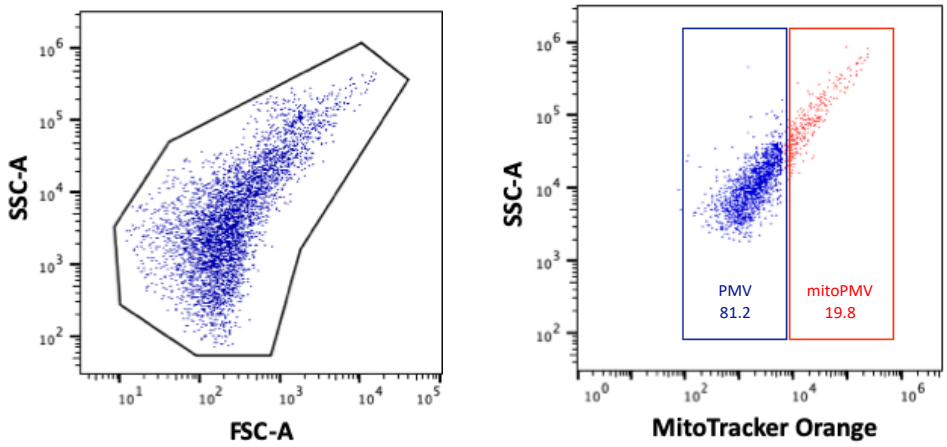

Figure 5.2 Gating strategy for sorting of mitochondria positive microvesicles

Flow cytometric scatter plot showing the **A.** forward and side scatter of the microvesicle population and **B.** the fluorescence intensity of MitoTracker Orange within the microvesicle population and the sorting gates to isolate mitochondria positive (mitoPMV) and mitochondria negative vesicles (PMV).

5.2.12 Assessment of neutrophil activation markers following incubation with platelet-derived vesicles

Isolated neutrophils (5 x 10^5) were incubated with mitochondria negative microvesicles (5 x 10^6), mitochondria positive microvesicles (5 x 10^6), or PBS as control for 30 minutes at 37˚C. Subsequently, the samples were fixed with PFA (2%) for 10 minutes and stained with an antibody cocktail described in Table 5.2. Samples were analysed using a BD LSRII, acquiring at least 5,000 CD45 positive events.

Table 5.2 Antibodies used for flow cytometric analysis of neutrophils

	Antibody	Concentration
Sample 1	CD45 PerCPCy5.5 CD66b Pacific blue	1:150 1:100
Sample 2	CD45 PerCPCy5.5 CD11b BV421	1:150 1:100
Sample 3	CD45 PerCPCy5.5 CXCR2 BV421	1:150 1:100

5.2.13 Statistical analysis

Graphs and statistical analysis were generated using GraphPad Prism v.8. Data were expressed as mean±SEM and all statistics were generated using a paired students t-test or a one-way ANOVA, with a Dunnett's or Tukey's multiple comparison test. Significance was defined as $p<0.05$.

5.3 Results

5.3.1 Platelet activation causes a reduction in the number of mitochondria

Immunofluorescence and confocal microscopy revealed that platelet activation by TRAP-6 caused a significant reduction in the number of mitochondria per platelet from 8±1 in resting platelets to 3±0.5 in stimulated platelets (Figure 5.3A, B and D). This was accompanied by a significant reduction in the platelet cross-sectional area from 8.2±1.2μm^2 to 4.2±0.2μm^2 (Figure 5.3A, B and C). Analysis of the mitochondrial size indicated that the reduction in mitochondria number was not as a result of mitochondrial fusion events as there was no significant difference in the mitochondria cross-sectional area; 151±5nm^2 in unstimulated platelets and 147±4nm^2 in stimulated platelets (Figure 5.4A-C).

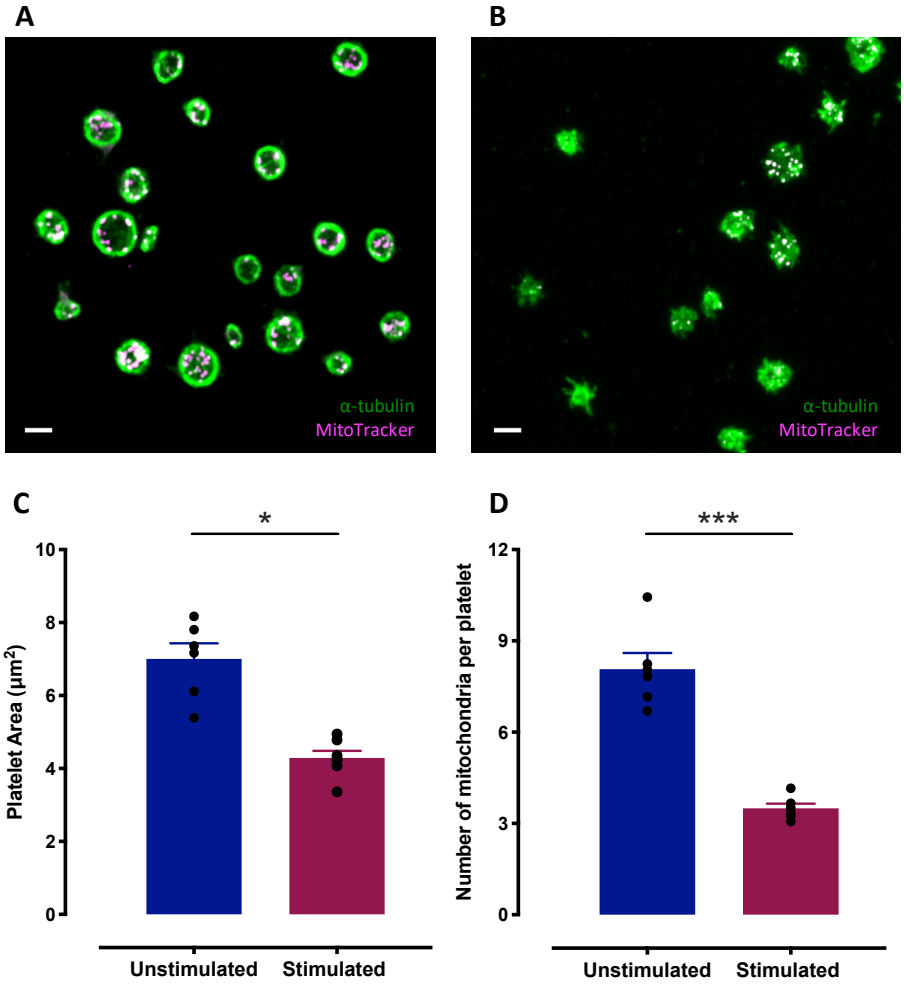

Figure 5.3 Airyscan confocal microscopy of mitochondria in unstimulated and stimulated platelets

Representative confocal microscopy images stained for α-tubulin (green) and MitoTracker Orange (magenta) in **A.** resting and **B.** TRAP-6 stimulated platelets. Scale bar represents 2µm. Quantification of **C.** platelet cross-sectional area and **D.** number of mitochondria per platelet. Data presented as mean±SEM, significance was determined by paired t-test (n=4, *p<0.05, ***p<0.005).

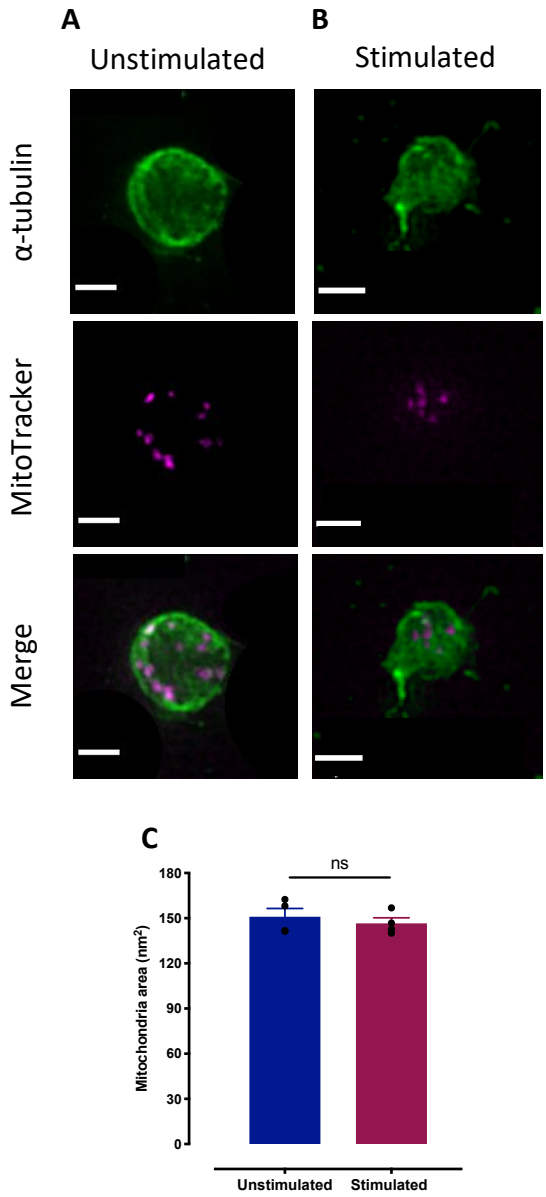

Figure 5.4 Assessment of mitochondrial size in unstimulated and stimulated platelets

Zoom of representative confocal images stained with α-tubulin (green) and MitoTracker Orange (magenta) in **A.** resting and **B.** TRAP-6 stimulated platelets. Scale bar represents 1µm. **C.** Quantification of mitochondria cross-sectional area. Data presented as mean±SEM, significance was determined by paired t-test (n=4).

5.3.2 Mitochondria in platelets have the capacity to undergo fission

Proteomic analysis of platelets has identified that platelets have the machinery required for mitochondrial fission and fusion, however it remains unknown if they have the ability to undergo these dynamic processes. Interestingly, following the initial decrease in mitochondria after TRAP-6 stimulation, there is a subsequent increase in the number of mitochondria at 30 minutes post-stimulation; from 8±0.7 in unstimulated to 3±0.3 at 5-minute stimulation, and 5±0.2 at 30-minute stimulation.

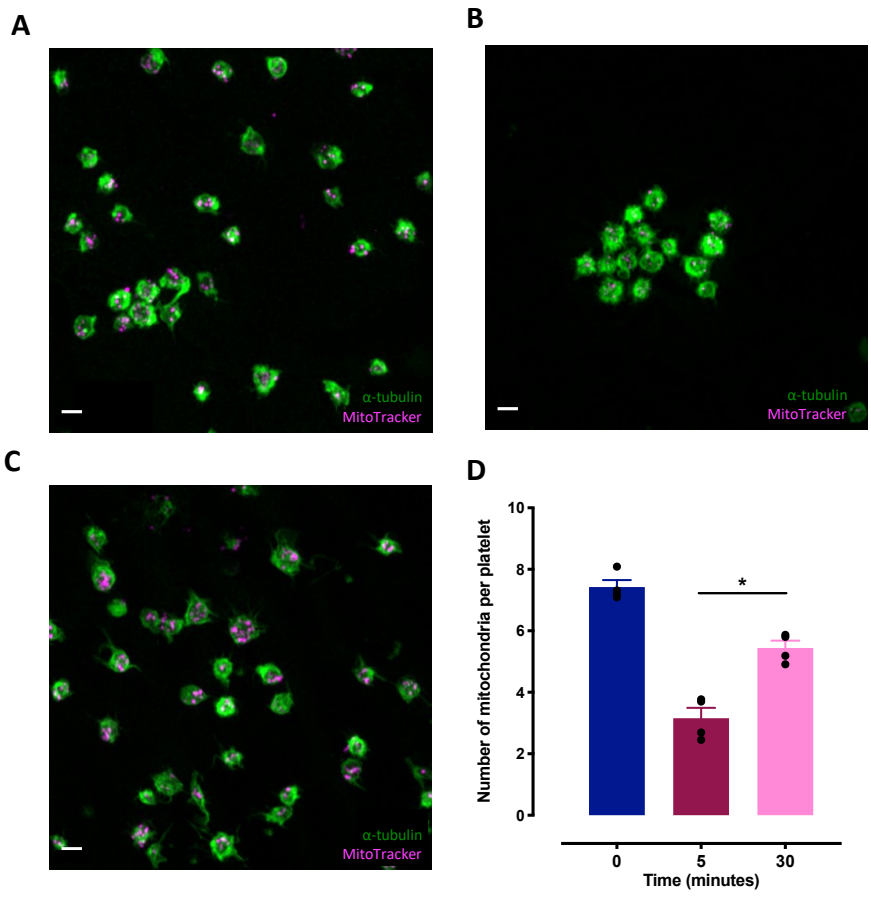

Figure 5.5 Platelet mitochondria have the capacity to undergo fission

Representative confocal microscopy images stained with α-tubulin (green) and MitoTracker Orange (magenta) in **A.** resting (0-minute), **B.** 5-minute TRAP-6 and **C.** 30-minute TRAP-6 stimulated platelets. Scale bar represents 2µm. **D.** Quantification of mitochondria number per platelet over the activation time course. Data presented as mean±SEM, significance was determined by paired one-way ANOVA with Dunnett's multiple comparisons (n=4, *p<0.05).

5.3.3 Platelets produce microvesicles through passive and active pathways

As the reduction in mitochondria number was not as a result of fusion events and there was a significant decrease in platelet cross-sectional area, I speculated that the mitochondria were being packaged and released into microvesicles.

Microvesicles can be isolated from both unstimulated (PBS) and TRAP-6 stimulated washed platelets. Flow cytometry was used to quantify microvesicle number, highlighting microvesicles released following incubation with PBS were produced at a lower concentration than following TRAP-6 activation (14926±5096 and 168075±65345 per sample following PBS and TRAP-6 stimulation respectively, Figure 5.6A). Furthermore, there was a higher number of microvesicles positive for the mitochondrial dye, MitoTracker Orange, produced when platelets were stimulated with TRAP-6; 26262±9153 vs. 2727±528 per sample (Figure 5.6B). Consistent with an increase in microvesicles containing mitochondria following TRAP-6 stimulation, the residual platelet pellet following microvesicle isolation had a significantly lower number of mitochondria positive events compared to the PBS incubated platelets (643825±90438 compared to 792307±106309 in the presence of PBS; Figure 5.6C). Furthermore, platelet activation on collagen coated coverslips causes the production and release of microvesicles which bleb from long pseudopodia (Figure 5.6D).

NanoSight analysis indicated that microvesicles generated from TRAP-6 stimulated platelets ranged in size from 30±1nm to 739±41nm (Figure 5.7). The modal value of detected vesicles was 129±4nm (Table 5.3).

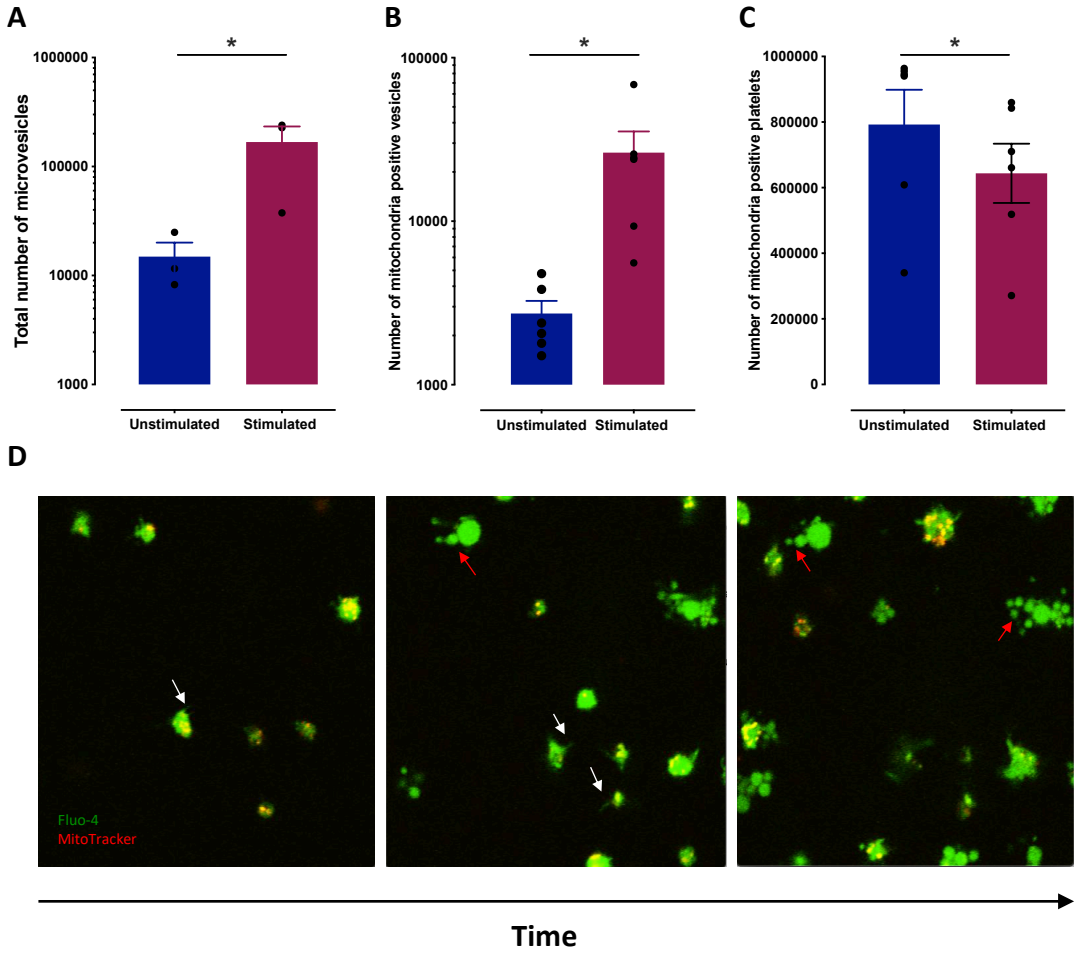

Figure 5.6 Platelets produce microvesicles through passive and active pathways

Flow cytometric analysis of microvesicles produced following incubation with PBS or TRAP-6 measured for 60 seconds triggered on **A.** side scatter and **B.** MitoTracker Orange fluorescence (PE). **C.** Flow cytometric analysis of the remaining platelet pellet following microvesicle production, measured for 60 seconds and triggered on MitoTracker Orange fluorescence (PE). **D.** Qualitative assessment of platelet activation on collagen. Platelets form pseudopodia (indicated by white arrows) and subsequently produce microvesicles (indicated by red arrows). Data presented as mean±SEM, significance was determined by paired t-test (n=4, *p<0.05).

A

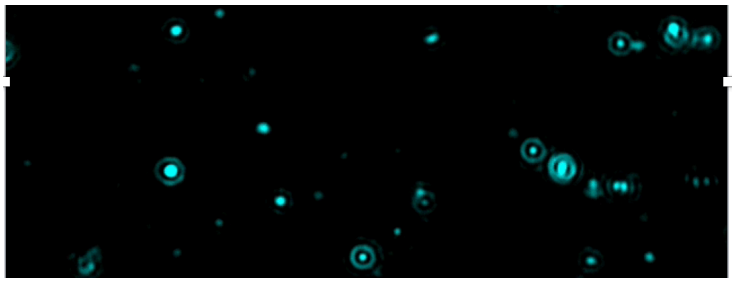

B

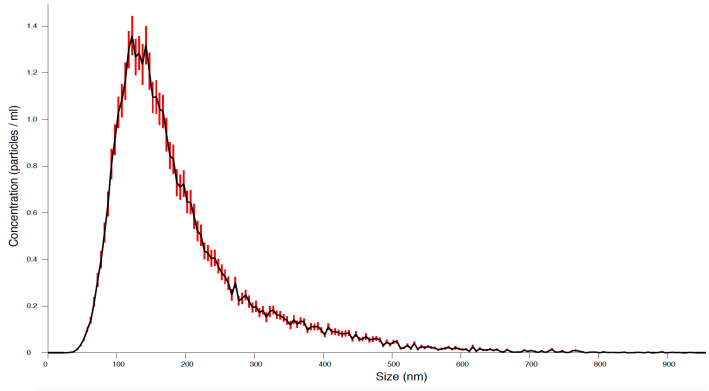

Figure 5.7 NanoSight tracking analysis of platelet-derived microvesicles

A. Representative image from the NanoSight tracking analysis showing the individual microvesicles (blue) tracked to estimate the size and concentration of the particles. **B.** Histogram showing the size range of microvesicles produced by platelets following incubation with TRAP-6.

Table 5.3 Size and concentration of platelet-derived microvesicles

Size (nm±SEM)			
Range	**Mean**	**Mode**	**Concentration**
29.9±1.1 – 738.6±140.6	193±7.5	128.7±3.6	3.7±0.4 x 10^9/ml

5.3.4 A subpopulation of platelet-derived microvesicles contain mitochondria and express high levels of activation markers

Characterisation of platelet microvesicles using imaging flow cytometry (Figure 5.8) revealed that 95% expressed CD41 (integrin alpha-IIb), 82% expressed annexin V (phosphatidylserine), 30% expressed P-selectin and 20% were positive for MitoTracker Orange (Figure 5.9).

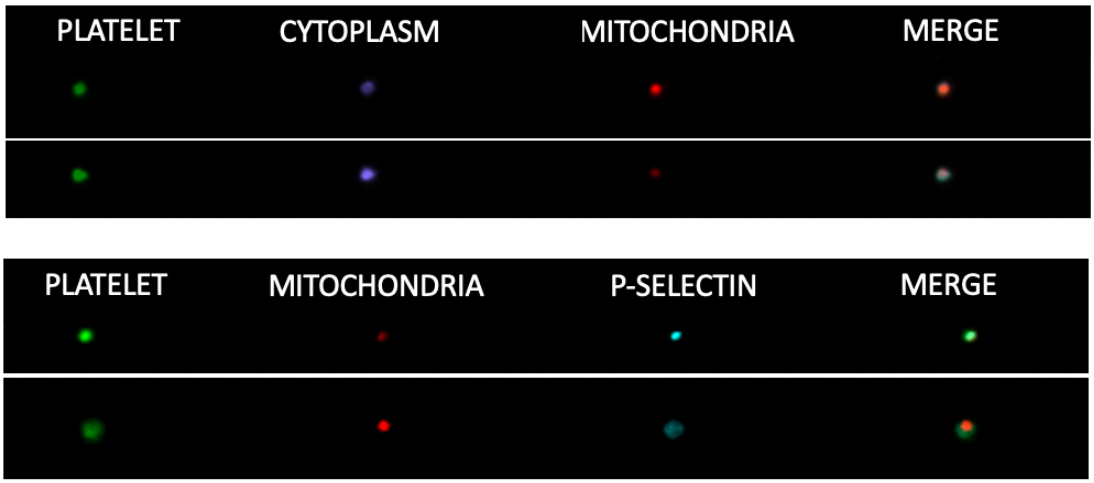

Figure 5.8 Image stream pictures of platelet-derived microvesicles

Representative image stream pictures of platelet microvesicles showing the localisation of the platelet marker (CD41), a cytoplasm dye (Cell Trace), mitochondria (MitoTracker Orange) and P-selectin (CD62P).

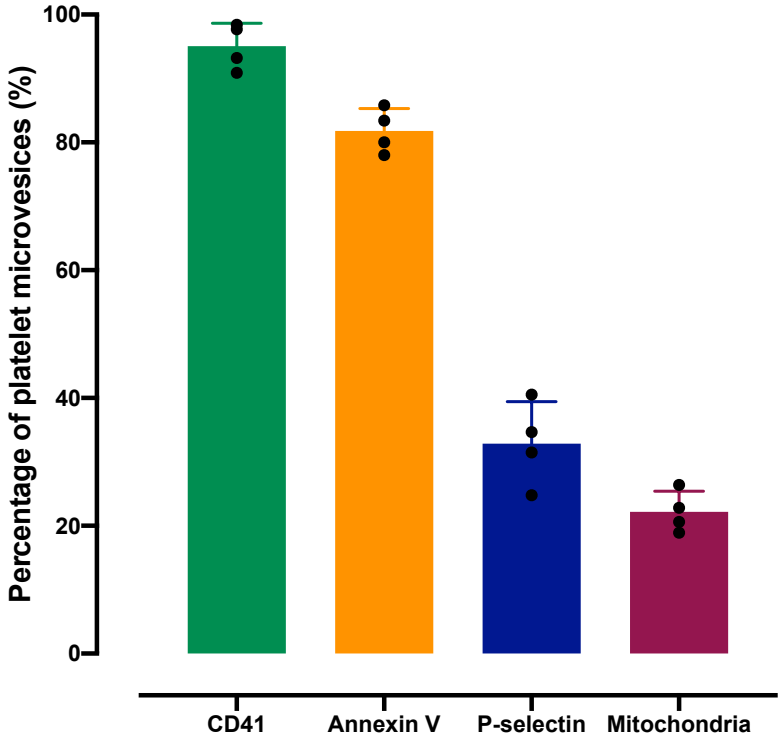

Figure 5.9 Characterisation of surface markers on platelet-derived microvesicles

Expression of surface and intracellular markers in platelet-derived microvesicles identify high levels of CD41 and annexin V, with lower levels of P-selectin and mitochondria. Data presented as mean±SEM (n=4).

As indicated in Figure 5.10A, the small proportion of microvesicles containing mitochondria (in red) were found to be generally the largest microvesicles within the population. Focused characterisation of microvesicles containing a mitochondrion (mitoPMV) revealed that the binding of annexin V remains constant to that of the whole population, with 80% of the microvesicles being positive for annexin V. Interestingly, when looking at P-selectin expression, this increased from 30% within the whole population to 95% in the mitochondria containing subpopulation, suggesting these microvesicles blebbed from the plasma membrane following release of the granular content (Figure 5.10B).

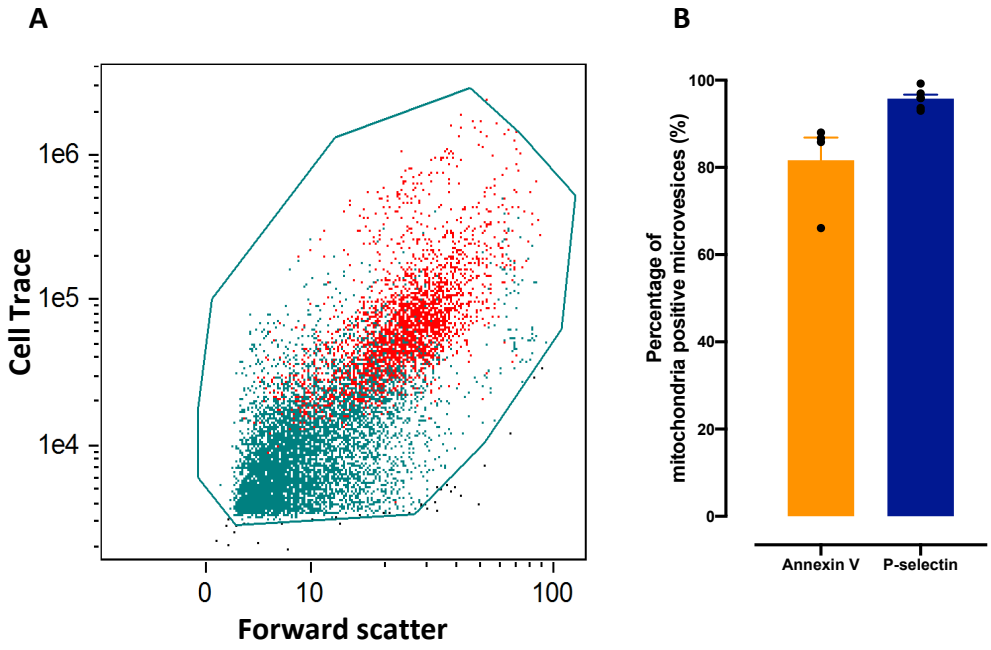

Figure 5.10 Characterisation of surface markers on mitochondria positive platelet-derived microvesicles

A. Scatter plot displaying size distribution of platelet microvesicles based on the forward scatter against the cytoplasm dye (Cell Trace), showing mitochondria containing vesicles in red and the rest of the population in blue. **B.** Expression of surface markers on microvesicle containing mitochondria. Data presented as mean±SEM (n=4-5).

5.3.5 Platelet-derived microvesicles contain active mitochondria

Despite identifying mitochondria within platelet microvesicles, the data thus far did not indicate whether they remained functional. As the primary role of mitochondria is in energy production through respiration, I sought to investigate if the mitochondria were respiring, and therefore consuming oxygen. As detailed in Figure 5.11, platelet microvesicles consume 36pmoles of oxygen per minute compared to 98pmoles of oxygen per minute in platelets, thus indicating the mitochondria are active, but to a lesser extent than in intact platelets.

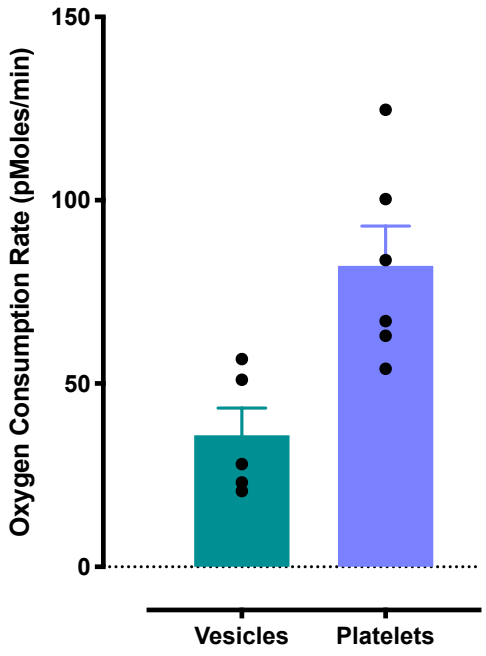

Figure 5.11 Basal oxygen consumption in platelet-derived microvesicles and platelets

Basal oxygen consumption rate of platelet microvesicles, normalised to starting platelet concentration ($3x10^8$/ml) and platelets ($6x10^7$) measured in an Agilent Seahorse analyser. Data presented as mean±SEM (n=4).

5.3.6 Platelet-derived microvesicles containing mitochondria interact with platelets and neutrophils

Activated platelets readily interact with other platelets as well as leukocytes, and growing evidence suggests that platelet microvesicles interact with leukocytes, therefore I wanted to determine if mitoPMVs interact with platelets and neutrophils.

Platelets interacted with mitoPMVs, in a time dependent manner, with an average of 3±0.1 mitoPMVs interacting with a platelet after 30 minutes, increasing to 5±0.5 after 60 minutes (Figure 5.12). Interestingly, mitoPMVs interacted more readily with isolated neutrophils than platelets, increasing in a time dependent manner; from 11±2 at 30 minutes to 33±6 at 60 minutes (Figure 5.13).

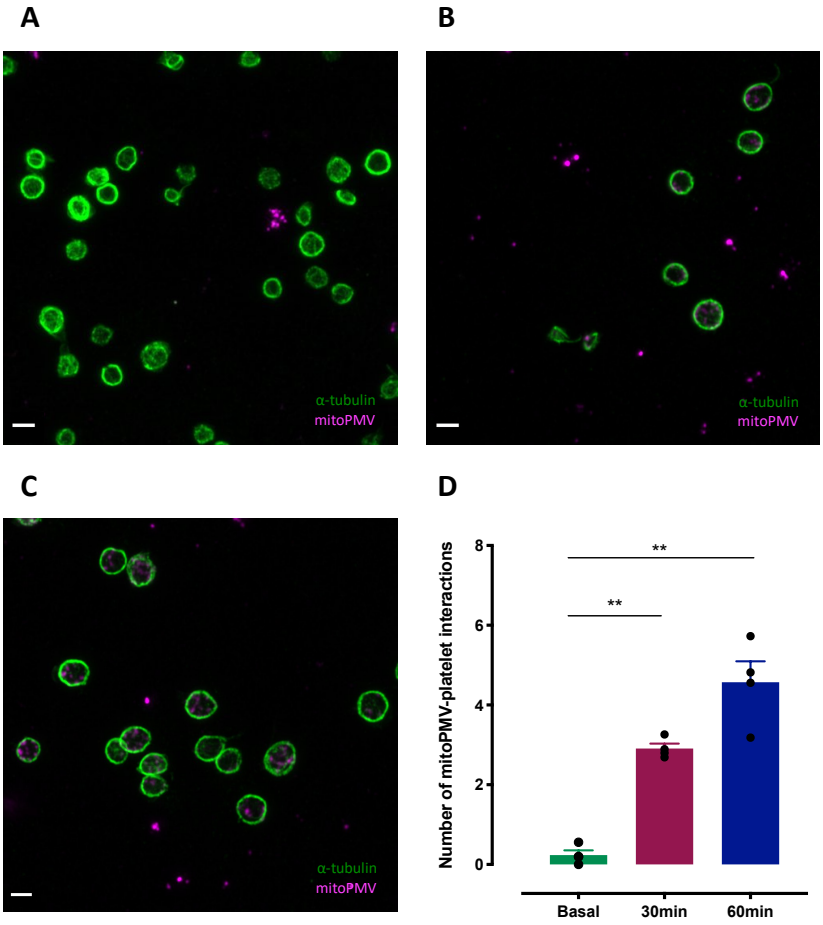

Figure 5.12: Platelet-derived mitochondria positive vesicles interact with platelets in a time dependent manner

Representative confocal microscopy images of platelets stained for α-tubulin (green) incubated with mitoPMVs (magenta) **A.** under basal conditions and for **B.** 30 minutes and **C.** 60 minutes. Scale bar represents 2µm. **D.** Quantification of the average number of mitoPMV-platelet interactions. Data presented as mean±SEM, significance was determined by one-way ANOVA with Tukey's multiple comparisons (n=4, **p<0.01).

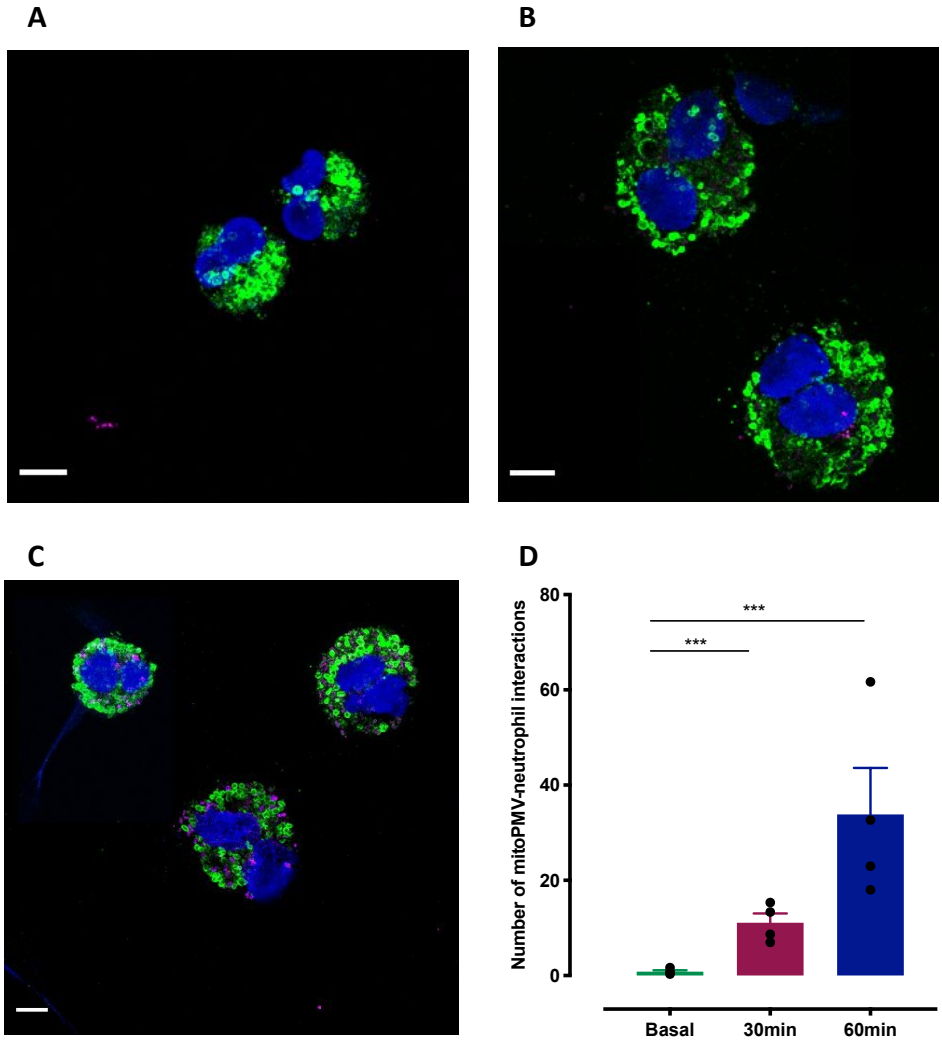

Figure 5.13: Platelet-derived mitochondria positive vesicles interact with neutrophils in a time dependent manner

Representative confocal microscopy images of neutrophils stained for LAMP1 (green) and DAPI (blue) incubated with mitoPMVs (magenta) **A.** under basal conditions and for **B.** 30 minutes and **C.** 60 minutes. Scale bar represents 5µm. **D.** Quantification of the average number of mitoPMV-neutrophils interactions. Data presented as mean±SEM, significance was determined by one-way ANOVA with Tukey's multiple comparisons (n=4, ***p<0.005).

5.3.7 Platelet microvesicles containing mitochondria alter the expression of neutrophil activation markers

Given that I had identified that mitoPMVs have higher expression levels of P-selectin, it raised the question as to whether they may be more likely to affect neutrophil function and phenotype than the remainder of the microvesicle population. To understand the functional significance of the impact of mitoPMVs on neutrophils, I sorted platelet microvesicles based on the fluorescence intensity of MitoTracker Orange into two subpopulations; mitochondria negative platelet microvesicles (PMVs) and mitochondrial positive platelet microvesicles (mitoPMVs).

Following incubation of neutrophils with mitoPMVs, there was a significant upregulation in two neutrophil activation markers, CD66b (carcinoembryonic antigen-related cell adhesion molecule 8) and CD11b (integrin αM), compared to that seen in control neutrophils. Interestingly, however, PMVs did not alter the expression levels of these surface markers (Figure 5.12A-B). Furthermore, incubation with mitoPMVs caused the downregulation of CXCR2 (C-X-C chemokine receptor type 2), whilst PMVs had no effect on the expression levels (Figure 5.14C).

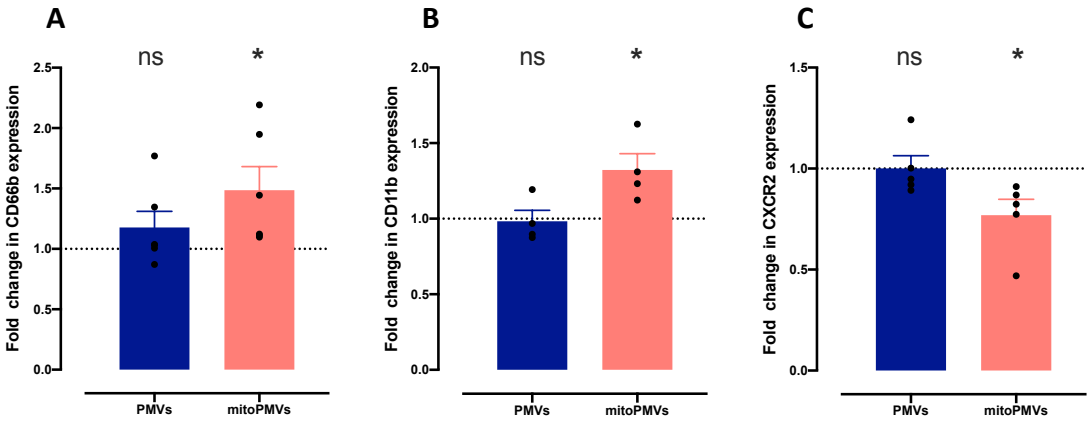

Figure 5.14: Characterisation of neutrophil surface markers following incubation with PMVs and mitoPMVs

Quantification of the expression of neutrophil surface markers after incubation with PMVs and mitoPMVs. Data expressed as a fold change in the expression of **A.** CD66b **B.** CD11b and **C.** CXCR2 in neutrophils under basal conditions. Data presented as mean±SEM, significance was determined by one-way ANOVA with Dunnett's multiple comparisons (n=5, *p<0.05).

5.4 Discussion

As platelets are small and anucleate, interest in their organelles to date has been limited. For the first time, using confocal microscopy I have shown that platelet activation causes a reduction in the number of mitochondria. The reduction in number of mitochondria could be explained by the engagement of two pathways; mitochondrial fusion or mitochondria release into microvesicles. Platelets are equipped with the machinery to support both mitochondrial fission and fusion, however neither of these processes have ever been documented in platelets. To understand if mitochondrial fusion had occurred, I quantified the cross-sectional area of individual mitochondria as an estimate of mitochondria size. As there was no change in the cross-sectional area it suggested that mitochondrial fusion was not the mechanism responsible for the reduction in mitochondrial number.

Mitochondrial fusion and fission are highly regulated processes in response to mitochondria stress, to ensure the maintenance of cellular health. Proteomic analysis has revealed that platelets contain the proteins responsible for these processes, namely mitofusin 1 and 2.[127] However, there is no literature indicating either of these processes occurs within platelets, so these proteins may be residual from the parent megakaryocyte. Although I identified that platelet activation does not cause mitochondrial fusion, I wanted to understand if platelet mitochondria have the capacity to undergo fission. Thus, following the initial reduction in mitochondria number following five minutes activation, I allowed the platelets to continue their cellular processes for a further 25 minutes. Interestingly, after the initial decrease, there was a subsequent increase in the number of mitochondria per platelet, suggesting the remaining mitochondria have undergone fission. In recent years research into platelet mitochondria has expanded greatly with reports demonstrating mitophagy occurring as a protective mechanism, however to date, mitochondrial fission and fusion dynamics have not been reported. Thus, this data may indicate that mitochondria within platelets have the ability to undergo mitochondrial fission. This is an interesting observation, but its significance is unknown and additional work using higher resolution microscopy is need to further

explore these pathways. However, it may suggest that despite having a short lifespan, mitochondria play an important role in platelet cellular function and thus need their health to be regulated. Indeed, given the small number of mitochondria contained within a platelet, it would seem necessary for them to have the ability to undergo fission therefore limiting the effect of accumulation of damage by extruding the damaged portion of the mitochondria.

Interestingly and somewhat unsurprisingly, platelet mitochondria are significantly smaller than those seen in other cells. Indeed, megakaryocytes have elaborate, interconnected mitochondrial networks, which raises the question as to when the alteration in mitochondrial architecture occurs leading to the small, discrete mitochondria seen in platelets. Recent research has demonstrated that dynamin-1 like protein 1 (Drp1) is essential in modulating mitochondrial fission during platelet biogenesis. Conditional knockout of Drp1 in the megakaryocyte lineage resulted in mitochondria within platelets forming extended networks, in contrast to the characteristic punctate mitochondria in wild type platelets.[278] Whilst the study of granule biogenesis and trafficking from megakaryocytes is well studied, there is limited information on the trafficking of mitochondria during platelet biogenesis. Thus, exploring mitochondrial trafficking in megakaryocytes could provide an exciting avenue of research, and may provide insights into the behaviour of platelet mitochondria.

In this work, I have shown that the reduction in mitochondria number is not as consequence of mitochondrial fusion, but rather the packing and release in microvesicles. Whilst it is well established that platelets produce microvesicles during physiological activation and apoptosis, here I have shown that they additionally release microvesicles through passive pathways. Interestingly, the concentration of microvesicles and mitochondrial content of microvesicles varies depending on the stimulus. Indeed, those release through passive pathways, are produced at a lower concentration and contain fewer mitochondria. On the other hand, strong stimulation with TRAP-6 produces a higher concentration of microvesicles, with a greater number of mitochondria positive microvesicles. The release of mitochondria

from platelets was first established by Boudreau et al, who demonstrated that the supernatant of activated platelets consumed oxygen, suggesting the presence of extracellular mitochondria.[156] Since this initial observation, mitochondria have been visualised in microvesicles using electron microscopy. Building on this work, I have used imaging flow cytometry to show microvesicles containing mitochondria are the largest, accounting for approximately 20% of the microvesicle population. Furthermore, supporting the work of Boudreau et al., I have shown that these platelet microvesicles consume oxygen indicative of functional mitochondria within them. However, this oxygen consumption could additionally be as a result of the presence of oxidative enzymes such as cyclooxygenase-1 within the microvesicles.[158] Focussed characterisation of mitoPMVs, revealed that these microvesicles had high levels of annexin V binding and high P-selectin expression. This data is interesting for two reasons. Firstly, it suggests that granule exocytosis may be higher in regions that are in close proximity to a mitochondrion. This raises the question as to whether mitochondria are trafficked towards the membrane, to facilitate the efficient transfer of energy needed during activation, or are granules that are resident close to a mitochondrion are more likely to undergo release reactions. Secondly, with higher P-selectin expression, are these microvesicles more likely to interact with leukocytes and endothelial cells, and therefore modulate their behaviour. The former of these would be a fascinating area of research, but given the intrinsic nature of platelets to want to activate, it would prove very challenging to live image platelets under resting conditions.

Platelet microvesicles express a wide array of surface receptors and molecules, and are thought of as important intracellular communication modulators. Indeed, evidence suggests that platelet microvesicles are selectively packaged with varying cargoes, therefore eliciting a variety of functions on other cells within the circulation. Here I have shown that mitoPMVs interact with platelets in a time dependent manner, with some evidence that they may be internalised, as indicated by the presence of the mitochondrial dye within the platelet cytoplasm. It is now widely known that platelets have the ability to endocytose plasma proteins, such as fibrinogen, albumin and vWF, but would it be possible for them to endocytose

mitochondria?[279] Interestingly, research has indicated that extracellular mitochondria have the ability to interact directly with platelets, forming complexes that have an increased procoagulant phenotype.[280] Despite evidence of these interactions between platelets and mitoPMVs, it is challenging to elucidate whether this is causing a change in platelet phenotype, as detection of alterations in surface receptors using flow cytometry will not discriminate between whether the fluorescence is coming from the platelet or mitoPMV.

In addition to interacting with platelets, I have shown that mitoPMVs readily interact with isolated neutrophils in a time dependent manner, supporting previous evidence showing that platelet microvesicles and mitochondria interact with and are internalised by neutrophils both *in vitro* and *in* vivo.[156,281] To understand if mitoPMVs elicit different functional effects on neutrophils in comparison to the rest of the PMV population, I sorted two distinct populations based on the fluorescence of MitoTracker Orange. Interestingly, incubation of neutrophils with mitoPMVs but not PMVs caused a change in the expression of several surface markers. Neutrophils express an extensive repertoire of surface receptors which facilitate the initiation of signalling pathways and alter neutrophil function. Amongst the vast array of molecules important in responding to physiological stimuli is CD66b, a glycoprotein present on granulocytes, which following neutrophil activation is increased on the cell surface.[282] Interestingly, following incubation of platelets with mitoPMVs, but not PMVs, expression of CD66b was significantly upregulated. Further evidence for mitoPMVs promoting neutrophil activation is the upregulation of CD11b.[283,284] This surface receptor is expressed basally on the neutrophil surface, however following activation, additional molecules are rapidly mobilised from within secretory granules.[282] Increased expression of CD66b and CD11b are important not only in neutrophil activation but also in their subsequent adhesion and migration within the vasculature. In addition to the upregulation in two activation markers, this work also demonstrates that incubation with mitoPMVs but not PMVs causes a downregulation of CXCR2. Consistent with neutrophil activation and subsequent alteration in phenotype, evidence has revealed a reduction in the expression of the chemokine receptors, CXCR1 and CXCR2 following phagocytosis.[285,286]

Neutrophils are mediators of the innate immune response, functioning through phagocytosis and degranulation. Here I suggest that mitoPMVs cause neutrophil activation and in doing so, facilitates their phagocytosis. The downstream effects of this remain to be elucidated, however I speculate that the phagocytosis of mitoPMVs may be affecting a number of pathways. Firstly, microvesicle clearance rates and mechanisms remain undefined, with some work suggesting they are engulfed within minutes of generation by phagocytic cells.[163,287] To understand if neutrophils are mediating the clearance of mitoPMVs, experiments investigating the levels of the autophagosomal machinery, namely LC3 may prove worthwhile. Secondly, phagocytosis of mitoPMVs may confer a functional benefit to the neutrophil, by increasing their respiratory capacity. I and others, have demonstrated that platelets release functional mitochondria, measured by their oxygen consumption capacity, which allows us to consider that following phagocytosis, the mitoPMVs may be able to combine with the existing neutrophil mitochondrial network and contribute towards the cellular energy generation.[156] To understand if mitoPMVs are indeed affecting neutrophil metabolism, measurement of oxygen consumption and glycolytic rates using the Aligent Seahorse Analyser or high resolution respirometry could provide insights into the neutrophil metabolic profile.[116]

MitoPMVs may also be acting as priming mediators of neutrophils, with their interaction promoting the upregulation of activation markers, which subsequently would promote neutrophil adhesion and migration within the vasculature.[288] To assess the role of mitoPMVs in neutrophil adhesion, flow adhesion assays on collagen or endothelial cell coated channels could be conducted. Furthermore, to elucidate if *in vitro* results are applicable *in vivo*, intravital microscopy could be performed following the injection of mitoPMvs, which would provide additional information on the transmigration capacity of the neutrophils. To support the flow adhesion assays, chemotaxis assays would provide insights into alterations in responses to chemokines, which may affect neutrophil adhesion and migration responses.

The relevance of mitochondria release from platelets and their subsequent effect on other cells remains to elucidated. However, there are numerous reports of elevated circulating levels of platelet microvesicles in pathological states, including diabetes mellitus, chronic kidney disease and cardiovascular diseases.[152] As my work has indicated that mitochondria are present within approximately 20% of microvesicles, it can be speculated that in diseases with elevated levels of platelet microvesicles there will also be higher mitoPMVs levels and that these would contribute to the underlying inflammatory phenotypes. Indeed, there is evidence that extracellular mitochondria have deleterious influences in traumatic injury where they promote procoagulant activity in platelets.[280] Furthermore, recent work has shown that microvesicles are abundant in platelet concentrates and that transfusions of platelet concentrates with higher levels of mitochondria DNA, as an indicator of mitoPMVs, are associated with increased adverse reactions.[289]

The data presented in this chapter shows that platelet mitochondria are dynamic in nature, and following the engagement of platelet activation pathways are packaged into microvesicles and released. These mitoPMVs express high levels of P-selectin on their surfaces and interact readily with neutrophils. Interestingly, mitoPMVs but not PMVs alter neutrophil activation markers, suggesting mitoPMVs are an important subject for microvesicle research. Indeed, my initial observations suggest that mitoPMVs are phagocytosed by neutrophils and promote neutrophil activation which may be relevant to the many diseases outlined above associated with enhanced inflammatory responses.

6 General Discussion

Platelets are fundamental for maintaining haemostasis, but following inappropriate activation can contribute to pathological thrombosis.[82] Following vascular injury, platelet activation proceeds through a serious of tightly regulated pathways, involving cytoskeletal rearrangement facilitating platelet shapes changes, and the activation of intracellular signalling pathways to promote the fusion and release of platelet granular contents[50,67]. These pathways facilitate the formation of platelet-platelet and platelet-leukocyte aggregates, encouraging the arrest of bleeding at the site of injury. Whilst the traditional function of platelets is to prevent blood loss, in recent years their role in other processes such as inflammation and immunity have been highlighted.[67] Indeed, platelets express a number of proteins and surface receptors that play no clear role in haemostasis, and as such there has long been speculation of alternative functions.

Platelets form a heterogenous population of ages, sizes and functions, primed to be activated when in the presence of stimuli such as exposed extracellular matrix components or soluble mediators. Whilst particular attention is paid to how platelets behave as a whole population, evidence indicates that only a small proportion of the total circulating platelets are needed for haemostasis. This interesting finding raises the questions as to why the remaining platelets are needed. The study of platelets is generally conducted at a whole population level in which, although there may be differences in the functions of certain subpopulations of platelets, the aggregate response is taken and assessed to whether it lies within the desirable ranges.[290] Whilst research has indicated there are subpopulations of platelets with different behavioural characteristics, the mechanisms underlying these differences remain elusive. One potential explanation for the observed differences between populations is the age of the platelets. It is well documented that platelets have a relatively short lifespan, approximately 10 days, but the changes in function and composition as they progress through their lifespan within the circulation have not been fully studied.

Platelet aggregation and activation assays fall within two categories; dynamic recordings over a set period, or endpoint assays, both of which have advantages and disadvantages.[219] Light transmission aggregometry was first developed in the 1960s by Gustav Born, and measures light transmission as an indicator of platelet aggregation.[291] Often referred to as the gold standard of platelet aggregation testing, this assay provides information as a dynamic trace on both aggregation and disaggregation within a sample. This assay is considered laborious and requires a relatively large sample volume. In response to this, the Optimul assay, a 96-well plate-based end point test, has been developed allowing for the more rapid testing of a much broader range of agonists.[292] The Optimul assay is easy and provides the user with the ability to run significantly more replicates in parallel, however it generally provides data at only a single time point, so evidence as to the dynamic nature of the response is lacking. Given that platelet activation is a sequential process, I sought to understand the dynamics of key phases of platelet activation including calcium signalling, granule release and changes in mitochondrial function.

In this thesis, I was able to show that calcium signalling precedes granule release, occurring in parallel with a transient $\Delta\Psi$m hyperpolarisation indicative of an increase in the proton motive force generated via oxidative phosphorylation. Sustained changes in $\Delta\Psi$m can lead to deleterious effects to the mitochondria, and so loss of membrane integrity, which could lead to the engagement of mitophagy or apoptotic pathways. Despite this transient $\Delta\Psi$m hyperpolarisation, changes in mitochondrial function, as measured by oxidative phosphorylation can be measured up to 20 minutes following platelet stimulation. This data supports previously published research indicating that thrombin activation causes an increase in mitochondrial consumption[224,293]. Furthermore, I have shown that treatment of platelets with a $P2Y_{12}$ receptor blocker, but not with aspirin, causes a significant reduction in calcium flux during platelet activation with TRAP-6 and U46619. Interestingly, both anti-platelet drugs cause a reduction in P-selectin expression following stimulation with U46619. This data supports previously published literature detailing a reduction in P-selectin expression in patients taking aspirin and $P2Y_{12}$ inhibitors. The use of flow cytometry to assess the effect of anti-platelet drugs on calcium flux and P-selectin

expression may not have been the most appropriate assay to accurately measure the dynamics of these responses. Indeed, both of these anti-platelet drugs target the secondary wave of aggregation and the generation of secondary mediators. In a system where the sample is dilute and passing through an artificial flow system, there may well not be the opportunity for the accumulation of secondary mediators and so observed differences may well not truly reflect genuine alterations in these pathways. Using a system with a spectrofluorometer would provide a more accurate assessment of the effects of inhibition of cyclooxygenase-1 and $P2Y_{12}$ receptors, as the platelets within the sample could aggregate and would not be removed from the tube for measurement, as happens during flow cytometric analysis. This would allow the accumulation of secondary mediators and so facilitate amplification of the activation response.

Interestingly, blockade of $P2Y_{12}$ receptors with AR-C66096 caused a significant reduction in the basal respiratory capacity of platelet mitochondria. The reasons for this reduction in oxygen consumption remain unclear, however there is evidence of $P2Y_{12}$ receptor expression on mitochondria within astrocytes, which suggests these receptors could also be present on platelet mitochondria.[230] Inhibition of $P2Y_{12}$ receptors within the mitochondrial membrane may affect the flow of ADP and could cause an imbalance in $\Delta\Psi m$ and so alter mitochondrial function. This interesting observation may provide additional insights into the mechanisms causing a reduction in platelet function following $P2Y_{12}$ receptor inhibition. Platelets have previously been described as metabolically plastic, having the ability to be able to switch readily between glycolysis and oxidative phosphorylation, providing compensatory mechanisms if needed. Thus, it would be intriguing to further explore the metabolic profile of platelets treated with a $P2Y_{12}$ receptor antagonist, to understand if the reduction in mitochondrial respiration is compensated for by an increase in glycolysis. Furthermore, in this work, I have only used one $P2Y_{12}$ antagonist, AR-C66096, so it would be beneficial to investigate whether this effect is specific to this compound or generally common to $P2Y_{12}$ receptor blockers. The data presented in this thesis come from studies looking at the acute treatment of platelets *in vitro*, however it would be exciting to look at the metabolism of platelets from healthy

individuals taking anti-platelet treatments for two weeks, and compare these to clinical samples from patients taking anti-platelet drugs as a secondary preventative measure.

As detailed previously, platelets form a heterogenous populations of sizes, ages and functions which work together to maintain vascular integrity and prevent blood loss. Interestingly however, research has indicated that only 5% of the total platelet count is required to maintain haemostasis, which raises the question, what are the other platelets needed for? Research in recent years has highlighted platelet subpopulations which respond differently to stimulation, but the triggers and determinants for these different responses remain unknown.[290,294,295] Despite this lack of information it is possible to arrive at the conclusion that platelet age is a key determinant of differences in function.

Research into platelet ageing within the circulation has become an interesting and somewhat controversial area of research. As the mechanisms controlling platelet lifespan remain unclear, there is no obvious way in which old platelets can be differentiated from young platelets. Nevertheless, evidence shows that following their initial entry into the circulation RNA contained within platelets is translated into protein or rapidly degraded.[73] Thus, there will be a small proportion of platelets, the most newly formed, that has a higher RNA content than the rest of the population. Using this knowledge, along with insights from commercially available machines such as the Sysmex, colleagues in my lab developed a cell sorting protocol that isolates platelets based on their RNA content, measured by thiazole orange fluorescence intensity.[41,296] During the development of this protocol, platelet specific mRNAs were measured and it was confirmed that thiazole orange low platelets exhibited a significant reduction in mRNA levels for platelet factor 4 and integrin alpha-IIb. Since the development of this protocol, other groups have suggested that thiazole orange may not be the best nucleic acid dye to define young and old platelets. Hille et al, outline an alternative staining protocol using the nucleic acid dye SYTO13 which has shown a longer duration of retention, and shows a strong correlation with the immature platelet fraction measured by the Sysmex.[243] As this paper has highlighted

differences in the retention of nucleic acid dyes, further work looking at identifying the most appropriate staining may be beneficial to enable a more robust characterisation of the platelet subpopulations.

The work presented in this thesis is the first to extensively characterise platelet function and composition in young and old platelets from healthy individuals (summarised in Figure 6.1). Previous research has indicated that newly formed, young platelets may be more reactive than older platelets, however the majority of this work has been conducted using blood from patients with altered platelet turnover.[21,37,38,297] Whilst these observations provide interesting insights, it is hard to unpick if platelet function is altered due to intrinsic changes in the platelet or as a consequence of changes in the vascular environment observed in these pathological states. One potential explanation that has been offered for this increased reactivity is that young platelets are larger, and therefore have more pro-thrombotic molecules packaged within them.[236,260,298,299] Indeed, there is a wealth of literature indicating that platelet size declines as platelets age. However, using confocal microscopy I have shown that the cross-sectional area of the platelet does not significantly change as platelets age. Interestingly, research in the 1980s hinted that platelet buoyant density, but not size declined with age.[261] This accords with the proteomic analysis conducted in this thesis, which demonstrated a decline in a number of subsets of proteins, notably cytoskeletal and mitochondrial proteins, as platelets age. Given that the cytoskeleton is a major component of maintaining platelet structure, this data would support the notion that platelet buoyant density but not size is reduced as platelets age within the circulation.

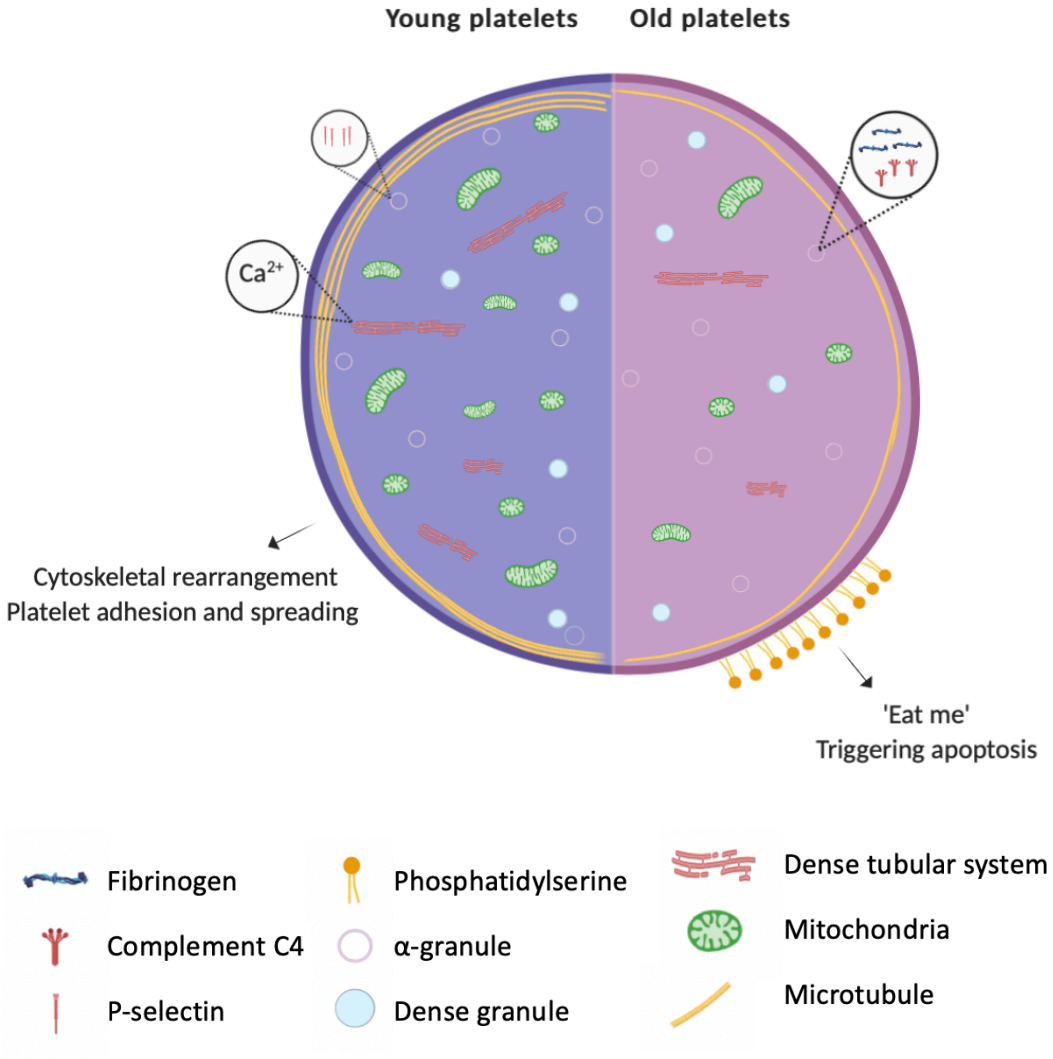

Figure 6.1 Summary of changes between young and old platelets

Representation of the structural changes between a young platelet (blue) and old platelet (pink) within the circulation of a healthy individual.

A number of mechanisms determining platelet lifespan have been proposed including desialyation and intrinsic apoptosis, which are thought to control the platelet 'molecular clock'. However the circumstances in which these pathways are engaged remains unknown.[24,34] The data presented in this thesis offers a novel insight into an alternative mechanism that may trigger the clearance of platelets from the circulation. Indeed, there is literature indicating that the loss of cytoskeletal proteins causes an instability in the structural integrity and subsequently an imbalance in the membrane phospholipids.[254] This imbalance causes the flipping of phosphatidylserine onto the outer leaflet membrane of the platelet, a well-known apoptotic trigger, which may act as an 'eat-me signal' and target older platelets for degradation. Furthermore, the reduction in mitochondria number may also contribute to the commitment of platelets to undergo degradation. Although I have shown that the number of mitochondria reduces as platelets age, the causes and mechanisms behind this still remain elusive. While mitochondria are dynamic organelles, there was no change in the size of the cross-sectional are of the mitochondria and therefore mitochondrial fusion is not responsible for the observed changes. Another explanation for this reduction could be the induction of mitophagy. During their lifespan within the circulation, platelets will experience cellular stresses which may lead to the accumulation of mitochondrial damage and cause the initiation of mitophagy. During the commitment of mitochondria to mitophagy, sustained $\Delta\Psi$m depolarisation causes the flipping of phosphatidylserine onto the outer leaflet of the plasma membrane.[272] As detailed above, the exposure of phosphatidylserine is an important apoptotic regulator, and therefore the reduction in mitochondria number coupled with the decrease in cytoskeletal integrity may trigger the commitment of platelets to undergo degradation and removal from the circulation.

As indicated above, previous research has suggested that newly formed platelets are hyper-reactive, but there was no definitive proof provided from studies in healthy individuals. In this work, I have demonstrated a reduction in calcium signalling in response to both TRAP-6 and ionomycin in old platelets, confirming the prediction of the ingenuity pathway analysis highlighting a reduction in calcium flux and quantity

of calcium in old platelets. Furthermore, I have shown that compared to young platelets, old platelets have marked reduction in adhesion and spreading to collagen. This interesting observation is likely a result of a reduction in cytoskeletal associated proteins such as gelsolin, emerin and myosin regulatory light chain 12A, which are important for both actin and tubulin dynamics. In addition, the reduction in calcium signalling may influence cytoskeletal dynamics, as a number of the motor proteins involved in the dynamic assembly and reorganisation of the cytoskeleton are calcium dependent.

This work has highlighted fundamental changes in structural and organelle composition as platelets age. Previous work performed within my laboratory indicated there is a reduction in granule secretion associated with platelet ageing, this information coupled to the proteomic analysis of a reduction in P-selectin and SNAP-23 raises the question of whether old platelets have fewer granules or whether there is an impairment in granule secretion. In favour of the former conclusion, there are indications that as platelets age there is a reduction in the number of dense granules.[300] Further work performing transmission electron microscopy on the sorted platelet samples would provide valuable information on the granule number, as well as providing confirmation on mitochondrial number and alteration in the cytoskeletal structure.

As demonstrated within the proteomic analysis there was a small subset of proteins that were present at a higher level in old platelets. Further work to understand the consequences of the relative increase in these proteins could provide insights into their roles within old platelets. Interestingly, the majority of the increased proteins are circulating proteins including complement proteins, haemoglobin and fibrinogen, which led me to speculate that these proteins are being bound and endocytosed as platelets circulate within the blood stream.[301] Indeed, using confocal microscopy, I was able to show that both fibrinogen and complement C4 were predominantly located within the platelet cytoplasm. However, recent research examining the transcriptome of differently aged platelets indicates a relative increase in complement protein mRNA in old platelets.[302] This work raises the question as to

where the mRNA and protein is coming from. Indeed, it is well established that platelets are able to transfer mRNA to other cells, but it remains less clear if they are able to endocytose mRNA themselves. If platelets are not able to endocytose mRNA, it may suggest that there is differential regulation in mRNA degradation. The recognition that both complement protein mRNA and protein increases as platelets age could provide an alternative method to distinguish between differently aged platelets, i.e. these could be used as markers of old platelets.

Whilst beyond the scope of this project, the significance of the upregulation of complement proteins warrants further investigation. The complement protein system is involved in innate immunity, promoting inflammation and assisting in the activation of phagocytic cells. As there was a relative increase in these proteins in old platelets, it may indicate a switch in phenotype and function as platelet age; potentially from rapid haemostatic responders to inflammatory modulators. To assess the inflammatory influences of these differently aged platelets, investigations into interactions with leukocytes and subsequent activation status and secretion of inflammatory molecules could provide interesting insights into functional switching during ageing.

This work has made important advances in our understanding of changes in platelets as they age within the circulation, highlighting an important association between mitochondrial and cytoskeletal loss and platelet age. With further evidence that these processes may be contributing to the exposure of phosphatidylserine this could provide novel insights into the underlying mechanisms governing platelet lifespan. This research also provides a foundation for future work investigating changes in composition and function of platelets from patients with diseases associated with alterations in platelet lifespan. The molecular mechanisms underlying the increase in platelet turnover observed in pathologies such as diabetes mellitus and cardiovascular disease remain unknown, thus extensively characterising these platelets subpopulations may provide a unique insight into the control of these processes in disease. The data presented here, demonstrating the importance of mitochondria to the process of platelet ageing, coupled with published research

indicating mitochondrial dysfunction in patients with diabetes may provide an interesting avenue of future research to explore if this may be a contributing factor to altered platelet lifespan.[148]

Research conducted in murine models to look at newly formed platelets generally depend upon depleting platelets by antibody treatment and then analysing the platelets that subsequently reappear. Whilst these studies provide useful understandings into the process of platelet production, it is unlikely that the rapidly reappearing platelets are 'normal'.[303] Total depletion of platelets using an anti-GPIbα antibody may cause vast stimulation of megakaryocyte differentiation to restore the platelet count, and may bypass some of the key stages of platelet packaging. This model may be of more benefit to understanding the changes in platelet function and composition induced by traumatic injury. As with this *in vivo* model, major trauma resulting in extensive blood loss may well stimulate mass production and release of platelets from the megakaryocytes. Given the unpredictable nature of major trauma, analysis of these samples may prove problematic. However, elective surgery can be a form of controlled trauma and could offer a model to test influences on platelet production and lifespan. Indeed, utilising platelet samples from elective surgery patients would allow for analysis of samples from pre- and post- 'trauma' which would allow for a strong comparison.

It is clear that mitochondria are important for platelet function, and may play a potential role in determining platelet lifespan. However, this thesis has highlighted a role for platelet mitochondria beyond haemostasis, and provided insights into the role of mitochondria packaged within platelet-derived microvesicles, in particular their ability to cause neutrophil phenotypic switching (discussed further below).

With advances in technologies, the field of extracellular vesicle research is greatly expanding.[150] Indeed, the ease of analysis using flow cytometry, and nanoparticle tracking analysis is providing potential avenues for the assessment of extracellular vesicles as biomarkers for the progression of conditions such as cardiovascular disease.[152] It is well documented that within the circulation, platelet-derived

microvesicles account for the largest proportion of vesicles, but the roles of circulating microvesicles remain unclear.[304] Interestingly, I was able to detect microvesicles within the circulation of healthy individuals, indicating they are not just involved in the progression of pathologies. Indeed, research has indicated that platelet derived-microvesicles are an important intracellular communicator, being able to transfer their contents to other cells within the circulation.[201,305] In this thesis I have shown that platelet microvesicles containing mitochondria, express significantly higher P-selectin levels than the remainder of the microvesicle population. Recent work has highlighted a potential for differential release of granules, although the mechanisms for this remain unknown.[67,68] As I have identified mitochondria encapsulated within microvesicles as having high P-selectin, and it is well established that platelet activation pathways are extremely energy dependent, it may be that granules with close proximity to a mitochondrion are preferentially secreted.

It remains unknown whether mitochondria within platelets are motile and dynamic in nature as they are within other cell types. It is well established that in neurons, mitochondria are required to be transported large distances from the cell body down the axon to ensure that energy is readily available throughout the length of the nerves.[270] Although there are several reports that platelets and neurons are similar, there are striking differences between these cell types, most notably the size and lifespan. Does a small platelet need the capacity for mitochondrial transport? This would be an exciting question to address, however there would be a number of technical issues, namely live imaging resting platelets is challenging. The inherent nature of platelets to readily activate makes it very difficult to attach them to a surface for imaging without some accompanying degree of activation.

The high expression of P-selectin on mitochondria containing microvesicles led me to hypothesise that these microvesicles were more likely to interact with other cells within the vasculature. Indeed, in this thesis I was able to show that mitochondria containing microvesicles are able to interact with neutrophils, which I speculate is mediated by the interaction between P-selectin and PSGL-1. Interestingly,

mitochondria containing microvesicles cause the upregulation of the classical neutrophil activation markers, CD11b and CD66b whilst causing the downregulation of CXCR2. The change in expression pattern of these markers is suggestive of the neutrophils taking on a phagocytic phenotype.[285,286,306] Further work investigating the downstream consequences of this platelet mitochondria-neutrophil interaction would be interesting in helping to understand if this is a clearance mechanism and if the microvesicles are degraded following internalisation. On the other hand, this interaction may be providing a functional benefit; if the platelet mitochondria are able to fuse into the resident neutrophil mitochondrial network, they may be able to increase the energy capacity and enhance the cells' function. In addition to the influence on neutrophils, future work looking at the effect of mitochondria containing microvesicles on monocyte and endothelial cell function would be interesting given that both these cell types express PSGL-1.

The release of mitochondria from platelets is an exciting concept, as it may have enormous ramifications for other cells. In the final stages of a platelet's lifespan, do they expel their remaining mitochondria so that they can be taken up by other cells within the vasculature to enhance their mitochondria function? Mitochondria are dynamic organelles and can undergo fission, fusion and mitophagy to eliminate any mitochondrial damage, however these processes are finite. Therefore, having a new source of mitochondria donated from platelets may enhance the cellular respiratory capacity and replenish the store of mitochondrial DNA of various other cells so prolonging their healthy lifespans.

More generally, it still remains unknown whether platelet-derived vesicles have a beneficial or negative effect on cells within the vasculature. Evidence would indicate that it depends on the circumstances underlying their production and the condition of the local environment. Indeed, levels of microvesicles have been associated with disease progression in both chronic pathologies such as chronic kidney disease and cardiovascular diseases, as well as in acute pathologies such as trauma.[167,169,307,308] Furthermore, platelet microvesicles have been shown to have enhanced procoagulant activity, and as such may be contributors to pathological thrombosis.

As a result of this link to pathological progression, targeting microvesicle release may be appealing therapeutically. As I have shown that a high percentage of microvesicles are positive for annexin V, targeting the exposure of phosphatidylserine, by inhibiting the scramblase responsible for the flipping of this negatively charged phospholipid onto the external surface of the platelet, may result in a reduction in microvesicle release and potentially a reduction in thrombotic events.[309,310]

Together, the investigations performed in this thesis have highlighted the importance of mitochondria in platelet function, indicating a role beyond classical energy production via oxidative phosphorylation. The work presented here has provided an insight into a potential mechanism in which mitochondria loss, coupled with cytoskeletal degradation, throughout the platelet lifespan may be contributing to the exposure of phosphatidylserine, and subsequently commitment of old platelets to undergo degradation. Furthermore, this work has shown that mitochondria are packaged into platelet-derived microvesicles and released into the circulation following physiological stimulation, subsequently acting as an intracellular communicator by modulating the phenotype of neutrophils.

Bibliography

1. Austin, S.K. Haemostasis. *Medicine (Baltimore).* **41**, 208–211 (2013).
2. van Hinsbergh, V.W.M. The endothelium: vascular control of haemostasis. *Eur. J. Obstet. Gynecol. Reprod. Biol.* **95**, 198–201 (2001).
3. Clemetson, K.J. Platelets and primary haemostasis. *Thromb. Res.* **129**, 220–4 (2012).
4. Minors, D. S. Haemostasis, blood platelets and coagulation. *Anaesth. Intensive Care Med.* **8**, 214–216 (2007).
5. Mackman, N. Tilley, R.E. & Key, N.S. Role of the Extrinsic Pathway of Blood Coagulation in Hemostasis and Thrombosis. *Arterioscler. Thromb. Vasc. Biol.* **27**, 1687–1693 (2007).
6. Palta, S. Saroa, R. & Palta, A. Overview of the coagulation system. *Indian J. Anaesth.* **58**, 515–23 (2014).
7. Chapin, J. C. & Hajjar, K.A. Fibrinolysis and the control of blood coagulation. *Blood Rev.* **29**, 17–24 (2015).
8. Yatsenko, T. Rybachuk, V. Kharchenko, S, Grinenko, T. & Yusova, E. Effect of fribrinigen degradation products on various stages of the fibrinolytic process. *J. Pre-Clinical Clin. Res.* **9**, 18–22 (2015).
9. Loof, T.G. Deicke, C. & Medina, E. The role of coagulation/fibrinolysis during Streptococcus pyogenes infection. *Front. Cell. Infect. Microbiol.* **4**, 128 (2014).
10. Machlus, K.R. & Italiano, J.E. The incredible journey: From megakaryocyte development to platelet formation. *J. Cell Biol.* **201**, 785–96 (2013).
11. Kuter, D. J. Beeler, D.L. & Rosenberg, R.D. *The purification of megapoietin: A physiological regulator of megakaryocyte growth and platelet production Physiology* **91**, (1994).
12. Nakamura-Ishizu, A. *et al.* Thrombopoietin Metabolically Primes Hematopoietic Stem Cells to Megakaryocyte-Lineage Differentiation. *Cell Rep.* **25**, 1772-1785.e6 (2018).
13. Poulter, N.S. & Thomas, S.G. Cytoskeletal regulation of platelet formation: Coordination of F-actin and microtubules. *Int. J. Biochem. Cell Biol.* **66**, 69–74 (2015).

14. Machlus, K.R. Thon, J.N. & Italiano, J.E. Interpreting the developmental dance of the megakaryocyte: a review of the cellular and molecular processes mediating platelet formation.
15. Patel, S.R. *et al.* Differential roles of microtubule assembly and sliding in proplatelet formation by megakaryocytes. *Blood* **106**, 4076–85 (2005).
16. Patel, S.R. Hartwig, J.H. & Italiano, J.E.The biogenesis of platelets from megakaryocyte proplatelets. *J. Clin. Invest.* **115**, 3348–54 (2005).
17. Richardson, J.L. *et al.* Mechanisms of organelle transport and capture along proplatelets during platelet production. *Blood* **106**, 4066–75 (2005).
18. Thon, J.N. *et al.* Cytoskeletal mechanics of proplatelet maturation and platelet release. *J. Cell Biol.* **191**, 861–74 (2010).
19. Cohen, J A. & Leeksma, C.H. Determination of the life span of human blood platelets using labelled diisopropylfluorophosphonate. *J. Clin. Invest.* **35**, 964–9 (1956).
20. Lebois, M. & Josefsson, E.C. Regulation of platelet lifespan by apoptosis. *Platelets* **27**, 497–504 (2016).
21. Winocour, P.D. Platelet turnover in advanced diabetes. *Eur. J. Clin. Invest.* **24**, 34–37 (1994).
22. Mustard, J.F. Rowsell, H.C. & Murphy, E.A. Platelet economy (platelet survival and turnover). *Br. J. Haematol.* **12**, 1–24 (1966).
23. Dowling, M.R. Josefsson, E.C. Henley, K.J. Hodgkin, P.D. & Kile, B.T. Platelet senescence is regulated by an internal timer, not damage inflicted by hits. *Blood* **116**, 1776–1778 (2010).
24. McArthur, K. Chappaz, S. & Kile, B.T. Apoptosis in megakaryocytes and platelets: the life and death of a lineage. *Blood* **131**, 605–610 (2018).
25. Rand, M.L. Procoagulant surface exposure and apoptosis in rabbit platelets: Association with shortened survival and steady-state senescence. *J. Thromb. Haemost.* **2**, 651–659 (2004).
26. Vanags, D.M. Orrenius, S. & Aguilar-Santelises, M. Alterations in Bcl-2/Bax protein levels in platelets form part of an ionomycin-induced process that resembles apoptosis. *Br. J. Haematol.* **99**, 824–831 (1997).
27. Pereira, J. *et al.* Platelet Aging In Vivo Is Associated with Activation of

Apoptotic Pathways: Studies in a Model of Suppressed Thrombopoiesis in Dogs. *Thromb. Haemost.* **87**, 905–909 (2002).

28. Mason, K.D. *et al.* Programmed Anuclear Cell Death Delimits Platelet Life Span. *Cell* **128**, 1173–1186 (2007).
29. Vogler, M. *et al.* BCL2/BCL-X L inhibition induces apoptosis, disrupts cellular calcium homeostasis, and prevents platelet activation. (2011).
30. Kile, B.T. The role of apoptosis in megakaryocytes and platelets. *Br. J. Haematol.* **165**, 217–226 (2014).
31. Sørensen, A.L. *et al.* Role of sialic acid for platelet life span: exposure of beta-galactose results in the rapid clearance of platelets from the circulation by asialoglycoprotein receptor-expressing liver macrophages and hepatocytes. *Blood* **114**, 1645–54 (2009).
32. Jansen, G. & Hoffmeister, K.M. Sialic Acid Loss Regulates Platelet Survival and Integrity. *Blood* **122**, (2013).
33. Cho, J. *et al.* Platelet storage induces accelerated desialylation of platelets and increases hepatic thrombopoietin production. *J. Transl. Med.* **16**, 199 (2018).
34. Grozovsky, R. Hoffmeister, K.M. & Falet, H. Novel clearance mechanisms of platelets. *Curr. Opin. Hematol.* **17**, 585–9 (2010).
35. Li, M. F. *et al.* Platelet desialylation is a novel mechanism and a therapeutic target in thrombocytopenia during sepsis: An open-label, multicenter, randomized controlled trial. *J. Hematol. Oncol.* **10**, 1–10 (2017).
36. Li, R. Hoffmeister, K.M. & Falet, H. Glycans and the platelet life cycle. *Platelets* **27**, 505–11 (2016).
37. Kakouros, N. Rade, J.J. Kourliouros, A. & Resar, J.R. Platelet Function in Patients with Diabetes Mellitus: From a Theoretical to a Practical Perspective. *Int. J. Endocrinol.* **2011**, (2011).
38. Mijovic, R. *et al.* Reticulated platelets and antiplatelet therapy response in diabetic patients. *J. Thromb. Thrombolysis* **40**, 203–210 (2015).
39. Tabit, C.E. Chung, W.B. Hamburg, N.M. & Vita, J.A. Endothelial dysfunction in diabetes mellitus: molecular mechanisms and clinical implications. *Rev. Endocr. Metab. Disord.* **11**, 61–74 (2010).
40. Audia, S. Mahévas, M. Samson, M. Godeau, B. & Bonnotte, B. Pathogenesis of

immune thrombocytopenia. *Autoimmun. Rev.* **16**, 620–632 (2017).

41. Imperiali, C.E. *et al.* Reference interval for immature platelet fraction on Sysmex XN haematology analyser in adult population. *Biochem. medica* **28**, 010708 (2018).
42. Bearer, E.L. & Friend, D.S. Lipids of the platelet membrane. *Lab. Invest.* **54**, 119–21 (1986).
43. Hankins, H.M. Baldridge, R.D. Xu, P. & Graham, T.R. Role of flippases, scramblases, and transfer proteins in phosphatidylserine subcellular distribution.
44. Nagata, S. Suzuki, J. Segawa, K. & Fujii, T. Exposure of phosphatidylserine on the cell surface. *Cell Death Differ.* **23**, 952–61 (2016).
45. Escolar, G. Leistikow, E. & White, J.G. *The Fate of the Open Canalicular System in Surface and Suspension-Activated Platelets*. *Blood* **74**, (1989).
46. Thomas, S.G. *The Structure of Resting and Activated Platelets*. *Platelets* (Elsevier Inc., 2019).
47. White, J.G. Platelets are covercytes, not phagocytes: Uptake of bacteria involves channels of the open canalicular system. *Platelets* **16**, 121–131 (2005).
48. Selvadurai, M.V. & Hamilton, J.R. Structure and function of the open canalicular system – the platelet's specialized internal membrane network. *Platelets* **29**, 319–325 (2018).
49. Patel-Hett, S. *et al.* Visualization of microtubule growth in living platelets reveals a dynamic marginal band with multiple microtubules. *Blood* **111**, 4605–16 (2008).
50. Bearer, E. L. Prakash, J.M. & Li, Z. Actin dynamics in platelets. *Int. Rev. Cytol.* **217**, 137–82 (2002).
51. Hartwig, J.H. Mechanisms of actin rearrangements mediating platelet activation. *J. Cell Biol.* **118**, 1421–1442 (1992).
52. Ebbeling, L. Robertson, C. Mcnicol, A. & Gerrard, J.M. *Rapid Ultrastructural Changes in the Dense Tubular System Following Platelet Activation*. *Blood* **80,** 718-723 (1992).
53. Van Nispen Tot Pannerden, H. *et al.* The platelet interior revisited: electron

tomography reveals tubular-granule subtypes. *Blood* **116**, 1147–1156 (2010).

54. van Nispen Tot Pannerden, H.E. van Dijk, S.M. Du, V. & Heijnen, H.F.G. Platelet protein disulfide isomerase is localized in the dense tubular system and does not become surface expressed after activation. *Blood* **114**, 4738–40 (2009).
55. Gerrard, J.M. White, J.G. & Peterson, D.A. The platelet dense tubular system: its relationship to prostaglandin synthesis and calcium flux. *Thromb. Haemost.* **40**, 224–31 (1978).
56. Blair, P. & Flaumenhaft, R. Platelet alpha-granules: basic biology and clinical correlates. *Blood Rev.* **23**, 177–89 (2009).
57. Sharda, A. & Flaumenhaft, R. The life cycle of platelet granules. *F1000Research* **7**, 236 (2018).
58. Maynard, D.M. Heijnen, H.F.G. Gahl, W.A. & Gunay-Aygun, M. The α-granule proteome: novel proteins in normal and ghost granules in gray platelet syndrome. *J. Thromb. Haemost.* **8**, 1786–96 (2010).
59. Hayward, C.P.M. Inherited disorders of platelet alpha-granules. *Platelets* **8**, 197–210 (1997).
60. Heijnen, H. & van der Sluijs, P. Platelet secretory behaviour: as diverse as the granules … or not? *J. Thromb. Haemost.* **13**, 2141–2151 (2015).
61. McNicol, A. *et al.* Platelet dense granules: structure, function and implications for haemostasis. *Thromb. Res.* **95**, 1–18 (1999).
62. Yadav, S. & Storrie, B. The cellular basis of platelet secretion: Emerging structure/function relationships. *Platelets* **28**, 108–118 (2017).
63. Flaumenhaft, R. Molecular basis of platelet granule secretion. *Arterioscler. Thromb. Vasc. Biol.* **23**, 1152–60 (2003).
64. Chen, D. Lemons, P.P. Schraw, T. & Whiteheart, S.W. *Molecular mechanisms of platelet exocytosis: role of SNAP-23 and syntaxin 2 and 4 in lysosome release*. *Blood.* **96,** 1782-1788 (2000).
65. Jonnalagadda, D., Izu, L. T. & Whiteheart, S. W. Platelet secretion is kinetically heterogeneous in an agonist-responsive manner. *Blood* **120**, 5209 (2012).
66. Whiteheart, S. W. Platelet granules: surprise packages. *Blood* **118**, 1190–1 (2011).
67. Golebiewska, E.M. & Poole, A.W. Platelet secretion: From haemostasis to

wound healing and beyond. *Blood Rev.* **29**, 153–62 (2015).

68. Golebiewska, E.M. & Poole, A.W. Secrets of platelet exocytosis - what do we really know about platelet secretion mechanisms? *Br. J. Haematol.* **165**, 204 (2013).
69. Thon, J.N. & Italiano, J.E. Platelets: Production, Morphology and Ultrastructure. in *Handbook of experimental pharmacology* 3–22 (2012).
70. Wanders, R.J.A. & Waterham, H.R. Biochemistry of Mammalian Peroxisomes Revisited. *Annu. Rev. Biochem.* **75**, 295–332 (2006).
71. Zharikov, S. & Shiva, S. Platelet mitochondrial function: from regulation of thrombosis to biomarker of disease. *Biochem. Soc. Trans.* **41**, (2013).
72. Friedman, J.R. & Nunnari, J. Mitochondrial form and function. *Nature* **505**, 335–43 (2014).
73. Rowley, J.W. Schwertz, H. & Weyrich, A.S. Platelet mRNA: the meaning behind the message. *Curr Opin Hematol*. **19,** 385–391 (2012).
74. Rowley, J.W. & Weyrich, A.S. Ribosomes in platelets protect the messenger. *Blood* **129**, 2343–2345 (2017).
75. McManus, D.D. & Freedman, J.E. MicroRNAs in platelet function and cardiovascular disease. *Nat. Rev. Cardiol.* **12**, 711–717 (2015).
76. Boilard, E. & Belleannée, C. (Dicer)phering roles of microRNA in platelets. *Blood* **127**, 1733–4 (2016).
77. Edelstein, L.C. *et al.* MicroRNAs in platelet production and activation. *J. Thromb. Haemost.* **11**, 340–350 (2013).
78. Pordzik, J. *et al.* The Potential Role of Platelet-Related microRNAs in the Development of Cardiovascular Events in High-Risk Populations, Including Diabetic Patients: A Review. *Front. Endocrinol. (Lausanne).* **9**, 74 (2018).
79. Landry, P. *et al.* Existence of a microRNA pathway in anucleate platelets. *Nat. Struct. Mol. Biol.* **16**, 961–6 (2009).
80. Marketou, M. *et al.* Platelet microRNAs in hypertensive patients with and without cardiovascular disease. *J. Hum. Hypertens.* **33**, 149–156 (2019).
81. Chesnutt, J.K.W. & Han, H.C. Effect of Red Blood Cells on Platelet Activation and Thrombus Formation in Tortuous Arterioles. *Front. Bioeng. Biotechnol.* **1**, (2013).

82. Bye, A.P., Unsworth, A.J. & Gibbins, J.M. Platelet signaling: a complex interplay between inhibitory and activatory networks. *J. Thromb. Haemost.* **14**, 918–30 (2016).

83. Tomokiyo, K. *et al.* Von Willebrand factor accelerates platelet adhesion and thrombus formation on a collagen surface in platelet-reduced blood under flow conditions. *Blood* **105**, 1078–84 (2005).

84. Li, Z. Delaney, M.K. O'Brien, K.A. & Du, X. Signaling During Platelet Adhesion and Activation. *Arterioscler. Thromb. Vasc. Biol.* **30**, 2341–2349 (2010).

85. Gibbins, J.M. Platelet adhesion signalling and the regulation of thrombus formation. *J. Cell Sci.* **117**, 3415–3425 (2004).

86. Sangkuhl, K. Shuldiner, A.R. Klein, T.E. & Altman, R.B. Platelet aggregation pathway. *Pharmacogenet. Genomics* **21**, 516–21 (2011).

87. Varga-Szabo, D. Braun, A. & Nieswandt, B. Calcium signaling in platelets. *J. Thromb. Haemost.* **7**, 1057–1066 (2009).

88. Saeed, S.A. *et al.* Signaling mechanisms mediated by G-protein coupled receptors in human platelets. *Acta Pharmacol. Sin.* **25**, 887–892 (2016).

89. Stalker, T.J. Newman, D.K. Ma, P. Wannemacher, K.M. & Brass, L. F. Platelet signaling. *Handb. Exp. Pharmacol.* 59–85 (2012).

90. Bennett, J.S. Platelet-Fibrinogen Interactions. *Ann. N. Y. Acad. Sci.* **936**, 340–354 (2006).

91. Rosenbaum, D.M. Rasmussen, S.G.F. & Kobilka, B.K. The structure and function of G-protein-coupled receptors. *Nature* **459**, 356–63 (2009).

92. Van Eps, N. *et al.* Gi- and Gs-coupled GPCRs show different modes of G-protein binding. *Proc. Natl. Acad. Sci. U. S. A.* **115**, 2383–2388 (2018).

93. Offermanns, S. Activation of platelet function through G protein-coupled receptors. *Circ. Res.* **99**, 1293–304 (2006).

94. Woulfe, D.S. Platelet G protein-coupled receptors in hemostasis and thrombosis. *J. Thromb. Haemost.* **3**, 2193–2200 (2005).

95. Nicholas, R.A. Insights into platelet P2Y12 receptor activation. *Blood* **125**, 893–5 (2015).

96. Dorsam, R.T. & Kunapuli, S.P. Central role of the P2Y12 receptor in platelet activation. *J. Clin. Invest.* **113**, 340–5 (2004).

97. Parise, L.V. Venton, D.L. & Le Breton, G.C. Arachidonic acid-induced platelet aggregation is mediated by a thromboxane A2/prostaglandin H2 receptor interaction. *J. Pharmacol. Exp. Ther.* **228**, (1984).

98. Vane, J. R. Bakhle, Y.S. & Botting, R.M. CYCLOOXYGENASES 1 AND 2. *Annu. Rev. Pharmacol. Toxicol.* **38**, 97–120 (1998).

99. FitzGerald, G.A. Mechanisms of platelet activation: Thromboxane A2 as an amplifying signal for other agonists. *Am. J. Cardiol.* **68**, B11–B15 (1991).

100. Paul, B.Z. Jin, J. & Kunapuli, S.P. Molecular mechanism of thromboxane A(2)-induced platelet aggregation. Essential role for p2t(ac) and alpha(2a) receptors. *J. Biol. Chem.* **274**, 29108–14 (1999).

101. Keularts, I.M. van Gorp, R.M. Feijge, M.A., Vuist, W.M. & Heemskerk, J.W. alpha(2A)-adrenergic receptor stimulation potentiates calcium release in platelets by modulating cAMP levels. *J. Biol. Chem.* **275**, 1763–72 (2000).

102. Adam, F. Verbeuren, T.J. Fauchere, J.L. Guillin, M.C. & Jandrot-Perrus, M. Thrombin-induced platelet PAR4 activation: role of glycoprotein Ib and ADP. *J. Thromb. Haemost.* **1**, 798–804 (2003).

103. Montague, S.J. *et al.* Soluble GPVI is elevated in injured patients: Shedding is mediated by fibrin activation of GPVI. *Blood Adv.* **2**, 240–251 (2018).

104. Mangin, P.H. *et al.* Immobilized fibrinogen activates human platelets through glycoprotein VI. *Haematologica* **103**, 898–907 (2018).

105. Slater, A. *et al.* Does fibrin(ogen) bind to monomeric or dimeric GPVI, or not at all? *Platelets* **30**, 281–289 (2019).

106. Pilla, C. *et al.* ATP diphosphohydrolase activity (apyrase, EC 3.6.1.5) in human blood platelets. *Platelets* **7**, 225–230 (1996).

107. Mitchell, J.A. Ali, F. Bailey, L. Moreno, L. & Harrington, L.S. Experimental Physiology-Symposium Report Role of nitric oxide and prostacyclin as vasoactive hormones released by the endothelium. *Exp Physiol* **93**, 141–147

108. Levin, G. *et al.* Differential metabolism of dihomo-gamma-linolenic acid and arachidonic acid by cyclo-oxygenase-1 and cyclo-oxygenase-2: implications for cellular synthesis of prostaglandin E1 and prostaglandin E2. *Biochem. J.* **365**, 489–96 (2002).

109. McFadyen, J.D. Schaff, M. & Peter, K. Current and future antiplatelet

therapies: emphasis on preserving haemostasis. *Nat. Rev. Cardiol.* **15**, 181–191 (2018).

110. Schrör, K. Aspirin and Platelets: The Antiplatelet Action of Aspirin and Its Role in Thrombosis Treatment and Prophylaxis. *Semin. Thromb. Hemost.* **23**, 349–356 (1997).
111. Bednar, F. *et al.* Antiplatelet efficacy of P2Y12 inhibitors (prasugrel, ticagrelor, clopidogrel) in patients treated with mild therapeutic hypothermia after cardiac arrest due to acute myocardial infarction. *J. Thromb. Thrombolysis* **41**, 549–555 (2016).
112. Deshpande, N.V. Admane, P. & Mardikar, H.M. Bleeding on dual antiplatelet therapy: real-life challenges. *Eur. Hear. J. Suppl.* **20**, B1–B9 (2018).
113. Hroudová, J. & Fišar, Z. Control mechanisms in mitochondrial oxidative phosphorylation. *Neural Regen. Res.* **8**, 363–75 (2013).
114. Doery, B.J.C.G. Hiii, J. & Cooper, A.I. *Energy Metabolism in Human Platelets :Interrelationship Between Glycolysis and Oxidative Metabolism*. *Blood* **36**, 159-168 (1970).
115. Aibibula, M. Naseem, K.M. & Sturmey, R.G. Glucose metabolism and metabolic flexibility in blood platelets. *J. Thromb. Haemost.* **16**, 2300–2314 (2018).
116. Kramer, P.A. Ravi, S. Chacko, B. Johnson, M. . & Darley-Usmar, V.M. A review of the mitochondrial and glycolytic metabolism in human platelets and leukocytes: implications for their use as bioenergetic biomarkers. *Redox Biol.* **2**, 206–10 (2014).
117. Ravera, S. *et al.* Extramitochondrial energy production in platelets. *Biol. Cell* **110**, 97–108 (2018).
118. Ravera, S. & Panfoli, I. Platelet aerobic metabolism: new perspectives. *J. Unexplored Med. Data* **4:7** (2019).
119. Chaban, Y. Boekema, E.J. & Dudkina, N.V. Structures of mitochondrial oxidative phosphorylation supercomplexes and mechanisms for their stabilisation. *Biochim. Biophys. Acta - Bioenerg.* **1837**, 418–426 (2014).
120. Freedman, J.E. Oxidative Stress and Platelets. A*rterioscler Thromb Vasc Biol* **28,** 11-16 (2008).
121. Avila, C. *et al.* Platelet mitochondrial dysfunction is evident in type 2 diabetes

in association with modifications of mitochondrial anti-oxidant stress proteins. *Exp. Clin. Endocrinol. Diabetes* **120**, 248–51 (2012).

122. Choo, H.J. Saafir, T.B. Mkumba, L. Wagner, M.B. & Jobe, S.M. Mitochondrial calcium and reactive oxygen species regulate agonist-initiated platelet phosphatidylserine exposure. *Arterioscler. Thromb. Vasc. Biol.* **32**, 2946–55 (2012).
123. Kile, B.T. The role of the intrinsic apoptosis pathway in platelet life and death. *J. Thromb. Haemost.* **7**, 214–217 (2009).
124. Schoenwaelder, S.M. *et al.* Two distinct pathways regulate platelet phosphatidylserine exposure and procoagulant function. *Blood* **114**, 663–6 (2009).
125. Suzuki, J. Denning, D.P. Imanishi, E., Horvitz, H.R. & Nagata, S. Xk-related protein 8 and CED-8 promote phosphatidylserine exposure in apoptotic cells. *Science* **341**, 403–6 (2013).
126. Scott, I. & Youle, R.J. Mitochondrial fission and fusion. *Essays Biochem.* **47**, 85–98 (2010).
127. Burkhart, J.M. *et al.* The first comprehensive and quantitative analysis of human platelet protein composition allows the comparative analysis of structural and functional pathways. *Blood* **120,** 73-82 (2012)
128. Zhang, W. Siraj, S. Zhang, R. & Chen, Q. Mitophagy receptor FUNDC1 regulates mitochondrial homeostasis and protects the heart from I/R injury. *Autophagy* **13**, 1080–1081 (2017).
129. Walsh, T.G. van den Bosch, M.T.J. Lewis, K.E. Williams, C.M. & Poole, A.W. Loss of the mitochondrial kinase PINK1 does not alter platelet function. *Sci. Rep.* **8**, 14377 (2018).
130. Kaur, A. & Gardiner, E.E. Parkin the bus to manage stress. *EMBO Mol. Med.* **11**, (2019).
131. Zhang, W. *et al.* Hypoxic mitophagy regulates mitochondrial quality and platelet activation and determines severity of I/R heart injury. *Elife* **5**, (2016).
132. Zhang, W. *et al.* Nix-mediated mitophagy regulates platelet activation and life span. *Blood Adv.* **3**, 2342–2354 (2019).
133. Wang, L. *et al.* Platelet mitochondrial dysfunction and the correlation with

human diseases. *Biochem. Soc. Trans.* **45**, 1213–1223 (2017).

134. Yoshino, H. Nakagawa-Hattori, Y. Kondo, T. & Mizuno, Y. Mitochondrial complex I and II activities of lymphocytes and platelets in Parkinson's disease. *J. Neural Transm. Park. Dis. Dement. Sect.* **4**, 27–34 (1992).
135. FiŠar, Z. *et al.* Mitochondrial Respiration in the Platelets of Patients with Alzheimer's Disease. *Curr. Alzheimer Res.* **13**, 930–941 (2016).
136. Parker, W.D. Boyson, S.J. Luder, A.S. & Parks, J.K. Evidence for a defect in NADH: ubiquinone oxidoreductase (complex I) in Huntington's disease. *Neurology* **40**, 1231–4 (1990).
137. Valla, J. *et al.* Impaired platelet mitochondrial activity in Alzheimer's disease and mild cognitive impairment. *Mitochondrion* **6**, 323–30 (2006).
138. Antony, P.M.A. *et al.* Platelet mitochondrial membrane potential in Parkinson's disease. *Ann. Clin. Transl. Neurol.* **2**, 67–73 (2015).
139. Protti, A. *et al.* Platelet mitochondrial dysfunction in critically ill patients: comparison between sepsis and cardiogenic shock. *Crit. Care* **19**, 39 (2015).
140. Wu, F. *et al.* Platelet mitochondrial dysfunction of DM rats and DM patients. *Int. J. Clin. Exp. Med.* **8**, 6937–46 (2015).
141. Protti, A. *et al.* Metformin overdose causes platelet mitochondrial dysfunction in humans. *Crit. Care* **16**, R180 (2012).
142. Vevera, J. *et al.* Statin-induced changes in mitochondrial respiration in blood platelets in rats and human with dyslipidemia.
143. Xu, W. Cardenes, N. Corey, C. Erzurum, S.C. & Shiva, S. Platelets from Asthmatic Individuals Show Less Reliance on Glycolysis. *PLoS One* **10**, e0132007 (2015).
144. Bronstein, J.M. *et al.* Platelet mitochondrial activity and pesticide exposure in early Parkinson's disease. *Mov. Disord.* **30**, 862–6 (2015).
145. Park, J.S. Davis, R.L. & Sue, C.M. Mitochondrial Dysfunction in Parkinson's Disease: New Mechanistic Insights and Therapeutic Perspectives. *Curr. Neurol. Neurosci. Rep.* **18**, 21 (2018).
146. Puskarich, M.A. *et al.* Early alterations in platelet mitochondrial function are associated with survival and organ failure in patients with septic shock. *J. Crit. Care* **31**, 63–7 (2016).

147. Gründler, K. *et al.* Platelet mitochondrial membrane depolarization reflects disease severity in patients with sepsis and correlates with clinical outcome. *Crit. Care* **18**, R31 (2014).

148. Lee, S.H. *et al.* Inducing mitophagy in diabetic platelets protects against severe oxidative stress. *EMBO Mol. Med.* **8**, 779–95 (2016).

149. Wolf, P. The Nature and Significance of Platelet Products in Human Plasma. *Br. J. Haematol.* **13**, 269–288 (1967).

150. Yuana, Y. Sturk, A. & Nieuwland, R. Extracellular vesicles in physiological and pathological conditions. *Blood Rev.* **27**, 31–39 (2013).

151. Antwi-Baffour, S. *et al.* Understanding the biosynthesis of platelets-derived extracellular vesicles. *Immunity, Inflamm. Dis.* **3**, 133–40 (2015).

152. Herring, J.M. McMichael, M.A. & Smith, S.A. Microparticles in Health and Disease. *J. Vet. Intern. Med.* **27**, 1020–1033 (2013).

153. Ponomareva, A.A. Nevzorova, T.A. Mordakhanova, E.R. Andrianova, I.A. & Litvinov, R.I. Structural characterization of platelets and platelet microvesicles. *Cell tissue biol.* **10**, 217–226 (2016).

154. Heijnen, H.F. *et al.* Multivesicular bodies are an intermediate stage in the formation of platelet alpha-granules. *Blood* **91**, 2313–25 (1998).

155. Zaborowski, M.P. Balaj, L. Breakefield, X.O. & Lai, C.P. Extracellular Vesicles: Composition, Biological Relevance, and Methods of Study. *Bioscience* **65**, 783–797 (2015).

156. Boudreau, L.H. *et al.* Platelets release mitochondria serving as substrate for bactericidal group IIA-secreted phospholipase A2 to promote inflammation. *Blood* **124**, (2014).

157. Aatonen, MT. *et al.* Isolation and characterization of platelet-derived extracellular vesicles. *J. Extracell. Vesicles* **3**, (2014).

158. Boilard, E. Extracellular vesicles and their content in bioactive lipid mediators: more than a sack of microRNA. *J. Lipid Res.* **59**, 2037–2046 (2018).

159. Biro, E. *et al.* The phospholipid composition and cholesterol content of platelet-derived microparticles: a comparison with platelet membrane fractions. *J. Thromb. Haemost.* **3**, 2754–2763 (2005).

160. Sinauridze, E.I. *et al.* Platelet microparticle membranes have 50-to 100-fold

higher specificprocoagulant activity than activated platelets Blood Coagulation, Fibrinolysis and CellularHaemostasis. *ThrombHaemost* **97**, 425–434 (2007).

161. Cortez-Espinosa, N. *et al.* Platelets and Platelet-Derived Microvesicles as Immune Effectors in Type 2 Diabetes. *Curr. Vasc. Pharmacol.* **15**, 207–217 (2017).
162. Vajen, T. Mause, S.F. & Koenen, R.R. Microvesicles from platelets: novel drivers of vascular inflammation. *Thromb. Haemost.* **114**, 228–36 (2015).
163. Badimon, L. Suades, R. Fuentes, E. Palomo, I. & Padró, T. Role of Platelet-Derived Microvesicles As Crosstalk Mediators in Atherothrombosis and Future Pharmacology Targets: A Link between Inflammation, Atherosclerosis, and Thrombosis. *Front. Pharmacol.* **7**, 293 (2016).
164. Dickhout, A. & Koenen, R.R. Extracellular Vesicles as Biomarkers in Cardiovascular Disease; Chances and Risks. *Front. Cardiovasc. Med.* **5**, 113 (2018).
165. Koga, H. *et al.* Elevated levels of remnant lipoproteins are associated with plasma platelet microparticles in patients with type-2 diabetes mellitus without obstructive coronary artery disease. *Eur. Heart J.* **27**, 817–823 (2006).
166. Fu, H. Hu, D. Zhang, L. & Tang, P. Role of extracellular vesicles in rheumatoid arthritis. *Mol. Immunol.* **93**, 125–132 (2018).
167. Melki, I. Tessandier, N. Zufferey, A. & Boilard, E. Platelet microvesicles in health and disease. *Platelets* **28**, 214–221 (2017).
168. Gaetani, E. *et al.* Microparticles Produced by Activated Platelets Carry a Potent and Functionally Active Angiogenic Signal in Subjects with Crohn's Disease. *Int. J. Mol. Sci.* **19**, (2018).
169. Vulliamy, P. *et al.* Histone H4 induces platelet ballooning and microparticle release during trauma hemorrhage. *Proc. Natl. Acad. Sci. U.S.A.* **116,** 17444-49 (2019).
170. Revenfeld, A.L.S. *et al.* Diagnostic and prognostic potential of extracellular vesicles in peripheral blood. *Clin. Ther.* **36**, 830–46 (2014).
171. Rodriguez, J.A. *et al.* Selective increase of cardiomyocyte derived extracellular vesicles after experimental myocardial infarction and functional effects on the

endothelium. *Thromb. Res.* **170**, 1–9 (2018).

172. Melo, S.A. *et al.* Glypican-1 identifies cancer exosomes and detects early pancreatic cancer. *Nature* **523**, 177–182 (2015).
173. Revenfeld, A.L.S. *et al.* Diagnostic and prognostic potential of extracellular vesicles in peripheral blood. *Clin. Ther.* **36**, 830–46 (2014).
174. Warkentin, T.E. Aird, W.C. & Rand, J.H. Platelet-endothelial interactions: sepsis, HIT, and antiphospholipid syndrome. *Hematol. Am. Soc. Hematol. Educ. Progr.* **2003**, 497–519 (2003).
175. Bombeli, T. Schwartz, B.R. & Harlan, J.M. Adhesion of Activated Platelets to Endothelial Cells: Evidence for a GPIIbIIIa-dependent Bridging Mechanism and Novel Roles for Endothelial Intercellular Adhesion Molecule 1 (ICAM-1), $\alpha_v \beta_3$ Integrin, and GPIbα. *J. Exp. Med.* **187**, 329–339 (1998).
176. Langer, H.F. & Chavakis, T. Leukocyte-endothelial interactions in inflammation. *J. Cell. Mol. Med.* **13**, 1211–20 (2009).
177. Hamilos, M. Petousis, S. & Parthenakis, F. Interaction between platelets and endothelium: from pathophysiology to new therapeutic options. *Cardiovasc. Diagn. Ther.* **8**, 568–580 (2018).
178. Wu, M. D. Atkinson, T.M. & Lindner, J.R. Platelets and von Willebrand factor in atherogenesis. *Blood* **129**, 1415–1419 (2017).
179. Lam, F. W. Vijayan, K.V. & Rumbaut, R.E. Platelets and Their Interactions with Other Immune Cells. *Compr. Physiol.* **5**, 1265–80 (2015).
180. Finsterbusch, M. Schrottmaier, W.C. Kral-Pointner, J.B., Salzmann, M. & Assinger, A. Measuring and interpreting platelet-leukocyte aggregates. *Platelets* **29**, 677–685 (2018).
181. Zarbock, A. Polanowska-Grabowska, R.K. & Ley, K. Platelet-neutrophil-interactions: Linking hemostasis and inflammation. *Blood Rev.* **21**, 99–111 (2007).
182. Armstrong, P.C.J. *et al.* Novel whole blood assay for phenotyping platelet reactivity in mice identifies ICAM-1 as a mediator of platelet-monocyte interaction. *Blood* **126**, e11-18 (2015).
183. da Costa Martins, P. *et al.* Platelet-monocyte complexes support monocyte adhesion to endothelium by enhancing secondary tethering and cluster

formation. *Arterioscler. Thromb. Vasc. Biol.* **24**, 193–9 (2004).

184. Cerletti, C. de Gaetano, G. & Lorenzet, R. Platelet-leukocyte interactions: multiple links between inflammation, blood coagulation and vascular risk. *Mediterr. J. Hematol. Infect. Dis.* **2**, e2010023 (2010).
185. van Gils, J.M. da Costa Martins, P.A. Mol, A. Hordijk, P.L. & Zwaginga, J.J. Transendothelial migration drives dissociation of plateletmonocyte complexes. *Thromb. Haemost.* **100**, 271–9 (2008).
186. D'Mello, C. Almishri, W. Liu, H. & Swain, M.G. Interactions Between Platelets and Inflammatory Monocytes Affect Sickness Behavior in Mice With Liver Inflammation. *Gastroenterology* **153**, 1416-1428.e2 (2017).
187. Totani, L. & Evangelista, V. Platelet-leukocyte interactions in cardiovascular disease and beyond. *Arterioscler. Thromb. Vasc. Biol.* **30**, 2357–61 (2010).
188. Ogura, H. *et al.* Activated platelets enhance microparticle formation and platelet-leukocyte interaction in severe trauma and sepsis. *J. Trauma* **50**, 801–9 (2001).
189. Gabbasov, Z. *et al.* Impact of platelet phenotype on myocardial infarction. *Biomarkers* **20**, 17–25 (2015).
190. Fateh-Moghadam, S. *et al.* Hyperresponsiveness of platelets in ischemic stroke. *Thromb. Haemost.* **97**, 974–8 (2007).
191. Cevik, O. Baykal, A.T. & Sener, A. Platelets Proteomic Profiles of Acute Ischemic Stroke Patients. *PLoS One* **11**, e0158287 (2016).
192. Yip, H.K. *et al.* Serial Changes in Platelet Activation in Patients After Ischemic Stroke Role of Pharmacodynamic Modulation. *Stroke* **35,** 1683-1687 (2004).
193. Li, A. *et al.* Comparison of ultrastructural and nanomechanical signature of platelets from acute myocardial infarction and platelet activation. *Biochem. Biophys. Res. Commun.* **486**, 245–251 (2017).
194. Furman, M.I. *et al.* Increased Platelet Reactivity and Circulating Monocyte-Platelet Aggregates in Patients With Stable Coronary Artery Disease. *J. Am. Coll. Cardiol.* **31**, 352–358 (1998).
195. Egan, K. *et al.* Platelet adhesion and degranulation induce pro-survival and pro-angiogenic signalling in ovarian cancer cells. *PLoS One* **6**, e26125 (2011).
196. Wang, S. Li, Z. & Xu, R. Human Cancer and Platelet Interaction, a Potential

Therapeutic Target. *Int. J. Mol. Sci.* **19**, (2018).

197. Menter, D.G. *et al.* Platelets and cancer: a casual or causal relationship: revisited. *Cancer Metastasis Rev.* **33**, 231–69 (2014).
198. Leblanc, R. & Peyruchaud, O. Metastasis: new functional implications of platelets and megakaryocytes. *Blood* **128**, 24–31 (2016).
199. Cho, M.S. *et al.* Platelets increase the proliferation of ovarian cancer cells. *Blood* **120**, 4869–72 (2012).
200. Schlesinger, M. Role of platelets and platelet receptors in cancer metastasis. *J. Hematol. Oncol.* **11**, 125 (2018).
201. Lazar, S. & Goldfinger, L.E. Platelet Microparticles and miRNA Transfer in Cancer Progression: Many Targets, Modes of Action, and Effects Across Cancer Stages. *Front. Cardiovasc. Med.* **5**, 13 (2018).
202. Dorsch, C.A. & Meyerhoff, J. Mechanisms of abnormal platelet aggregation in systemic lupus erythematosus. *Arthritis Rheum.* **25**, 966–973 (1982).
203. Harifi, G. & Sibilia, J. Pathogenic role of platelets in rheumatoid arthritis and systemic autoimmune diseases. Perspectives and therapeutic aspects. *Saudi Med. J.* **37**, 354–60 (2016).
204. Wang, F. Wang, N.S. Yan, C.G. Li, J.H. & Tang, L.Q. The significance of platelet activation in rheumatoid arthritis. *Clin. Rheumatol.* **26**, 768–771 (2007).
205. Gasparyan, A.Y. & Kitas, G.D. Platelets in rheumatoid arthritis: exploring the anti-inflammatory and antithrombotic potential of TNF inhibitors. *Ann. Rheum. Dis.* **75**, 1426–7 (2016).
206. Gowert, N.S. *et al.* Blood platelets in the progression of Alzheimer's disease. *PLoS One* **9**, e90523 (2014).
207. Yamakawa, K. *et al.* Platelet mitochondrial membrane potential correlates with severity in patients with systemic inflammatory response syndrome. *J Trauma Acute Care Surg.* **74,** 411-418 (2013).
208. Kholmukhamedov, A. & Jobe, S. Platelet respiration. *Blood Adv.* **3**, 599–602 (2019).
209. Ravi, S. *et al.* Metabolic Plasticity in Resting and Thrombin Activated Platelets. *PLoS ONE* **10(4),** e0123597 (2015).
210. Packham, M.A. Role of platelets in thrombosis and hemostasis. *Can. J. Physiol.*

Pharmacol. **72**, 278–284 (1994).

211. Wang, Y. *et al.* Platelets in thrombosis and hemostasis: old topic with new mechanisms. *Cardiovasc. Hematol. Disord. Drug Targets* **12**, 126–32 (2012).
212. Koupenova, M., Kehrel, B. E., Corkrey, H. A. & Freedman, J. E. Thrombosis and platelets: an update. *European Heart Journal* **38**, 785-791 (207).
213. Hennekens, C.H. Buring, J.E. Sandercock, P. Collins, R. & Peto, R.*U* Clinical Progress Series Aspirin and Other Antiplatelet Agents in the Secondary and Primary Prevention of Cardiovascular Disease.*Circulation* **80,** 749-756 (1989).
214. Altman, R. Luciardi, H.L. Muntaner, J. & Herrera, R.N. The antithrombotic profile of aspirin. Aspirin resistance, or simply failure? *Thromb. J.* **2**, 1 (2004).
215. McKenzie, M.E. *et al.* Aspirin inhibits surface glycoprotein IIb/IIIa, P-selectin, CD63, and CD107a receptor expression on human platelets. *Blood Coagul. Fibrinolysis* **14**, 249–253 (2003).
216. Michelson, A.D. Platelet function testing in cardiovascular diseases. *Circulation* **110**, e489-93 (2004).
217. Ibanez, B. Vilahur, G. & Badimon, J.J. Pharmacology of thienopyridines: rationale for dual pathway inhibition. *European Heart Journal Supplements* **8,** G3-G9 (2006).
218. Leon, C. Ravanat, C. Freund, M. Cazenave, J.P. & Gachet, C. Differential involvement of the P2Y1 and P2Y12 receptors in platelet procoagulant activity. *Arterioscler. Thromb. Vasc. Biol.* **23**, 1941–7 (2003).
219. Chan, M.V Leadbeater, P.D. Watson, S.P. & Warner, T.D. Not all light transmission aggregation assays are created equal: qualitative differences between light transmission and 96-well plate aggregometry. *Platelets* **29**, 686–689 (2018).
220. Nesbitt, W.S. *et al.* Intercellular calcium communication regulates platelet aggregation and thrombus growth. *J. Cell Biol.* **160**, 1151–61 (2003).
221. Zorova, L.D. *et al.* Mitochondrial membrane potential. *Anal. Biochem.* **552**, 50–59 (2018).
222. Hansford, R.G. & Zorov, D. Role of mitochondrial calcium transport in the control of substrate oxidation. *Mol. Cell. Biochem.* **184**, 359–69 (1998).
223. Kholmukhamedov, A. Janecke, R. Choo, H. & Jobe, S.M. Mitochondrial Calcium

Entry Is Essential in Agonist-Induced Procoagulant Platelet Formation. *Blood* **128**, (2016).

224. Sowton, A.P. Millington-Burgess, S.L. Murray, A.J. & Harper, M.T. Rapid kinetics of changes in oxygen consumption rate in thrombin-stimulated platelets measured by high-resolution respirometry. *Biochem. Biophys. Res. Commun.* **503**, 2721–2727 (2018).
225. Koopman, M. *et al.* A screening-based platform for the assessment of cellular respiration in Caenorhabditis elegans. **11**, 1798–1816 (2017).
226. Crescente, M. Menke, L. Chan, M.V. Armstrong, P.C. & Warner, T.D. Eicosanoids in platelets and the effect of their modulation by aspirin in the cardiovascular system (and beyond). *Br. J. Pharmacol.* **176**, 988–999 (2019).
227. Ding, X.Z. Hennig, R. & Adrian, T.E. Lipoxygenase and cyclooxygenase metabolism: New insights in treatment and chemoprevention of pancreatic cancer. *Mol. Cancer* **2**, 1–12 (2003).
228. Behan, M.W.H. Fox, S.C. Heptinstall, S. & Storey, R.F. Inhibitory effects of $P2Y_{12}$ receptor antagonists on TRAP-induced platelet aggregation, procoagulant activity, microparticle formation and intracellular calcium responses in patients with acute coronary syndromes. *Platelets* **16**, 73–80 (2005).
229. Suzuki, Y. Inoue, T. & Ra, C. NSAIDs, Mitochondria and Calcium Signaling: Special Focus on Aspirin/Salicylates. *Pharmaceuticals (Basel).* **3**, 1594–1613 (2010).
230. Krzeminski, P. Misiewicz, I. Pomorski, P. Kasprzycka-Guttman, T. & Brańska, J. Mitochondrial localization of P2Y1, P2Y2 and P2Y12 receptors in rat astrocytes and glioma C6 cells. *Brain Res. Bull.* **71**, 587–592 (2007).
231. Thon, J.N. & Italiano, J.E. Platelet formation. *Semin. Hematol.* **47**, 220–6 (2010).
232. Lindemann, S. & Gawaz, M. The Active Platelet: Translation and Protein Synthesis in an Anucleate Cell. *Semin. Thromb. Hemost.* **33**, 144–150 (2007).
233. Clancy, L. & Freedman, J.E. New paradigms in thrombosis: novel mediators and biomarkers platelet RNA transfer. *J. Thromb. Thrombolysis* **37**, 12–6 (2014).
234. Risitano, A. Beaulieu, L.M. Vitseva, O. & Freedman, J.E. Platelets and platelet-like particles mediate intercellular RNA transfer. *Blood* **119**, 6288–95 (2012).

235. Laffont, B. *et al.* Activated platelets can deliver mRNA regulatory Ago2• microRNA complexes to endothelial cells via microparticles. *Blood* **122**, 253–61 (2013).

236. Ibrahim, H. *et al.* Association of Immature Platelets With Adverse Cardiovascular Outcomes. *J. Am. Coll. Cardiol.* **64**, 2122–2129 (2014).

237. Lee, E.Y. Kim, S.J. Song, Y.J. Choi, S.J. & Song, J. Immature platelet fraction in diabetes mellitus and metabolic syndrome. *Thromb. Res.* **132**, 692–695 (2013).

238. Armstrong, P.C. *et al.* Newly Formed Reticulated Platelets Undermine Pharmacokinetically Short-Lived Antiplatelet Therapies. *Arterioscler. Thromb. Vasc. Biol.* **37**, 949–956 (2017).

239. Grande, R. *et al.* Platelet-Derived Microparticles From Obese Individuals: Characterization of Number, Size, Proteomics, and Crosstalk With Cancer and Endothelial Cells. *Front. Pharmacol.* **10**, 7 (2019).

240. Fujii, T. Shimomura, T. Fujimoto, T.T. Kimura, A. & Fujimura, K.A New Approach to Detect Reticulated Platelets Stained with Thiazole Orange in Thrombocytopenic Patients. *Thromb. Res.* **97**, 431–440 (2000).

241. Balduini, C.L. *et al.* Relationship between size and thiazole orange fluorescence of platelets in patients undergoing high-dose chemotherapy. *British Journal of Haemotology* **106**, 202-207 (1999).

242. Dale, G.L. Friese, P. Hynes, L.A. & Burstein, S.A. Demonstration That Thiazole-Orange-Positive Platelets in the Dog Are Less Than 24 Hours Old. *Blood* **85,** 1822-1825 (1995).

243. Hille, L. *et al.* Evaluation of an Alternative Staining Method Using SYTO 13 to Determine Reticulated Platelets. *Thromb. Haemost.* **119**, 779–785 (2019).

244. Desjardins, P. Hansen, J.B. & Allen, M. Microvolume protein concentration determination using the NanoDrop 2000c Spectrophotometer. *J. Vis. Exp.* 3–5 (2010).

245. Kono, M. *et al.* Morphological and optical properties of human immature platelet-enriched population produced in immunodeficient mice. *Platelets* 1–6 (2018).

246. van der Bliek, A.M. Shen, Q. & Kawajiri, S. Mechanisms of mitochondrial fission and fusion. *Cold Spring Harb. Perspect. Biol.* **5**, a011072 (2013).

247. Jin, S.M. & Youle, R.J. PINK1- and Parkin-mediated mitophagy at a glance. *J. Cell Sci.* **125**, 795–9 (2012).

248. Palikaras, K. Lionaki, E. & Tavernarakis, N. Mechanisms of mitophagy in cellular homeostasis, physiology and pathology. *Nat. Cell Biol.* **20**, 1013–1022 (2018).

249. Flaumenhaft, R. *et al.* The actin cytoskeleton differentially regulates platelet-granule and dense-granule secretion. *Blood **105,** 3879-3887* (2005).

250. Thomas, S.G. Calaminus, S.D. Auger, J.M. Watson, S.P. & Machesky, L.M. Studies on the actin-binding protein HS1 in platelets. *BMC Cell Biol.* **8**, 46 (2007).

251. Choo, H.J. Kholmukhamedov, A. Zhou, C. & Jobe, S. Inner Mitochondrial Membrane Disruption Links Apoptotic and Agonist-Initiated Phosphatidylserine Externalization in Platelets. *Arterioscler. Thromb. Vasc. Biol.* **37**, 1503–1512 (2017).

252. Lhermusier, T. Chap, H. & Payrastre, B. Platelet membrane phospholipid asymmetry: from the characterization of a scramblase activity to the identification of an essential protein mutated in Scott syndrome. *J. Thromb. Haemost.* **9**, 1883–1891 (2011).

253. Comfurius, P. Bevers, E.M. & Zwaal, R.F.A. Interaction between phosphatidylserine and the isolated cytoskeleton of human blood platelets. *Biochim. Biophys. Acta - Biomembr.* **983**, 212–216 (1989).

254. Desouza, M. Gunning, P.W. & Stehn, J.R. The actin cytoskeleton as a sensor and mediator of apoptosis. *Bioarchitecture* **2**, 75–87 (2012).

255. Segawa, K. & Nagata, S. An Apoptotic 'Eat Me' Signal: Phosphatidylserine Exposure. *Trends Cell Biol.* **25**, 639–650 (2015).

256. Reddy, E.C. *et al.* Analysis of procoagulant phosphatidylserine-exposing platelets by imaging flow cytometry. *Res. Pract. Thromb. Haemost.* **2**, 736–750 (2018).

257. Stritt, S. *et al.* Twinfilin 2a regulates platelet reactivity and turnover in mice Key Points. *Blood* **130,** 1746-1756 (2017).

258. Williams, C.M. Li, Y. Brown, E. & Poole, A.W. Platelet-specific deletion of SNAP23 ablates granule secretion, substantially inhibiting arterial and venous thrombosis in mice. *Blood Adv.* **2**, 3627–3636 (2018).

259. Asmat, U. Abad, K. & Ismail, K. Diabetes mellitus and oxidative stress-A concise review. *Saudi Pharm. J. SPJ Off. Publ. Saudi Pharm. Soc.* **24**, 547–553 (2016).
260. Rinder, H.M. *et al.* Correlation of Thrombosis With Increased Platelet Turnover in Thrombocytosis. *Blood* **91,** 1288-1294 (1998).
261. Mezzano, D. Hwang, K. Catalano, P. & Aster, R.H. Evidence that platelet buoyant density, but not size, correlates with platelet age in man. *Am. J. Hematol.* **11**, 61–76 (1981).
262. Handtke, S. *et al.* Role of Platelet Size Revisited—Function and Protein Composition of Large and Small Platelets. *Thromb. Haemost.* **119**, 407–420 (2019).
263. Klement, G.L. *et al.* Platelets actively sequester angiogenesis regulators. *Blood* **113**, 2835–42 (2009).
264. Kerr, B.A. & Byzova, T.V. Platelet Sequestered Proteins Mediate Pre-Metastatic Communication Between Tumors and Bone. *Blood* **122**, (2013).
265. Sonmez, O. & Sonmez, M. Role of platelets in immune system and inflammation. *Porto Biomed. J.* **2**, 311–314 (2017).
266. Gros, A. Ollivier, V. & Ho-Tin-Noé, B. Platelets in inflammation: regulation of leukocyte activities and vascular repair. *Front. Immunol.* **5**, 678 (2014).
267. Galluzzi, L. Kepp, O. Trojel-Hansen, C. & Kroemer, G. Mitochondrial control of cellular life, stress, and death. *Circ. Res.* **111**, 1198–207 (2012).
268. Hollenbeck, P.J. & Saxton, W.M. The axonal transport of mitochondria. *J. Cell Sci.* **118**, 5411 (2005).
269. Melkov, A. & Abdu, U. Regulation of long-distance transport of mitochondria along microtubules. *Cell. Mol. Life Sci.* **75**, 163–176 (2018).
270. Frederick, R.L. & Shaw, J.M. Moving mitochondria: establishing distribution of an essential organelle. *Traffic* **8**, 1668–75 (2007).
271. Wu, M. Kalyanasundaram, A. & Zhu, J. Structural and biomechanical basis of mitochondrial movement in eukaryotic cells. *Int. J. Nanomedicine* **8**, 4033–42 (2013).
272. Kubli, D.A. & Gustafsson, Å.B. Mitochondria and mitophagy: the yin and yang of cell death control. *Circ. Res.* **111**, 1208–21 (2012).
273. Bozza, F.A. & Weyrich, A.S. Mitochondria push platelets past their prime.

Blood **111**, 2496–2497 (2008).

274. Jobe, S.M. *et al.* Critical role for the mitochondrial permeability transition pore and cyclophilin D in platelet activation and thrombosis. *Blood* **111,** 1257-1265 (2008).
275. Agbani, E.O. & Poole, A.W. Procoagulant platelets: generation, function, and therapeutic targeting in thrombosis. *Blood* **130**, 2171–2179 (2017).
276. Puhm, F. *et al.* Mitochondria Are a Subset of Extracellular Vesicles Released by Activated Monocytes and Induce Type I IFN and TNF Responses in Endothelial Cells. *Circ. Res.* **125**, 43–52 (2019).
277. Torralba, D. Baixauli, F. & Sánchez-Madrid, F. Mitochondria Know No Boundaries: Mechanisms and Functions of Intercellular Mitochondrial Transfer. *Front. Cell Dev. Biol.* **4**, 107 (2016).
278. Tugolukova, E.A. *et al.* Mitochondrial Fission Protein Drp1 Regulates Megakaryocyte and Platelet Mitochondrial Morphology, Platelet Numbers, and Platelet Function. *Blood* **130**, (2017).
279. Lowenstein, C.J. VAMP-3 mediates platelet endocytosis. *Blood* **130**, 2816–2818 (2017).
280. Zhao, Z. *et al.* Extracellular mitochondria released from traumatized brains induced platelet procoagulant activity. *Haematologica **105,** 209-217* (2020).
281. Duchez, A.C. *et al.* Platelet microparticles are internalized in neutrophils via the concerted activity of 12-lipoxygenase and secreted phospholipase A2-IIA. *Proc. Natl. Acad. Sci. U.S.A.* **112**, E3564 (2015).
282. Fortunati, E. Kazemier, K.M. Grutters, J.C. Koenderman, L. & Van den Bosch, van J.M.M. Human neutrophils switch to an activated phenotype after homing to the lung irrespective of inflammatory disease. *Clin. Exp. Immunol.* **155**, 559–66 (2009).
283. Abdel-Salam, B.K.A. & Ebaid, H. Expression of CD11b and CD18 on polymorphonuclear neutrophils stimulated with interleukin-2. *Cent. J. Immunol.* **39**, 209–15 (2014).
284. Hentzen, E.R. *et al.* Sequential binding of CD11a/CD18 and CD11b/CD18 defines neutrophil capture and stable adhesion to intercellular adhesion molecule-1. *Blood* **95,** 911-920 (2000).

285. Doroshenko, T. *et al.* Phagocytosing neutrophils down-regulate the expression of chemokine receptors CXCR1 and CXCR2. *Blood **100,** 2668-2671*(2002).
286. Lane, T. *et al.* Phagocytosis-induced modulation of human neutrophil chemotaxis receptors. *Blood* **58**, 228–236 (2002).
287. Dasgupta, S.K. *et al.* Lactadherin and clearance of platelet-derived microvesicles. *Blood* **113**, 1332–9 (2009).
288. Miralda, I. Uriarte, S.M. & McLeish, K.R. Multiple Phenotypic Changes Define Neutrophil Priming. *Front. Cell. Infect. Microbiol.* **7**, 217 (2017).
289. Marcoux, G. *et al.* Platelet-derived extracellular vesicles convey mitochondrial DAMPs in platelet concentrates and their levels are associated with adverse reactions. *Transfusion* **59**, 2403–2414 (2019).
290. Handtke, S. Steil, L. Greinacher, A. & Thiele, T. Toward the Relevance of Platelet Subpopulations for Transfusion Medicine. *Front. Med.* **5**, 17 (2018).
291. Born, G.V.T. Aggregation of blood platelet by adenosine diphosphate. *Nature* **194**, 927–9 (1962).
292. Chan, M.V. Armstrong, P.C.J. Papalia, F. Kirkby, N.S. & Warner, T.D. Optical multichannel (optimul) platelet aggregometry in 96-well plates as an additional method of platelet reactivity testing. *Platelets* **22**, 485–494 (2011).
293. Ravi, S. *et al.* Metabolic Plasticity in Resting and Thrombin Activated Platelets. *PLoS ONE* **10(4),** e0123597 (2015).
294. Södergren, A.L. & Ramström, S. Platelet subpopulations remain despite strong dual agonist stimulation and can be characterised using a novel six-colour flow cytometry protocol. *Sci. Reports 2018 81* **8**, 1–12 (2018).
295. Lesyk, G. & Jurasz, P. Advances in Platelet Subpopulation Research. *Front. Cardiovasc. Med.* **6**, 138 (2019).
296. Hoffmann, J. Reticulated platelets: analytical aspects and clinical utility Formation and maturation of megakaryocytes. *Clin. Chem. Lab. Med.* **52,** 1107-1117 (2014).
297. Grove, E.L. Hvas, A.M. Mortensen, S.B. Larsen, S.B. & Kristensen, S.D. Effect of platelet turnover on whole blood platelet aggregation in patients with coronary artery disease. *J. Thromb. Haemost.* **9**, 185–191 (2011).
298. Thompson, C.B. Love, D.G. Quinn, P.G. & Valeri, C.R. *Platelet Size Does Not*

Correlate With Platelet Age. *Blood* **62**, (1983).

299. Thompson, C.B. Jakubowski, J.A. Quinn, P.G. Deykin, D. & Valeri, C.R. *Platelet Size and Age Determine Platelet Function Independently*. *Blood* **63**, (1984).
300. Robinson, M. Machin, S. Mackie, I. & Harrison, P. In vivo biotinylation studies: specificity of labelling of reticulated platelets by thiazole orange and mepacrine. *Br. J. Haematol.* **108**, 859–864 (2000).
301. Banerjee, M. & Whiteheart, S.W. The ins and outs of endocytic trafficking in platelet functions. *Curr. Opin. Hematol.* **24**, 467–474 (2017).
302. Bongiovanni, D. *et al.* Transcriptome Analysis of Reticulated Platelets Reveals a Prothrombotic Profile. *Thromb. Haemost.* **119**, 1795–1806 (2019).
303. Gupta, S. *et al.* GPVI signaling is compromised in newly formed platelets after acute thrombocytopenia in mice. *Blood* **131**, 1106–1110 (2018).
304. Tao, S.C. Guo, S.C. & Zhang, C.Q. Platelet-derived Extracellular Vesicles: An Emerging Therapeutic Approach. *Int. J. Biol. Sci.* **13**, 828–834 (2017).
305. Żmigrodzka, M. Guzera, M. Miśkiewicz, A. Jagielski, D. Winnicka, A. The biology of extracellular vesicles with focus on platelet microparticles and their role in cancer development and progression. *Tumor Biol.* **37,** 14391-14401 (2016).
306. Lakschevitz, F.S. *et al.* Identification of neutrophil surface marker changes in health and inflammation using high-throughput screening flow cytometry. *Exp. Cell Res.* **342**, 200–209 (2016).
307. Shamekhi Amiri, F. Microparticles in kidney diseases: focus on kidney transplantation. *Ren. Replace. Ther.* **3**, 24 (2017).
308. Piccin, A. Murphy, W.G. & Smith, O.P. Circulating microparticles: pathophysiology and clinical implications. *Blood Rev.* **21**, 157–171 (2007).
309. Fujii, T. Sakata, A. Nishimura, S. Eto, K. & Nagata, S. TMEM16F is required for phosphatidylserine exposure and microparticle release in activated mouse platelets. *Proc. Natl. Acad. Sci. U.S.A.* **112,** 12800-12805 (2015).
310. Yang, H. *et al.* TMEM16F forms a Ca2+-activated cation channel required for lipid scrambling in platelets during blood coagulation. *Cell* **151**, 111–22 (2012).

Appendix 1: The proteome of thiazole orange sorted platelets

Protein ID	Protein	Protein Name	Young Z score	Intermediate Z Score	Old Z Score
P01624	KV315	Immunoglobulin kappa variable 3-15	-0.1474	-0.3070	0.4545
H7BXI1	H7BXI1	Extended synaptotagmin-2	0.3308	-0.5546	0.2237
B9A064	IGLL5	Immunoglobulin lambda-like polypeptide 5	-0.9803	-0.0275	1.0077
O00139	KIF2A	Kinesin-like protein KIF2A	0.1685	-0.0517	-0.1167
O00151	PDLI1	PDZ and LIM domain protein 1	0.4820	-0.5625	0.0804
O00161	SNP23	Synaptosomal-associated protein 23	1.0689	-0.9345	-0.1345
O00194	RB27B	Ras-related protein Rab-27B	0.5364	0.4026	-0.9389
O00231	PSD11	26S proteasome non-ATPase regulatory subunit 11	0.5913	-0.4430	-0.1483
O00264	PGRC1	Membrane-associated progesterone receptor component 1	0.8114	0.2005	-1.0119
O00299	CLIC1	Chloride intracellular channel protein 1	0.3917	0.4727	-0.8644
O00429	DNM1L	Dynamin-1-like protein	0.7850	-0.8775	0.0926
O00483	NDUA4	Cytochrome c oxidase subunit NDUFA4	0.4168	-0.6326	0.2158
O14745	NHRF1	Na(+)/H(+) exchange regulatory cofactor NHE-RF1	-0.6044	0.3637	0.2407
O14773	TPP1	Tripeptidyl-peptidase 1	-0.2922	-0.0538	0.3460
O14791	APOL1	Apolipoprotein L1	-0.0103	-0.3329	0.3431
P19105	ML12A	Myosin regulatory light chain 12A	0.5900	0.4342	-1.0242
O15117	FYB1	FYN-binding protein 1	0.6664	-0.0960	-0.5704
O15127	SCAM2	Secretory carrier-associated membrane protein 2	0.2373	0.0334	-0.2707
O15143	ARC1B	Actin-related protein 2/3 complex subunit 1B	0.6574	-0.2447	-0.4127
O15144	ARPC2	Actin-related protein 2/3 complex subunit 2	-0.4238	0.3461	0.0777
O15145	ARPC3	Actin-related protein 2/3 complex subunit 3	0.5962	0.1430	-0.7392
O15173	PGRC2	Membrane-associated progesterone receptor component 2	-0.8051	0.1953	0.6098
O15400	STX7	Syntaxin-7	0.2862	-0.1618	-0.1244
O15511	ARPC5	Actin-related protein 2/3 complex subunit 5	-0.2274	-0.0518	0.2791
O43182	RHG06	Rho GTPase-activating protein 6	0.5095	-0.0513	-0.4582
O43242	PSMD3	26S proteasome non-ATPase regulatory subunit 3	0.0495	-0.0980	0.0485
O43294	TGFI1	Transforming growth factor beta-1-induced transcript 1 protein	0.0042	-0.3130	0.3088
O43396	TXNL1	Thioredoxin-like protein 1	-0.3235	0.3648	-0.0412
O43399	TPD54	Tumor protein D54	-0.4045	0.8384	-0.4339
O43488	ARK72	Aflatoxin B1 aldehyde reductase member 2	0.4159	0.3286	-0.7445
O43639	NCK2	Cytoplasmic protein NCK2	0.2032	0.5176	-0.7208
O43707	ACTN4	Alpha-actinin-4	0.7094	-0.1288	-0.5807
O43852	CALU	Calumenin	0.2445	-0.1638	-0.0807
H7BXZ5	H7BXZ5	Kalirin	0.7039	-0.1638	-0.5401
O60234	GMFG	Glia maturation factor gamma	-0.3571	0.2895	0.0676
O60493	SNX3	Sorting nexin-3	0.5480	-0.3107	-0.2373
O60496	DOK2	Docking protein 2	0.3402	-0.3667	0.0265
A0A140T8Z0	A0A140T8Z0	Protein diaphanous homolog 1	0.8132	-0.4855	-0.3277
O60664	PLIN3	Perilipin-3	-0.2622	0.1731	0.0890
Q99879	H2B1M	Histone H2B type 1-M	0.6530	-0.5617	-0.0912
O75083	WDR1	WD repeat-containing protein 1	0.3186	-0.1524	-0.1662
O75116	ROCK2	Rho-associated protein kinase 2	0.6090	-0.2670	-0.3420
K7EMR7	K7EMR7	Reticulon	0.5958	-0.5897	-0.0060
O75368	SH3L1	SH3 domain-binding glutamic acid-rich-like protein	0.7935	0.0317	-0.8252
B4DJV2	B4DJV2	Citrate synthase	0.9785	-0.1853	-0.7932
O75396	SC22B	Vesicle-trafficking protein SEC22b	-0.4229	-0.0011	0.4240
O75558	STX11	Syntaxin-11	0.5805	-0.1788	-0.4017
O75563	SKAP2	Src kinase-associated phosphoprotein 2	0.4727	-0.4048	-0.0679
O75874	IDHC	Isocitrate dehydrogenase [NADP] cytoplasmic	0.5785	-0.1520	-0.4265
O75915	PRAF3	PRA1 family protein 3	0.3390	0.5713	-0.9102
E9PN17	E9PN17	ATP synthase subunit g, mitochondrial	0.8459	-0.4409	-0.4050
O76074	PDE5A	cGMP-specific 3',5'-cyclic phosphodiesterase	0.5675	-0.1024	-0.4651
O94886	CSCL1	CSC1-like protein 1	0.4651	-0.5345	0.0694
O94919	ENDD1	Endonuclease domain-containing 1 protein	0.5352	-0.1813	-0.3539
O95336	6PGL	6-phosphogluconolactonase	-0.1147	0.2583	-0.1436

O95721	SNP29	Synaptosomal-associated protein 29	-0.1028	0.0055	0.0973
O95810	CAVN2	Caveolae-associated protein 2	-0.6124	0.0696	0.5428
O95870	ABHGA	Phosphatidylserine lipase ABHD16A	0.4504	0.2067	-0.6571
P00338	LDHA	L-lactate dehydrogenase A chain	1.1609	-0.7740	-0.3868
P00387	NB5R3	NADH-cytochrome b5 reductase 3	0.4708	-0.5806	0.1098
P00390	GSHR	Glutathione reductase, mitochondrial	0.0430	-0.2538	0.2108
P00403	COX2	Cytochrome c oxidase subunit 2	1.1537	-0.7474	-0.4063
E9PFZ2	E9PFZ2	Ceruloplasmin	0.3836	-0.3125	-0.0711
P00488	F13A	Coagulation factor XIII A chain	0.6420	0.0848	-0.7268
P00491	PNPH	Purine nucleoside phosphorylase	0.0522	0.4891	-0.5413
P00492	HPRT	Hypoxanthine-guanine phosphoribosyltransferase	0.1173	-0.3906	0.2733
P00505	AATM	Aspartate aminotransferase, mitochondrial	0.2134	0.1097	-0.3231
P00558	PGK1	Phosphoglycerate kinase 1	0.4851	-0.4472	-0.0379
P00734	THRB	Prothrombin	-0.7134	0.3020	0.4114
P00738	HPT	Haptoglobin	-0.7868	0.0861	0.7007
P00747	PLMN	Plasminogen	-0.2407	0.4019	-0.1612
P00751	CFAB	Complement factor B	-0.1651	-0.2591	0.4242
E5RHP7	E5RHP7	Carbonic anhydrase 1	-0.7988	0.1774	0.6213
P00918	CAH2	Carbonic anhydrase 2	0.0164	-0.3463	0.3299
P01011	AACT	Alpha-1-antichymotrypsin	0.2723	-0.4827	0.2103
P01019	ANGT	Angiotensinogen	-0.0545	-0.1215	0.1760
P01023	A2MG	Alpha-2-macroglobulin	-0.0315	-0.0573	0.0888
P01024	CO3	Complement C3	-0.5167	0.2111	0.3056
P01031	CO5	Complement C5	-1.1780	0.3225	0.8555
P01042	KNG1	Kininogen-1	0.2735	0.0531	-0.3266
P01137	TGFB1	Transforming growth factor beta-1 proprotein	0.6435	-0.0320	-0.6115
C9JA05	C9JA05	Immunoglobulin J chain	-0.5973	0.3554	0.2419
P01619	KV320	Immunoglobulin kappa variable 3-20	-0.4159	-0.0974	0.5133
P01834	IGKC	Immunoglobulin kappa constant	-0.4685	0.2527	0.2157
P01857	IGHG1	Immunoglobulin heavy constant gamma 1	-0.4547	-0.1718	0.6265
P01859	IGHG2	Immunoglobulin heavy constant gamma 2	0.7095	-0.8263	0.1168
P01861	IGHG4	Immunoglobulin heavy constant gamma 4	0.3383	-0.5976	0.2593
P01871	IGHM	Immunoglobulin heavy constant mu	-0.2259	-0.0999	0.3258
P01876	IGHA1	Immunoglobulin heavy constant alpha 1	-0.0221	0.3126	-0.2905
P01889	1B07	HLA class I histocompatibility antigen, B-7 alpha chain	0.1469	-0.3539	0.2070
P02647	APOA1	Apolipoprotein A-I	-0.5187	0.4593	0.0594
P02649	APOE	Apolipoprotein E	-0.8205	0.0608	0.7598
V9GYE3	V9GYE3	Apolipoprotein A-II	-0.3954	0.4269	-0.0315
K7ERI9	K7ERI9	Apolipoprotein C-I	-0.0203	-0.0555	0.0758
P02656	APOC3	Apolipoprotein C-III	-0.3143	-0.0261	0.3404
P02671	FIBA	Fibrinogen alpha chain	-0.6393	-0.4206	1.0598
P02675	FIBB	Fibrinogen beta chain	0.3155	-0.6102	0.2946
P02679	FIBG	Fibrinogen gamma chain	0.2556	0.0735	-0.3291
P02747	C1QC	Complement C1q subcomponent subunit C	-0.4371	-0.2205	0.6576
P02748	CO9	Complement component C9	-0.1710	-0.2786	0.4496
P02751	FINC	Fibronectin	-0.6961	0.1441	0.5519
P02765	FETUA	Alpha-2-HS-glycoprotein	0.2250	0.1955	-0.4205
P02774	VTDB	Vitamin D-binding protein	-0.8792	0.5003	0.3790
P02775	CXCL7	Platelet basic protein	0.9185	-0.1984	-0.7201
P02776	PLF4	Platelet factor 4	0.4097	0.1234	-0.5331
P02787	TRFE	Serotransferrin	-0.1881	0.6245	-0.4364
P02790	HEMO	Hemopexin	0.1202	0.0687	-0.1889
P04003	C4BPA	C4b-binding protein alpha chain	0.6354	-0.2375	-0.3979
P04004	VTNC	Vitronectin	0.0939	-0.0037	-0.0903
P04040	CATA	Catalase	0.0518	-0.1180	0.0662
P04075	ALDOA	Fructose-bisphosphate aldolase A	0.8716	-0.5173	-0.3543
P04114	APOB	Apolipoprotein B-100	-0.8012	0.2129	0.5883
P04179	SODM	Superoxide dismutase [Mn], mitochondrial	0.7702	0.0397	-0.8098
P04196	HRG	Histidine-rich glycoprotein	0.3137	-0.3132	-0.0005
M0R009	M0R009	Alpha-1B-glycoprotein	-0.6742	-0.0513	0.7255
P04275	VWF	von Willebrand factor	0.7588	0.0430	-0.8018
P04406	G3P	Glyceraldehyde-3-phosphate dehydrogenase	0.5385	-0.4752	-0.0633
P04632	CPNS1	Calpain small subunit 1	0.8143	-0.5378	-0.2764

P04792	HSPB1	Heat shock protein beta-1	-0.0924	-0.0969	0.1893
P04843	RPN1	Dolichyl-diphosphooligosaccharide--protein glycosyltransferase subunit 1	0.9500	-0.6285	-0.3214
P04844	RPN2	Dolichyl-diphosphooligosaccharide--protein glycosyltransferase subunit 2	0.8019	0.1668	-0.9687
P04899	GNAI2	Guanine nucleotide-binding protein G	0.1722	-0.5154	0.3433
A0A0A0MRG2	A0A0A0MRG2	Amyloid-beta precursor protein	0.1229	0.2457	-0.3686
P05090	APOD	Apolipoprotein D	0.1229	-0.1271	0.0042
P05106	ITB3	Integrin beta-3	1.1148	-0.5295	-0.5853
P05121	PAI1	Plasminogen activator inhibitor 1	0.3155	0.0321	-0.3476
P05141	ADT2	ADP/ATP translocase 2	0.7893	0.0635	-0.8528
P05155	IC1	Plasma protease C1 inhibitor	0.6589	-0.2648	-0.3940
P05546	HEP2	Heparin cofactor 2	-0.8674	0.1169	0.7505
P05556	ITB1	Integrin beta-1	0.2930	0.3656	-0.6586
P05771	KPCB	Protein kinase C beta type	0.7954	-0.4960	-0.2994
P05976	MYL1	Myosin light chain 1/3, skeletal muscle isoform	0.3953	-0.2455	-0.1498
P06396	GELS	Gelsolin	0.2257	-0.2591	0.0334
P06576	ATPB	ATP synthase subunit beta, mitochondrial	1.1680	-0.1766	-0.9914
P06702	S10A9	Protein S100-A9	0.2012	0.1233	-0.3245
R4GN98	R4GN98	Protein S100	-0.1548	0.1616	-0.0067
P06727	APOA4	Apolipoprotein A-IV	-0.9149	0.4312	0.4837
P06733	ENOA	Alpha-enolase	0.0896	-0.1775	0.0879
P06737	PYGL	Glycogen phosphorylase, liver form	0.4084	-0.4048	-0.0037
P06744	G6PI	Glucose-6-phosphate isomerase	0.9360	-0.6537	-0.2823
P07195	LDHB	L-lactate dehydrogenase B chain	0.9135	-0.3526	-0.5608
A0A087WUQ6	A0A087WUQ6	Glutathione peroxidase	0.7072	-0.5574	-0.1497
P07225	PROS	Vitamin K-dependent protein S	0.5930	-0.5915	-0.0015
P07237	PDIA1	Protein disulfide-isomerase	0.8638	-0.1058	-0.7580
A0A1B0GW44	A0A1B0GW44	Cathepsin D	0.4187	-0.5287	0.1100
A0A0C4DGZ8	A0A0C4DGZ8	Glycoprotein Ib	0.2228	-0.0713	-0.1514
P07360	CO8G	Complement component C8 gamma chain	-0.8899	0.1192	0.7707
P07384	CAN1	Calpain-1 catalytic subunit	1.0486	-0.4221	-0.6265
Q5JP53	Q5JP53	Tubulin beta chain	-0.1129	-0.0225	0.1354
P07737	PROF1	Profilin-1	0.8387	-0.4228	-0.4160
P07741	APT	Adenine phosphoribosyltransferase	0.2597	-0.5326	0.2729
P07900	HS90A	Heat shock protein HSP 90-alpha	0.4970	0.0644	-0.5614
P07948	LYN	Tyrosine-protein kinase Lyn	0.5703	-1.1055	0.5352
P07954	FUMH	Fumarate hydratase, mitochondrial	0.4718	0.0257	-0.4976
P08238	HS90B	Heat shock protein HSP 90-beta	0.7131	0.0701	-0.7832
P08514	ITA2B	Integrin alpha-IIb	0.8581	-0.0641	-0.7940
P08567	PLEK	Pleckstrin	0.6812	-0.8487	0.1675
B0YJC4	B0YJC4	Vimentin	0.4616	-0.2150	-0.2466
P08697	A2AP	Alpha-2-antiplasmin	-0.0452	-0.5230	0.5682
P09211	GSTP1	Glutathione S-transferase P	0.4351	-0.5854	0.1504
P09486	SPRC	SPARC	0.6691	0.0010	-0.6700
P09496	CLCA	Clathrin light chain A	0.2061	-0.4427	0.2366
A0A087X232	A0A087X232	Complement C1s subcomponent	-0.8260	-0.2758	1.1019
P0C0L4	CO4A	Complement C4-A	-1.1248	0.6892	0.4356
J3QS39	J3QS39	Polyubiquitin-B	0.9078	-0.3107	-0.5971
P0DMV9	HS71B	Heat shock 70 kDa protein 1B	0.5691	0.4524	-1.0215
P0DOY3	IGLC3	Immunoglobulin lambda constant 3	-0.5571	0.3849	0.1722
P0DP25	CALM3	Calmodulin-3	0.5700	0.2155	-0.7855
P10124	SRGN	Serglycin	0.3487	-0.2160	-0.1327
P10316	1A69	HLA class I histocompatibility antigen, A-69 alpha chain	0.0831	-0.7798	0.6967
O19617	O19617	HLA class I antigen	0.6290	-0.0160	-0.6130
P10599	THIO	Thioredoxin	0.2602	-0.0483	-0.2119
P10619	PPGB	Lysosomal protective protein	0.1571	-0.1601	0.0030
P10644	KAP0	cAMP-dependent protein kinase type I-alpha regulatory subunit	0.3536	-0.5828	0.2292
P10809	CH60	60 kDa heat shock protein, mitochondrial	0.5336	0.0798	-0.6134
P10909	CLUS	Clusterin	-0.8031	0.4768	0.3262
P11021	BIP	Endoplasmic reticulum chaperone BiP	0.1261	0.0859	-0.2120
P11142	HSP7C	Heat shock cognate 71 kDa protein	0.4433	-0.2225	-0.2208

P11169	GTR3	Solute carrier family 2, facilitated glucose transporter member 3	0.7026	-0.5511	-0.1515
P11177	ODPB	Pyruvate dehydrogenase E1 component subunit beta, mitochondrial	-0.4359	0.2224	0.2135
P11216	PYGB	Glycogen phosphorylase, brain form	0.7281	-0.3924	-0.3357
P11234	RALB	Ras-related protein Ral-B	0.7081	-0.2789	-0.4291
P11413	G6PD	Glucose-6-phosphate 1-dehydrogenase	0.9199	-0.6463	-0.2735
P12236	ADT3	ADP/ATP translocase 3	0.3307	0.3484	-0.6791
P12259	FA5	Coagulation factor V	1.0488	-0.2452	-0.8036
P12814	ACTN1	Alpha-actinin-1	0.8861	-0.2685	-0.6177
P12931	SRC	Proto-oncogene tyrosine-protein kinase Src	0.7118	0.1840	-0.8958
P13073	COX41	Cytochrome c oxidase subunit 4 isoform 1, mitochondrial	-0.0396	0.8311	-0.7916
P13224	GP1BB	Platelet glycoprotein Ib beta chain	0.7086	-0.4889	-0.2197
P13489	RINI	Ribonuclease inhibitor	-0.1310	0.7623	-0.6314
P13639	EF2	Elongation factor 2	-0.3593	-0.2274	0.5867
P13667	PDIA4	Protein disulfide-isomerase A4	0.9672	-0.8148	-0.1523
P13693	TCTP	Translationally-controlled tumor protein	0.7447	-0.5084	-0.2362
P13746	1A11	HLA class I histocompatibility antigen, A-11 alpha chain	0.5025	-0.0073	-0.4952
A0A0A0MSQ0	A0A0A0MSQ0	Plastin-3	-0.3449	0.4436	-0.0987
P14314	GLU2B	Glucosidase 2 subunit beta	0.5275	-0.6081	0.0806
P14543	NID1	Nidogen-1	0.9876	0.0102	-0.9979
P14618	KPYM	Pyruvate kinase PKM	-0.0979	-0.6695	0.7674
P14625	ENPL	Endoplasmin	0.8180	-0.0726	-0.7454
P14770	GPIX	Platelet glycoprotein IX	0.6158	0.0031	-0.6189
B1AH77	B1AH77	Ras-related C3 botulinum toxin substrate 2	0.6435	-0.3765	-0.2671
Q5R345	Q5R345	P-selectin	0.6565	0.2754	-0.9319
P16152	CBR1	Carbonyl reductase [NADPH] 1	-0.3123	-0.0601	0.3723
P16615	AT2A2	Sarcoplasmic/endoplasmic reticulum calcium ATPase 2	0.0671	0.2488	-0.3158
E7EU05	E7EU05	Platelet glycoprotein 4	0.5017	0.1404	-0.6421
P16930	FAAA	Fumarylacetoacetase	0.1283	0.1499	-0.2782
P17301	ITA2	Integrin alpha-2	0.7801	-0.2604	-0.5197
P17987	TCPA	T-complex protein 1 subunit alpha	-0.0089	-0.5276	0.5365
P18031	PTN1	Tyrosine-protein phosphatase non-receptor type 1	-0.3843	-0.2658	0.6500
P18054	LOX12	Arachidonate 12-lipoxygenase, 12S-type	-0.2973	-0.3082	0.6054
P18085	ARF4	ADP-ribosylation factor 4	0.9704	-0.1732	-0.7972
P18206	VINC	Vinculin	0.1387	-0.0849	-0.0538
P18669	PGAM1	Phosphoglycerate mutase 1	1.0374	-0.7292	-0.3083
P19086	GNAZ	Guanine nucleotide-binding protein G (z) subunit alpha	0.8054	-0.4680	-0.3373
P19367	HXK1	Hexokinase-1	0.6968	0.3524	-1.0493
Q5T985	Q5T985	Inter-alpha-trypsin inhibitor heavy chain H2	-0.8814	0.1265	0.7549
P19827	ITIH1	Inter-alpha-trypsin inhibitor heavy chain H1	-0.5873	-0.0094	0.5968
P19971	TYPH	Thymidine phosphorylase	0.3691	-0.1098	-0.2592
P20042	IF2B	Eukaryotic translation initiation factor 2 subunit 2	-0.5102	0.1533	0.3569
P20073	ANXA7	Annexin A7	-0.4698	-0.4200	0.8898
P20340	RAB6A	Ras-related protein Rab-6A	-0.2965	0.6748	-0.3783
P20674	COX5A	Cytochrome c oxidase subunit 5A, mitochondrial	0.4243	-0.2454	-0.1788
P21291	CSRP1	Cysteine and glycine-rich protein 1	0.8161	-0.6364	-0.1797
P21333	FLNA	Filamin-A	0.7785	-0.1956	-0.5829
P21796	VDAC1	Voltage-dependent anion-selective channel protein 1	0.8156	-0.2870	-0.5286
A6NNI4	A6NNI4	Tetraspanin	0.3965	0.5119	-0.9083
P22061	PIMT	Protein-L-isoaspartate	0.2402	-0.0661	-0.1741
P22314	UBA1	Ubiquitin-like modifier-activating enzyme 1	0.7475	-0.4888	-0.2587
P22694	KAPCB	cAMP-dependent protein kinase catalytic subunit beta	0.8894	-0.6926	-0.1968
P22695	QCR2	Cytochrome b-c1 complex subunit 2, mitochondrial	-0.1795	-0.2117	0.3912
P23219	PGH1	Prostaglandin G/H synthase 1	0.6503	-0.1735	-0.4768
P23229	ITA6	Integrin alpha-6	0.6886	0.0186	-0.7072
P23284	PPIB	Peptidyl-prolyl cis-trans isomerase B	0.5992	-0.5759	-0.0233
A0A1W2PQH3	A0A1W2PQH3	Malic enzyme	1.1079	-0.7047	-0.4032
P23528	COF1	Cofilin-1	-0.9427	0.1587	0.7841
P24534	EF1B	Elongation factor 1-beta	0.6289	-0.5369	-0.0920
Q5QNZ2	Q5QNZ2	ATP synthase F	0.6026	-0.3954	-0.2073
P24557	THAS	Thromboxane-A synthase	0.4773	0.2974	-0.7747

G5E9R5	G5E9R5	Acid phosphatase 1, soluble, isoform CRA_d	-0.4562	0.6854	-0.2292
P24844	MYL9	Myosin regulatory light polypeptide 9	0.8529	-0.3458	-0.5070
P25325	THTM	3-mercaptopyruvate sulfurtransferase	0.2912	-0.1820	-0.1092
P25705	ATPA	ATP synthase subunit alpha, mitochondrial	0.3000	0.3282	-0.6281
P25788	PSA3	Proteasome subunit alpha type-3	0.0320	0.1632	-0.1952
P25789	PSA4	Proteasome subunit alpha type-4	0.0059	-0.3484	0.3425
P26038	MOES	Moesin	0.8711	-0.4954	-0.3757
P26447	S10A4	Protein S100-A4	0.4495	-0.5071	0.0575
A6NLN1	A6NLN1	Polypyrimidine tract binding protein 1, isoform CRA_b	-0.5447	0.1670	0.3778
P26639	SYTC	Threonine--tRNA ligase, cytoplasmic	-0.5048	0.2534	0.2514
P26641	EF1G	Elongation factor 1-gamma	0.7797	-0.2273	-0.5525
P27105	STOM	Erythrocyte band 7 integral membrane protein	0.5839	-0.1518	-0.4320
P27169	PON1	Serum paraoxonase/arylesterase 1	-0.9258	0.1241	0.8017
P27338	AOFB	Amine oxidase [flavin-containing] B	0.7860	-0.2196	-0.5665
P27348	1433T	14-3-3 protein theta	0.4867	0.4613	-0.9480
P27797	CALR	Calreticulin	0.3311	0.2591	-0.5903
P27824	CALX	Calnexin	0.7127	-0.6917	-0.0210
P29144	TPP2	Tripeptidyl-peptidase 2	0.9334	-0.9834	0.0500
P29350	PTN6	Tyrosine-protein phosphatase non-receptor type 6	0.9086	0.0927	-1.0013
P29401	TKT	Transketolase	0.8768	-0.7039	-0.1729
E9PK01	E9PK01	Elongation factor 1-delta	1.1153	-0.4526	-0.6627
P30040	ERP29	Endoplasmic reticulum resident protein 29	0.1779	0.1136	-0.2915
P30041	PRDX6	Peroxiredoxin-6	0.4661	-0.0469	-0.4191
P30044	PRDX5	Peroxiredoxin-5, mitochondrial	0.2217	-0.0278	-0.1939
P30048	PRDX3	Thioredoxin-dependent peroxide reductase, mitochondrial	0.3947	-0.0642	-0.3305
P30085	KCY	UMP-CMP kinase	0.4156	0.1526	-0.5682
P30086	PEBP1	Phosphatidylethanolamine-binding protein 1	0.2594	0.2210	-0.4803
P30101	PDIA3	Protein disulfide-isomerase A3	0.7007	-0.2069	-0.4938
P30153	2AAA	Serine/threonine-protein phosphatase 2A 65 kDa regulatory subunit A alpha isoform	0.8201	-0.1863	-0.6337
P30273	FCERG	High affinity immunoglobulin epsilon receptor subunit gamma	0.4046	0.1318	-0.5364
P30405	PPIF	Peptidyl-prolyl cis-trans isomerase F, mitochondrial	0.3149	-0.4800	0.1651
P30740	ILEU	Leukocyte elastase inhibitor	0.5389	-0.1087	-0.4302
P31146	COR1A	Coronin-1A	0.8047	-0.6710	-0.1337
P31150	GDIA	Rab GDP dissociation inhibitor alpha	0.4181	-0.0790	-0.3391
P31323	KAP3	cAMP-dependent protein kinase type II-beta regulatory subunit	0.4322	0.1980	-0.6302
P31946	1433B	14-3-3 protein beta/alpha	0.7555	-0.4379	-0.3176
P31948	STIP1	Stress-induced-phosphoprotein 1	0.1429	0.1917	-0.3346
P32119	PRDX2	Peroxiredoxin-2	-0.1724	0.3916	-0.2193
P35232	PHB	Prohibitin	0.3362	0.6084	-0.9446
P35237	SPB6	Serpin B6	0.5624	-0.3319	-0.2305
P35542	SAA4	Serum amyloid A-4 protein	-0.9693	0.3400	0.6293
P35579	MYH9	Myosin-9	0.9123	-0.3532	-0.5592
P35606	COPB2	Coatomer subunit beta'	0.3649	-0.4408	0.0759
P35908	K22E	Keratin, type II cytoskeletal 2 epidermal	-0.3629	-0.2207	0.5835
P36542	ATPG	ATP synthase subunit gamma, mitochondrial	0.7018	-0.4979	-0.2040
P36871	PGM1	Phosphoglucomutase-1	0.2248	-0.3376	0.1128
P36957	ODO2	Dihydrolipoyllysine-residue succinyltransferase component of 2-oxoglutarate dehydrogenase complex, mitochondrial	-0.4221	0.6882	-0.2661
P37802	TAGL2	Transgelin-2	0.6475	-0.2158	-0.4317
P37837	TALDO	Transaldolase	0.4866	0.6037	-1.0903
E7EPV7	E7EPV7	Alpha-synuclein	0.8015	-0.2627	-0.5388
P38117	ETFB	Electron transfer flavoprotein subunit beta	0.4264	-0.2691	-0.1573
P38606	VATA	V-type proton ATPase catalytic subunit A	0.7755	-0.2578	-0.5178
P38646	GRP75	Stress-70 protein, mitochondrial	0.7181	0.2657	-0.9838
A0A0C4DGS1	A0A0C4DGS1	Dolichyl-diphosphooligosaccharide--protein glycosyltransferase 48 kDa subunit	0.9212	-0.7944	-0.1268
P40197	GPV	Platelet glycoprotein V	0.2377	-0.3275	0.0898
P40227	TCPZ	T-complex protein 1 subunit zeta	0.5758	-0.0561	-0.5197

P40925	MDHC	Malate dehydrogenase, cytoplasmic	0.5635	-0.1320	-0.4315
P40926	MDHM	Malate dehydrogenase, mitochondrial	0.8399	-0.1194	-0.7206
P40939	ECHA	Trifunctional enzyme subunit alpha, mitochondrial	0.1592	-0.2909	0.1317
P41226	UBA7	Ubiquitin-like modifier-activating enzyme 7	-0.0649	0.0251	0.0398
P41240	CSK	Tyrosine-protein kinase CSK	0.2925	-0.5496	0.2571
B1AUU8	B1AUU8	Epidermal growth factor receptor substrate 15	-0.4881	0.5501	-0.0620
P43304	GPDM	Glycerol-3-phosphate dehydrogenase, mitochondrial	0.8513	-0.0369	-0.8143
P45880	VDAC2	Voltage-dependent anion-selective channel protein 2	0.8161	0.0249	-0.8411
P46109	CRKL	Crk-like protein	-0.1028	0.1981	-0.0952
I3L0N3	I3L0N3	Vesicle-fusing ATPase	-0.8436	0.4108	0.4328
G5E9W8	G5E9W8	Glycogenin 1, isoform CRA_e	-0.7136	0.4215	0.2921
P46977	STT3A	Dolichyl-diphosphooligosaccharide--protein glycosyltransferase subunit STT3A	0.1594	-0.5164	0.3570
P47755	CAZA2	F-actin-capping protein subunit alpha-2	1.1223	-0.6475	-0.4748
P48047	ATPO	ATP synthase subunit O, mitochondrial	0.5189	-0.4953	-0.0237
P48059	LIMS1	LIM and senescent cell antigen-like-containing domain protein 1	0.0498	0.2573	-0.3070
P48426	PI42A	Phosphatidylinositol 5-phosphate 4-kinase type-2 alpha	0.3124	-0.0709	-0.2416
P48444	COPD	Coatomer subunit delta	0.4059	0.0201	-0.4260
P48643	TCPE	T-complex protein 1 subunit epsilon	0.7251	-0.0578	-0.6673
P48735	IDHP	Isocitrate dehydrogenase [NADP], mitochondrial	0.6843	0.1374	-0.8217
A0A0U1RQF0	A0A0U1RQF0	Fatty acid synthase	0.2205	0.3127	-0.5331
P49368	TCPG	T-complex protein 1 subunit gamma	0.8387	-1.0077	0.1690
P49411	EFTU	Elongation factor Tu, mitochondrial	1.2314	-0.3900	-0.8414
P49748	ACADV	Very long-chain specific acyl-CoA dehydrogenase, mitochondrial	0.8999	-0.1809	-0.7190
P49755	TMEDA	Transmembrane emp24 domain-containing protein 10	1.2023	-0.5442	-0.6581
P50148	GNAQ	Guanine nucleotide-binding protein G	1.0175	-0.5350	-0.4825
P50395	GDIB	Rab GDP dissociation inhibitor beta	0.2585	0.4745	-0.7329
P50402	EMD	Emerin	0.9401	-0.5890	-0.3511
P50416	CPT1A	Carnitine O-palmitoyltransferase 1, liver isoform	-0.1130	-0.2637	0.3767
P50453	SPB9	Serpin B9	-0.1141	0.7161	-0.6020
P50502	F10A1	Hsc70-interacting protein	0.9564	-0.7047	-0.2517
P50552	VASP	Vasodilator-stimulated phosphoprotein	0.4689	-0.0237	-0.4451
P50851	LRBA	Lipopolysaccharide-responsive and beige-like anchor protein	1.1979	-0.6610	-0.5368
P50990	TCPQ	T-complex protein 1 subunit theta	0.7130	0.1258	-0.8388
P50991	TCPD	T-complex protein 1 subunit delta	0.7980	-0.7660	-0.0320
P50995	ANX11	Annexin A11	0.9843	-0.5619	-0.4224
P51148	RAB5C	Ras-related protein Rab-5C	0.7185	-0.7172	-0.0013
P51149	RAB7A	Ras-related protein Rab-7a	0.7417	-0.1499	-0.5917
P51452	DUS3	Dual specificity protein phosphatase 3	0.2737	0.3024	-0.5761
P51572	BAP31	B-cell receptor-associated protein 31	0.5096	-0.2185	-0.2911
P51575	P2RX1	P2X purinoceptor 1	-0.5415	-0.0122	0.5537
A6NKZ2	A6NKZ2	N-acylglucosamine 2-epimerase	0.2141	0.3002	-0.5143
P51659	DHB4	Peroxisomal multifunctional enzyme type 2	0.8200	0.0450	-0.8650
P52209	6PGD	6-phosphogluconate dehydrogenase, decarboxylating	0.6421	-0.3272	-0.3150
J3KTF8	J3KTF8	Rho GDP-dissociation inhibitor 1	0.4492	-0.4133	-0.0359
P52566	GDIR2	Rho GDP-dissociation inhibitor 2	0.6936	0.2811	-0.9746
P52907	CAZA1	F-actin-capping protein subunit alpha-1	0.9567	-0.6785	-0.2782
P53396	ACLY	ATP-citrate synthase	-0.2361	0.4947	-0.2586
P53621	COPA	Coatomer subunit alpha	0.1348	0.4788	-0.6136
A8MXQ1	A8MXQ1	Pituitary tumor-transforming gene 1 protein-interacting protein	0.3226	-0.2373	-0.0854
P54577	SYYC	Tyrosine--tRNA ligase, cytoplasmic	0.4589	0.3402	-0.7991
F8W1A4	F8W1A4	Adenylate kinase 2, mitochondrial	0.6173	-0.6181	0.0008
P54920	SNAA	Alpha-soluble NSF attachment protein	0.9064	-0.1367	-0.7697
P55072	TERA	Transitional endoplasmic reticulum ATPase	0.5275	-0.3396	-0.1879
P55084	ECHB	Trifunctional enzyme subunit beta, mitochondrial	0.9434	-0.4403	-0.5030
P55160	NCKPL	Nck-associated protein 1-like	-0.0364	0.3671	-0.3307
F8W020	F8W020	Nucleosome assembly protein 1-like 1	0.9221	-0.0376	-0.8845
E9PLK3	E9PLK3	Aminopeptidase	0.7735	-0.2126	-0.5609
P58546	MTPN	Myotrophin	0.7155	-0.5447	-0.1707

P59998	ARPC4	Actin-related protein 2/3 complex subunit 4	0.3763	-0.2492	-0.1271
P60174	TPIS	Triosephosphate isomerase	-0.3786	-0.5179	0.8965
F8W1R7	F8W1R7	Myosin light polypeptide 6	0.4915	-0.3666	-0.1250
P60709	ACTB	Actin, cytoplasmic 1	-0.4308	0.2579	0.1729
P60842	IF4A1	Eukaryotic initiation factor 4A-I	0.9324	-0.2565	-0.6759
G3V295	G3V295	Proteasome subunit alpha type	-0.4402	0.0476	0.3926
P60953	CDC42	Cell division control protein 42 homolog	-0.1759	-0.0203	0.1963
P61006	RAB8A	Ras-related protein Rab-8A	0.3815	-0.8774	0.4959
P61026	RAB10	Ras-related protein Rab-10	0.7075	-0.6435	-0.0641
P61088	UBE2N	Ubiquitin-conjugating enzyme E2 N	0.4930	-0.2679	-0.2251
P61106	RAB14	Ras-related protein Rab-14	0.2035	-0.1185	-0.0850
P61158	ARP3	Actin-related protein 3	0.4576	-0.0147	-0.4429
P61160	ARP2	Actin-related protein 2	0.5320	0.1142	-0.6462
P84077	ARF1	ADP-ribosylation factor 1	0.8529	-0.6342	-0.2188
P61224	RAP1B	Ras-related protein Rap-1b	0.6322	-0.0439	-0.5883
P61225	RAP2B	Ras-related protein Rap-2b	0.3720	-0.5342	0.1622
P61586	RHOA	Transforming protein RhoA	0.9411	-0.4023	-0.5388
P61604	CH10	10 kDa heat shock protein, mitochondrial	0.6587	0.4455	-1.1042
P61769	B2MG	Beta-2-microglobulin	0.5604	0.0901	-0.6505
F5GXX5	F5GXX5	Dolichyl-diphosphooligosaccharide--protein glycosyltransferase subunit DAD1	0.1003	0.1504	-0.2507
P61970	NTF2	Nuclear transport factor 2	0.2541	-0.0666	-0.1875
P61981	1433G	14-3-3 protein gamma	0.3664	-0.4411	0.0747
P62136	PP1A	Serine/threonine-protein phosphatase PP1-alpha catalytic subunit	0.1223	-0.1303	0.0080
P62140	PP1B	Serine/threonine-protein phosphatase PP1-beta catalytic subunit	0.1224	-0.7427	0.6204
P62258	1433E	14-3-3 protein epsilon	0.8144	-0.3640	-0.4504
P62328	TYB4	Thymosin beta-4	0.2400	0.0406	-0.2805
P62805	H4	Histone H4	0.9348	-0.3412	-0.5937
P62820	RAB1A	Ras-related protein Rab-1A	0.1629	0.1037	-0.2666
P62826	RAN	GTP-binding nuclear protein Ran	0.1532	-0.4079	0.2546
P62873	GBB1	Guanine nucleotide-binding protein G	0.6624	0.2126	-0.8750
P62937	PPIA	Peptidyl-prolyl cis-trans isomerase A	0.5483	-0.6501	0.1018
P62942	FKB1A	Peptidyl-prolyl cis-trans isomerase FKBP1A	0.7793	-0.6904	-0.0889
P62993	GRB2	Growth factor receptor-bound protein 2	-0.4835	0.1505	0.3330
P63000	RAC1	Ras-related C3 botulinum toxin substrate 1	0.1795	0.4611	-0.6406
P63104	1433Z	14-3-3 protein zeta/delta	0.8121	-0.4100	-0.4021
P63218	GBG5	Guanine nucleotide-binding protein G	-0.3256	0.4897	-0.1641
P67936	TPM4	Tropomyosin alpha-4 chain	0.5637	-0.2579	-0.3057
P68133	ACTS	Actin, alpha skeletal muscle	0.3086	-0.1102	-0.1984
P68036	UB2L3	Ubiquitin-conjugating enzyme E2 L3	0.8832	-0.1674	-0.7158
Q5VTE0	EF1A3	Putative elongation factor 1-alpha-like 3	1.1317	-0.4696	-0.6621
P68363	TBA1B	Tubulin alpha-1B chain	0.1248	0.2979	-0.4227
P68366	TBA4A	Tubulin alpha-4A chain	0.4798	-0.1421	-0.3378
P68371	TBB4B	Tubulin beta-4B chain	0.0216	-0.0676	0.0460
P68871	HBB	Hemoglobin subunit beta	-0.3656	-0.5690	0.9346
P69905	HBA	Hemoglobin subunit alpha	-0.2842	-0.7962	1.0803
P78371	TCPB	T-complex protein 1 subunit beta	1.0300	-0.8718	-0.1582
P78417	GSTO1	Glutathione S-transferase omega-1	0.9420	-0.4786	-0.4634
P81605	DCD	Dermcidin	-0.5421	0.4187	0.1234
C9JFR7	C9JFR7	Cytochrome c	-0.1339	0.0000	0.1339
Q00013	EM55	55 kDa erythrocyte membrane protein	0.0712	-0.7718	0.7005
Q00325	MPCP	Phosphate carrier protein, mitochondrial	1.0049	-0.6570	-0.3479
Q00610	CLH1	Clathrin heavy chain 1	0.9941	-0.1188	-0.8753
Q01082	SPTB2	Spectrin beta chain, non-erythrocytic 1	-0.1400	-0.4078	0.5479
Q01433	AMPD2	AMP deaminase 2	0.7985	-0.5272	-0.2713
Q01518	CAP1	Adenylyl cyclase-associated protein 1	0.5478	-0.8651	0.3173
Q01813	PFKAP	ATP-dependent 6-phosphofructokinase, platelet type	0.7681	-0.2801	-0.4880
I3L1P8	I3L1P8	Mitochondrial 2-oxoglutarate/malate carrier protein	0.4165	-0.3046	-0.1120
Q04917	1433F	14-3-3 protein eta	0.8251	-0.3659	-0.4591
A0A0U1RQP1	A0A0U1RQP1	Dynamin-1	-0.1930	0.5224	-0.3295
Q05209	PTN12	Tyrosine-protein phosphatase non-receptor type 12	0.7431	-0.0402	-0.7029

E7EX44	E7EX44	Caldesmon	0.6988	-0.6218	-0.0770
A0A087WW43	A0A087WW43	Inter-alpha-trypsin inhibitor heavy chain H3	-0.5483	0.1507	0.3977
Q06187	BTK	Tyrosine-protein kinase BTK	0.8373	-0.8979	0.0606
Q06323	PSME1	Proteasome activator complex subunit 1	-0.1239	-0.0155	0.1395
Q06830	PRDX1	Peroxiredoxin-1	0.2212	0.2328	-0.4541
Q07960	RHG01	Rho GTPase-activating protein 1	0.9012	-0.5485	-0.3527
Q08495	DEMA	Dematin	0.4021	-0.3233	-0.0788
Q08722	CD47	Leukocyte surface antigen CD47	0.5337	-0.1969	-0.3368
Q0ZGT2	NEXN	Nexilin	0.4250	-0.2115	-0.2135
Q10567	AP1B1	AP-1 complex subunit beta-1	0.6684	-0.7398	0.0714
Q12913	PTPRJ	Receptor-type tyrosine-protein phosphatase eta	0.7203	-0.6173	-0.1030
Q13011	ECH1	Delta	0.3499	0.4398	-0.7897
Q13045	FLII	Protein flightless-1 homolog	0.2366	-0.4819	0.2453
A0A0D9SGG1	A0A0D9SGG1	Lymphocyte cytosolic protein 2	0.7009	-0.0619	-0.6390
Q13162	PRDX4	Peroxiredoxin-4	0.2750	-0.2539	-0.0211
Q13177	PAK2	Serine/threonine-protein kinase PAK 2	-0.8073	-0.0693	0.8766
Q13201	MMRN1	Multimerin-1	1.0038	0.1346	-1.1384
Q13418	ILK	Integrin-linked protein kinase	0.2417	-0.1320	-0.1097
Q13423	NNTM	NAD(P) transhydrogenase, mitochondrial	0.9707	-0.1371	-0.8337
Q13576	IQGA2	Ras GTPase-activating-like protein IQGAP2	0.6244	-0.2652	-0.3593
Q13586	STIM1	Stromal interaction molecule 1	1.1748	-0.3993	-0.7754
Q13637	RAB32	Ras-related protein Rab-32	0.9240	-0.3089	-0.6150
Q14008	CKAP5	Cytoskeleton-associated protein 5	-0.0340	-0.0816	0.1156
Q14019	COTL1	Coactosin-like protein	0.3017	0.2054	-0.5070
B1AMS2	B1AMS2	Septin 6	0.5477	-0.5490	0.0013
Q14165	MLEC	Malectin	0.6982	-0.7394	0.0412
Q14247	SRC8	Src substrate cortactin	0.5952	0.0166	-0.6119
Q14344	GNA13	Guanine nucleotide-binding protein subunit alpha-13	0.4602	-1.0135	0.5533
Q14554	PDIA5	Protein disulfide-isomerase A5	0.4490	0.0596	-0.5086
Q14624	ITIH4	Inter-alpha-trypsin inhibitor heavy chain H4	-1.2222	0.3275	0.8947
Q14644	RASA3	Ras GTPase-activating protein 3	0.3415	-0.4135	0.0720
Q14677	EPN4	Clathrin interactor 1	0.7505	-0.8329	0.0824
Q14697	GANAB	Neutral alpha-glucosidase AB	1.0518	-0.5139	-0.5378
Q14766	LTBP1	Latent-transforming growth factor beta-binding protein 1	0.8044	-0.4834	-0.3210
Q14847	LASP1	LIM and SH3 domain protein 1	0.6850	0.1772	-0.8622
Q14974	IMB1	Importin subunit beta-1	-0.0105	-0.1282	0.1386
Q15019	Sep-02	Septin-2	-0.0327	-0.5337	0.5664
E9PAP1	E9PAP1	Histone-lysine N-methyltransferase SETDB1	0.6858	-0.5260	-0.1597
Q15084	PDIA6	Protein disulfide-isomerase A6	0.5199	-0.0940	-0.4259
Q15149	PLEC	Plectin	0.6996	-0.3853	-0.3143
A6PVN5	A6PVN5	Serine/threonine-protein phosphatase 2A activator	0.1750	-0.6348	0.4599
Q15365	PCBP1	Poly(rC)-binding protein 1	0.8565	-0.1874	-0.6691
Q15404	RSU1	Ras suppressor protein 1	0.3951	-0.2005	-0.1946
Q15555	MARE2	Microtubule-associated protein RP/EB family member 2	-0.3329	-0.5762	0.9092
Q15691	MARE1	Microtubule-associated protein RP/EB family member 1	1.1245	-0.7737	-0.3508
Q15746	MYLK	Myosin light chain kinase, smooth muscle	0.8434	-0.6271	-0.2163
Q15833	STXB2	Syntaxin-binding protein 2	0.6533	-0.0304	-0.6229
Q15836	VAMP3	Vesicle-associated membrane protein 3	0.7695	-0.5726	-0.1969
Q15907	RB11B	Ras-related protein Rab-11B	0.5519	0.1375	-0.6894
Q15942	ZYX	Zyxin	0.4441	-0.3928	-0.0513
E7ES33	E7ES33	Septin 7	0.6866	-0.6956	0.0090
Q16643	DREB	Drebrin	0.8253	-0.7151	-0.1102
Q16698	DECR	2,4-dienoyl-CoA reductase, mitochondrial	0.6858	-0.3473	-0.3385
Q16762	THTR	Thiosulfate sulfurtransferase	-0.5117	0.4601	0.0517
Q16799	RTN1	Reticulon-1	0.9025	-0.5261	-0.3764
A0A087WYS1	A0A087WYS1	UTP--glucose-1-phosphate uridylyltransferase	-0.2628	-0.0540	0.3167
Q27J81	INF2	Inverted formin-2	0.9142	-0.0610	-0.8532
Q3ZCW2	LEGL	Galectin-related protein	0.5047	0.4213	-0.9260
Q4KMQ2	ANO6	Anoctamin-6	0.2674	-0.3633	0.0959
Q53GQ0	DHB12	Very-long-chain 3-oxoacyl-CoA reductase	0.3932	-0.1859	-0.2073
Q5JSH3	WDR44	WD repeat-containing protein 44	0.8692	-0.1196	-0.7496
Q5SQ64	LY66F	Lymphocyte antigen 6 complex locus protein G6f	0.4975	-0.5026	0.0051

Q6DD88	ATLA3	Atlastin-3	0.5991	-0.3364	-0.2628
Q6IBS0	TWF2	Twinfilin-2	1.0176	-0.4944	-0.5232
Q6PJW8	CNST	Consortin	0.3642	-0.1280	-0.2361
Q6ZNJ1	NBEL2	Neurobeachin-like protein 2	0.2821	-0.0618	-0.2202
Q70J99	UN13D	Protein unc-13 homolog D	0.9147	-0.0936	-0.8211
Q7KZF4	SND1	Staphylococcal nuclease domain-containing protein 1	0.7114	-0.4354	-0.2760
Q7L576	CYFP1	Cytoplasmic FMR1-interacting protein 1	0.7666	-0.5392	-0.2274
Q9H8S9	MOB1A	MOB kinase activator 1A	-0.3353	-0.3098	0.6451
Q7LDG7	GRP2	RAS guanyl-releasing protein 2	1.0204	-0.2363	-0.7841
Q7Z406	MYH14	Myosin-14	0.1736	-0.3742	0.2006
Q7Z434	MAVS	Mitochondrial antiviral-signaling protein	0.8244	-0.2740	-0.5504
Q86UX7	URP2	Fermitin family homolog 3	0.8351	-0.4279	-0.4072
Q86VP6	CAND1	Cullin-associated NEDD8-dissociated protein 1	0.2460	-0.2649	0.0189
Q86WI1	PKHL1	Fibrocystin-L	-0.9329	0.7943	0.1386
Q86YW5	TRML1	Trem-like transcript 1 protein	0.1406	0.1581	-0.2988
Q8IVB4	SL9A9	Sodium/hydrogen exchanger 9	-0.4070	0.2119	0.1952
Q8N392	RHG18	Rho GTPase-activating protein 18	0.8585	-0.2640	-0.5945
H0YDV5	H0YDV5	Myc target protein 1	0.1309	-0.3020	0.1712
Q8NBX0	SCPDL	Saccharopine dehydrogenase-like oxidoreductase	-0.0327	-0.2580	0.2907
Q8NG06	TRI58	E3 ubiquitin-protein ligase TRIM58	0.1736	0.1027	-0.2762
Q8TC12	RDH11	Retinol dehydrogenase 11	0.4747	-0.1561	-0.3186
Q8TF42	UBS3B	Ubiquitin-associated and SH3 domain-containing protein B	0.5271	-0.2376	-0.2895
Q8WUM4	PDC6I	Programmed cell death 6-interacting protein	0.6306	-0.2705	-0.3601
Q8WWA1	TMM40	Transmembrane protein 40	0.9408	-1.0558	0.1150
Q8WXF7	ATLA1	Atlastin-1	-0.4146	0.2160	0.1986
Q92619	HMHA1	Rho GTPase-activating protein 45 [Cleaved into: Minor histocompatibility antigen HA-1	0.2049	-0.0421	-0.1628
Q92686	NEUG	Neurogranin	0.5871	-0.5098	-0.0773
Q93084	AT2A3	Sarcoplasmic/endoplasmic reticulum calcium ATPase 3	0.4496	0.0400	-0.4897
K7EIJ0	K7EIJ0	WW domain-binding protein 2	-0.1134	-0.1404	0.2538
Q96AP7	ESAM	Endothelial cell-selective adhesion molecule	0.2177	-0.4196	0.2019
Q96C24	SYTL4	Synaptotagmin-like protein 4	0.7340	-0.3756	-0.3584
C9JAI6	C9JAI6	CKLF-like MARVEL transmembrane domain-containing protein 5	1.0520	-0.6655	-0.3865
Q96G03	PGM2	Phosphoglucomutase-2	0.2172	0.0254	-0.2426
Q96HC4	PDLI5	PDZ and LIM domain protein 5	0.9747	-0.2098	-0.7649
Q96KP4	CNDP2	Cytosolic non-specific dipeptidase	0.6967	-0.3372	-0.3595
Q96QK1	VPS35	Vacuolar protein sorting-associated protein 35	-0.5904	0.4118	0.1786
C9JJV6	C9JJV6	Myeloid-associated differentiation marker	0.6577	-0.3355	-0.3222
B4DDF4	B4DDF4	Calponin	0.7415	-0.7612	0.0197
Q99497	PARK7	Protein/nucleic acid deglycase DJ-1	-0.2924	0.4372	-0.1448
J3KPX7	J3KPX7	Prohibitin-2	1.0744	-0.6020	-0.4724
Q99798	ACON	Aconitate hydratase, mitochondrial	0.2679	-0.1981	-0.0698
Q99832	TCPH	T-complex protein 1 subunit eta	0.7068	-0.5817	-0.1251
E7EMB8	E7EMB8	Tyrosine-protein phosphatase non-receptor type 18	0.3481	-0.4600	0.1120
Q9BR76	COR1B	Coronin-1B	0.7586	-0.0842	-0.6744
Q9BS26	ERP44	Endoplasmic reticulum resident protein 44	0.6734	-0.2697	-0.4037
Q9BSJ8	ESYT1	Extended synaptotagmin-1	0.7285	-0.1269	-0.6016
Q9BUL8	PDC10	Programmed cell death protein 10	0.3967	0.7672	-1.1639
Q9BV40	VAMP8	Vesicle-associated membrane protein 8	0.1419	-0.4064	0.2645
Q9BX10	GTPB2	GTP-binding protein 2	0.4647	-0.4744	0.0096
Q9BX67	JAM3	Junctional adhesion molecule C	0.4212	0.4108	-0.8320
Q9BXS5	AP1M1	AP-1 complex subunit mu-1	-0.1086	0.3572	-0.2486
Q9C0C9	UBE2O	(E3-independent) E2 ubiquitin-conjugating enzyme	-0.5038	-0.3065	0.8103
Q9H0U4	RAB1B	Ras-related protein Rab-1B	0.5962	-0.2820	-0.3142
Q5T123	Q5T123	SH3 domain-binding glutamic acid-rich-like protein 3	-0.5444	-0.0302	0.5746
Q9H2K8	TAOK3	Serine/threonine-protein kinase TAO3	0.5807	-0.7124	0.1317
Q9H3N1	TMX1	Thioredoxin-related transmembrane protein 1	-0.2665	-0.1846	0.4510
Q9H4B7	TBB1	Tubulin beta-1 chain	0.6461	-0.3353	-0.3108
Q9H4M9	EHD1	EH domain-containing protein 1	0.7736	-0.3656	-0.4080
Q9H939	PPIP2	Proline-serine-threonine phosphatase-interacting protein 2	0.8059	-0.3131	-0.4927

Q9HBI1	PARVB	Beta-parvin	0.6341	-0.1969	-0.4372
Q9HCN6	GPVI	Platelet glycoprotein VI	0.4634	-0.2183	-0.2452
Q9NQ75	CASS4	Cas scaffolding protein family member 4	0.0606	-0.8132	0.7526
Q9NQC3	RTN4	Reticulon-4	0.5636	-0.0380	-0.5256
Q9NR12	PDLI7	PDZ and LIM domain protein 7	0.2192	-0.3539	0.1347
Q9NR31	SAR1A	GTP-binding protein SAR1a	0.5832	-0.0572	-0.5259
Q9NRW1	RAB6B	Ras-related protein Rab-6B	0.5735	-0.1626	-0.4109
Q9NTJ5	SAC1	Phosphatidylinositide phosphatase SAC1	0.7642	-0.0388	-0.7253
D6RGI3	D6RGI3	Septin 11	-0.1914	0.4913	-0.2999
Q9NX76	CKLF6	CKLF-like MARVEL transmembrane domain-containing protein 6	-0.6163	0.8677	-0.2514
Q9NXH8	TOR4A	Torsin-4A	0.9091	-0.6770	-0.2321
Q9NY65	TBA8	Tubulin alpha-8 chain	0.4761	0.2295	-0.7057
Q9NYL9	TMOD3	Tropomodulin-3	0.9531	-0.5632	-0.3899
Q9NYU2	UGGG1	UDP-glucose:glycoprotein glucosyltransferase 1	0.1245	0.0921	-0.2166
Q9NZ08	ERAP1	Endoplasmic reticulum aminopeptidase 1	0.0389	0.2609	-0.2998
Q9NZN3	EHD3	EH domain-containing protein 3	0.8105	-0.0520	-0.7585
Q9P0L0	VAPA	Vesicle-associated membrane protein-associated protein A	0.4442	-0.4815	0.0374
M0R165	M0R165	Epidermal growth factor receptor substrate 15-like 1	-0.5369	-0.1240	0.6609
Q9UBW5	BIN2	Bridging integrator 2	-0.0114	-0.5321	0.5435
Q9UDY2	ZO2	Tight junction protein ZO-2	0.8942	-0.2814	-0.6128
Q9UFN0	NPS3A	Protein NipSnap homolog 3A	0.4206	-0.0095	-0.4111
Q9UHQ9	NB5R1	NADH-cytochrome b5 reductase 1	-0.2030	0.2071	-0.0041
Q9UIB8	SLAF5	SLAM family member 5	0.5316	-0.4992	-0.0325
Q9UJU6	DBNL	Drebrin-like protein	0.6805	-0.1940	-0.4865
Q9ULV4	COR1C	Coronin-1C	0.3131	-0.6689	0.3558
Q9Y251	HPSE	Heparanase	0.5297	-0.1456	-0.3841
Q9Y277	VDAC3	Voltage-dependent anion-selective channel protein 3	0.1362	0.4486	-0.5848
Q9Y2A7	NCKP1	Nck-associated protein 1	0.0804	-0.2498	0.1694
Q9Y2Q3	GSTK1	Glutathione S-transferase kappa 1	0.4354	-0.7115	0.2762
Q9Y2Q5	LTOR2	Ragulator complex protein LAMTOR2	-0.5681	1.1751	-0.6071
Q9Y490	TLN1	Talin-1	0.2747	-0.0283	-0.2464
A0A087X054	A0A087X054	Hypoxia up-regulated protein 1	1.0611	-0.7530	-0.3082
Q9Y613	FHOD1	FH1/FH2 domain-containing protein 1	0.4356	-0.0406	-0.3949
Q9Y624	JAM1	Junctional adhesion molecule A	0.3475	-0.0757	-0.2717
Q9Y6C2	EMIL1	EMILIN-1	1.0385	-0.3888	-0.6497
A0A024R6I7	A0A024R6I7	Alpha-1-antitrypsin	0.7338	-0.5484	-0.1854
A0A075B738	PECA1	Platelet endothelial cell adhesion molecule	0.4971	-0.5093	0.0122
S4R460	S4R460	Immunoglobulin heavy variable 3/OR16-9	-0.0282	-0.1225	0.1507
A0A140T9L8	A0A140T9L8	C6orf25	0.4291	-0.2005	-0.2286
A6NJA2	A6NJA2	Ubiquitin carboxyl-terminal hydrolase 14	-0.4161	0.2318	0.1843
B1AK87	B1AK87	F-actin-capping protein subunit beta	0.7187	0.1552	-0.8739
B4DR80	B4DR80	Serine/threonine-protein kinase 24	0.2516	0.0931	-0.3447
G3XAH0	G3XAH0	HCG2002594, isoform CRA_c	0.3869	-0.4908	0.1039
H7BYY1	H7BYY1	Tropomyosin 1 (Alpha), isoform CRA_m	0.4126	0.1657	-0.5783
J3KN67	J3KN67	Tropomyosin alpha-3 chain	0.6050	-0.3564	-0.2486
Q32Q12	Q32Q12	Nucleoside diphosphate kinase	0.7783	-0.5312	-0.2472
Q5HYB6	Q5HYB6	Epididymis luminal protein 189	0.4511	-0.2486	-0.2024
Q5JXI8	Q5JXI8	Four and a half LIM domains protein 1	0.1467	0.0352	-0.1819
Q5T0I0	Q5T0I0	Gelsolin	1.0373	-0.5118	-0.5255
Q6ZN40	Q6ZN40	Tropomyosin 1 (Alpha), isoform CRA_f	0.4406	0.0878	-0.5284

Appendix 2: Significantly altered proteins between young, intermediate and old platelets

Protein ID	Protein	Protein Name	Young Z score	Intermediate Z score	Old Z score	p value
M0R009	A1BG	Alpha-1B-glycoprotein	-0.9429	0.1061	0.8367	0.0197
Q8N392	ARHGAP18	Rho GTPase-activating protein 18	0.8620	-0.0950	-0.7670	0.0494
P52566	ARHGDIB	Rho GDP-dissociation inhibitor 2	0.6936	0.2811	-0.9746	0.0278
P06576	ATP5F1B	ATP synthase subunit beta, mitochondrial	1.1680	-0.1766	-0.9914	0.0001
P48047	ATP5PO	ATP synthase subunit O, mitochondrial	0.8588	-0.7887	-0.0701	0.0457
A0A087X232	C1S	Complement C1s subcomponent	-0.6595	-0.4318	1.0913	0.0079
P0C0L4	C4A	Complement C4-A	-1.1248	0.6892	0.4356	0.0043
P01031	C5	Complement C5	-1.1690	0.4508	0.7182	0.0017
P07360	C8G	Complement component C8 gamma chain	-0.9833	0.0274	0.9559	0.0056
P07384	CAPN1	Calpain-1 catalytic subunit	1.0486	-0.4221	-0.6265	0.0149
P49368	CCT3	T-complex protein 1 subunit gamma	0.9158	-0.9266	0.0108	0.0133
P50991	CCT4	T-complex protein 1 subunit delta	0.7858	-1.0102	0.2243	0.0138
P23528	CFL1	Cofilin-1	-0.9427	0.1587	0.7841	0.0259
Q00610	CLTC	Clathrin heavy chain 1	0.9551	-0.0839	-0.8713	0.0144
C9JAI6	CMTM5	CKLF-like MARVEL transmembrane domain-containing protein 5	1.0555	-0.4296	-0.6259	0.0137
P13073	COX4I1	Cytochrome c oxidase subunit 4 isoform 1, mitochondrial	0.0394	0.7994	-0.8388	0.0488
B4DJV2	CS	Citrate synthase	0.9569	-0.1444	-0.8125	0.0200
A0A0C4DGS1	DDOST	Dolichyl-diphosphooligosaccharide--protein glycosyltransferase 48 kDa subunit	0.9496	-0.5912	-0.3584	0.0435
Q5VTE0	EEF1A1P5	Putative elongation factor 1-alpha-like 3	1.0931	-0.1623	-0.9307	0.0017
E9PK01	EEF1D	Elongation factor 1-delta	0.9422	-0.6864	-0.2558	0.0375
P60842	EIF4A1	Eukaryotic initiation factor 4A-I	0.8928	-0.1212	-0.7716	0.0397

P50402	EMD	Emerin	0.9439	-0.4975	-0.4464	0.0499
Q9Y6C2	EMILIN1	EMILIN-1	1.0280	-0.3463	-0.6817	0.0168
Q9BSJ8	ESYT1	Extended synaptotagmin-1	0.8537	-0.0542	-0.7995	0.0448
P12259	F5	Coagulation factor V	1.0488	-0.2452	-0.8036	0.0081
P02671	FGA	Fibrinogen alpha chain	-0.6393	-0.4206	1.0598	0.0126
P11413	G6PD	Glucose-6-phosphate 1-dehydrogenase	0.9112	-0.6806	-0.2306	0.0484
Q14697	GANAB	Neutral alpha-glucosidase AB	1.0670	-0.4191	-0.6479	0.0113
Q14344	GNA13	Guanine nucleotide-binding protein subunit alpha-13	0.8965	-0.8411	-0.0554	0.0273
P50148	GNAQ	Guanine nucleotide-binding protein G	1.0175	-0.5350	-0.4825	0.0236
P43304	GPD2	Glycerol-3-phosphate dehydrogenase, mitochondrial	0.8130	0.0812	-0.8942	0.0323
P06744	GPI	Glucose-6-phosphate isomerase	0.9212	-0.6576	-0.2636	0.0478
Q5T0I0	GSN	Gelsolin	1.1058	-0.7632	-0.3425	0.0045
P78417	GSTO1	Glutathione S-transferase omega-1	0.9498	-0.4130	-0.5368	0.0463
Q9BX10	GTPBP2	GTP-binding protein 2	0.4992	-0.9628	0.4636	0.0419
P55084	HADHB	Trifunctional enzyme subunit beta, mitochondrial	0.9566	-0.6524	-0.3042	0.0364
P69905	HBA1;	Hemoglobin subunit alpha	-0.2842	-0.7962	1.0803	0.0056
P19367	HK1	Hexokinase-1	0.6968	0.3524	-1.0493	0.0125
P0DMV9	HSPA1B	Heat shock 70 kDa protein 1B	0.5691	0.4524	-1.0215	0.0220
P38646	HSPA9	Stress-70 protein, mitochondrial	0.7189	0.2886	-1.0075	0.0186
P61604	HSPE1	10 kDa heat shock protein, mitochondrial	0.6560	0.4488	-1.1047	0.0065
A0A087X054	HYOU1	Hypoxia up-regulated protein 1	0.8908	-0.7725	-0.1183	0.0401
P01859	IGHG2	Immunoglobulin heavy constant gamma 2	0.7569	-1.0082	0.2513	0.0160
B9A064	IGLL5	Immunoglobulin lambda-like polypeptide 5	-0.9803	-0.0275	1.0077	0.0033
Q27J81	INF2	Inverted formin-2	0.9248	-0.1883	-0.7365	0.0364
P08514	ITGA2B	Integrin alpha-IIb	0.8581	-0.0641	-0.7940	0.0448

P05106	ITGB3	Integrin beta-3	1.1148	-0.5295	-0.5853	0.0061
Q5T985	ITIH2	Inter-alpha-trypsin inhibitor heavy chain H2	-0.8814	0.1265	0.7549	0.0460
Q14624	ITIH4	Inter-alpha-trypsin inhibitor heavy chain H4	-1.2222	0.3275	0.8947	0.0001
P00338	LDHA	L-lactate dehydrogenase A chain	1.1609	-0.7740	-0.3868	0.0016
Q3ZCW2	LGALSL	Galectin-related protein	0.6028	0.4044	-1.0071	0.0248
P50851	LRBA	Lipopolysaccharide-responsive and beige-like anchor protein	1.1215	-0.9221	-0.1994	0.0011
P07948	LYN	Tyrosine-protein kinase Lyn	0.4737	-1.0078	0.5341	0.0263
Q15691	MAPRE1	Microtubule-associated protein RP/EB family member 1	1.1064	-0.7125	-0.3939	0.0054
A0A1W2PQH3	ME2	Malic enzyme	1.1021	-0.5683	-0.5338	0.0075
Q13201	MMRN1	Multimerin-1	1.0038	0.1346	-1.1384	0.0002
P00403	MT-CO2	Cytochrome c oxidase subunit 2	1.2085	-0.8838	-0.3247	0.0002
P19105	MYL12A	Myosin regulatory light chain 12A	0.5900	0.4342	-1.0242	0.0209
P14543	NID1	Nidogen-1	1.0075	0.1286	-1.1361	0.0002
Q13423	NNT	NAD(P) transhydrogenase, mitochondrial	0.9269	-0.0713	-0.8556	0.0201
P18669	PGAM1	Phosphoglycerate mutase 1	1.0077	-0.6126	-0.3951	0.0242
J3KPX7	PHB2	Prohibitin-2	1.1294	-1.0367	-0.0927	0.0002
Q86WI1	PKHD1L1	Fibrocystin-L	-1.0000	0.2339	0.7661	0.0168
P27169	PON1	Serum paraoxonase/arylesterase 1	-0.9258	0.1241	0.8017	0.0272
P02775	PPBP	Platelet basic protein	0.9185	-0.1984	-0.7201	0.0405
P30153	PPP2R1A	Serine/threonine-protein phosphatase 2A 65 kDa regulatory subunit A alpha isoform	0.8129	0.1300	-0.9429	0.0225
P05771	PRKCB	Protein kinase C beta type	1.0061	-0.2489	-0.7572	0.0164
A6NLN1	PTBP1	Polypyrimidine tract binding protein 1, isoform CRA_b	-0.7988	-0.1566	0.9554	0.0218
P29350	PTPN6	Tyrosine-protein phosphatase non-receptor type 6	1.0043	-0.2040	-0.8003	0.0137
Q7LDG7	RASGRP2	RAS guanyl-releasing protein 2	0.9852	-0.3341	-0.6511	0.0281

P61586	RHOA	Transforming protein RhoA	0.9411	-0.4023	-0.5388	0.0498
P04843	RPN1	Dolichyl-diphosphooligosaccharide--protein glycosyltransferase subunit 1	1.0420	-0.7063	-0.3357	0.0133
P04844	RPN2	Dolichyl-diphosphooligosaccharide--protein glycosyltransferase subunit 2	0.8292	0.1204	-0.9496	0.0195
Q16799	RTN1	Reticulon-1	1.1585	-0.6249	-0.5336	0.0026
Q8NBX0	SCCPDH	Saccharopine dehydrogenase-like oxidoreductase	0.6500	-1.0046	0.3546	0.0233
Q5R345	SELP	P-selectin	0.7351	0.2861	-1.0212	0.0152
O75368	SH3BGRL	SH3 domain-binding glutamic acid-rich-like protein	0.8471	0.2033	-1.0504	0.0062
Q00325	SLC25A3	Phosphate carrier protein, mitochondrial	0.9957	-0.5474	-0.4484	0.0296
P05141	SLC25A5	ADP/ATP translocase 2	0.8051	0.0528	-0.8579	0.0425
O00161	SNAP23	Synaptosomal-associated protein 23	1.0689	-0.9345	-0.1345	0.0023
Q7KZF4	SND1	Staphylococcal nuclease domain-containing protein 1	0.8334	0.1226	-0.9559	0.0180
P12931	SRC	Proto-oncogene tyrosine-protein kinase Src	0.7118	0.1840	-0.8958	0.0490
P50502	ST13	Hsc70-interacting protein	1.0891	-0.8654	-0.2238	0.0032
Q13586	STIM1	Stromal interaction molecule 1	1.1641	-0.4928	-0.6713	0.0021
P37837	TALDO1	Transaldolase	0.4604	0.5746	-1.0350	0.0188
P01137	TGFB1	Transforming growth factor beta-1 proprotein [Cleaved into: Latency-associated peptide	0.6628	0.3600	-1.0228	0.0186
P49755	TMED10	Transmembrane emp24 domain-containing protein 10	1.2180	-0.5790	-0.6390	0.0006
O94886	TMEM63A	CSC1-like protein 1	0.8545	-0.8713	0.0168	0.0299
Q9NYL9	TMOD3	Tropomodulin-3	0.9454	-0.4448	-0.5006	0.0492
P49411	TUFM	Elongation factor Tu, mitochondrial	1.1144	-0.2063	-0.9081	0.0014
Q6IBS0	TWF2	Twinfilin-2	1.1051	-0.4982	-0.6069	0.0070
P68036	UBE2L3	Ubiquitin-conjugating enzyme E2 L3	0.9614	0.0037	-0.9651	0.0064
Q70J99	UNC13D	Protein unc-13 homolog D	0.9046	-0.0879	-0.8167	0.0295
Q15836	VAMP3	Vesicle-associated membrane protein 3	0.8917	-0.9159	0.0242	0.0172

Appendix 3: Significantly altered proteins between young and old platelets

Protein ID	Protein	Protein Name	Young Z score	Old Z score	p value	T test difference
M0R009	A1BG	Alpha-1B-glycoprotein	-0.9429	0.8367	0.0193	-1.7796
Q8N392	ARHGAP18	Rho GTPase-activating protein 18	0.8620	-0.7670	0.0127	1.6290
P52566	ARHGDIB	Rho GDP-dissociation inhibitor 2	0.6936	-0.9746	0.0031	1.6682
P06576	ATP5F1B	ATP synthase subunit beta, mitochondrial	1.1680	-0.9914	0.0001	2.1594
A0A087X232	C1S	Complement C1s subcomponent	-0.6595	1.0913	0.0063	-1.7509
P0C0L4	C4A	Complement C4-A	-1.1248	0.4356	0.0153	-1.5604
P07360	C8G	Complement component C8 gamma chain	-0.9833	0.9559	0.0065	-1.9392
P07384	CAPN1	Calpain-1 catalytic subunit	1.0486	-0.6265	0.0104	1.6751
P23528	CFL1	Cofilin-1	-0.9427	0.7841	0.0149	-1.7268
Q00610	CLTCL1	Clathrin heavy chain 1	0.9551	-0.8713	0.0138	1.8264
C9JAI6	CMTM5	CKLF-like MARVEL transmembrane domain-containing protein 5	1.0555	-0.6259	0.0144	1.6814
P01031	CO5	Complement C5	-1.1690	0.7182	0.0042	-1.8873
B4DJV2	CS	Citrate synthase	0.9569	-0.8125	0.0063	1.7694
Q5VTE0	EEF1A1P5	Putative elongation factor 1-alpha-like 3	1.0931	-0.9307	0.0019	2.0238
P60842	EIF4A1	Eukaryotic initiation factor 4A-I	0.8928	-0.7716	0.0255	1.6644
P50402	EMD	Emerin	0.9439	-0.4464	0.0123	1.3903
Q9Y6C2	EMILIN1	EMILIN-1	1.0280	-0.6817	0.0104	1.7097
Q9BSJ8	ESYT1	Extended synaptotagmin-1	0.8537	-0.7995	0.0247	1.6532
P12259	F5	Coagulation factor V	1.0488	-0.8036	0.0033	1.8523
P02671	FGA	Fibrinogen alpha chain	-0.6393	1.0598	0.0218	-1.6991
Q14697	GANAB	Neutral alpha-glucosidase AB	1.0670	-0.6479	0.0085	1.7149

P50148	GNAQ	Guanine nucleotide-binding protein G	1.0175	-0.4825	0.0249	1.5000
P43304	GPD2	Glycerol-3-phosphate dehydrogenase, mitochondrial	0.8130	-0.8942	0.0147	1.7072
P06744	GPI	Glucose-6-phosphate isomerase	0.9212	-0.2636	0.0096	1.1848
Q5T0I0	GSN	Gelsolin	1.1058	-0.3425	0.0270	1.4483
P78417	GSTO1	Glutathione S-transferase omega-1	0.9498	-0.5368	0.0048	1.4866
P55084	HADHB	Trifunctional enzyme subunit beta, mitochondrial	0.9566	-0.3042	0.0224	1.2607
P69905	HBA	Hemoglobin subunit alpha	-0.2842	1.0803	0.0309	-1.3645
P19367	HK1	Hexokinase-1	0.6968	-1.0493	0.0234	1.7461
P61604	HSP70-10	10 kDa heat shock protein, mitochondrial	0.6560	-1.1047	0.0074	1.7607
P0DMV9	HSPA1B	Heat shock 70 kDa protein 1B	0.5691	-1.0215	0.0082	1.5906
P38646	HSPA9	Stress-70 protein, mitochondrial	0.7189	-1.0075	0.0107	1.7265
B9A064	IGLL5	Immunoglobulin lambda-like polypeptide 5	-0.9803	1.0077	0.0008	-1.9880
Q27J81	INF2	Inverted formin-2	0.9248	-0.7365	0.0003	1.6613
P08514	ITGA2B	Integrin alpha-IIb	0.8581	-0.7940	0.0242	1.6520
P05106	ITGB3	Integrin beta-3	1.1148	-0.5853	0.0086	1.7001
Q5T985	ITIH2	Inter-alpha-trypsin inhibitor heavy chain H2	-0.8814	0.7549	0.0160	-1.6362
Q14624	ITIH4	Inter-alpha-trypsin inhibitor heavy chain H4	-1.2222	0.8947	0.0002	-2.1170
P00338	LDHA	L-lactate dehydrogenase A chain	1.1609	-0.3868	0.0053	1.5477
Q3ZCW2	LGALSL	Galectin-related protein	0.6028	-1.0071	0.0199	1.6099
P50851	LRBA	Lipopolysaccharide-responsive and beige-like anchor protein	1.1215	-0.1994	0.0113	1.3209
Q15691	MAPRE1	Microtubule-associated protein RP/EB family member 1	1.1064	-0.3939	0.0243	1.5002
A0A1W2PQH3	ME2	Malic enzyme	1.1021	-0.5338	0.0014	1.6359
Q13201	MMRN1	Multimerin-1	1.0038	-1.1384	0.0010	2.1423
P00403	MT-CO2	Cytochrome c oxidase subunit 2	1.2085	-0.3247	0.0039	1.5332
P19105	MYL12A	Myosin regulatory light chain 12A	0.5900	-1.0242	0.0406	1.6141

P14543	NID1	Nidogen-1	1.0075	-1.1361	0.0008	2.1436
Q13423	NNT	NAD (P) transhydrogenase, mitochondrial	0.9269	-0.8556	0.0096	1.7825
J3KPX7	PHB2	Prohibitin-2	1.1294	-0.0927	0.0096	1.2222
Q86WI1	PKHD1L1	Fibrocystin-L	-1.0000	0.7661	0.0023	-1.7660
P27169	PON1	Serum paraoxonase/arylesterase 1	-0.9258	0.8017	0.0248	-1.7274
P02775	PPBP	Platelet basic protein	0.9185	-0.7201	0.0220	1.6386
P30153	PPP2R1A	Serine/threonine-protein phosphatase 2A 65 kDa regulatory subunit A alpha isoform	0.8129	-0.9429	0.0042	1.7558
P05771	PRKCB	Protein kinase C beta type	1.0061	-0.7572	0.0139	1.7633
A6NLN1	PTBP1	Polypyrimidine tract binding protein 1, isoform CRA_b	-0.7988	0.9554	0.0207	-1.7542
P29350	PTPN6	Tyrosine-protein phosphatase non-receptor type 6	1.0043	-0.8003	0.0188	1.8046
Q7LDG7	RASGRP2	RAS guanyl-releasing protein 2	0.9852	-0.6511	0.0292	1.6363
P61586	RHOA	Transforming protein RhoA	0.9411	-0.5388	0.0481	1.4799
P04843	RPN1	Dolichyl-diphosphooligosaccharide--protein glycosyltransferase subunit 1	1.0420	-0.3357	0.0382	1.3777
P04844	RPN2	Dolichyl-diphosphooligosaccharide--protein glycosyltransferase subunit 2	0.8292	-0.9496	0.0237	1.7788
Q16799	RTN1	Reticulon-1	1.1585	-0.5336	0.0032	1.6921
Q5R345	SELPLG	P-selectin	0.7351	-1.0212	0.0188	1.7563
O75368	SH3BGRL	SH3 domain-binding glutamic acid-rich-like protein	0.8471	-1.0504	0.0003	1.8976
Q00325	SLC25A3	Phosphate carrier protein, mitochondrial	0.9957	-0.4484	0.0127	1.4441
P05141	SLC25A5	ADP/ATP translocase 2	0.8051	-0.8579	0.0305	1.6630
O00161	SNAP23	Synaptosomal-associated protein 23	1.0689	-0.1345	0.0388	1.2034
Q7KZF4	SND1	Staphylococcal nuclease domain-containing protein 1	0.8334	-0.9559	0.0107	1.7893
P12931	SRC	Proto-oncogene tyrosine-protein kinase Src	0.7118	-0.8958	0.0449	1.6076
P50502	ST13	Hsc70-interacting protein	1.0891	-0.2238	0.0053	1.3129
Q13586	STIM1	Stromal interaction molecule 1	1.1641	-0.6713	0.0038	1.8354
P37837	TALDO1	Transaldolase	0.4604	-1.0350	0.0488	1.4954

P01137	TGFB1	Transforming growth factor beta-1 proprotein	0.6628	-1.0228	0.0153	1.6856
P49755	TMED10	Transmembrane emp24 domain-containing protein 10	1.2180	-0.6390	0.0020	1.8570
Q9NYL9	TMOD3	Tropomodulin-3	0.9454	-0.5006	0.0405	1.4460
P49411	TUFM	Elongation factor Tu, mitochondrial	1.1144	-0.9081	0.0001	2.0225
Q6IBS0	TWF2	Twinfilin-2	1.1051	-0.6069	0.0171	1.7121
P68036	UBE2L3	Ubiquitin-conjugating enzyme E2 L3	0.9614	-0.9651	0.0011	1.9264
Q70J99	UNC13D	Protein unc-13 homolog D	0.9046	-0.8167	0.0062	1.7213